Adsorption of Nitrogen, Methane, and Carbon Monoxide on Aluminosilicate and Aluminophosphate Molecular Sieves

Ligia Predescu

A thesis submitted to the School of Graduate Studies and Research

in partial fulfillment of the requirements for the degree of

M. A. Sc. in Chemical Engineering (Environmental)

Department of Chemical Engineering

University of Ottawa

ISBN 0-612-15753-9

Canada

UNIVERSITÉ D'OTTAWA
UNIVERSITY OF OTTAWA

ABSTRACT

Considering the difficulties associated with the experimental determination of binary mixture adsorption isotherms, pure-gas adsorption information becomes vital in the prediction of these isotherms and the corresponding phase equilibria necessary in the design of adsorptive separation units. Experimental equilibrium isotherms describing the adsorption of pure N_2, CH_4, and CO in a natural aluminosilicate molecular sieve (clinoptilolite from Cuba) and two synthetic small-pore aluminophosphate molecular sieves ($AlPO_4$-17 and $AlPO_4$-18) have been determined using the volumetric method at 40°C over a pressure range up to about 1000 mm Hg, and subsequently fitted with the Langmuir and Flory-Huggins Vacancy Solution Theory equations. Additional Langmuir and FH-VST fits of equilibrium isotherms previously measured over the same pressure range at room temperature and 40°C to describe the equilibrium adsorption of the same three adsorbates in two aluminosilicate molecular sieves (natural clinoptilolite from Turkey and zeolite 5A), as well as in a medium-pore aluminophosphate molecular sieve $AlPO_4$-11 were also obtained. The Freundlich equation was found to yield a better fit than either the Langmuir or FH-VST equations for the experimental adsorption isotherms of N_2 and CO on $AlPO_4$-17. The higher capacities of the aluminosilicate molecular sieves, compared to those of the aluminophosphate molecular sieves, for the adsorbates investigated were attributed to the energetic heterogeneity conferred by the presence of framework-charge compensating cations.

The model parameters obtained by fitting the experimental pure-component adsorption isotherms permitted the prediction of the mixture adsorption phase diagrams and the binary adsorption isotherms by the Extended Langmuir Model and the Flory-Huggins Vacancy Solution Model for the three possible binary mixtures at 101.3 kPa total pressure and the pure-component adsorption temperatures investigated. The Ideal Adsorbed Solution Theory was also applied by calculating the spreading pressures of the mixture components with the Langmuir fits. An explanation of the behaviour predicted by each model for each adsorption system was attempted.

ACKNOWLEDGMENTS

I would like to thank my supervisor, Dr. F. Handan Tezel, for giving me the opportunity to have a close look at the fascinating world of molecular sieves, and for guiding my steps into the captivating and challenging field of adsorption. Her relentless support, encouragement, and optimism, whether professionnally related or not, have been invaluable at all times, and I have gained tremendous knowledge – while deriving great strength – from my collaboration with her.

My heartfelt thanks go to Messrs. Sudhir Chopra and Robert Triebe for enlightening discussions on adsorption measurements and diffusion mechanisms. I also feel indebted toward my fellow graduate students, especially Messrs. Boguslaw Kruczek and Sameer Al-Asheh, who shared with me some of their expertise on data processing tools.

The experimental work could not have been carried out without the molecular sieve samples. Professor Serge Kaliaguine of Université Laval in Ste-Foy, Quebec, kindly supplied the aluminophosphate molecular sieve samples, while Mr. G. Mrazek from the Department of Geology at the University of Ottawa, provided the Cuban clinoptilolite samples.

In addition, I am grateful to Messrs. Louis Tremblay, Frank Ziroldo, and Gérard Nina – whose technical skills were much needed in solving equipment-related problems – for providing excellent laboratory work conditions.

Last but not least, my gratitude goes to my family: it is they who made it all possible, with their help and understanding which kept me going and made all the efforts worthwhile and rewarding.

Table of Contents

List of Figures

List of Tables

Nomenclature

A - surface area of the adsorbent [m^2]
B_i, B_j - Langmuir constants [1/Pa]
b_i - Henry's law constant [mol/kg Pa]
k - Freundlich parameter [m^3/Pa]
M - monovalent (alkali) metal atom
N - divalent (alkali-earth) metal atom
n - Freundlich parameter [dimensionless]
n_i - amount of species i adsorbed [mol/kg]
n_i^0 - amount of species i adsorbed at pressure P_i^0 [mol/kg]
n_m - Langmuir monolayer capacity for pure gas adsorbed [mol/kg]
n_{mi} - Langmuir monolayer capacity for species i adsorbed from mixture [mol/kg]
n_m^∞, n_m^{inf} - total limiting amount of adsorption [mol/kg]
n_1^∞, n_1^{inf} - limiting amount of adsorption [mol/kg]
n_t - total amount of mixture adsorbed [mol/kg]
P - pressure [Pa]
P_i, P_j - partial pressure of species i in the gas phase mixture [Pa]
P_i^0 - equilibrium pressure of pure component i at the same temperature and spreading pressure as the adsorbed mixture [Pa]
q - charge of cation on the surface of the adsorbent [dimensionless]
R - universal gas constant [m^3Pa/mol K]
r - distance between the adsorbing atom or molecule and the surface of the adsorbent [m]
T - absolute temperature [K]
T - atom capable of forming tetrahedra (Si, Al, P)
v - volume of gas adsorbed [m^3]
v_i - volume of gas adsorbed from a mixture [m^3]
v_m - monolayer volume of pure gas adsorbed [m^3]
v_{mi} - monolayer volume of species i adsorbed [m^3]
v_M (= v_{Mi}) - averaged monolayer volume [m^3]
w - number of water molecules per unit cell
x - total number of AlO_4 tetrahedra per unit cell of zeolite
X_i, x_i - experimental mole fraction of species i in the adsorbed phase [dimensionless]
x_i^s - mole fraction of species i in the adsorbed phase [dimensionless] (i represents either of the components in the adsorbed mixture as well as the vacancy)
y - total number of SiO_4 tetrahedra per unit cell of zeolite
Y_i, y_i - mole fraction of species i in the gas phase [dimensionless]
z - distance between the adsorbate molecule and the adsorbent surface [m]

Greek Letters

α_1 - adsorbent polarizability [cm^3]
α_{12} - equilibrium adsorption separation factor (selectivity) [dimensionless]
α_{1v} - gas-vacancy interaction parameter [dimensionless]
γ_i - Flory-Huggins activity coefficient of species *i* in the vacancy solution representing the adsorbed multicomponent mixture [dimensionless] (*i* represents either of the components in the adsorbed mixture as well as the vacancy)
θ - fractional coverage of adsorbent surface [dimensionless]
θ_i - partial fractional coverage of adsorbent surface by adsorbed molecules of species *i* in the mixture [dimensionless]
π_i - spreading pressure of species i in the mixture [Pa]
ϕ_A - "non-specific" (adsorbent-related) adsorption potential [V]
ϕ_a - "specific" (adsorbate-related) adsorption potential [V]
$\phi(z)$ - local adsorption potential [V]
ϕ_D - adsorption potential due to dispersive interactions [V]
$\phi_{F\mu}$ - adsorption potential due to field-dipole interactions [V]
ϕ_{FQ} - adsorption potential due to field gradient - quadrupole interactions [V]
ϕ_P - adsorption potential due to the polarizing energy of the adsorbent [V]
ϕ_R - adsorption potential due to repulsive interactions [V]
ϕ_{SP} - self potential [V]

Abbreviations

a-ELM - averaging-approach Extended Langmuir Model
d-ELM - direct-approach Extended Langmuir Model
IAST - Ideal Adsorbed Solution Theory
FH-VST - Flory-Huggins Vacancy Solution Theory

CHAPTER 1

INTRODUCTION

The discovery of adsorptive properties in the natural microporous crystalline aluminosilicate molecular sieves known as zeolites in the eighteenth century has triggered extensive research which has exponentially grown over the past decades. Although the initial focus was kept on naturally-occurring zeolites, advances in chemical synthesis techniques have led to the advent of synthetic aluminosilicate molecular sieves in the 1950's, followed by the synthesis of aluminophosphate molecular sieves for which no natural counterparts are known but whose frameworks are, in many cases, homologous to those of natural zeolites.

Unlike activated alumina, silica gel, activated carbon, and carbon molecular sieves which are characterized by pore size distributions, aluminosilicate and aluminophosphate molecular sieves possess a uniform pore size which is responsible for the sieving effect known to be exerted on gaseous molecules on the basis of steric considerations. Intermolecular forces (due to dispersion, close-range repulsion, polarization, and electrostatic interactions) and a fine interplay between the various types of adsorbent-adsorbate interactions determine, however, the amount of gas adsorbed at equilibrium and the kinetics of the adsorption process. Structural information on the adsorbent and the physico-chemical properties of the adsorbate can provide initial qualitative information on the behaviour of pure-gas systems which can be validated only through measurement of the pure-gas adsorption isotherms.

As adsorptive processes currently constitute a major means for purification and bulk separation of gaseous streams, the behaviour of adsorption systems representative for air purification and important hydrocarbon processing (such as removal of impurities from natural gas) must be known in depth in order to improve the current technology. With economic and environmental issues becoming more pressing every day, information related to the optimization of adsorption separation processes (whose share of the industrial market has been continuously growing) appears to be in constant demand.

Knowledge of the adsorptive properties of systems involving readily available synthetic molecular sieves or sufficiently pure natural zeolites abundant enough to allow large-scale commercialization, as well as their interaction with adsorbates featuring specific physical and chemical properties plays an important part in adsorber design, which is heavily dependent on multicomponent adsorption equilibria information (e.g. the adsorption capacity of the adsorbent for the pure gas or for the components of a gas mixture, the adsorption separation factor or selectivity). In those cases in which experimental binary adsorption phase diagrams and isotherms are not available the usual approach is modelling of experimental single-component adsorption isotherms in order to predict the binary mixture adsorption data at a chosen total pressure and the temperatures at which the pure-gas isotherms had been determined.

Important advances have been recorded in the development of modelling tools for adsorption processes, and most of the theoretical models published in the literature, while acknowledged as extremely accurate for several types of adsorption systems, still need further testing with various other adsorption systems before they can be considered "universal". Given the large number and types of adsorption systems encountered in industrial practice, this becomes an overwhelming task when one sets out to perform work involving pure-component adsorption, let alone multicomponent adsorption. While it is impossible to avoid pure-gas adsorption experiments for a clue on the behaviour of any adsorbate-adsorbent system, one may obtain a few qualitative hints by using the pure-component adsorption information, turn to one or several theoretical models to fit the data, and then model the multicomponent adsorption behaviour without having to necessarily resort to laborious experimental setups and procedures.

A modest share of the work necessary to provide comprehensive information on single- and multicomponent adsorption systems is undertaken in this study, in an attempt to improve the understanding of the underlying phenomena and to compare the modelling performance of several predictive tools which are gaining increasing recognition in the field of adsorptive separation process design.

1.1 OBJECTIVES OF THE PRESENT STUDY

The importance of adsorption among separation processes has increased considerably over the past decades, with bulk separation and purification of gaseous mixtures continuing to remain the foremost industrial applications. Consequently, there is a constant need for experimental data to enlarge the existing database, and to permit the prediction of the behaviour of binary gas mixtures using literature models which have been successfully applied in adsorption separation units in the industry. The design of an adsorption separation process requires not only the use of a suitable adsorbent with high capacity for a specific gas, but also the knowledge of suitable conditions to improve the selectivity of the adsorbent for one or more components present in the gaseous mixture.

The selection of the adsorbates was performed with industrial applications in mind. The inert N_2 could be considered the representative of air and a "standard" on the scale of adsorbate chemical reactivity when compared to the two other adsorbates chosen – CO which was selected to represent highly toxic gases yielded in many industrial processes and whose concentration in the environment is regulated with increasing strictness, and the combustible CH_4, which is the primary component of natural gas and an important raw material for the chemical and petrochemical industry involved in important industrial bulk separations. On a different scale suggested by the difference in the polarity of these three gases, non-polar CH_4 can be looked upon as the "origin" with polar CO at the other end and quadrupolar N_2 occupying an intermediate position ($CH_4 < N_2 << CO$). Thus, the prediction of the adsorptive separation of binary mixtures of these three gases would be meaningful in the areas of air purification (CO-N_2 mixtures) and natural gas enrichment or bulk separation (CO-CH_4 and CH_4-N_2).

The overall objective of this study was to determine the best adsorbent from the set of six investigated for the separation of N_2-CO, CH_4-CO, and N_2-CH_4 mixtures, at 101.3 kPa total pressure. Predicted binary equilibria information can improve the understanding of the mechanisms governing physical adsorption, especially in the case of novel materials like aluminophosphate molecular sieves.

The first objective of this work was to use the volumetric method for measurement of adsorption data to provide the pure gas adsorption data bank with experimental equilibrium isotherms for adsorption systems involving N_2, CH_4, and CO. The adsorbents chosen were natural clinoptilolite from Cuba to represent the class of natural aluminosilicate molecular sieves, and two representatives of the synthetic aluminophosphate molecular sieves, $AlPO_4$-17 (the structural analogue of erionite) and $AlPO_4$-18 (structually related to chabazite), which feature approximately the same small pore size (4.3 Å, according to Wilson [1991]), only slightly larger than the kinetic diameters of the three adsorbates (3.64 Å for N_2, 3.76 Å for CO, and 3.80 Å for CH_4). Comparison of the pure-gas adsorption behaviour of these three molecular sieves would permit a better understanding of the adsorptive properties resulting from the differences in their respective structural, physical, and chemical characteristics, and would subsequently provide the means to take full advantage of these differences to optimize adsorptive separation processes of multicomponent mixtures.

The second objective of this investigation was to model the Cuban clinoptilolite, $AlPO_4$-17, and $AlPO_4$-18 isotherms obtained experimentally in this study along with previously measured experimental equilibrium isotherms describing the adsorption of N_2, CH_4, and CO in zeolite 5A, clinoptilolite from Turkey, and $AlPO_4$-11. Modelling would thus provide a picture of the performance of the Langmuir theory and the Vacancy Solution Theory for various classes of adsorbents when the same adsorbates are used, and enable a qualitative estimate regarding the reliability of subsequently predicted binary information.

The third and last objective of this work was to predict binary mixture equilibria using the Extended Langmuir Model and the Vacancy Solution Theory for mixtures with the pure-gas parameters previously determined for all six adsorbents, at the temperatures

previously used and a constant total pressure. The Ideal Adsorbed Solution Theory was also applied using the Langmuir fits for the single-component isotherms. The binary predictions yielded by these three modelling tools for the adsorption of N_2-CO, CH_4-CO, and N_2-CH_4 mixtures in the six adsorbents (clinoptilolite from Cuba and Turkey, zeolite 5A, $AlPO_4$-17, $AlPO_4$-18, and $AlPO_4$-11) were compared for the same total pressure (101.3 kPa) and temperature (40°C). In addition, the availability of experimental equilibrium data on zeolite 5A, Turkish clinoptilolite, and $AlPO_4$-11 at room temperature (Stelmack, 1994) permitted the prediction of binary data at that temperature and 101.3 kPa total pressure. The explanation of the discrepancies between the predictions yielded by each model for each adsorption system investigated is related to the structural, physical, chemical, and energetic characteristics of both adsorbent and adsorbate, as well as the assumptions on which each theory is based and the way these underlying assumptions account for the characteristics of both the adsorbent and the adsorbate.

1.2 CONTRIBUTIONS OF THE PRESENT WORK

The current study investigates experimentally the single-component equilibrium adsorption of N_2, CO, and CH_4 in Cuban clinoptilolite, $AlPO_4$-17 and $AlPO_4$-18, and predicts the separation ability of these adsorbents when in contact with binary mixtures of these adsorbates.

In order to obtain a more thorough overview of the behaviour of binary gas mixture adsorption systems involving aluminosilicate and aluminophosphate molecular sieves, equilibrium experimental data previously collected for single-component adsorption systems involving the same adsorbates and three different adsorbents (zeolite 5A, Turkish clinoptilolite, and $AlPO_4$-11) were fitted with the Langmuir equation and the FH-VST equation, the fits being subsequently used to predict the performance of these adsorbents in the separation of the same binary gas mixtures. Table 1.1 summarizes the extent of the work contributed by the present study.

Table 1.1 Contributions of the present study to the investigation of the adsorptive behaviour of N_2, CH_4, CO, and their binary gas mixtures (at 101.3 kPa total pressure)

Adsorbent	Experimental single-component equilibrium isotherms	Fitted experimental single-component isotherms	Predicted binary gas mixture adsorption at equilibrium
Zeolite 5A	Stelmack (1994)	Present	Present
Turkish clinoptilolite	Stelmack (1994)	Present	Present
Cuban clinoptilolite	Present	Present	Present
$AlPO_4$-11	Stelmack (1994)	Present	Present
$AlPO_4$-17	Present	Present	Present
$AlPO_4$-18	Present	Present	Present

CHAPTER 2

LITERATURE REVIEW

2.1 ALUMINOSILICATE MOLECULAR SIEVES

2.1.1 General Characteristics

Zeolites are defined as hydrated crystalline aluminosilicates of mono- and divalent bases which can be reversibly dehydrated to varying degrees without undergoing cation exchange. The general composition of zeolites is given by the formula $(M_2,N)O \cdot Al_2O_3 \cdot nSiO_2 \cdot mH_2O$ where M and N are mono- and divalent cations, respectively, present in the zeolite structure.

Since the valence of the Si atom is IV (four electrons in the outer shell) and the valence of the Al atom is III (three electrons in the outer shell), aluminosilicate molecular sieves would feature an excess negative charge in the absence of cations. Cations are therefore necessary to compensate the excess negative charge so that the neutrality (and therefore stability) of the zeolitic framework be maintained. A zeolite will accommodate only a given maximum number of monovalent or divalent cations, corresponding to the number of negative charges which must be compensated in the framework or, in other words, to the number of Al atoms present in the framework. Consequently, there is a direct relationship between the number of aluminum atoms present in the framework and the exchange capacity of a zeolite. According to Iijima (1971), high-silica zeolites generally feature a lower exchange capacity and contain more univalent cations than

low-silica varieties which have a higher exchange capacity and contain divalent cations preferably.

Aluminosilicate molecular sieves are restricted to frameworks with only four-coordinated Al atoms (Pluth and Smith, 1987), but their Al/Si ratios cover a wide range which accordingly trigger order/disorder phenomena not encountered in aluminophosphate materials. Aluminophosphate molecular sieve structures feature four-, five-, and six-coordinated Al atoms but are restricted to only one Al/P ratio equal to unity, given the valencies of the Al (+3) and P (-3) atoms, which explains therefore the absence of framework charge compensating cations. Irrespective of the type of molecular sieve, micropores whose apertures are somewhat smaller than the kinetic diameter of the adsorbate molecules can be accessed as a result of the effects of vibration of both the diffusing molecules and the crystal lattice (Ruthven, 1984).

The presence of cations in aluminosilicate molecular sieves confers energetic heterogeneity to the adsorption surface. Three categories of factors influence energetic heterogeneity (Barrer, 1978):

a) adsorbate-related factors such as adsorbate molecular size (i.e. heterogeneity is reduced for large molecules which are unable to access small pores);

b) outgassing conditions which can allow the presence of various amounts of residual water, which – given its small molecular diameter and high polarity – is likely to "quench" the high potential of strongly adsorbing sites and thus contribute to the reduction of energetic heterogeneity;

c) adsorbent-related factors such as the presence of impurities, the presence of a mixed cation population with varying proportions of cations in different cavities as well as framework defects (more likely to be encountered in natural zeolites such as clinoptilolite), and an uneven distribution of aluminum and silicon atoms in the framework of zeolites (which all have Si : Al > 1) which may lead to local cationic charges that cannot be fully neutralized in some areas of the lattice; energetic heterogeneity is also boosted by the presence of cations of small sizes (H^+ being the exception).

The presence of a polar adsorbate in the vicinity of an energetically heterogeneous adsorbent surface results in the "specific", adsorbate-related potential

energy (ϕ_s) consisting in the sum of the field - dipole and field gradient - quadrupole interactions, as well as the "self potential", which depends on the amount already adsorbed (Barrer, 1978). In the absence of a polar adsorbate, the adsorption potential consists only of the "non-specific" component, which represents the summation of the potentials corresponding to the dispersive interactions, close-range repulsion interactions, and polarization interactions. Thus, the overall potential between the adsorbate molecule and the surface is constant at a certain distance z from the surface of the adsorbent, and is the summation of these individual adsorption potentials:

$$\phi(z) = \phi_A + \phi_s = \phi_D + \phi_R + \phi_P + \phi_{F\mu} + \phi_{FQ} + \phi_{SP} \qquad (2.1)$$

Uses of zeolites have stemmed from properties such as reversible dehydration, cation exchange, adsorption, and acid and thermal stability (Hansley and Sheppard, 1993). In addition to large-scale gas separation, applications include sewage-effluent treatment, radioactive wase treatment, use as fertilizers and as dietary supplement for livestock.

2.1.2 Zeolite 5A

Zeolite A was synthesized by R.M. Milton in 1959. The framework topology shown in Figure 2.1a reveals the presence of two types of polyhedra: the small one is a cubic arrangement of eight TO_2 tetrahedra, and the large one is the beta cage encountered in the sodalite structure, i.e. an octahedron consisting of 24 TO_2 tetrahedra, whose free diameter is 6.6 Å. The cavity generated by the cubic arrangement of the beta cages is also known as the alpha (or sodalite) cage.

Ruthven and Derrah (1975) describe the crystal lattice of zeolite 5A as a cubic array of nearly spherical cavities with a free diameter of approximately 11.4 Å, interconnected by windows of aperture 4.8 Å resulting from the presence of Ca^{+2} cations. The volume of the large cavity in zeolite A is known to be 776 $Å^3$ (Dubinin, 1964), which corresponds to a specific micropore volume of approximately 0.27 $cm^3\ g^{-1}$ (Loughlin and Ruthven, 1972). The smaller cavities in the sodalite units (beta cages) present in the framework contribute approximately 150 $Å^3$ per unit cell, or 0.05 $cm^3\ g^{-1}$ to the total specific micropore volume, but these cavities are not accessible to large gas molecules.

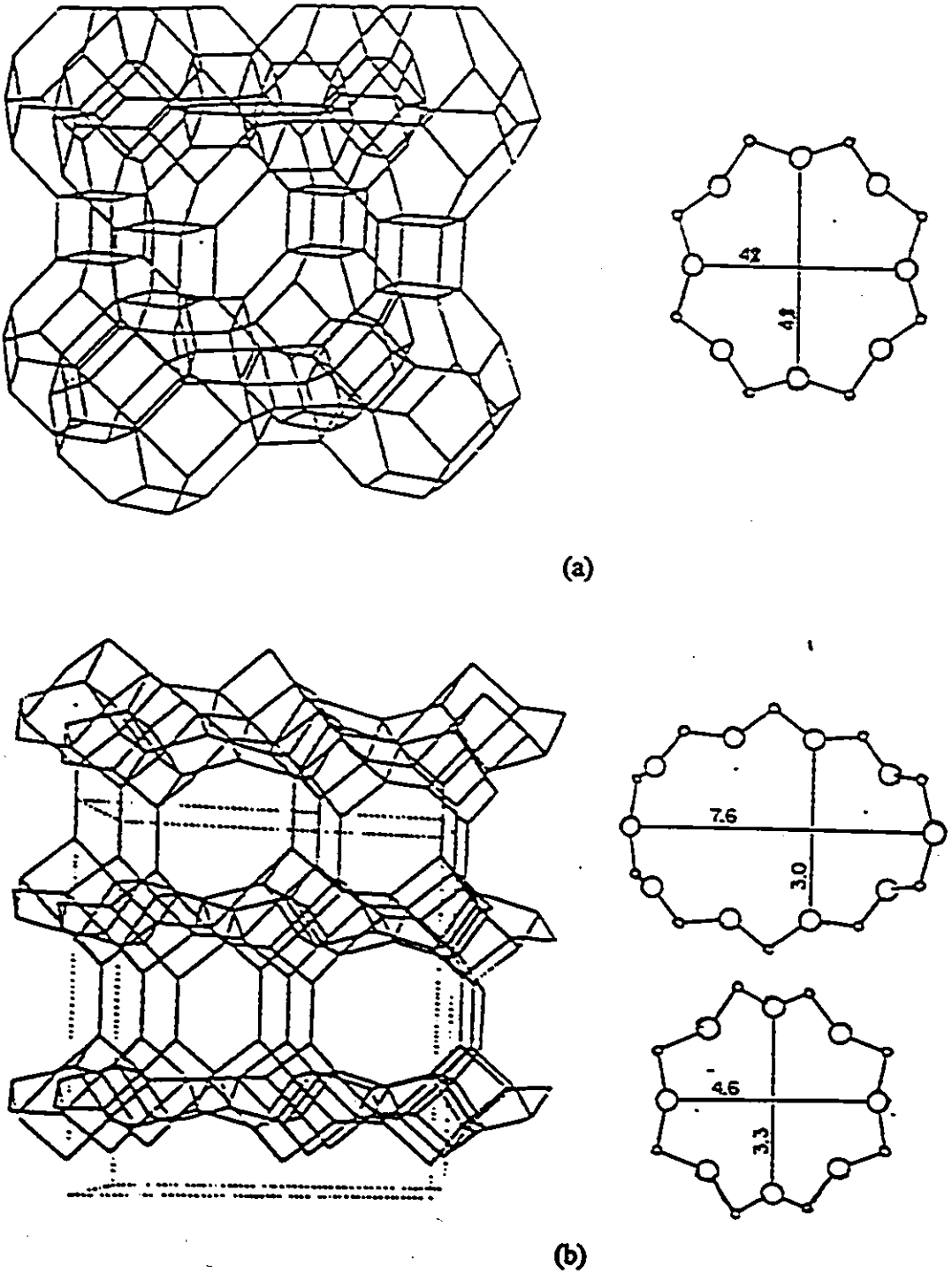

Figure 2.1 Channel and pore geometries in (a) zeolite 5A; (b) clinoptilolite (Meier and Olson, 1992)

The pore structure of zeolite A is three-dimensional with 8-member oxygen rings as pore apertures.

Ion exchange does not produce significant alterations in the framework dimensions, therefore the equilibrium adsorptive properties of zeolite A are expected to be the same for all cationic forms of zeolite A when non-polar gases are involved (Loughlin and Ruthven, 1972). Sorption kinetics, however, are expected to feature large differences depending on the type of exchangeable cation obstructing the cavity aperture.

2.1.3 Clinoptilolite

Clinoptilolite was first identified by Schaller in the Hoodoo mountains in Wyoming (U.S.A.) in the 1930s, then recognized by Kostov as a heulandite rich in silica, and eventually classified by Berman and Pabst as a distinct mineral in the heulandite group (U.S. EPA, 1971). While the properties of clinoptilolite approximate those of heulandite (same type of framework with monoclinic symmetry), clinoptilolite exhibits increased thermal stability (above 450°C, up to 700°C in air) due to its higher content of silica. Unlike heulandite which can be found in hydrothermal or deeply buried deposits, clinoptilolite is characteristic of low-temperature, near-surface, silicic tuffaceous sedimentary deposits. Beside a higher Si:Al ratio (>4.0), clinoptilolite features a higher content of monovalent alkaline ions with respect to the total content of alkaline and alkaline-earth ions (Na+K : Na+K+Ca+Mg > 0.6), as well as a lower mean index of refraction (<1.485) attributed to the presence of ferric oxide and a high calcium content (as a result of calcium substitution for potassium and sodium). The chemical composition of natural clinoptilolite is (Ackley and Yang, 1991a):

$$(Li, Na, K)_a(Mg, Ca, Sr, Ba)_d[Al_{(a+2d)}Si_{n-(a+2d)}O_{2n}] \cdot mH_2O$$

with n = 36 and m = 24. The water association depends on the type of exchangeable cations (Szostak, 1992). Clinoptilolite can be synthesized from an $Al_2O_3 - SiO_2 - Na_2O - H_2O$ gel at 200-250°C (Szostak, 1992).

The framework topology is shown in Figure 2.1b. The layered structure of clinoptilolite features alternating channels defined by 8- and 10-member oxygen rings, (whose dimensions are 4.6 x 3.3 Å and 7.6 x 3.0 Å, respectively), which are intersected .by channels of 8-member oxygen rings.

Esenli and Kumbasar (1994) have compared the thermal and dehydration behaviour of heulandites and clinoptilolites from Western Anatolia, Turkey, including samples from Bigadic, and have found that the chemical composition is an important factor. Heulandites dehydrate at higher temperatures than clinoptilolites, but the latter retain water at higher temperatures as their divalent cation content increases. The Bigadic samples (90 and 95% zeolite content), taken from diferent levels of the formation, featured Si/Al ratios of 4.58 and 4.62, respectively, and Na+K/Ca+Mg ratios of 0.58 and 1.35, respectively (the sample taken from the lower level having higher thermal stability and cationic ratio value). The amount of Na^+ was found to be negligible.

Table 2.1 summarizes some of the structural characteristics of the investigated aluminosilicate molecular sieves.

Table 2.1 Structural characteristics of investigated aluminosilicate molecular sieves (Szostak, 1992)

	Zeolite 5A	Clinoptilolite
Chemical composition	$\{Ca_6[Al_{12}Si_{12}O_{48}].27\ H_2O\}$[1]	$\{Ca_x(Na,K)_{6-2x}[Al_6Si_{30}O_{72}].27\ H_2O\}$[2]
Si/Al ratio	1.0	> 4.0
Symmetry	cubic	monoclinic
Channel system	three-dimensional	two-dimensional
Ring system	8-member	10-member and 8-member
Pore dimensions [Å]	4.8	3.0 x 7.6 and 3.3 x 4.6

[1] Meier and Olson (1992)
[2] Hansley and Sheppard (1993)

The commercial value of clinoptilolite is mainly due to its ability to accommodate large cations (NH_4^+, Cs^+, Sr^{2+}, heavy metals) which enables it to remove ammonium ions from sewage effluents (making it a less expensive alternative in water treatment when compared to synthetic organic ion-exchange resins) and radioactive cesium (Cs^{137}) and strontium (Sr^{90}) from wastewater nuclear power plants--clinoptilolite being more stable in the presence of nuclear-particle bombardment. Beside playing an important part in gas- and liquid-drying processes and for the separation of gases, clinoptilolite is used as an additive in paper fillings, fertilizers, pet litter, and as building-stone aggregate.

2.2 ALUMINOPHOSPHATE MOLECULAR SIEVES

Aluminophosphate differ from aluminosilicate molecular sieves through three distinct features (Bennett *et al.*, 1986):

(i) the electrostatic neutrality of the $AlPO_4$ moiety (absence of specific adsorption sites);

(ii) the occurrence of some Al atoms in five or six coordination with oxygen species (OH, H_2O) -- which provides geometric and electrostatic flexibility translated into the adoption of new structure types not represented by aluminosilicate molecular sieves;

(iii) the strict alternation of Al and P atoms (Al/P = 1) on tetrahedral nodes which generate even-numbered atom rings.

Pluth and Smith (1987) describe the aluminophosphate structures as frameworks of linked AlO_4 and PO_4 tetrahedra as well as Al octahedra in which some Al atoms which have more than four near neighbors are five- and six-coordinated. The tetrahedra and octahedra link by corner sharing to form 4-, 6-, 8-, 10-, 12-, 14-, 18-, and 20-member rings, which generate channels that extend in one or more dimensions and are responsible for the molecular sieve nature of $AlPO_4$ materials (Rudolf and Crowder, 1990). The alternation of Al and P atoms in $AlPO_4$ frameworks despite the variation in the Al coordination restricts the order of a ring to an even number (Bennett *et al.*, 1986).

The type of rings present in aluminophosphate molecular sieves allows the classification of these synthetic materials into condensed or dense (very small pore, with 4- and 6-member rings of diameter ~3 Å), small-pore (8-member rings of diameter ~4 Å), medium-pore (10-member rings of diameter ~6 Å), large-pore (12-member rings of diameter ~7-8 Å), and very large pore (18- and 20-member rings of diameter > 12.5 Å). Large pore diameters of 12-13 Å and up pave the way to industrial applications of aluminophosphate molecular sieves in catalytic processes, separation processes, etc., in which "bulky" chemical species could be adsorbed. Structure types range therefore from dense phases (with low surface areas) through the hydrates and semi-dense phases, to eventually the microporous materials yielded by the removal of the encapsulated organic template (Bennett *et al.*, 1986).

The Al/P ratio of 1, characteristic for aluminophosphate molecular sieves, determines therefore the complete absence of cations in the framework as both Al and P atoms are trivalent. According to Davis (1991), the aluminophosphate lattice is the "3-5" analogue of the "4-4" pure SiO_2. Although the electrically neutral $AlPO_4$ frameworks feature no ion-exchange capacity, they possess a mildly hydrophilic surface selectivity (Rabo, 1992), lower than that of aluminosilicate zeolites. According to Malla and Komarneni (1991), the mild hydrophilicity has been attributed to the electronegativity difference between Al and P or capillary condensation and/or water bonded by coordination. Their low surface acidity explains why aluminophosphate molecular sieves have not been used as acid catalysts (Theocharis and Gelsthorpe, 1988). Saturation water pore volumes are comparable to those observed in aluminosilicate molecular sieves, as they range from 0.16 to 0.35 cm^3/g (Wilson, 1991).

Even though aluminophosphate molecular sieves are considered globally neutral, adsorbate molecules featuring permanent electric moments (known as 'specific' molecules) can interact with a local non-zero framework electric field (Grillet *et al.*, 1994). However, the stronger interactions existing in smaller-pore aluminophosphate molecular sieves have a greater effect on 'non-specific' (i.e. non-polar) molecules (CH_4) than on 'specific' molecules. As the pore size decreases, the short-range dispersive forces become more important than the long-range Coulombic forces. In micropores of size comparable to the

size of the adsorbate molecules, the micropore wall exerts an attractive force on the gas molecules which start to fill the micropore volumetrically – a phenomenon similar to capillary condensation that occurs in large pores at high partial pressures (Suzuki, 1990). The adsorbed phase in the micropores is different from the liquid phase resulting from capillary condensation because of the effect of the force field of the pore wall. Adsorption of non-polar molecules in the micropores would have a non-localized character (Grillet *et al.*, 1994).

Table 2.2 summarizes information related to $AlPO_4$-11, $AlPO_4$-17, and $AlPO_4$-18, while Figure 2.2 presents their framework topologies and pore geometries.

Table 2.2 Structural characteristics of investigated aluminophosphate molecular sieves (Szostak, 1992)

	$AlPO_4$-11	$AlPO_4$-17	$AlPO_4$-18
Chemical composition	$[Al_{20}P_{20}O_{80}]$	$[Al_{18}P_{18}O_{72}]$	$[Al_{24}P_{24}O_{96}]$
Symmetry	orthorhombic	hexagonal	monoclinic
Channel system	unidimensional	three-dimensional	three-dimensional
Ring system	10-member	8-member	8-member
Pore dimensions [Å]	3.9 x 6.3 [1]	3.6 x 5.1	3.8 x 3.8
Saturation H_2O pore volume [2] [cc/g]	0.16	0.28	0.35

[1] Meier and Olson (1992)
[2] Wilson (1991)

X-ray powder diffraction and neutron powder diffraction studies indicate that $AlPO_4$-17 is the aluminophosphate structural analogue of erionite (Wilson *et al.*, 1984), possessing two large cages (15.1 Å x 6.3 Å) per unit cell, accessible through eight-member rings. From the adsorption point of view, only the large cavities with eight-member ring openings of free aperture 3.6 x 5.1 Å in erionite are relevant. The ERI framework topology (Figure 2.2b) shows columns formed by cancrinite cages connected to adjacent columns by single six-member rings and alternately rotated by 60°, thereby

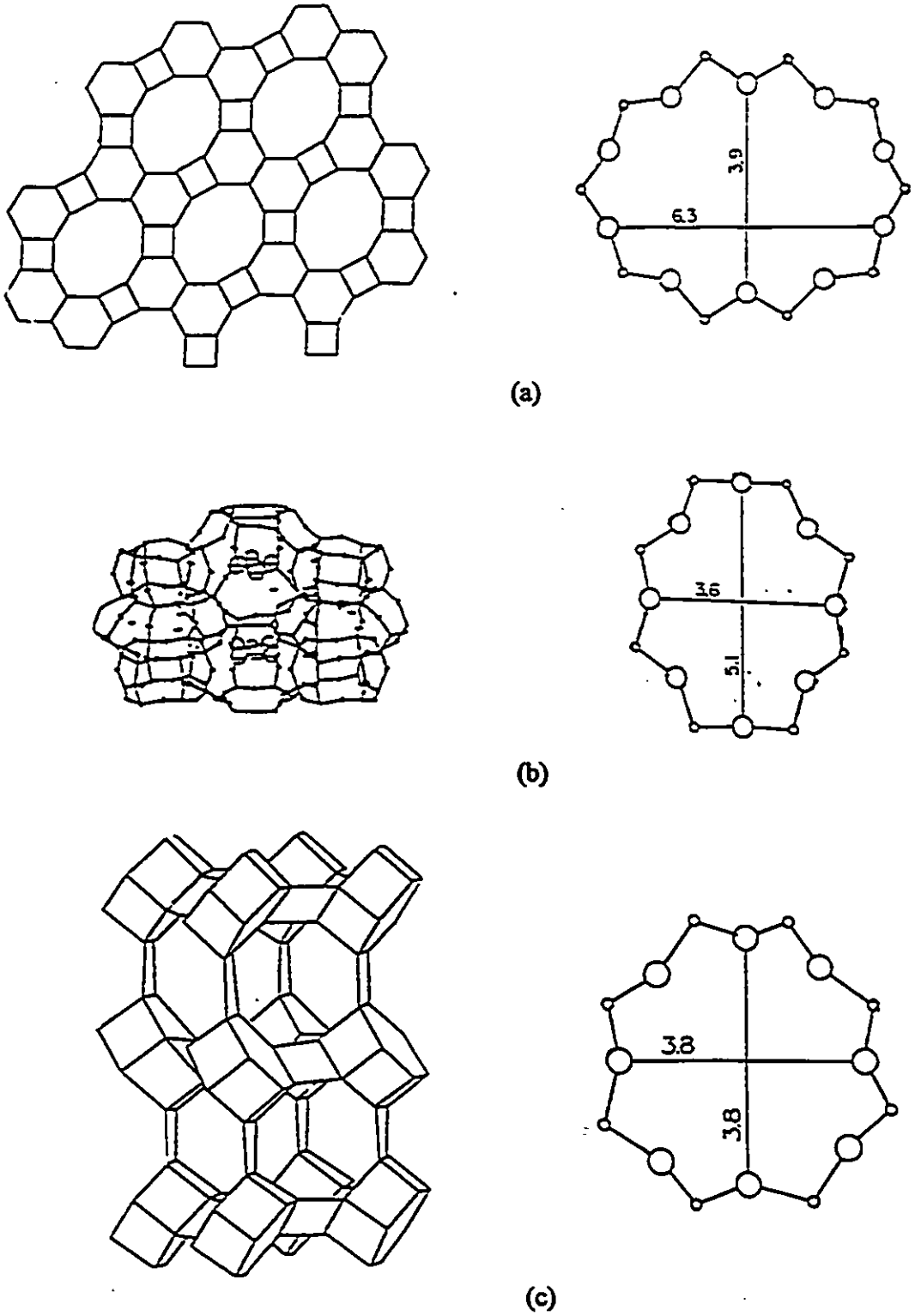

Figure 2.2 Framework topologies (Szostak, 1992) and pore geometries (Meier and Olson, 1992) in (a) $AlPO_4$-11; (b) $AlPO_4$-17; (c) $AlPO_4$-18.

placing the connecting single six-ring unit into the main channel at regular distance intervals, i.e. 15.2 Å in erionite (Szostak, 1992).

$AlPO_4$-18 features monoclinic symmetry like clinoptilolite and chabazite, but its novel structure is more closely related to the latter. The structure of $AlPO_4$-18 is presented for comparison in Figure 2.2c (Szostak, 1992). The framework structure consists of layers of tilted double six-member rings that give rise to a three-dimensional channel system and pear-shaped pores accessed through eight-member ring apertures like those in zeolite A (Simmen *et al.*, 1991). The structural difference between chabazite and $AlPO_4$-18 is the direction in which the double six-rings (D6R units) are tilted: in the same direction in chabazite, and in opposite directions from one plane of D6R units to the other in $AlPO_4$-18 (Lillerud and Akporiaye, 1994). Unlike $AlPO_4$-17 which is thermally and hydrothermally stable, $AlPO_4$-18 is thermally stable only below 600°C, and it undergoes reversible changes with hydration and dehydration.

Applications of aluminophosphate molecular sieves include the alignment of molecular sieve crystals ($AlPO_4$-5) to measure anisotropic molecular self-diffusion with a special NMR technique (Werner *et al.*, 1992). The separation of chlorinated aromatics such as chloro- and dichlorotoluenes, and dichloro- and trichlorobenzenes may be performed using $AlPO_4$-11 which separates 2,6-dichlorotoluene from its 2,4- and 2,5-isomers retained by the sieve. Very large pore $AlPO_4$-based materials are likely to be utilized as heavy-feedstock-processing catalysts (Wilson, 1991) and to enlarge the potential of molecular sieves in the separation of organic compounds. Framework substitution with Si or other elements Me (divalent metals such as Co, Mg, etc.) yields SAPO's (silicoaluminophosphate molecular sieves) or MeAPO's (metal-substituted aluminophosphate molecular sieves), generates Bronsted acidity and thus enhances their catalytic potential (Peeters *et al.*, 1992). Most $AlPO_4$-based materials (e.g. $AlPO_4$-5, $AlPO_4$-11 and $AlPO_4$-17) adsorb water readily which enhances their potential as drying materials. In addition, the separation of gaseous mixtures containing organic halides and water can be performed using aluminophosphate molecular sieve $AlPO_4$-5. Finally, they can be used in scientific studies which require appropriately sized particles and focus on transport mechanism, diffusion phenomena, and crystal structure zoning.

All the aluminophosphate molecular sieves used in the present study were synthesized for the first time by the Union Carbide Corporation (Szostak, 1992).

2.3 ADSORPTION STUDIES

A good deal of attention has been granted to the adsorptive separation of industrially relevant gases, and especially to the separation of toxic and combustible gases (such as CO and CH_4, respectively) from N_2, which is the major constituent of air, using various types of molecular sieves. Pioneering work has revealed from the very beginning that the separation of CH_4 from N_2 is more difficult than that of CO from either N_2 or CH_4.

2.3.1 Adsorption in Zeolite 5A

Tezel and Apolonatos (1993) studied chromatographically the adsorption kinetics and equilibrium of N_2, CH_4, and CO in zeolite 5A as well as the separation potential of zeolite 5A for N_2-CO, N_2-CH_4, and CH_4-CO gas mixtures at 101.3 kPa total pressure and room temperature as well as 40°C, concluding on the basis of adsorption equilibrium selectivities that the 5A sieve is a promising adsorbent only for the separation of CO-N_2 and CO-CH_4 mixtures at these temperatures. Their investigation showed that for the separation of CO from N_2 using zeolite 5A the adsorption temperature does not exert a strong influence on the dynamic adsorption capacity, but does affect the values of the kinetic separation factors, with faster kinetics at higher temperatures. They also found that the equilibrium separation factors for CH_4-N_2 gas mixtures, although too low to allow separation, were higher at 40°C.

Ruthven (1976) investigated the adsorption of pure N_2 at various temperatures ranging from 145 to 273 K, the adsorption of pure CH_4 at temperatures ranging from 195 to 253 K, and the adsorption of pure CO at 145 K (with adsorbate equilibrium pressure values below 1000 torr in each case). He predicted the behaviour of the N_2-CO mixture in the presence of zeolite 5A using the statistical thermodynamic model which was found to be accurate only in the case of zeolitic systems (Yang, 1987). Ruthven (1976) also used

data on adsorption systems involving N_2 and CH_4 to develop a model applicable to zeolites of type A, and predicted that mixtures of two sorbates with equal molecular volumes should display approximately ideal solution behaviour in the adsorbed phase.

Danner and Wenzel (1969) determined the single-component adsorption isotherms of N_2 and CO at -200°F (144.26 K) and investigated the adsorption of N_2-CO mixtures in zeolite 5A at -200°F and 1 atm total pressure. According to these authors, zeolite 5A possesses surface selectivity, and therefore, the separation of binary gas mixtures involving species of relatively similar diameter is not related to the molecular sieving effect. The predictive capability of the Ideal Adsorbed Solution Theory (IAST) developed by Myers and Prausnitz (1965) was also investigated, and proved to yield relatively poor fits for the N_2-CO/5A adsorption systems under those operating conditions.

Lederman (1966) determined single-component adsorption isotherms of N_2 and CH_4 in zeolite 5A, as well as binary equilibrium information concerning the adsorption of their mixtures in this sieve at 195 and 295 K for superatmospheric pressures ranging from 3 to 100 atm, which were not maintained constant. However, according to Ruthven (1976), for this binary gas mixture in which the molecular volumes of the components are essentially the same, the X-Y diagram is expected to depend only upon the ratio of the Henry constants for the two components and to be independent of the total pressure. In this case the adsorbed phase is therefore expected to behave ideally. It is possible that the effective molecular volume feature a slight dependence of pressure (what Ruthven or Lederman considers a simple compressibility effect) which may be pronounced at the higher temperature because of the correspondingly higher pressure range.

Shah and Ruthven (1977) determined equilibrium isotherms for the adsorption of CH_4 in zeolite 5A using the chromatographic method, and found that the diffusion of CH_4 in zeolite 5A is extremely rapid, an observation made earlier by Oberholtzer and Rogers (1969). Ruthven and Derrah (1975) studied the diffusion of N_2 and other diatomic and monatomic gases in zeolite 5A, reporting an inverse dependence of diffusivity on concentration in Henry's law region, attributing the observed behaviour to a collisional transport mechanism. They also concluded that the diffusion of light hydrocarbons in zeolite 5A is essentially independent of concentration, and that the kinetics of sorption of

N_2 are controlled in both the crystal and the pellet by the intracrystalline diffusion rather than by the macropore diffusion.

Haq and Ruthven (1986) investigated the sorption and diffusion of N_2 and CH_4 in commercial 5A zeolite using the chromatographic method, which did not allow a reliable evaluation of the intracrystalline diffusivities due to the rapidity of intracrystalline diffusion of these two small molecules.

Ruthven *et al.* (1973) measured zeolitic diffusivities of CH_4 in zeolite 5A over small differential concentration steps, and concluded that intracrystalline diffusivities show a pronounced increase with sorbate concentration – an effect attributed to the nonlinearity of the isotherms – and that the intrinsic mobilities are essentially independent of concentration. Ruthven and Derrah (1972) applied the transition state theory of zeolitic transport in order to interpret experimental diffusivity data on the molecular scale.

Yeh and Yang (1989) reported equilibrium adsorption and diffusivity data on systems involving CH_4 and zeolite 5A containing mixed Na^+ and K^+ cations which are representative of porous structures with blocked pores and covered adsorption/reaction sites.

Sievers and Mersmann (1994) determined experimentally the single-component isotherms of N_2, CH_4, and CO in zeolite 5A at 303, 323, 343, and 363 K at high pressures (10^{-4} to 10 MPa), as well as the corresponding binary mixture adsorption equilibria at 303 and 323 K, at 0.1, 0.6, and 3.0 MPa total pressure. In addition, they obtained satisfactory predictions of the binary equilibria using the Ideal Adsorbed Solution Theory based on the temperature-dependent Toth equation with five parameters.

2.3.2 Adsorption in Clinoptilolite

The structural/adsorption/diffusion characteristics of clinoptilolite are difficult to associate due to the mixture of cations present in this natural zeolite (Ackley and Yang, 1991b).

A chromatographic study of the adsorption of N_2 and CO in calcium-rich Turkish clinoptilolite was conducted by Triebe and Tezel (1995), concluding that the

presence of divalent cations in clinoptilolite yields promising equilibrium separation factors for N_2-CO mixtures at 1 atm and in the 323-473 K temperature range, and that micropore diffusion is the dominant mass transfer mechanism for both adsorbates. They also found that the kinetic selectivity of Turkish clinoptilolite would favor the adsorption of N_2 but its equilibrium selectivity would favor the adsorption of CO from the binary mixture with N_2. The chromatographic method was also used to investigate the adsorptive behaviour of CH_4 in the presence of Turkish clinoptilolite (Triebe *et al.*, 1995).

Frankiewicz and Donnelly (1983) investigated the potential of clinoptilolite for the difficult separation of N_2-CH_4 mixtures by selective adsorption of N_2 to determine the optimum process conditions, and concluded that at ambient temperature the kinetic selectivity favors the adsorption of N_2 and that only clinoptilolites with the appropriate cation content can efficiently take advantage of the kinetic selectivity for separation purposes. They showed that calcium-impregnated clinoptilolite features a superior ability to separate CH_4-N_2 mixtures both because of molecular sieving of CH_4 and because of the stronger electrostatic interactions between the quadrupole moment of N_2 molecules and the Ca^{2+} cations.

Ackley and Yang (1991b) have used cation manipulation in clinoptilolite to produce selectivity values higher than 1 for the reputably difficult adsorptive separation of the N_2-CH_4 mixture, and concluded that tailoring zeolites through ion exchange in order to perform certain gas separations depends on the relationship between the zeolite structure and the gas adsorption/diffusion characteristics. The adsorption isotherms of N_2 and CH_4 they determined at 300 and 323 K confirmed the molecular sieving effect exerted on the non-polar CH_4 molecules by the fully-exchanged Na^+ and Ca^{2+} forms of the zeolite, and the energetic heterogeneity exhibited by the Ca^{2+} form in the presence of the weakly polar N_2. Internal electrostatic fields present in the pore space of clinoptilolite strongly influence adsorption of gas molecules such as N_2 and CH_4 in the microporous channels, since the dimensions of these channels are not much larger than the adsorbate molecules diffusing through them. The framework ions (the charge-balancing cations) and the adsorbate molecules contribute to these internal fields in an interdependent fashion.

2.3.3 Adsorption in Aluminophosphate Molecular Sieves

Aluminophosphate materials being very recent additions to the molecular sieve scene, most of the research undertaken so far has been focused on synthesis and characterization issues. The work performed in the area of adsorption has involved only a few adsorbates such as water, oxygen, *i*-butane (for all three aluminophosphate molecular sieves investigated) as well as *n*-butane (for $AlPO_4$-11 and $AlPO_4$-18), neopentane (for $AlPO_4$-11 and $AlPO_4$-17), *n*-hexane (for $AlPO_4$-17), and cyclohexane (for $AlPO_4$-11) (Szostak, 1992). It is known that aluminophosphate molecular sieves exhibit Type I isotherms with N_2 and other nonpolar adsorbates (Malla and Komarneni, 1991). Adsorption isotherms of type I are, as described by Grillet *et al.* (1994), the result of "adsorbate confinement" due to the overlap of potential fields from neighbouring walls in close proximity (small-diameter micropores).

Type I adsorption isotherms for N_2, CO, and CH_4 at different cryogenic temperatures were determined in $AlPO_4$-11 by Reichert *et al.* (1994) within a study focusing on the influence of aluminophosphate structures with unidimensional channels of different diameters. They showed that the isosteric heat of sorption is correlated with the pore size, and that the 10-member ring $AlPO_4$-11 behaved like an 8-member ring because of its elliptical channels (3.9 x 6.3 Å) with a small diameter identical to the diameter 8-member rings in aluminophosphate molecular sieves such as $AlPO_4$-39. In addition, Reichert *et al.* (1994) observed in the variation of the heats of sorption with the relative amount adsorbed two energy plateaux in the case of quadrupolar N_2 and the polar CO; the step in the energy curve occurred exactly at the point corresponding to the half filling of the pores where more than one molecule has to share the elliptical channel of the AEL framework structure. A similar graph plotted for the non-polar CH_4 did not feature these two plateaux, which led to the conclusion that specific interactions of the quadrupolar N_2 and the polar CO in $AlPO_4$-11 would be responsible for the presence of the step in the isosteric heat curves. The values of the isosteric heat of sorption of N_2, CO, and CH_4 determined experimentally on $AlPO_4$-11 through isothermal microcalorimetry at the

temperature of liquid nitrogen were 18.0 / 14.1 kJ/mol for N_2 (two energy plateaux), 19.3 / 15.0 kJ/mol for CO (two energy plateaux), and 18.2 kJ/mol for CH_4, respectively.

Grillet *et al.* (1994) have found by measuring the initial net differential enthalpies of adsorption that there is little difference between the adsorption behaviour of N_2 (quadrupole moment) and that of CO (dipole moment) in systems involving aluminophosphate molecular sieves like $AlPO_4$-11, despite the larger electric moment of CO. It appears that molecular sieves with smaller pores enhance the adsorptive properties of an adsorbate molecule featuring a smaller electric moment and a smaller kinetic diameter. A smaller molecule like N_2 (kinetic diameter 3.64 Å) is more likely to be adsorbed than a CO molecule, even though it may possess only a quadrupole moment, because its lower kinetic diameter permits access to the surface of the adsorbent within a smaller distance, and thus the intensity of electrostatic interactions between the electric moment of the molecule and the local non-zero framework electric field increases. The larger kinetic diameter of CO impedes the interaction of its dipole moment with the local electric field because the molecule cannot approach the adsorbent surface from too close a distance and the electrostatic interactions are thereby reduced to about the magnitude of those between quadrupolar N_2 molecules and the same local electric field.

The adsorption studies published to date provide some insight on the potential behavior of polar and non-polar adsorbates, with hydrocarbons such as CH_4 at the lower end of the polarity scale and water at the other end. A parallel could therefore be drawn for the set of adsorbates investigated in this work, i.e. CH_4, N_2, and CO, in which CH_4 would represent the lower end of a smaller range on the polarity scale (zero polarity), and CO would represent the category of polar adsorbates (dipole moment 0.1 Debye), being expected to behave similarly to water which is considered one of the most polar chemical species (the dipole moment of the H_2O molecule is 1.84 Debye).

Malla and Komarneni (1991) have investigated the water sorption properties of $AlPO_4$-11 and $AlPO_4$-17, obtaining unusual isotherm shapes with little or no initial adsorption followed by steep upward adsorption leading to volume filling by hydrogen bonding and cooperative interaction in micropores. Martens and Jacobs (1994) maintain that all aluminophosphate molecular sieves exhibit hysteresis extending to very low

pressures, and explain the water sorption behaviour of all $AlPO_4$'s by chemisorption in specific framework aluminum sites that are transformed in aluminum dihydrate sites.

Aluminophosphate molecular sieves like the ten-member ring $AlPO_4$-11 (whose micropore system is unidimensional and tubular) feature permanent dipoles oriented according to the channel direction (Martens and Jacobs, 1994); because of the lower electronegativity of the Al atom with respect to the P atoms, each pair of adjacent Al-P atoms represents a permanent dipole.

The polar properties are less pronounced in the eight-member ring aluminophosphate molecular sieves $AlPO_4$-17 and $AlPO_4$-18, because of their three-dimensional channel system which does not allow for the representation of framework as stacked 2-D nets alternately linked by Al and P atoms.

2.4 THEORY

Theories attempting to mathematically describe the phenomena occurring during physical adsorption processes can be basically viewed as belonging to two categories: theories which ignore the interactions between the adsorbate molecules in the adsorbed phase (such as the Langmuir model), and theories which account not only for such interactions but also for interactions with the adsorbent (such as the Vacancy Solution Theory).

2.4.1 Modelling of Single-Component Adsorption Equilibria

Given an adsorption system consisting of a gas and a solid, the amount adsorbed at equilibrium is given by a mathematical expression relating the volume of gas adsorbed to the temperature and the pressure. At constant temperature this mathematical expression yields equations for adsorption isotherms.

2.4.1.1 The Langmuir Isotherm

Accorging to Yang (1987), the Langmuir isotherm remains the most useful for data correlation in separation processes based on physical and chemical adsorption. Although derived for the ideal case of localized adsorption on a uniform surface without lateral interaction, this isotherm fits experimental data for a surprisingly large number of systems. Graham (1959) attributes this performance to the fact that large adsorbate molecules tend to average out the effects of heterogeneity on an atomic scale.

The Langmuir approach assumes that the adsorption system is in dynamic equilibrium and is based upon the assumptions that molecules or atoms may adsorb only on a fixed number of well-defined, localized sites which can hold one and only one molecule or atom with no interaction between molecules or atoms adsorbed on neighboring sites, and that the energy of adsorption is constant over all sites. The equation for the Langmuir isotherm (Langmuir, 1918) results from the equality between the rate of adsorption and the rate of desorption at dynamic equilibrium and expresses the relationship between the equilibrium pressure P in the gas phase and the fractional coverage of the surface of the adsorbent, θ:

$$\theta = \frac{v}{v_m} = \frac{BP}{1+BP} \tag{2.2}$$

As P --> 0, the Langmuir isotherm reduces to Henry's law form, $\theta = BP$ and the value of Henry's law constant becomes equal to Bv_m. At infinite pressure, the fractional coverage is equal to 1. The two Langmuir parameters, Langmuir's adsorption constant B and the monolayer volume, v_m, are determined through linear regression of a plot of P/v vs. P obtained by rearranging equation (2.2):

$$\frac{P}{v} = \frac{1}{Bv_m} + \frac{P}{v_m} \tag{2.3}$$

The variation of heats of sorption, a direct consequence of energetic heterogeneity as described by Barrer (1978), is indicative of the strength of the bond

between the guest molecule and the host crystal and of the applicability of the Langmuir model to the prediction of pure-gas adsorption isotherms.

2.4.1.2 The Freundlich Isotherm

The Langmuir approach provides for physical adsorption on nonuniform surfaces through an empirical equation obtained by Zeldowitsh (1935) who assumed an exponentially decaying function of site density with respect to the heat of adsorption:

$$v = kP^{1/n} \tag{2.4}$$

According to this isotherm, the amount adsorbed will increase indefinitely with pressure. At low coverage, the Freundlich isotherm assumes the existence of adsorption sites with very high heat of adsorption. As is the case with all empirical equations, the parameters have no significant meaning and therefore do not allow extrapolation beyond the range of operating conditions under which they have been determined (Suzuki, 1990).

2.4.1.3 The Flory-Huggins Vacancy Solution Theory

The Vacancy Solution Theory is based on the assumption that each of the two phases involved in any adsorptive separation process (the gas phase and the adsorbed phase) are binary solutions of adsorbate and vacancy, featuring different compositions at equilibrium. As defined by Cochran *et al.* (1985a), the vacancy is an imaginary entity used to quantify the vacuum space which acts as a solvent for the system.

The predictive abilities of the Flory-Huggins three-parameter form of the Vacancy Solution Theory have been proven superior to those of the Wilson four-parameter form (Cochran *et al.*, 1985b) despite the lower number of parameters involved. The complexity of the equations of the Wilson form of the Vacancy Solution Theory also makes it more difficult to obtain physically significant parameters from the regression of limited isothermal data sets. The fact that the number of isothermal data sets available was limited, contributed to the selection of the three-parameter form of the

Flory-Huggins Vacancy Solution Theory against the five-parameter form, which permits the correlation of the pure-gas data over a range of temperatures and therefore includes the effect of temperature (Cochran *et al.*, 1985a).

Cochran *et al.* (1985a) obtained the expression of the adsorption isotherm equation from an equation of state for the adsorbed phase, derived by equating the chemical potentials of the gas and adsorbed phases, and from the Gibbs adsorption equation. Thus, the adsorption isotherm is expressed as a function relating the equilibrium pressure in the gas phase to the fractional coverage of the surface of the molecular sieve upon adsorption:

$$P = \frac{n_1^{\infty}}{b_1}\frac{\theta}{1-\theta}\exp\frac{\alpha_{1v}^2\theta}{1+\alpha_{1v}\theta} \qquad (2.5)$$

where $\theta = \frac{n_1}{n_1^{\infty}}$ represents the fractional coverage of the surface of the molecular sieve.

The three regression parameters are the limiting amount of adsorption n_1^{∞}, Henry's law constant b_1, and the gas-solid (adsorbate-vacancy) interaction parameter α_{1v}. The Flory-Huggins VST isotherm equation reduces to the Langmuir equation for $\alpha_{1v} = 0$, that is, the adsorbed phase is considered ideal as there are no interactions between the adsorbate molecules and the vacancy in this phase. The value of Henry's law constant in the Langmuir equation is determined at very low pressure, i.e. in the limit of P –> 0 (when $\theta << 1$), and is equal to Bv_m. Rewriting equation (2.5) by substituting the Langmuir parameter v_m for n_1^{∞} and the product of the Langmuir parameters, Bv_m, for b_1 leads to the expression of the Langmuir equation.

As the model is most sensitive to the value of Henry's law constant, b_1, the ability to obtain experimental data points at low pressures has proven extremely beneficial from the modelling point of view. The accurate prediction of Henry's law constant (the most important parameter as far as multicomponent equilibria prediction using the Vacancy Solution Theory is concerned) is crucial not only for the modelling of pure gas adsorption isotherms, but also for the evaluation of binary isotherms from pure component adsorption data, considering the difficulty associated with the collection of binary adsorption experimental data.

2.4.2 Modelling of Binary Gas Mixture Adsorption Equilibria

The most important information required to describe binary gas mixture adsorption equilibria are phase diagrams, considered a precious tool in the selection of optimal adsorbents, and binary isotherms, which provide first-hand information on the capacity of a certain adsorbent for various adsorbates.

Displacement and competition are the predominant phenomena encountered in multicomponent adsorption systems, in which the components compete for the limited number of adsorption sites available on the surface of the adsorbent, and the capacity of the adsorbent for one component of the mixture is restricted by the presence of the other component(s) (Noll *et al.*, 1992). The strongly adsorbed species usually occupies a larger portion of adsorbent surface than the weakly adsorbed species and consequently the capacity of the adsorbent for the latter in the mixture decreases more considerably than it does for the strongly adsorbed species. The displacement phenomenon becomes more significant when the adsorbates in the mixture feature different adsorptive characteristics.

2.4.2.1 The Extended Langmuir Model (ELM)

The Extended Langmuir Model (ELM) for multicomponent gas mixture adsorption is based on the same assumptions used for the Langmuir single-component isotherm. For a binary mixture adsorption system the partial pressures of the components in the gas phase, P_1 and P_2, are in equilibrium with fractional coverages θ_1 and θ_2 on the adsorbent surface, and the Extended Langmuir Model equation results from the equality of the rate of adsorption and the rate of desorption at dynamic equilibrium (Markham and Benton, 1931). Thus, the fractional coverage for species 1 in the binary mixture is:

$$\theta_1 = \frac{v_1}{v_{m1}} = \frac{B_1 P_1}{1 + B_1 P_1 + B_2 P_2} \qquad (2.6)$$

Similarly, the fractional coverage for species *i* in an *n*-component mixture is:

$$\theta_i = \frac{B_i P_i}{1 + \Sigma B_j P_j} \tag{2.7}$$

If each species in the mixed adsorbed phase maintains its own molecular area (the area covered by one molecule that is not influenced, as in single-component adsorption, by the presence of other molecules on the surface), then the amount of species *i* adsorbed from the mixture is:

$$v_i = \frac{v_{mi} B_i P_i}{1 + \Sigma B_j P_j} \tag{2.8}$$

where v_{mi} is the monolayer amount for *i* obtained through linear regression from the single-component adsorption data. In this study, equation (2.8) has been viewed as a direct-approach Extended Langmuir Model and has been labeled d-ELM.

According to Broughton (1948), equation (2.8) can hold only for limited ranges of mixture compositions or, for the entire range of mixture compositions provide there is no mutual displacement between the adsorbed species ($B_1P_1 << 1$ and $B_2P_2 << 1$), i.e. $v_{m1} = v_{m2}$. The thermodynamic consistency condition introduced by Broughton (1948) requires that the monolayer adsorption capacities be equal for all the species in the mixture, i.e. $v_{M1} = v_{M2}$. In other words, the areas occupied by each molecular species on the surface of the adsorbent must be independent of the areas occupied by the other species.

Kemball *et al.* (1948) acknowledged considerable interaction between adsorbed molecules from the reduction in the area available for the adsorption of each species when binary mixture adsorption occurs, compared to the area available for adsorption during single-component adsorption. To account for the interactions present in the adsorbed phase for binary mixtures, Innes and Rowley (1947) calculated an averaged monolayer volume, $v_M = v_{M1} = v_{M2}$, from the pure-component monolayer volumes (v_{m1}, v_{m2}) and the mole fractions in the adsorbed phase (x_1, x_2):

$$\frac{1}{v_{M1}} = \frac{x_1}{v_{m1}} + \frac{x_2}{v_{m2}} = \frac{1}{v_{M2}} = \frac{1}{v_M} \tag{2.9}$$

When this averaged monolayer volume is utilized, equation (2.8) becomes:

$$v_i = \frac{v_{Mi} B_i P_i}{1 + \Sigma B_j P_j} \tag{2.10}$$

Equation (2.10), viewed in this study as the averaging-approach Extended Langmuir Model and accordingly labeled a-ELM, has been the major model used in adsorber design involving dynamics for multicomponent adsorption (Yang, 1987). However, according to Innes and Rowley (1947), for an agreement between the experimental results and the averaging-approach equation (2.10), the amount adsorbed is determined as a function of the mole fraction of the adsorbate only when the overall fractional coverage approaches 1, i.e. upon the saturation of the surface of the adsorbent. Innes *et al.* (1951) resort to the averaging approach equation only after assuming that when the surface of the adsorbent is completely covered the areas occupied by one species are not affected by the areas occupied by the other species.

Both equations (2.8) and (2.10) lead to the conclusion that the ELM separation factor for a binary mixture is constant (and equal to the ratio of the temperature-dependent Langmuir constants, in the case of a-ELM). This is the reason why the Extended Langmuir Model is known as the "constant-selectivity" model (Ruthven, 1984):

$$\alpha_{12} = \frac{(x_1/x_2)}{(y_1/y_2)} = \frac{B_1}{B_2} \tag{2.11}$$

2.4.2.2 The Ideal Adsorbed Solution Theory (IAST)

According to the Ideal Adsorbed Solution Theory (IAST) which was developed by Myers and Prausnitz (1965) as an adsorption analog of Raoult's law for vapour-liquid equlibria, there are no interactions between adsorbate molecules in a binary mixture and equilibrium is attained at constant temperature when the spreading pressures of the components in the mixture are equal. The physical meaning of spreading pressure is analogous to that of a monomolecular film at the gas-liquid interface (Yang, 1987). The spreading pressure is given by the area under the single-component isotherm, which means

therefore that for a weakly adsorbed component extrapolation of the isotherm is necessary in order to satisfy the equilibrium condition. With adequate Langmuir fits for the experimental pure gas adsorption isotherms, analytical integration of the Langmuir isotherm equations allows the determination of the spreading pressures of the components, hence the prediction of the phase diagrams and binary isotherms of mixture adsorption systems. Therefore, the expression allowing the calculation of spreading pressure when the Langmuir fits are acceptable is:

$$\frac{\pi_i A}{RT} = \int_0^{P_i^o} \frac{\nu_i}{P} dP = \nu_{mi} \ln(1 + B_i P_i^o) \qquad (2.12)$$

The equality of the spreading pressures for the two components of a binary mixture is then used in conjunction with "Raoult's law" applied for each pure component to determine the equilibrium saturation pressure at the temperature and pressure of the mixture, i.e. $y_i P = x_i P_i^o$, to obtain the relationship between the mole fraction in the gas phase y_i and the mole fraction in the adsorbed phase x_i which will generate the equilibrium XY diagram:

$$\nu_{m1} \ln(1 + \frac{B_1 y_1 P}{x_1}) = \nu_{m2} \ln(1 + \frac{B_2 y_2 P}{x_2}) \qquad (2.13)$$

The x_i values calculated with equation (2.13) permit the calculation of the total amount of mixture adsorbed, and the amount of each species adsorbed from the mixture:

$$n_i^0 = \frac{n_{mi}^0 B_i P_i^0}{1 + \sum B_j P_j^0} \quad (2.14); \qquad \frac{1}{n_t} = \sum \frac{x_i}{n_i^0} \quad (2.15); \qquad n_i = x_i n_t \quad (2.16)$$

The Ideal Adsorbed Solution Theory is considered more reliable than the Extended Langmuir Model (Suzuki, 1990), but may not be accurate, however, when a binary mixture forms an azeotrope since the assumption of ideal adsorbed solution is not likely to apply. Valenzuela and Myers (1989) maintain that IAST predictions are accurate when the amount adsorbed is less than half the saturation capacity of the adsorbent.

At the same time, if the pure-gas adsorption isotherms on the basis of which the IAST predictions are determined are measured for pressure ranges below 101.3 kPa and

At the same time, if the pure-gas adsorption isotherms on the basis of which the IAST predictions are determined are measured for pressure ranges below 101.3 kPa and the difference in polarity of the gaseous species is not too large, then the predictions are very likely to be accurate since at those pressures the assumption of ideal behaviour can be considered valid (Valenzuela and Myers, 1989). IAST predictions could also be sensitive to the choice of method used in determining the spreading pressure of each component (the area under the corresponding experimental isotherm). If the experimental isotherm fits are not satisfactory but the isotherms are favourable, analytical integration of the isotherm should be abandoned in favour of a graphical integration using Simpson's rule. IAST cannot be used, however, for adsorption systems whose components feature unfavourable pure-gas equilibrium isotherms accurately correlated by the Freundlich equation.

2.4.2.3 The Flory-Huggins Vacancy Solution Theory for Mixtures (FH-VST)

The Flory-Huggins Vacancy Solution Theory is acknowledged to be able to predict highly nonideal equilibria such as adsorption azeotropes (Cochran *et al.*, 1985a). The Vacancy Solution Theory treats gas-mixture adsorption as an equilibrium between two vacancy solutions of different compositions. The components of these solutions (adsorbate and vacancy) are characterized by individual activity coefficients with a Flory-Huggins or Wilson type of expression to account for the departure from ideal behavior of the adsorbed phase, and the presence of these components in each phase is quantified by mole fractions specific for each phase. The activity coefficients actually describe the composition dependence of the nonideal solute-solvent (vacancy) interactions during pure and multicomponent adsorption, and solute-solute interactions during multicomponent adsorption. The extent of the departure from unity of the values of the activity coefficients reflect therefore the intensity of the adsorbent-adsorbate and adsorbate-adsorbate interactions in the adsorbed phase. The vacancy in the adsorbed phase is described by its own activity coefficient, γ_v, which is a function of the composition of the adsorbed vacancy solution.

The Vacancy Solution Theory applied to binary mixtures introduces expressions for activity coefficients for both adsorbates and the vacancy (γ_1, γ_2, and γ_v). In addition, it provides various relationships allowing the calculation of the molar fractions of adsorbates and vacancy in the adsorbed phase (x_1^s, x_2^s, and x_v^s), the individual amounts of pure gases adsorbed from the mixture (n_1 and n_2), as well as the capacity of the adsorbent for the binary mixture (n_m), thereby yielding the data necessary to plot binary isotherms. The activity coefficient in the adsorbed phase, γ_v, is a function of the composition of the adsorbed vacancy solution (x_1^s, x_2^s, and x_v^s). A system of equations is solved iteratively to provide values for the mole fractions of the adsorbates in the gas phase (Y_1 and Y_2), the mole fractions of the adsorbates and the vacancy in the adsorbed phase (x_1^s, x_2^s, and x_v^s), the experimental mole fractions in the adsorbed phase (X_1 and X_2), the total limiting amount of adsorption (n_m^∞), the activity coefficients for the adsorbates and the vacancy (γ_1, γ_2, and γ_v), as well as the capacity of the adsorbent for the mixture and the amounts of individual components adsorbed (n_m, n_1, and n_2). The procedure is described in detail by Cochran *et al.* (1985a). The system of equations was solved by setting the fugacity coefficients of the components equal to 1 (assumption valid at low pressures), and by selecting the composition of the adsorbed phase (X_1) and the total pressure (101.3 kPa).

CHAPTER 3

EXPERIMENTAL

3.1 APPARATUS

The volumetric adsorption apparatus used to determine the pure-component adsorption isotherms was the Accusorb 2100E Physical Adsorption Analyzer, provided by the Micromeritics Instrument Corporation of Atlanta, Georgia. The schematic diagram is shown in Figure 3.1. Due to the pressure limitations imposed by the pressure transducers (5-8 psig), isotherms could be determined only for pressure ranges up to 1000 torr (133.3 kPa). The two pressure transducers, one for the low-pressure range (0-40 torr, i.e. 0-5.33 kPa) and the other for the higher pressure range (0-1000 torr, i.e. 133.3 kPa), calibrated by the manufacturer, provided the pressure readings. The volumes and the temperatures corresponding to the distributing manifold and interconnecting tubing within the apparatus were provided by the manufacturer (Appendix A). The sample flask was introduced in a jacket during the runs at room temperature and 40°C, with electric heating provided only for the higher temperature runs. A thermocouple was used to monitor the temperature around the sample flask.

3.2 MATERIALS

The adsorbents investigated were clinoptilolite from Cuba (25 x 42) mesh, and two aluminophosphate molecular sieves in powder form, $AlPO_4$-17 and $AlPO_4$-18,

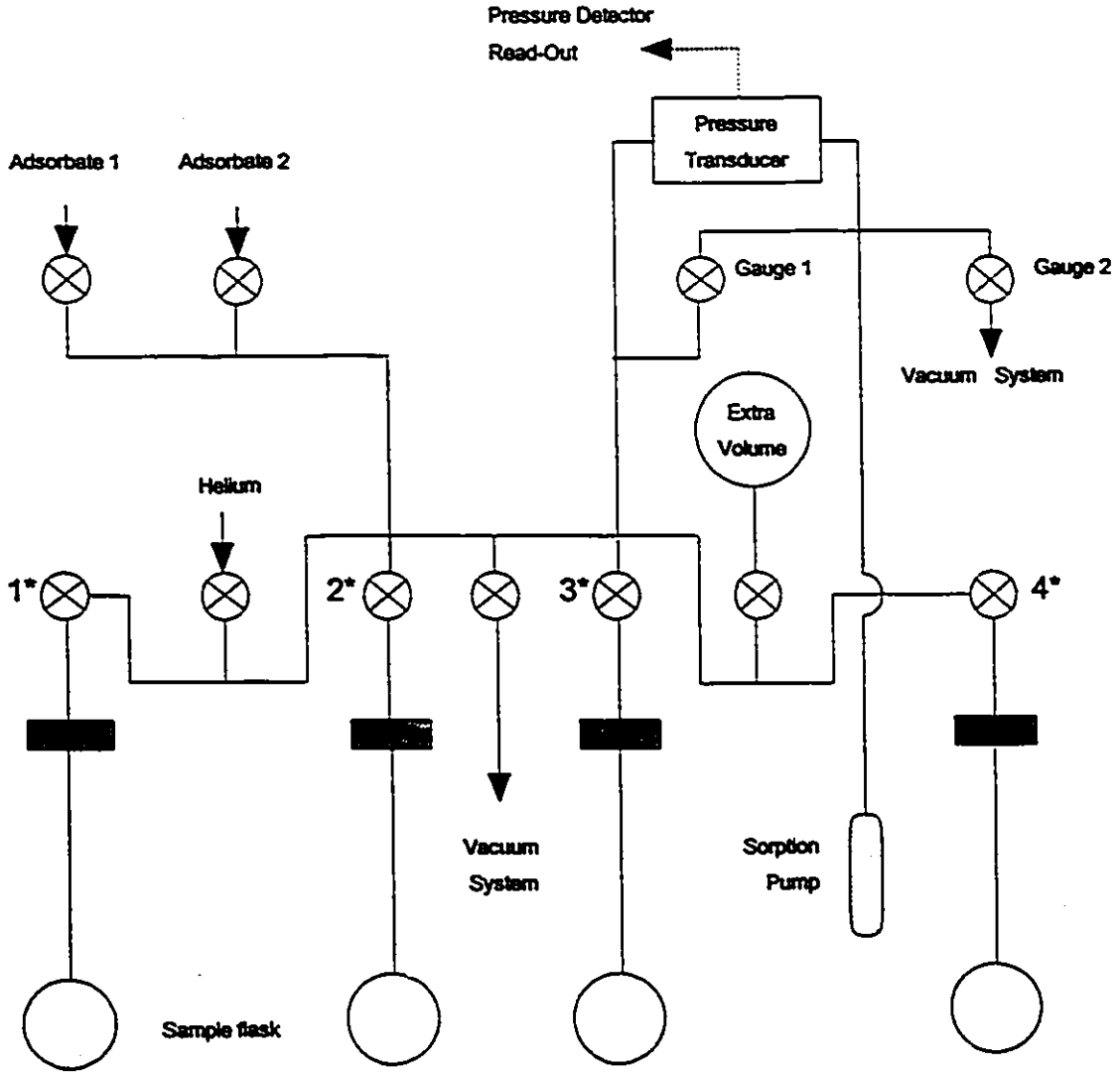

Figure 3.1 Diagram of Micromeritics Accusorb 2100E volumetric apparatus used in pure-component experimental data collection.

synthesized and kindly supplied by Dr. Serge Kaliaguine of Laval University, Ste-Foy, Quebec, Canada.

The gases used were nitrogen (min. 99.99%) and methane (99.99%) from Air Products, as well as carbon monoxide and helium (99.995%) from Matheson. Table 3.1 presents several characteristics of these gases. Liquid nitrogen was necessary to maintain the sorption pump of the volumetric apparatus at a low temperature in order to ensure that all impurities are adsorbed on the reference side of the pressure transducer.

Table 3.1 Synopsis of relevant physical characteristics of the adsorbates investigated.

	N_2	CH_4	CO
Molecular configuration	linear	tetrahedral	linear
Pauling molecular dimensions[1] [Å]	3.0 x 4.1	4.2	3.7 x 4.2
Kinetic diameter[1] [Å]	3.64	3.8	3.76
Formula weight	28	16	28
Normal boiling point [°C]	-195.8	-161.4	-192
Quadrupole moment[2] [x 10^{40} Cm^2]	-5.0	—	-12.3
Dipole moment[2] [x 10^{30} Cm]	—	—	0.39
Polarizability [x 10^{24} cm^3]	1.74	2.593	1.844

[1] Breck (1974)
[2] Grillet *et al.* (1994)

3.3 PROCEDURE

Prior to each run, approximately one gram of adsorbent was regenerated by heating it in the sample glass flask at 623 K under vacuum (< 10 Pa) for a period of minimum 11 hours. After cooling the sample flask to the run temperature and checking the outgassing rate, the dead-space volume around the sample was determined using helium, assumed to be adsorbed in negligible quantities at the run temperatures and capable of entering the void volume present in the zeolite crystals because of its small molecular size. After the completion of the dead-space evaluation, the helium was evacuated and the experiment was initiated by admitting adsorbate in the manifold and

recording the pressure, and then releasing the adsorbate into the sample flask and recording the subsequent equilibrium pressure. Depending on the nature of the adsorbent and the adsorbate, phase equilibrium was attained in periods ranging from one hour to 6 weeks for one datapoint on the isotherm. At the end of each equilibration period, the valve isolating the sample from the manifold was closed to allow admission of an additional quantity of gas in stepwise fashion until the maximum pressure allowed by the pressure transducers in the apparatus (1000 torr) was attained. The amount adsorbed at each step was determined from PVT measurements applied in a material balance analysis.

Isotherms were determined for the adsorption of N_2, CH_4, and CO in Cuban clinoptilolite, $AlPO_4$-17, and $AlPO_4$-18 at only one temperature, i.e. 40°C. Time limitations did not permit measurement of the adsorption capacity at room temperature: equilibration periods were expected to be even longer than those necessary at 40°C, considering the expected decrease in diffusivity of the adsorbate.

The measurement of the CH_4 adsorption isotherm in $AlPO_4$-18 at 40°C was repeated (Figure 3.2), the standard deviation being ±0.0986 cc STP/g (= ±0.0044 mol/kg). The experimental error associated with this measurement was found to be less than 7%, and could be attributed to the difference in the regeneration procedure (a longer regeneration period leading to a much "cleaner" surface in the second run).

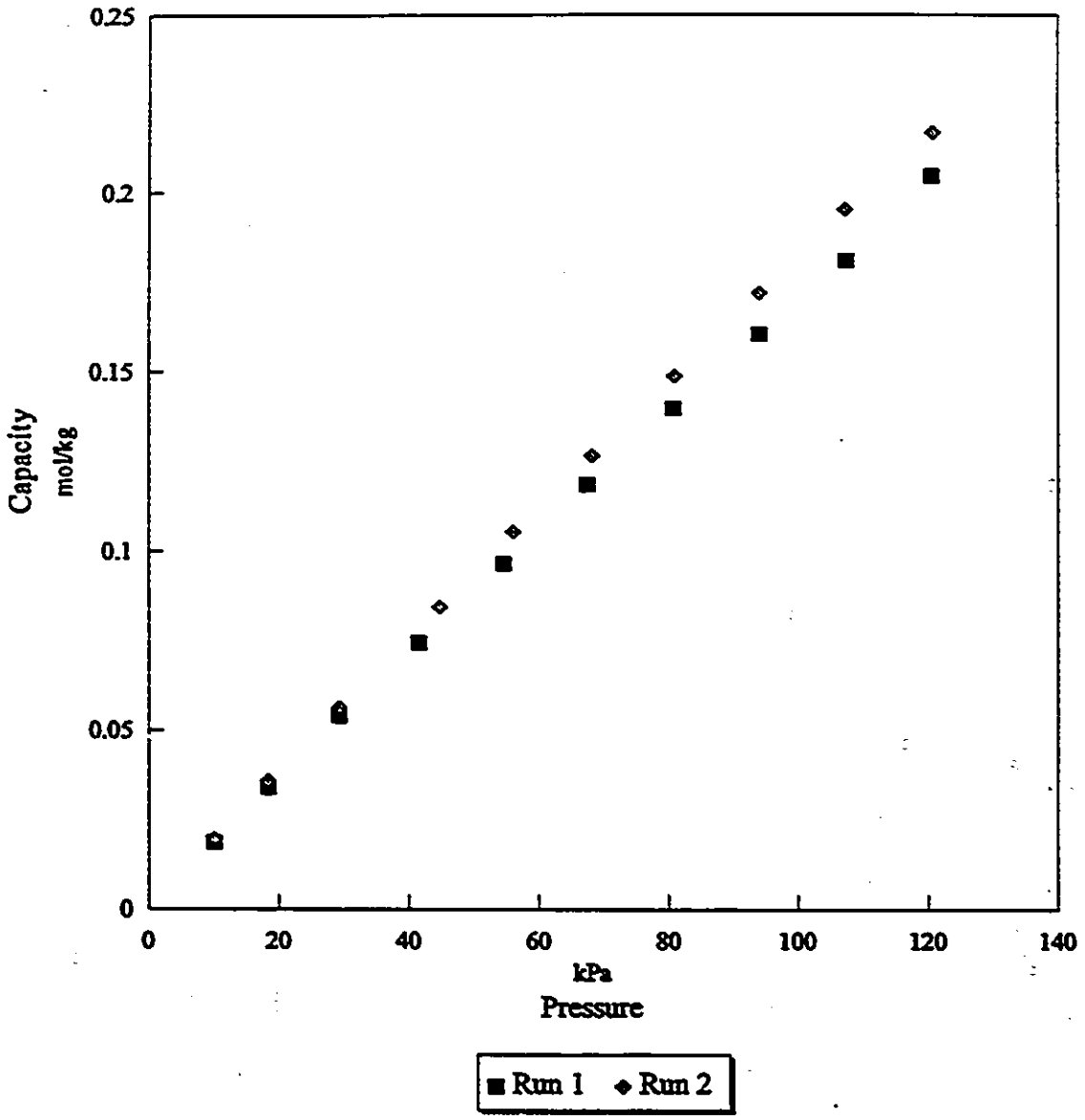

Figure 3.2. Experimental reproducibility of the measurement of the adsorption of CH4 on AlPO4-18 at 40°C

CHAPTER 4

RESULTS AND DISCUSSION

4.1 PURE-GAS ADSORPTION ISOTHERMS

Langmuir and FH-VST fits were determined for all the pure gas adsorption systems involving aluminosilicate molecular sieves. Single-component experimental isotherms measured for the adsorption in $AlPO_4$-11 and $AlPO_4$-18 were fitted using the Langmuir and FH-VST equations. In the case of $AlPO_4$-17 adsorption systems, Freundlich fits proved to be an excellent alternative when polar CO and quadrupolar N_2 were involved, as the Langmuir equation was unable to fit the experimental isotherms corresponding to these systems. The Langmuir equation could adequately represent the CH_4 / $AlPO_4$-17 adsorption system, but the Freundlich fit was determined as well in order to check the applicability of the Freundlich fit to all the $AlPO_4$-17 single-component systems investigated. The FH-VST parameters were regressed for each individual pure gas adsorption isotherm, using the isothermal computational method described by Cochran *et al.* (1985a). This method resorts to a non-linear regression procedure based on the Marquardt algorithm and available in the Statistical Analysis System (SAS) software package.

Details of the calculation and tabulation of the data corresponding to each adsorption system are given in Appendices A, B, C, and D.

4.1.1 Aluminosilicate Molecular Sieves

4.1.1.1 Single-Component Equilibrium Adsorption in Zeolite 5A

The experimental pure-component isotherms of N_2, CH_4, and CO in zeolite 5A at room temperature and 40°C (Stelmack, 1994) and the corresponding Langmuir and FH-VST fits determined in this study are presented in Figure 4.1. The parameters of the fitting equations (Langmuir and FH-VST) are given in Table 4.1.

At both temperatures the capacity of zeolite 5A for the three gases follows the expected decreasing trend corresponding to the decrease in adsorbate polarity, given the relatively small aperture of pores in zeolite 5A and the high energetic heterogeneity. Thus, the capacity of zeolite 5A for polar CO is, as expected, the highest as a result of the intense adsorbate-adsorbent interactions.

Table 4.1 Langmuir and FH-VST parameters for single-component / 5A adsorption isotherms.

Adsorption System	Temperature [°C]	n_1^{sat} [mol/kg]	b_1 [mol/kg Pa] x 10^6	α_{1v}	n_m [mol/kg]	B_1 [1/Pa] x 10^6
N_2 / 5A	39.8	2.51	2	0	3.57	0.5
CH_4 / 5A	40.1	2.37	2.7	-0.715	1.52	2
CO / 5A	40	2.59	12.3	1.6363	1.25	9
N_2 / 5A	22.7	1.67	5.06	-0.0108	1.61	3
CH_4 / 5A	22.8	1.26	4.7	0	1.2	4
CO / 5A	22.6	1.47	19	0	1.36	14.8

The higher adsorption capacity of zeolite 5A for N_2 than for CH_4 at room temperature and atmospheric pressure can also be explained through the specific adsorption potential that reflects the interaction between the quadrupole moment of the N_2 molecule and the Ca^{2+} ions which determine the diameter of the pore aperture. The smaller the pore aperture and volume, the more intense the interaction of the quadrupolar N_2 with the framework. Although the polarizability of the CH_4 molecule is higher than

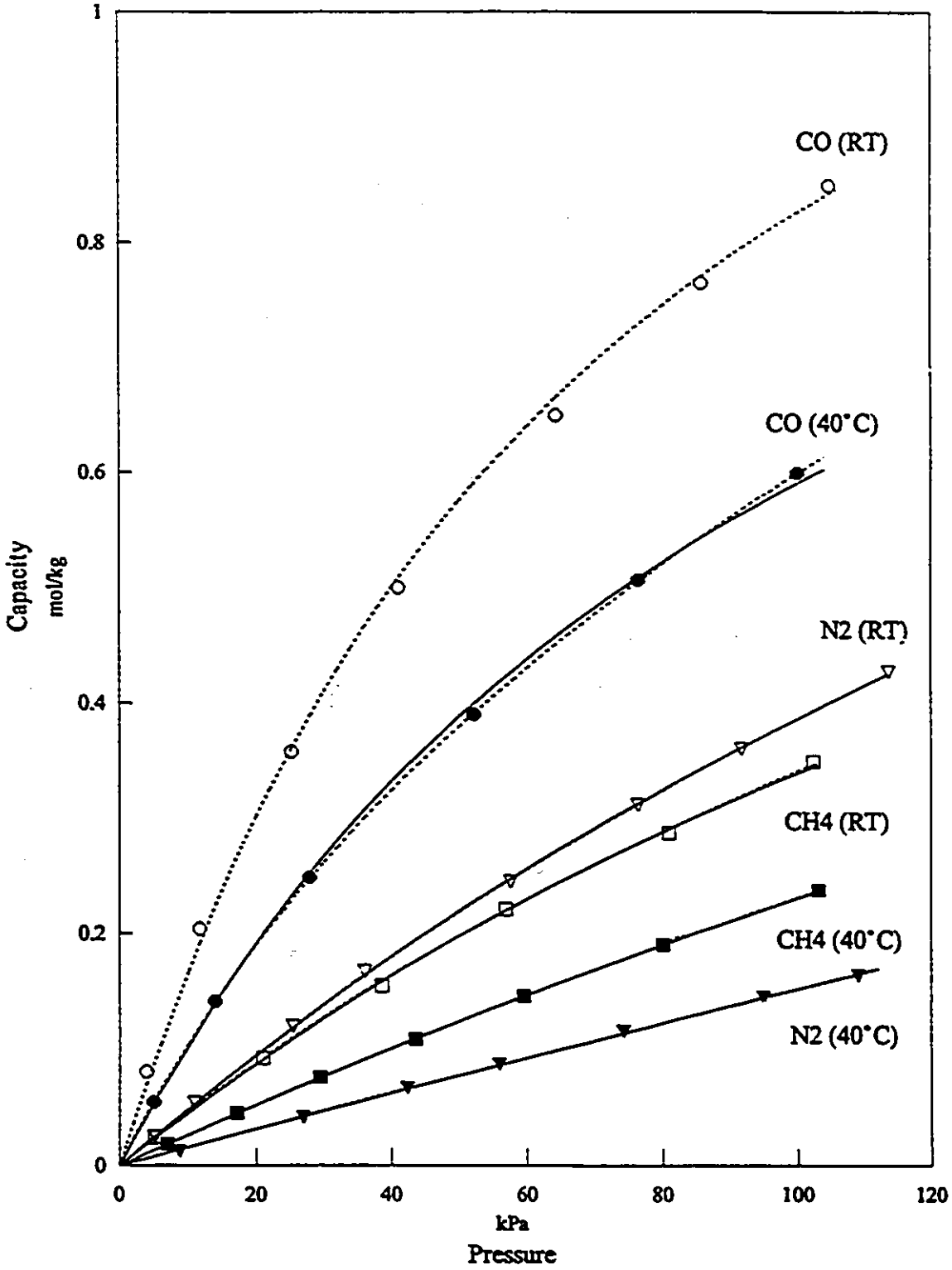

Figure 4.1 Adsorption isotherms for zeolite 5A at room temperature (RT) and 40°C (experimental points [Stelmack, 1994] and fits [present work])
_____ Langmuir fit - - - - - - - - FH-VST fit

that of the N_2 molecule (Table 3.1), the stronger interaction of N_2 molecules with this zeolite more than compensates for its lower polarizability.

The higher loss in capacity due to the increase in temperature for N_2 adsorption compared to CH_4 (Figure 4.1) could be explained as follows: N_2 having smaller molecular dimensions gains greater mobility for the same temperature increment, and the adsorptive forces are less able to hold the N_2 molecules on the surface of the adsorbent. The quadrupole moment of the N_2 molecules, which benefits adsorption capacity at the lower temperature, cannot offset the increased mobility gained at the higher temperature.

The superior capacities of zeolite 5A for CO can be explained by the beneficial association of adsorbate polarity and adsorbent energetic heterogeneity, which is also responsible for much higher capacities for N_2 than for CH_4 at room temperature. This fine interplay leads to more intense adsorbent-adsorbate interactions proportionally reflected in the value of the isotherm slope. As long as the adsorbent-adsorbate interactions are very intense compared to the adsorbate-adsorbate interactions, the slope of the isotherm is high. The value of this slope decreases as the adsorbate-adsorbate interactions increase and progressively approach the magnitude of the adsorbent-adsorbate interactions.

All 5A isotherms are equally well fitted by the Langmuir equation and the FH-VST equation in the case of N_2 and CH_4 gases. For CO, the Langmuir equation slightly overestimates the capacity at intermediate pressures, while slightly underestimating it at the ends of the pressure range investigated (Figure 4.1). The excellent FH-VST fits obtained are a consequence of the availability of data in the low-pressure range (<1000 mm Hg) which permitted the determination of accurate values for Henry's law constant, b_1, the quantitative indicator of adsorbate-adsorbent interactions at infinite dilution (Cochran *et al.*, 1985). The discrepancy in the predicted values of the Langmuir monolayer capacity and the FH-VST limiting amount of adsorption at infinite pressure or zeolite saturation (Table 4.1) is a result of the difference in the predicted slopes of the isotherm, that is the product of the Langmuir parameters, Bn_m (in the case of the Langmuir model), and the FH-VST Henry's law constant, b_1 (in the case of the FH-VST equation). While the Langmuir monolayer capacity is a concept valid only within the context of monolayer adsorption, its FH-VST homologue (i.e. the limiting amount of adsorption) can

be valid for monolayer as well as multilayer adsorption. As these two concepts are not equivalent, the values of the slopes yielded by the fit corresponding to each model are different.

As emphasized by Cochran *et al.* (1985a), one should not attach too much significance to the value of the α_{1v} parameter. The adsorption of CH_4 as interpreted by FH-VST is interesting to discuss, though, because two equally good fits of the isotherm at ambient temperature can be obtained with two different values of the adsorbate-vacancy parameter, α_{1v}. The values of the coverages predicted by FH-VST at 101.3 kPa could influence the choice of the better set of FH-VST parameters. Table 4.2 presents the coverages predicted by FH-VST at 101.3 kPa, and the values of the adsorbate-vacancy parameter responsible for equally excellent fits.

Table 4.2 FH-VST-predicted fractional coverages in zeolite 5A at 101.3 kPa.

Adsorbate	Temperature [°C]	α_{1v}	Fractional Coverage
N_2	22.7	-0.0107	0.2354
	39.8	0.0000	0.0614
CH_4	22.8	2.0927	0.0795
	22.8	0.0000	0.2736
	40.1	-0.7150	0.0990
CO	22.6	0.0000	0.5677
	40.0	1.6363	0.2334

Given the value of the coverage predicted at 40.1°C (0.0990), it would appear logical to choose the zero value of α_{1v} at room temperature, for which the coverage is higher (0.2736), rather than the non-zero value of α_{1v} which yields a coverage value at room temperature lower than the coverage value at 40.1°C. The zero value of α_{1v} reduces the FH-VST equation to the Langmuir equation, and it is not surprising therefore that the Langmuir and FH-VST fits agree for the CH_4/5A adsorption system.

4.1.1.2 Single-Component Equilibrium Adsorption in Turkish Clinoptilolite

The experimental pure-component isotherms of N_2, CH_4, and CO for Turkish clinoptilolite at room temperature and 40°C (Stelmack, 1994) as well as the corresponding Langmuir and FH-VST fits determined in this study are presented in Figure 4.2. The constants in the fitting equations (Langmuir and FH-VST) are given in Table 4.3.

The experimental adsorption isotherms of N_2, CH_4, and CO in Turkish clinoptilolite feature the "knee-bend" shape characteristic of strong adsorbents able to reach the saturation capacity at only slightly superatmospheric pressures. At both temperatures, the adsorption capacity of this natural zeolite for these gases at atmospheric pressure decreases in the order: $CO > CH_4 > N_2$. The adsorption capacity of Turkish clinoptilolite for CO exceeds by far that for either CH_4 or N_2. Unlike the highly polar zeolite A (Si/Al = 1), the less polar Turkish clinoptilolite (Si/Al = 4.25) favours the adsorption of CH_4 over N_2, thereby confirming the influence of the adsorbent energetic heterogeneity dictated by the higher Al content and, consequently, by the larger cation content. It is understandable that pure CH_4 is better adsorbed than N_2 at equilibrium in a zeolite richer in silica like Turkish clinoptilolite because the higher the Si/Al ratio of an aluminosilicate molecular sieve, the higher the capacity of the adsorbent for non-polar molecules.

Table 4.3 Langmuir and FH-VST parameters for single-component / Turkish clinoptilolite (TC) adsorption isotherms.

Adsorption System	Temperature [°C]	n_i^{sat} [mol/kg]	b_i [mol/kg Pa]	$\alpha_{i\infty}$	n_∞ [mol/kg]	B_i [1/Pa]
N_2 / TC	40.1	0.73	3.06×10^{-3}	6.8066	0.53	6.00×10^{-5}
CH_4 / TC	40	1.19	5.60×10^{-5}	2.1939	0.81	4.00×10^{-5}
CO / TC	40	1.04	2.70×10^{-2}	6.599	1.05	9.00×10^{-5}
N_2 / TC	22.7	0.82	6.51×10^{-3}	7.1046	1.61	3.00×10^{-4}
CH_4 / TC	22.8	1.08	1.05×10^{-4}	1.9706	0.94	5.76×10^{-5}
CO / TC	22.8	1.25	1.9	9.9	1.21	3.81×10^{-4}

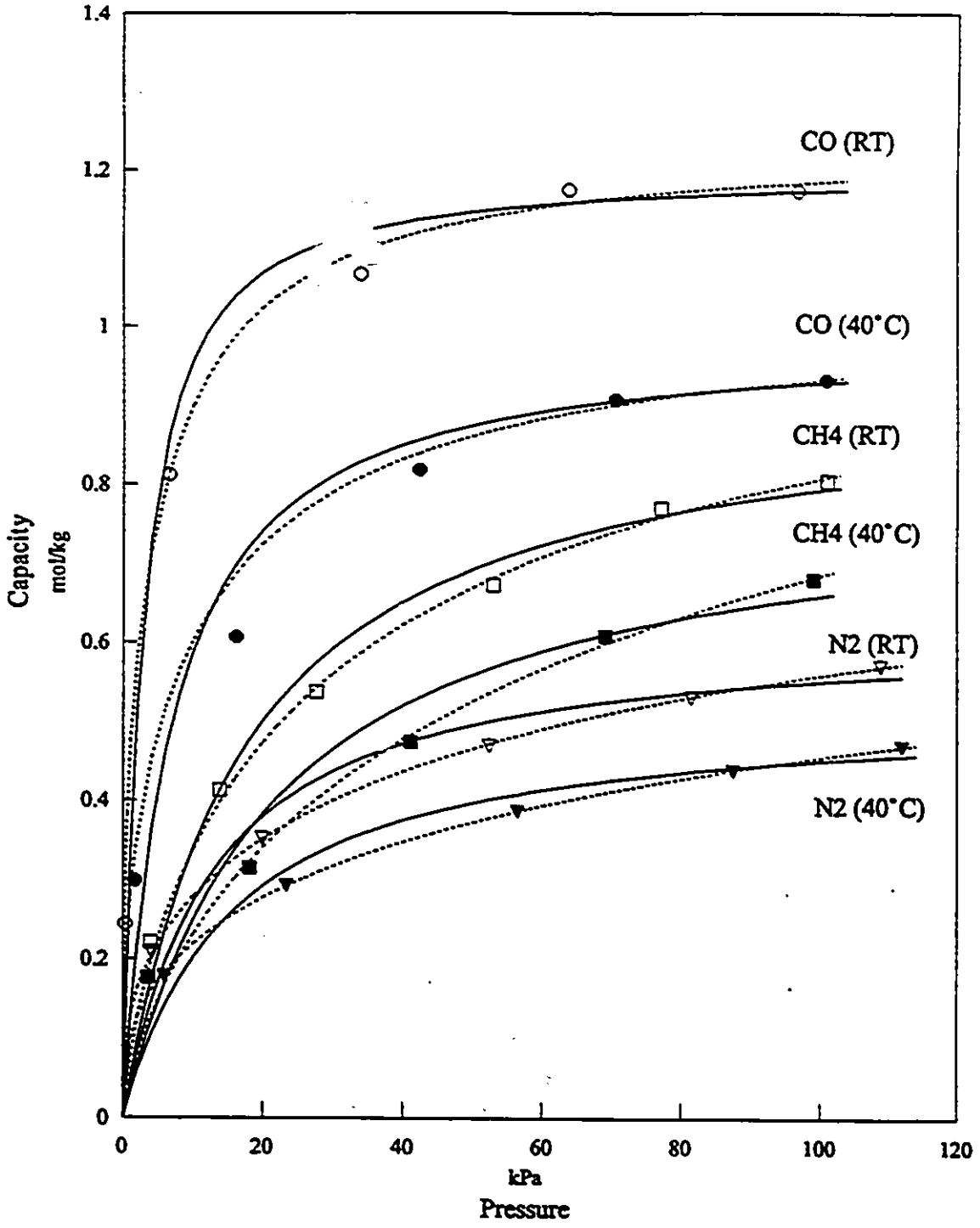

Figure 4.2 Adsorption isotherms for Turkish clinoptilolite at room temperature (RT) and 40°C (experimental points [Stelmack, 1994] and fits [present work])
_____ Langmuir fit - - - - - - - - FH-VST fit

Although the experimental isotherms do not actually cross, the FH-VST fits show a crossing at low pressure (4 kPa at room temperature and 8 kPa at 40°C), which should result in prediction of azeotrope formation when binary mixture adsorption data are evaluated using FH-VST. Ackley and Yang (1991b) have observed similar crossovers with experimental isotherms of N_2 and CH_4 in natural clinoptilolite at very low pressures.

At lower pressures, the quadrupole moment and the smaller kinetic diameter of the N_2 molecules favour their adsorption and diffusion within the energetically heterogeneous adsorbent. At higher coverages, the close-range repulsions between the quadrupolar N_2 molecules in the adsorbed phase become much stronger than those between the nonpolar (but polarizable) CH_4 molecules, thus leading to a lower capacity for N_2 at higher pressures. Over a larger pressure range, the higher polarizability of CH_4 is thus able to compensate for its total lack of polarity, therefore adsorbing in higher amounts at equilibrium.

The type of cations compensating the negative charge in the framework of natural clinoptilolite could also explain the preferential adsorption of CH_4 with respect to N_2 at equilibrium. Turkish clinoptilolite is predominantly rich in divalent cations (Mg^{2+} and Ca^{2+}) which generate stronger electric fields than monovalent cations such as Na^+ and K^+ (Table 4.4).

Table 4.4 Unit cell composition of investigated natural clinoptilolite samples (based on 72 atoms)

	Si (# atoms)	Al (# atoms)	Fe (# atoms)	Na (# atoms)	K (# atoms)	Ca (# atoms)	Mg (# atoms)	Si/Al ratio
Turkish[1]	28.98	6.82	0.36	0.22	1.34	1.46	1.02	4.25
Cuban	29.16	5.6	1.07	1.57	0.95	1.58	0.32	5.2

[1] Sirkecioglu *et al.* (1995)

The number of cations per unit cell decreases in the order $Ca^{2+} > Mg^{2+} > K^+ >> Na^+$. The stronger electric field generated by the divalent cations induces dipoles in the highly polarizable CH_4 molecules which, as a result of the field - induced dipole interactions, are more strongly held in the adsorbed phase than the quadrupolar N_2.

As far as the effect of temperature on adsorption is concerned, as shown in Figure 4.2, the capacity for CO is affected the most by the change in temperature, indicating the highest heat of adsorption and, consequently, the highest interaction between CO molecules and Turkish clinoptilolite. CH_4 and N_2 molecules follow CO in the decreasing order of interaction intensity with this adsorbent.

The Langmuir fits are less accurate for the adsorption systems involving Turkish clinoptilolite than for those involving zeolite 5A. The FH-VST fits are very good for the CH_4 adsorption isotherms at the two temperatures, and excellent for the N_2 adsorption isotherm. As far as CO is concerned, the FH-VST fits are much better than the Langmuir ones, but not as good as the ones obtained for the other adsorption systems.

The surface coverages in Turkish clinoptilolite at 101.3 kPa are higher than those in zeolite 5A at the same pressure (see Figures 4.1 and 4.2). This is not surprising considering the shape of the isotherms and the corresponding α_{1v} values (Tables 4.1 and 4.3). It seems that α_{1v} values reflect, indeed, the intensity of interaction expected from the nature of the components of the adsorption system: the values at a particular adsorption temperature are highest for the polar adsorbate, and lowest for the non-polar adsorbate (Table 4.3). In other words, this adsorbate-vacancy parameter appears to be related to the strength of interaction. Although α_{1v} is higher at the lower temperature for N_2 and CO systems, the opposite is true for the CH_4 systems.

The rectangular shape of the Turkish clinoptilolite isotherms indicates that this adsorbent would be ideally suited in purification applications rather than bulk separation of gas mixtures.

4.1.1.3 Single-Component Equilibrium Adsorption in Cuban Clinoptilolite

The experimental pure-component isotherms of N_2, CH_4, and CO in Cuban clinoptilolite at 40°C and the corresponding Langmuir and FH-VST fits are presented in Figure 4.3. The constants in the fitting equations (Langmuir and FH-VST) are given in Table 4.5.

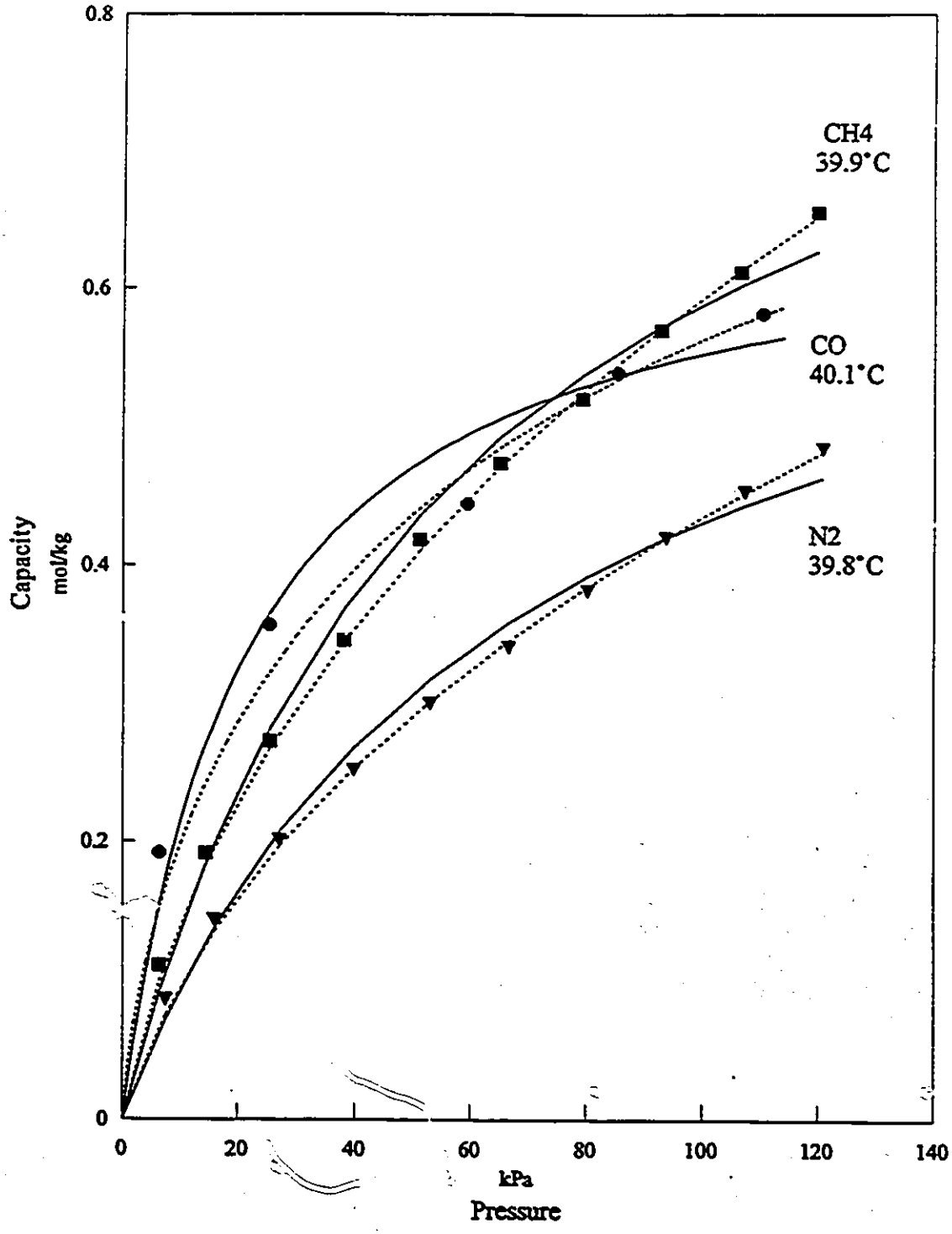

Figure 4.3 Adsorption isotherms for Cuban clinoptilolite at 40°C (experimental points and fits)

_____ Langmuir fit - - - - - - - - - FH-VST fit

Table 4.5 Langmuir and FH-VST parameters for single-component / Cuban Clinoptilolite (CC) adsorption isotherms.

Adsorption System	Temperature [°C]	n_1^{sat} [mol/kg]	b_1 [mol/kg Pa] x 10^5	α_{1v}	n_∞ [mol/kg]	B_1 [1/Pa] x 10^5
N_2 / CC	40	2.39	1.3	2.7	0.72	1.48
CH_4 / CC	39.9	4.05	2.05	3.3	0.94	2
CO / CC	40.1	0.94	5.31	2.28	0.67	4.72

The unit cell composition of Cuban clinoptilolite (Table 4.4) was approximated from the percentages related to the corresponding oxide mass present in 100 g sample, and may not necessarily reflect accurately the presence of the charge-compensating Ca^{2+} since Ca^{2+} may also be present in the sample as carbonate. Fe^{3+} also can be present as impurity. The typical chemical analysis also reveals the presence of Mn, Ti, and P, which would amount to roughly 0.11, 0.087, and 0.094 atoms per unit cell, respectively.

As mentioned in the experimental procedure section, the pressure equilibration periods during the measurement of the adsorption isotherms were extremely long in the case of Cuban clinoptilolite, thus indicating that adsorption in this natural aluminosilicate molecular sieve is diffusion-controlled. Equilibration periods varied with the nature of the adsorbate, being the lowest for N_2 (6 to 24 hours per datapoint, depending on the pressure) and the highest for CO which constituted the most severe case of diffusion-controlled adsorption (two to six weeks per datapoint, depending on the pressure). The long equilibration periods may be due to the presence of a larger number of Na^+ cations per unit cell in Cuban clinoptilolite with respect to Turkish clinoptilolite (Table 4.4), which preferentially occupy the sites at the intersection of the 10-member ring channel with the 8-member ring channel, as well as the sites at the intersection of the two 8-member ring channels (Koyama and Takeuchi, 1977), thus partially blocking the access to the pores and decreasing diffusivities. Only high pressures can help overcome these "obstacles", thereby increasing accessibility to partially "blocked" pores. These effects are especially important in the case of adsorbents whose reduced aperture diameter approach the value of the kinetic diameter of the adsorbate molecule.

Just like in the case of Turkish clinoptiloiite, the experimental adsorption isotherm of CO in Cuban clinoptilolite features the "knee-bend" shape. It is less pronounced than that found with Turkish clinoptilolite. Efficient pressure-swing processes require a less rectangular shape of the adsorption isotherm to ensure rapid desorption cycles, and this requirement appears to be better met by Cuban clinoptilolite than by Turkish clinoptilolite for CO. The N_2 and CH_4 isotherms for the Cuban clinoptilolite are much smoother than the ones for CO.

The Langmuir fits follow the known trend, underestimating the adsorption capacity at the extremes of the pressure ranges and overestimating it at intermediate pressures studied. The FH-VST fits are very good for the N_2 and CH_4 isotherms, but imperfect for the CO isotherm.

Both clinoptilolites adsorb CO in the highest amounts and N_2 in the lowest amounts at 40°C and pressures below 80 kPa (Figures 4.2 and 4.3). Cuban clinoptilolite contains more monovalent cations than divalent cations (Table 4.4), which means a lower strength of the polarizing field compared to divalent cations and, therefore, a weaker interaction with quadrupolar N_2, retained by this adsorbent in lowest amounts at equilibrium. Unlike Turkish clinoptilolite, however, Cuban clinoptilolite adsorbs CH_4 in higher amounts than CO at pressures above 80 kPa. The CH_4 and CO isotherms cross at about 80 kPa, an observation which leads to the conclusion that a mixture of the two gases will feature an azeotrope. This fact can be used as an assessment tool for the predictive performance of the binary mixture adsorption models.

Isotherm cross-over in the case of Cuban clinoptilolite could be explained by the difference in the cation compositions of these clinoptilolite samples (Table 4.4). A higher Si/Al ratio and a larger number of univalent cations favour the adsorption of non-polar molecules like CH_4. Although the energetic heterogeneity of Cuban clinoptilolite is slightly lower than that of Turkish clinoptilolite, the mixed cation population contains approximately equal numbers of Na^+ and Ca^{2+} cations which would possess enough polarizing power to induce electric moments in the CH_4 molecules and eventually interact with the polarized CH_4 molecules. The crossing of the isotherms is ultimately due to the

increase in the close-range repulsive interactions exerted between the adsorbed polar CO molecules at higher coverages.

The N_2 and CH_4 isotherms in Cuban clinoptilolite do not cross, illustrating therefore the fact that at equilibrium the higher polarizability of CH_4 overcomes unfavourable steric factors for this molecule and turn the handicap related to the absence of polarity into an advantage since no close-range repulsions come into play at higher coverages the way they do in the case of N_2.

4.1.2 Aluminophosphate Molecular Sieves

4.1.2.1 Single-Component Equilibrium Adsorption in $AlPO_4$-11

The experimental pure-component isotherms of N_2, CH_4, and CO in $AlPO_4$-11 at 40°C and room temperature (Stelmack, 1994) are presented in Figure 4.4 along with the corresponding Langmuir and FH-VST fits determined in this study. All six experimental isotherms are favourable, which supports the hypothesis of the relationship between the shape of an isotherm and the steric constrictions encountered by the adsorbate molecule at the micropore aperture: with medium-sized pores like those of $AlPO_4$-11 (3.9 x 6.3 Å), the three adsorbates (molecular dimensions 3.0 x 4.1 Å for N_2, 4.2 Å for CH_4, and 3.7 x 4.2 Å) do not have to overcome steric impediments and the isotherms are therefore favourable. Given the linearity of virtually all the six isotherms in the pressure range investigated, predicted saturation capacities are expected to be high.

Figure 4.4 shows that over the investigated pressure range $AlPO_4$-11 features the highest adsorption capacity for CH_4 and the lowest for N_2, with CO being in between. This is an expected result of "equal access" offered by this medium-pore molecular sieve to all gaseous adsorbates of similar molecular dimensions, smaller than those of its pore aperture. CH_4 being the largest molecule is trapped easily within the pores, while N_2 being the smallest molecule can easily leave the adsorbed phase. The capacity for CO accordingly features intermediate values. The Langmuir and FH-VST regressed parameters, valid for the pressure range investigated, are listed in Table 4.6.

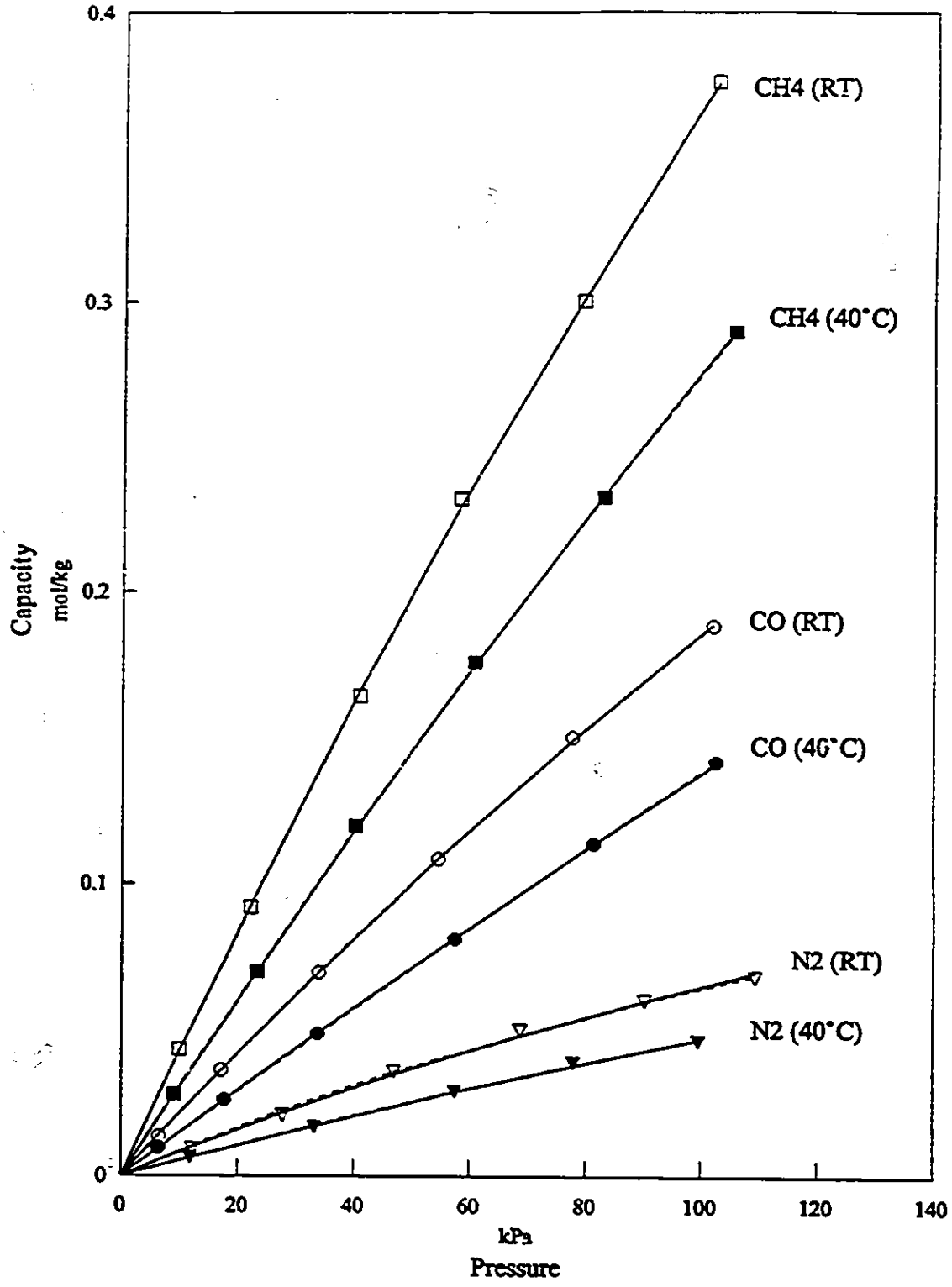

Figure 4.4 Adsorption isotherms for AlPO4-11 at room temperature (RT) and 40°C (experimental points [Stelmack, 1994] and fits [present work])
———— Langmuir - - - - - - - - FH-VST

Table 4.6 Langmuir and FH-VST parameters for single-component / $AlPO_4$-11 (A11) adsorption isotherms.

Adsorption System	Temperature [°C]	n_1^{sat} [mol/ kg]	$b_1 \times 10^6$ [mol/kg Pa]	α_{1v}	n_m [mol/kg]	$B_1 \times 10^6$ [1/Pa]
N_2 / A11	40	0.3	0.56	0	0.34	1.62
CH_4 / A11	40	2.51	3.11	0	2.71	1.14
CO / A11	40	2.58	1.47	0	1.92	0.78
N_2 / A11	22.8	0.23	0.9	0	0.29	2.92
CH_4 / A11	22.8	2.3	4.38	0	2.26	1.94
CO / A11	22.8	1.27	2.19	0	1.32	1.65

As expected, the slope of the isotherms as well as the capacities decrease with increasing temperature.

With the gas-vacancy interaction parameters equal to zero for all six adsorption isotherms, it is not surprising that both the Langmuir and the FH-VST fits are excellent, since the FH-VST equation reduces to the Langmuir equation at very low pressures.

4.1.2.2 Single-Component Equilibrium Adsorption in $AlPO_4$-17

The experimental pure-component isotherms of N_2, CH_4, and CO in $AlPO_4$-17 at 40°C are presented in Figure 4.5, along with the corresponding Langmuir (or Freundlich) and FH-VST fits. The Langmuir and FH-VST parameters are listed in Table 4.7.

The FH-VST fit for the CH_4 isotherm is perfect. The FH-VST fit for the CO isotherm resembles the type-I trend characteristic to the Langmuir equation and therefore fails to follow the experimental datapoints closely. The same tendency of the FH-VST fit is observed in the N_2 isotherm, but to a lesser extent. Figure 4.4 shows that at 40°C $AlPO_4$-17 prefers to adsorb CH_4 much more than N_2 and CO, probably because of the larger molecular size of CH_4 and the energetic homogeneity of the adsorbent. Neighbouring quadrupolar N_2 molecules would repel each other to a lesser extent than neighbouring dipolar CO molecules. That is why the N_2 isotherm lies above the CO isotherm in the case of $AlPO_4$-17, even though these two isotherms are fairly close.

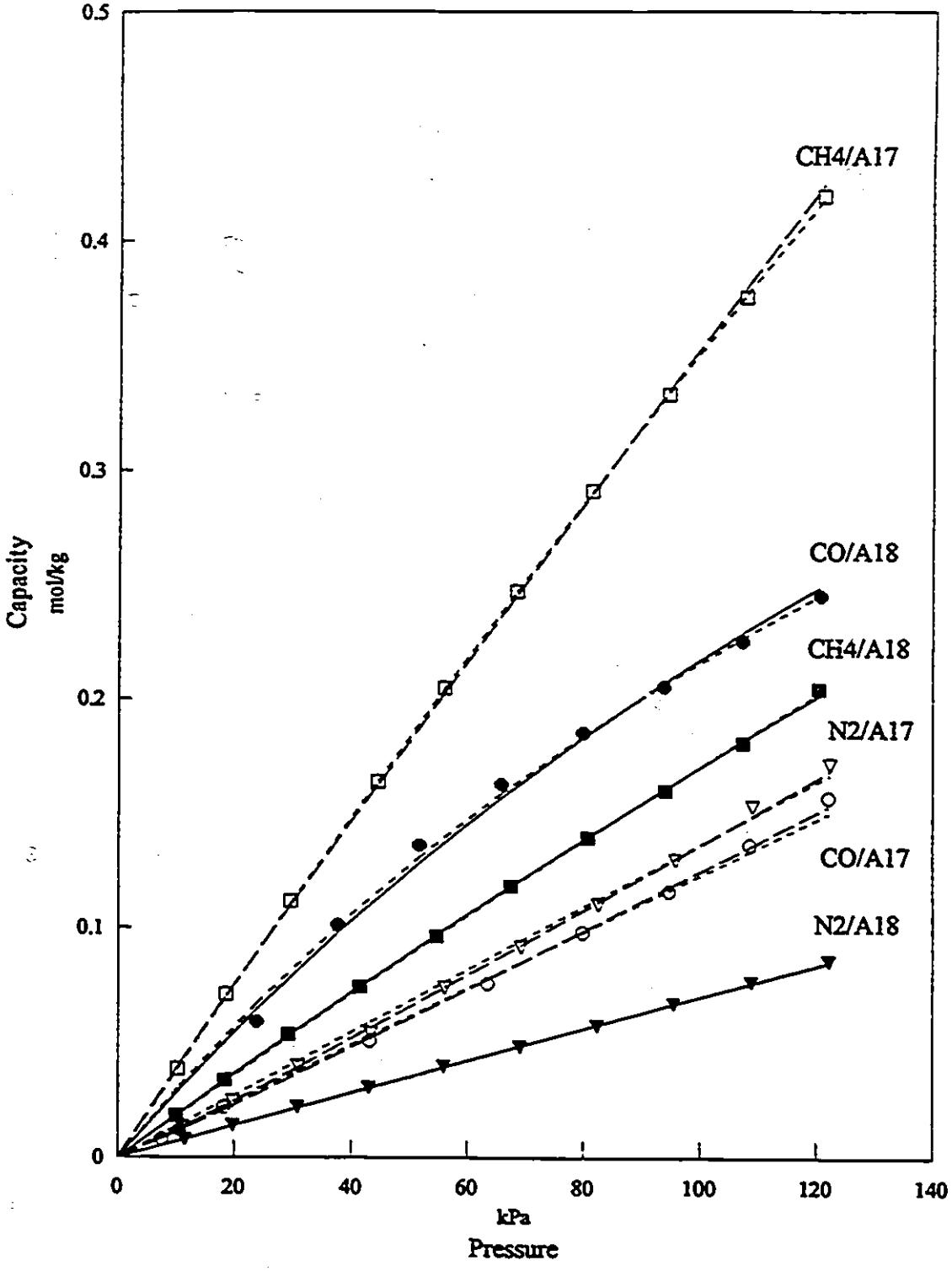

Figure 4.5 Adsorption isotherms for AlPO4-17 (A17) and AlPO4-18 (A18) at 40°C (experimental points and fits)
_____ Langmuir or _ _ _ _ Freundlich, and _____ FH-VST

Table 4.7. Langmuir and FH-VST parameters for single-component / $AlPO_4$-17 (A17) adsorption isotherms.

Adsorption System	Temperature [°C]	n_i^{sat} [mol/kg]	$b_i \times 10^6$ [mol/kg Pa]	$\alpha_{1i} \times 10^6$	n_∞ [mol/kg]	$B_i \times 10^6$ [1/Pa]
N_2/A17	39.6	1.27	1.53	4.44	2.68	0.48
CH_4/A17	40	4.12	3.85	0	3.88	0.99
CO/A17	40	0.58	1.56	-4.58	n/a	n/a

The slightly "unfavourable" shape observed in the experimental CO / $AlPO_4$-17 and N_2 / $AlPO_4$-17 isotherms is due to the steric hindrance encountered by these adsorbate molecules when attempting to penetrate the micropores. $AlPO_4$-17 is a structural analogue of erionite and presents the same "ink-bottle" type of pore geometry, with elliptical pore apertures which may constitute an impediment for less spherical molecules like N_2 and CO. As shown in Table 3.1, the molecular dimensions of N_2 are 3.0 x 4.1 Å (kinetic diameter 3.64 Å) and those of CO are 3.7 x 4.2 Å (kinetic diameter 3.76 Å). The adsorption of these molecules in $AlPO_4$-17 would depend on their orientation when approaching the elliptical opening of a micropore (3.6 x 5.1 Å). The capacity of the sieve would be the result of the probability that the "candidate" molecules feature the adequate orientation, as well as the result of the pressure necessary to assist in "pushing" the molecule with the right orientation through the elliptical micropore aperture. Steric hindrance is therefore responsible for the lower capacity for CO. In the case of CH_4 of tetrahedral molecular dimension 4.2 Å (kinetic diameter 3.8 Å), the tetrahedral geometry of the molecules facilitates pore penetration when the molecules approach the opening with one of their four vertices, and then ease themselves as a result of their translational, rotational, and vibrational energies (still present even though reduced upon adsorption on the external surface of the crystal).

Given the inability of the Langmuir equation in fitting the slightly "unfavourable" CO experimental isotherm, the Freundlich equation was used and an excellent correlation was obtained. The Freundlich parameters are provided in Table 4.8.

Several desorption points were also determined on the CO / $AlPO_4$-17 isotherm (Figure 4.6), revealing considerable adsorption irreversibility in the investigated pressure

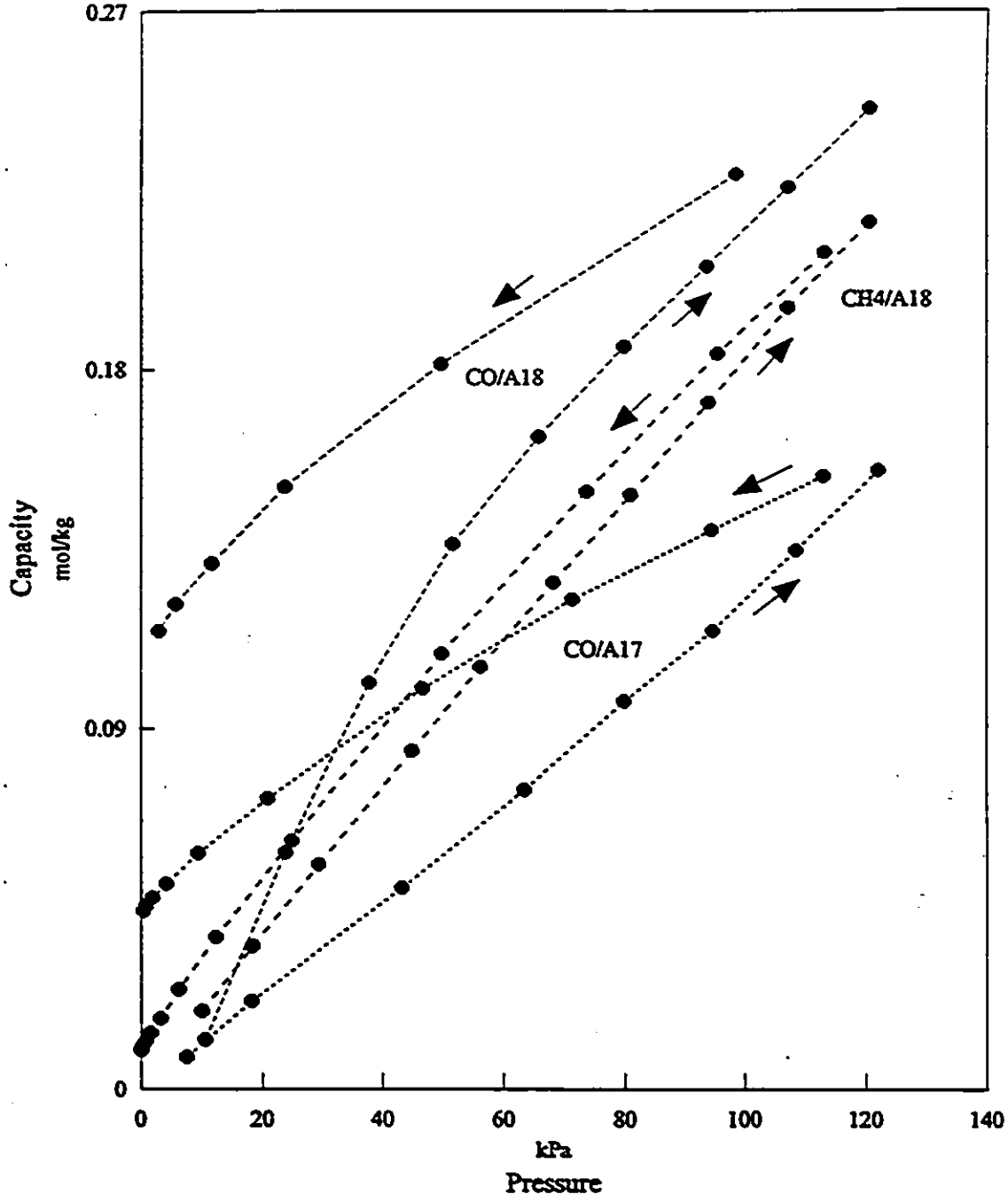

Figure 4.6 Hysteresis effect in small-pore aluminophosphate molecular sieves AlPO4-17 (A17) and AlPO4-18 (A18) at 40°C

range and the necessity to resort to ultra-high vacuum to desorb most of the CO adsorbed, and ultimately to thermal desorption. The irreversibility curve appears to indicate that once the CO molecules are adsorbed in the micropores, steric considerations concur in impeding desorption once the pressure is reduced. The CO molecules do not have the same translational, rotational, and vibrational freedom (energy) in the micropore cavity, and therefore cannot orient themselves in the position that would permit them to exit the micropore and return to the gas phase above the external surface of the $AlPO_4$-17 crystals, no matter how high the vacuum applied is.

Table 4.8 Freundlich parameters for single-component / $AlPO_4$-17 adsorption isotherms.

Adsorbate	Temperature [°C]	k [mol/kg $Pa^{1/n}$]	n
N_2	39.6	7.0×10^{-7}	0.949
CH_4	40.0	5.7×10^{-6}	1.044
CO	40.0	7.8×10^{-7}	0.961

4.1.2.3 Single-Component Equilibrium Adsorption in $AlPO_4$-18

The experimental pure-component isotherms of N_2, CH_4, and CO in $AlPO_4$-18 at 40°C are presented in Figure 4.5, along with the corresponding Langmuir and FH-VST fits. The Langmuir and FH-VST parameters are provided in Table 4.9.

Table 4.9 Langmuir and FH-VST parameters for single-component / $AlPO_4$-18 (A18) adsorption isotherms.

Adsorption System	Temperature [°C]	n_1^{sat} [mol/kg]	$b_1 \times 10^6$ [mol/kg Pa]	α_{1v}	n_m [mol/kg]	$B_1 \times 10^6$ [1/Pa]
N_2 / A18	40.1	4.07	0.72	0	3.35	0.22
CH_4 / A18	40	2.44	1.84	0	1.97	0.95
CO / A18	40.1	0.71	3.13	0	0.84	3.52

The capacity of $AlPO_4$-18 for the three adsorbates investigated decreases in the order CO > CH_4 >> N_2, with the N_2 and CH_4 isotherms featuring obvious linearity. The capacity hierarchy could be explained in terms of steric hindrance effects, given the circular pore openings of $AlPO_4$-18 (3.8 x 3.8 Å) and the molecular dimensions of each adsorbate (Table 3.1).

N_2 is adsorbed in the smallest amounts by $AlPO_4$-18 because of two reasons. Firstly, the larger dimension of the "capsular" N_2 molecule (3.0 x 4.1 Å) cannot fit easily into a circular pore aperture of slightly smaller diameter. Molecular sieves with circular pore apertures are less accessible to "nonspherical" molecules like N_2 or tetrahedral molecules like CH_4 (4.2 Å). Secondly, the weak quadrupole moment in the N_2 molecules is unable to induce electric moments in the atoms on the surface of the adsorbent.

CH_4 is more easily accommodated than N_2 since it can be more easily trapped in the micropores of $AlPO_4$-18. The smaller adsorption capacity range of $AlPO_4$-18 for CH_4 with respect to CO is due to the higher kinetic diameter of the CH_4 molecule -- equal to the diameter of the pore opening (3.8 Å) – and to its tetrahedral molecular configuration.

The slightly unfavourable shape of the CO isotherm up to 25 kPa could be interpreted as a result of the conjugated effect of energetic interactions and steric factors. Although the kinetic diameter of the CO molecule is 3.76 Å (lower than the diameter of the $AlPO_4$-18 pore aperture), the molecular dimensions are 3.7 x 4.2 Å (Table 3.1). The kinetic diameter may slightly increase, approaching the molecular dimensions (which define a "static" molecule) once the molecule is adsorbed and has less energy to translate, rotate, and vibrate (fewer degrees of freedom). It appears that at low pressure when the concentration of the polar CO molecules in the gas phase is small, the first few molecules end up in the adsorbed phase as a result of the non-specific (adsorbent-related) interactions. The pressure being so low, the first molecules adsorbed in the micropores are probably those which, after being initially adsorbed on the external surface of the crystal, diffuse toward and through the pore openings drawn by the non-specific (adsorbent-related) adsorption potential, and happen to have the adequate orientation necessary to enter the micropore cavity, i.e. they approach the pore window with their smaller molecular dimension (3.7 Å).

The unfavourable part of the CO isotherm in the very low pressure region appears to enforce the idea that pressure was insufficient to help a large number of CO molecules get adsorbed on the external surface of the $AlPO_4$-18 crystals and then diffuse with the appropriate orientation toward and through the pore apertures. Given the energetic homogeneity of the adsorbent, the adsorption potential of the system is also too low at those low pressures (the self-potential contribution paid by only a small number of molecules adsorbed is insufficient to enhance the overall adsorption potential of the system). As soon as some more CO molecules are adsorbed, the self-potential component increases and continues to do so with further adsorption of additional CO molecules.

The adsorbed CO molecules induce "mirror" dipole and quadrupole moments in the framework atoms in the vicinity of which they are lying, thus polarizing the surface of the adsorbent. These moments can be more easily induced in the case of this adsorption system because of the close values of the kinetic diameter of the adsorbate and the pore aperture diameter of the adsorbent. As pressure is increased, the concentration of CO in the gas phase above the surface of the adsorbent increases, and the interactions between these gaseous molecules and the polarized adsorbent surface -- which now features "self-made" adsorption sites -- intensify. Self-potential increases with continuous buildup of adsorbed molecules on the surface of the aluminophosphate sieve and thus, the overall adsorption potential increases from contributions of dipole-field and quadrupole-field gradient interactions and self-potential to the inherent non-specific potential.

The number of molecular collisions in the gas phase above the crystal also increases with increasing pressure, thus increasing the probability that the molecules in the vicinity of the pore openings have the proper orientation permitting diffusion into the micropore cavities. There appears to be a "threshold" pressure at which the self-potential has reached a value corresponding to a sufficiently polarized surface for the non-polar aluminophosphate molecular material to start behaving like a polar adsorbent with high-potential sites analogous to the cationic sites in zeolites. Above that pressure the slope of the isotherm increases abruptly only to start decreasing the way any favourable type I isotherm flattens when the saturation capacity is approached and close-range repulsions between adsorbed molecules become dominant.

Several desorption points were also determined on the CH_4 / $AlPO_4$-18 and the CO / $AlPO_4$-18 isotherms (Figure 4.6), revealing that the hysteresis effect is quite important in the investigated pressure range. The magnitude of this effect was less for the adsorption of CO in $AlPO_4$-17 at the same temperature (40°C). Again, the presence of this effect can be explained in terms of steric factors: the adsorbed molecules (whether CH_4 or CO) cannot translate, rotate, and vibrate within the micropores in order to orient themselves in the position that would allow them to leave the micropores and the adsorbed phase in favour of the gas phase around the $AlPO_4$-18 crystals. During desorption, steric hindrance cannot be overcome by a gradient of pressure (as in pressure-swing adsorption). The solution to this problem would be thermal-swing desorption, in which case the amplitude and frequency of vibration of the framework increases allowing the adsorbed molecules to exit the micropores at higher temperatures.

Just like in the case of the CO / $AlPO_4$-17 adsorption system, $AlPO_4$-18 appears to be inadequate for industrial separations involving pressure-swing adsorption of CH_4 from gaseous mixtures, unless thermal-swing adsorption can be used at low costs or the synthesis of the aluminophosphate material is inexpensive and allows disposal. Similarly, $AlPO_4$-18 is expected to be a useful adsorbent for gas molecules of much lower diameter (e.g. CO_2, NO), and a good desiccant. According to Wilson *et al.* (1984), the capacity of $AlPO_4$-18 for water at 24°C and 101.3 kPa (about 1.4 mol/kg) is superior with respect to that of $AlPO_4$-11 (about 0.6 mol/ kg) and $AlPO_4$-17 (about 1.1 mol/kg).

4.1.3 Final Overview on Single-Component Adsorption

Adsorption of pure gases onto aluminosilicate molecular sieves appears to be regulated by the degree of energetic heterogeneity featured by the adsorbent, while the adsorption of the same gases onto aluminophosphate molecular sieves seems to be governed by steric effects.

As discussed by Kärger and Ruthven (1992), the investigation of the adsorptive properties of aluminosilicate and aluminophosphate molecular sieves brings out the importance of the two types of driving force responsible for gas adsorption processes: the

gradient of chemical potential and the gradient of concentration (pressure). Table 4.10 reflects the relationship between these acting driving forces and the fractional coverage attained on the surface of the adsorbent.

The gradient of chemical potential is predominantly related to the energetic heterogeneity, the polarizability, and polarity of the adsorbent and indicates the strength of adsorbent-adsorbate interactions, while the pressure gradient appears to assist the adsorbate in the adsorption process. Both driving forces work to help the adsorbate migrate to the adsorption site and then remain adsorbed in equilibrium with the gas phase. The gradient in chemical potential is responsible for the actual adsorption of a molecule which is in the vicinity of a vacant adsorption site; the gradient in concentration is responsible for the diffusion of the molecules through the channels (succession of micropores with a certain degree of tortuosity) to reach the next vacant adsorption sites. While the gradient of chemical potential and the gradient of concentration cooperate during adsorption, they work against each other during desorption. The larger the difference between the absolute values of the two gradients (the less compensating the actions of the two gradients are during desorption), the more important the hysteresis.

Table 4.10 Acting driving forces in the adsorption process according to the magnitude of coverage.

Molecular sieve	Low coverages		High coverages
	Low intrinsic potential	High intrinsic potential	
Aluminosilicate	concentration gradient	chemical potential & concentration gradients	concentration gradient
Aluminophosphate	concentration gradient		concentration gradient

The behaviour of adsorption systems featuring aluminosilicate molecular sieves as adsorbents is enhanced and modified by the properties of the adsorbent (Si/Al ratio, cation type and content). On the other hand, the behaviour of adsorption systems in which the adsorbent is an aluminophosphate molecular sieve is primarily dependent on the nature of the adsorbate (i.e. its polarity, kinetic diameter, geometric configuration, boiling point,

degree of unsaturation, and system pressure). The magnitude of the chemical potential increases with the polarity of the adsorbate and the cationic charge density in the adsorbent. The higher the cationic charge density of an adsorbent the higher its intrinsic potential, i.e. the chemical potential at zero adsorbate pressure. The larger the quadrupole or dipole moment of the adsorbate molecule, the higher its specific potential, i.e. the contribution of the molecule to the total adsorption potential. The ability of a non-polar adsorbate to interact with an adsorbent is related to its polarizability. In the case of a polar adsorbate, its polarizability enhances the interactive ability given by its polarity.

In an adsorption system involving an energetically heterogeneous adsorbent (such as an aluminosilicate molecular sieve) and an arbitrary adsorbate, the gradient of chemical potential will be the major driving force at lower coverages, with the adsorbate pressure playing a minor role in counteracting any repulsive interactions which might arise because of the polar nature of the adsorbate. The larger the gradient of chemical potential, the more rectangular the isotherm. As the adsorption sites are progressively occupied, the gradient in chemical potential decreases, and so does the degree of energetic heterogeneity, the gradient of concentration becoming the dominant driving force at higher coverages; at still higher pressures the adsorption mechanism is the result of a micropore-filling process which is physically limited by the value of the saturation volume (Table 2.2). As long as there are unoccupied vacant sites in the zeolite framework, the adsorbed molecules will diffuse within the channels toward those vacant sites; previously occupied sites are vacated and become available for the adsorption of additional molecules at sufficiently high pressure.

In an adsorption system consisting of an energetically homogeneous molecular sieve (such as an aluminophosphate molecular sieve), the gradient of chemical potential is very small because of the absence of cations (energetic heterogeneity), and the success of the adsorption process relies almost exclusively, even at the lowest pressures, on the concentration gradient. Volume filling becomes the predominant mechanism of sorption at high pressures in the gas phase, which permit a large number of molecules to "squeeze" in the micropores. The adsorption capacity is measured through the degree of pore filling,

which replaces the concept of surface coverage. With aluminophosphate molecular sieves, saturation pore volumes become the structural parameter analogous to surface area.

The adsorption capacities of aluminophosphate molecular sieves are influenced by the nature of the adsorbate. Thus, non-polar and larger molecules would be preferentially adsorbed since the lack of repulsive interactions at high pore fillings enable neighbouring molecules to tolerate the proximity of their peers, and their larger molecular dimensions allows them to be more easily entrapped within the pores. Polar and smaller molecules would be adsorbed in the lowest amounts because of the intense repulsive interactions which are likely to appear at high pore fillings and the smaller molecular dimensions which allow them to readily exit the micropores and thus return into the gas phase.

The hysteresis effect occurring in single-component adsorption is influenced by steric factors such as the pore dimensions and geometry, as well as the adsorbate molecular dimensions and geometry. The larger the difference between the micropore aperture diameter and the dimensions of the gas molecule, the less likely the hysteretic behaviour of an adsorption system. If steric factors are not favourable (too close pore size and molecular dimensions, and different pore and molecule geometries), the adsorbed molecules are not likely to leave the micropores easily when the pressure is reduced (desorption). The presence of hysteresis reduces the eligibility of a microporous material for industrial pressure-swing adsorptive separations, unless the use of temperature-swing is incorporated to effect desorption.

Confirmation of the reliability of each theory as far as pure gas adsorption modeling is concerned would involve determination of experimental data in the high superatmospheric pressure range.

Of the three aluminosilicate molecular sieves investigated, zeolite 5A features the highest energetic heterogeneity with its Si/Al ratio of 1, followed by Turkish clinoptilolite (Si/Al = 4.25) and Cuban clinoptilolite (Si/Al = 5.20). As reflected by the FH-VST predicted limiting amounts of adsorption in Tables 4.1, 4.3, and 4.5, the Ca^{2+} content of zeolite 5A permits higher saturation capacities than the natural clinoptilolites for gas molecules featuring electric moments (CO and N_2). Depending on the qualitative

composition of the gas mixtures to be separated, the mixed cation populations of the clinoptilolites investigated can be seen as both an advantage (if non-polar gases like CH_4 are involved) and a drawback (if polar gases such as CO are present in the mixture). This leads to the conclusion that synthetic zeolites with a population of the same strongly polarizing divalent cations (Ca^{2+}) yield high adsorption capacities, and can be successfully utilized in bulk separations of gas mixtures containing polar species by using pressure-swing adsorption (PSA).

A comparison of adsorbent performance among the aluminosilicate molecular sieves can be made through the degree of rectangularity of the adsorption isotherms at 40°C. The best N_2 adsorbent appears to be Cuban clinoptilolite at pressures atmospheric, and Turkish clinoptilolite in the subatmospheric pressure range. T. clinoptilolite is the best for CH_4 and CO adsorption over the entire pressure range investigated, but the capacity of zeolite 5A for CO is likely to surpass that of Turkish clinoptilolite at very high pressures (because of the more "linear" shape of the isotherms over the pressure range investigated).

As far as energetically homogeneous molecular sieves are concerned, $AlPO_4$-11 and $AlPO_4$-17 adsorb CH_4 in the highest amounts in the pressure range investigated, while $AlPO_4$-18 prefers to accommodate CO in higher amounts because of similar pore and molecular dimensions (which lead to enhanced interactions). The smaller molecular dimensions of N_2 are responsible for the inability of $AlPO_4$-11 and $AlPO_4$-18 to retain it in large amounts, thus proving that steric factors are of tremendous importance in gas adsorption processes going on in aluminophosphate molecular sieves. Steric hindrance is also responsible for the low adsorption capacity of CO in $AlPO_4$-17.

The experimental data lead to the conclusion that in the absence of steric constraints imposed by the geometry of the molecule and that of the pore aperture (e.g. in large-pore aluminophosphate molecular sieves), CH_4 would be preferentially adsorbed ("trapped") in all three molecular sieves. The respective geometries of the pore aperture and the adsorbate molecule determine the equilibrium adsorption capacity through the ability of the gas molecule to interact with the micropore walls. Table 4.11 summarizes steric accessibility granted by each aluminophosphate molecular sieve to each adsorbate.

Table 4.11 Extent of steric accessibility for the adsorption of N_2, CO, CH_4 in $AlPO_4$-11, $AlPO_4$-17, and $AlPO_4$-18.

Adsorbate	$AlPO_4$-11	$AlPO_4$-17	$AlPO_4$-18
N_2	full	high	very high
CO	full	low[1]	high[2]
CH_4	full	very high	medium[1]

[1] molecular sieving effect; [2] especially at higher pressures

Consequently, it is possible to anticipate the adsorbate-adsorbent affinity ranking resulting from the single-component experimental isotherms. The observed preferences of each aluminophosphate molecular sieve are summarized below:

$AlPO_4$-11 (elliptical pores 3.9 x 6.3 Å; unidimensional channel structure):	$CH_4 > CO > N_2$
$AlPO_4$-17 ("ink-bottle" pores 3.6 x 5.1 Å, three-dimensional channel structure):	$CH_4 >> N_2 > CO$
$AlPO_4$-18 (pear-shape pores 3.8 x 3.8 Å, three-dimensional channel structure):	$CO > CH_4 >> N_2$

In the case of isotherm measurement in small-pore aluminophosphate molecular sieves, steric effects are likely to lead to hysteresis: the pressure measured is higher in the gas phase than the equilibrium pressure during adsorption, and it is lower in the gas phase than the equilibrium pressure during desorption. Thus, steric constraints could explain the hysteresis effect observed experimentally at 40°C for the CO / $AlPO_4$-17, CO / $AlPO_4$-18, and CH_4 / $AlPO_4$-18 isotherms. During adsorption, these constraints impose a slightly higher adsorption pressure in order to attain a certain capacity. During desorption, the impeding steric factors are probably responsible for a higher pressure within the micropores. This hypothesis could be checked with adsorbate molecules of smaller kinetic diameter such as carbon dioxide, CO_2 (3.3 Å) and nitric oxide, NO (3.17 Å). Other small molecules such as water, acetylene, C_2H_2 (3.3 Å), ammonia NH_3 (2.6 Å) may be too well

retained by the aluminophosphate molecular sieves whose framework oxygen atoms could form hydrogen bonds with the hydrogen atoms available in these adsorbate molecules.

4.2 PREDICTED BINARY MIXTURE ADSORPTION ISOTHERMS

Binary gas mixture isotherms provide quantitative information pertaining to the amount of individual components adsorbed, as well as to the behaviour of the adsorption system as a function of the sorbate concentration. Generally, a mixture can be considered to behave ideally in the absence of interactions or in the presence of weak interactions between its components. Strong interactions between mixture components would classify the adsorbed mixture as non-ideal. The degree of curvature in the binary adsorption isotherms reflects the intensity of the interactions between the sorbent and the sorbate: the greater the curvature of the component isotherms, the stronger the sorbent-sorbate interactions.

Equilibrium XY diagrams provide important qualitative information on the selectivity of the solid adsorbent used to separate the gaseous mixture. The farther away the XY curve is from the X = Y line, the higher the value of the equilibrium separation factor. As far as the modelling theories applied in the present study for the prediction of gas mixture adsorption are concerned, ELM yields a constant separation factor, whereas the separation factor varies with composition in the case of FH-VST and IAST.

All predictions have been determined for a total pressure of 101.3 kPa. In order to achieve a better separation, Ruthven (1976) recommends a low operating pressure for systems in which the more strongly adsorbed species has the larger molecular volume. In the case of the adsorbates investigated in this study the kinetic diameters are fairly similar and the separation factors are considered to be essentially independent of pressure.

ELM predictions can be obtained using either equation (2.8) which calculates the capacity of the adsorbent for each component in the mixture from the Langmuir monolayer capacities of the pure components (termed herein "direct-approach" ELM and abbreviated d-ELM), or equation (2.10), resulting from the amendment of equation (2.8)

with the thermodynamic consistency equation (2.9), based on the averaged monolayer capacity of the adsorbent for the mixture (termed herein "averaging-approach" ELM and abbreviated a-ELM).

4.2.1 Aluminosilicate Molecular Sieves

4.2.1.1 Binary Mixture Equilibrium Adsorption in Zeolite 5A

Carbon Monoxide - Nitrogen / 5A. Figures 4.7 and 4.8 reveal that all the models predict a better separation of CO-N_2 mixtures at 40°C compared to room temperature. A slight increase in selectivity at 40°C with a decrease in the CO content of the mixture (according to IAST and FH-VST) confirms the adequacy of zeolite 5A as a good adsorbent in air purification applications. This temperature-enhanced selectivity is probably due to the fact that a higher temperature means, despite the decrease in component and mixture capacities, lower coverage and therefore less intense repulsions between adsorbed molecules featuring electric moments.

The increase in temperature appears to augment the discrepancy between the predictions of a-ELM and the other models (IAST, FH-VST, and d-ELM). a-ELM is likely to yield erroneous predictions because it grants too much weight to the weakly adsorbed component at the expense of the strongly adsorbed component. Binary gas mixtures involving species for which zeolite 5A has very different affinities could be especially prone to inadequate a-ELM predictions, because the equality of the monolayer volumes of the components in the mixture cannot be easily attained and the thermodynamic consistency condition is not met. Furthermore, this condition (equation 2.9) cannot hold if the total pressure is not approaching the value for which the monolayer volumes of the components in the mixture are equal. Since the isotherm is not fully determined, assessing the applicability of the thermodynamic consistency equation could be a risky undertaking in the present study.

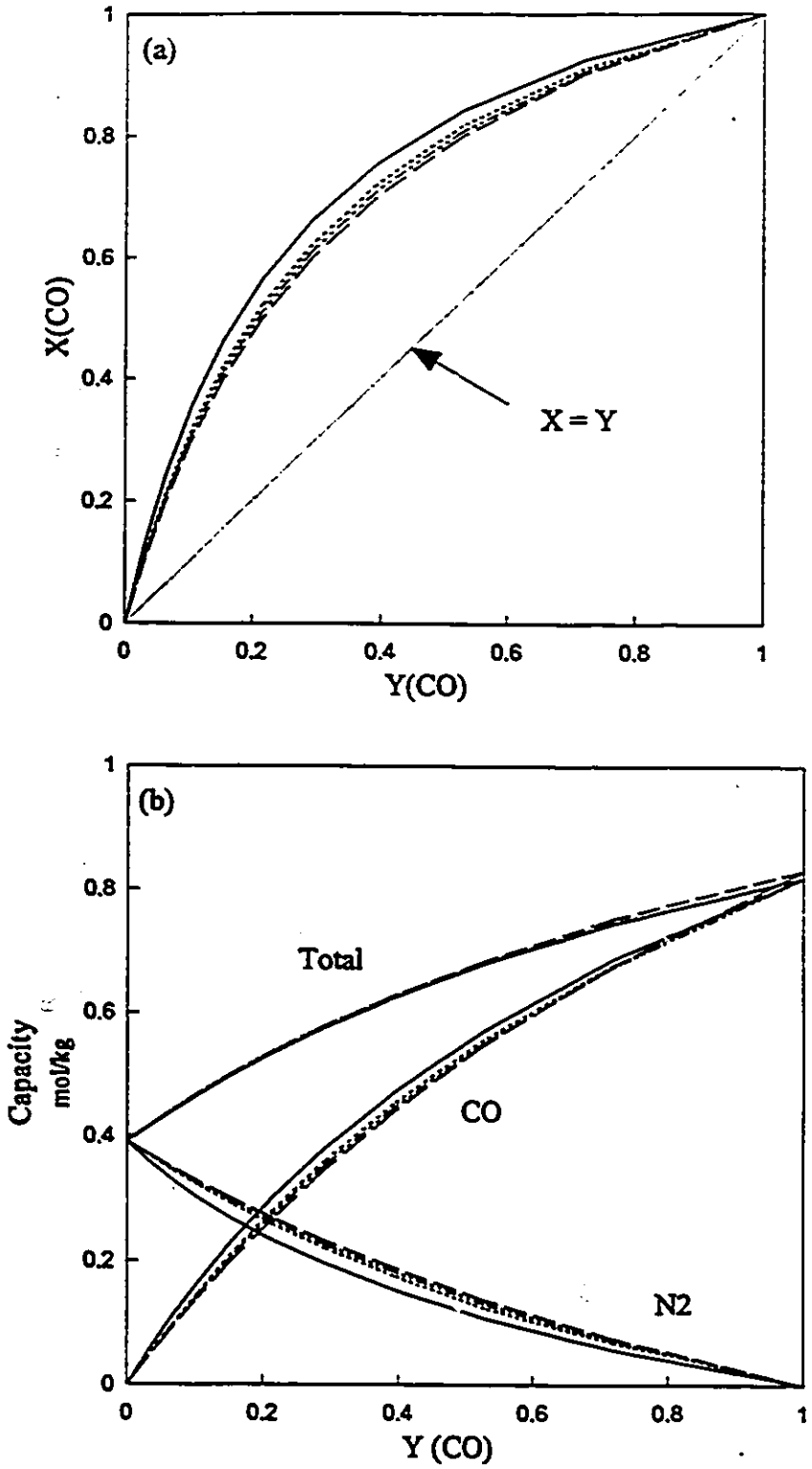

Figure 4.7 Predicted (a) X-Y diagram and (b) binary equilibrium isotherm for CO-N2 adsorption on zeolite 5A at 22.6-22.7°C and 101.3 kPa total pressure
_____ a-ELM _ _ _ _ FH-VST _ _ _ _ IAST ——— d-ELM

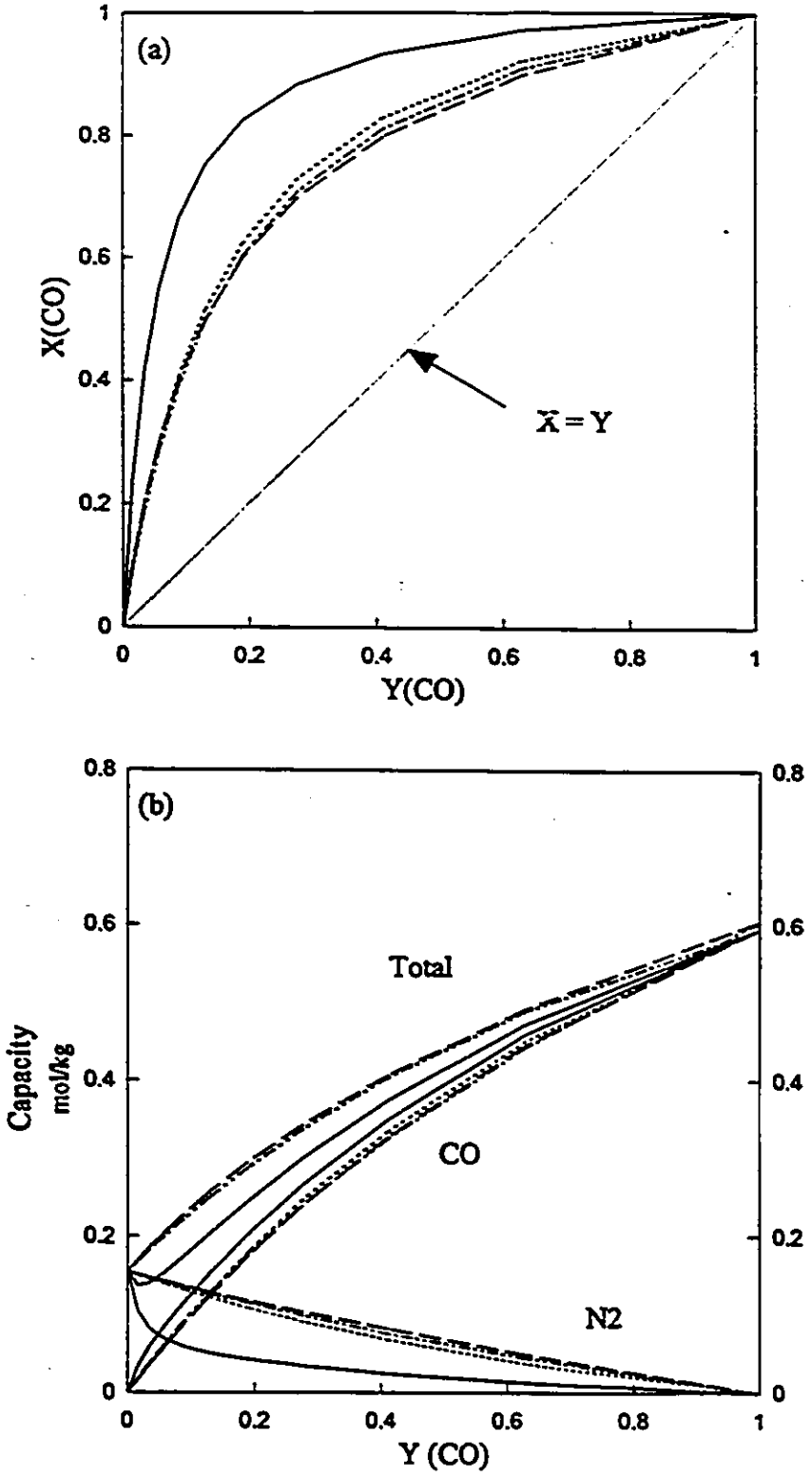

Figure 4.8 Predicted (a) X-Y diagram and (b) binary equilibrium isotherm for CO-N2 adsorption on zeolite 5A at 39.8-40.0°C and 101.3 kPa total pressure
_____ a-ELM _ _ _ _ FH-VST _ _ _ IAST ——— d-ELM

CO is the better adsorbed component, which is not surprising given its polarity and larger molecular dimensions. The affinity of the energetically heterogeneous zeolite 5A framework for polar CO and the smaller molecular dimensions as well as the quadrupolarity of N_2 facilitate the displacement of adsorbed N_2 molecules. Zeolite 5A will always preferentially adsorb the adsorbate which can provide a higher specific contribution to the total adsorption potential of the system (CO). In the case of the CO-N_2 gas mixture, the equilibrium separation factor of CO relative to N_2 is higher at the higher temperature because, as explained in the single-component equilibrium adsorption section, zeolite 5A cannot hold strongly the highly mobile N_2 molecules at 40°C. At this temperature, the individual and total adsorption capacities will obviously be lower but the selectivity will be higher for the polar molecule able to contribute specific adsorption potential.

According to a-ELM, traces of CO in the mixture would "inhibit" or "discourage" the adsorption of N_2 at 40°C (Figure 4.8), unless the N_2 partial pressure in the gas phase is very high. However, a-ELM does not predict a correspondingly higher adsorption capacity of zeolite 5A for CO, as expected from the experimental pure-component information. The "hook" featured by the a-ELM curve representing the total amount adsorbed apparently means that small amounts of CO cause the displacement (desorption) of large amounts of N_2 without the corresponding adsorption of equal or larger amounts of CO. This is a very unrealistic situation since single-component adsorption data have revealed that CO is better adsorbed than N_2 and, therefore, CO should be adsorbed in amounts equivalent to the amounts of N_2 displaced.

At 40°C IAST, FH-VST, and d-ELM do not forecast this particular type of behaviour at high N_2 partial pressures, but they acknowledge slightly more intense interactions for the CO molecules (the CO branch of the binary equilibrium isotherm is curvier than the N_2 branch). FH-VST provides quantitative proof to this effect through the composition-dependent values of the activity coefficients (Appendix D): γ_{N2} values are very close to unity, while γ_{CO} values increase with increasing CO partial pressure.

At room temperature the three models (IAST, FH-VST, and d-ELM) are in much closer agreement. The lower CO selectivity of zeolite 5A at room temperature can

be understood in terms of close-range repulsions: since the coverage is higher at a lower temperature, repulsive interactions would be accordingly higher. All these models acknowledge a slightly stronger interaction of N_2 with the adsorbent (curvier N_2 branch) at room temperature compared to that at 40°C, due to the lower mobility of the N_2 molecules which allows more intense field gradient - quadrupole interactions.

The much higher selectivity values predicted by a-ELM compared to the other models can be attributed to the averaging procedure which leads to an expression of the separation factor which is a function of the Langmuir constants B_i, but not of the averaged monolayer volumes v_M or the individual pure-component monolayer volumes v_{mi}. Thus, the averaging procedure enhances the contribution of the less adsorbed component too much.

Carbon Monoxide - Methane / 5A. In the case of this system, the difference in the polarity of the gas species is the largest since CH_4 is non-polar while CO features a dipole moment in addition to the quadrupole moment. CH_4, however, has the higher polarizability.

Figures 4.9 and 4.10 show binary mixture predictions of different models for the CO-CH_4 / 5A adsorption system. CO is the better adsorbed component in this binary gas mixture, as expected from the pure-gas adsorption data. The selectivity values/ranges predicted by all the models for zeolite 5A are relatively similar for both adsorption temperatures (Table 4.12).

Table 4.12 Predicted equilibrium separation factors for zeolite 5A at 101.3 kPa total pressure for all the adsorption systems.

Binary gas mixture adsorption system (1) - (2) / Adsorbent	Temperature [°C]	Predicted equilibrium separation factors a-ELM	d-ELM	IAST	FH-VST
CO-N_2 / 5A	39.8-40.0	20.39	7.09	6.77-5.98	7.42-5.31
	22.6-22.7	4.73	3.98	3.86-3.71	2.86-3.54
CO-CH_4 / 5A	40.0-40.1	5.11	4.16	4.07-3.89	5.22-2.67
	22.6-22.8	3.71	4.25	4.35-4.52	4.19-4.23
CH_4-N_2 / 5A	39.8-40.1	3.99	1.71	1.65-1.63	1.65-1.57
	22.7-22.8	1.28	0.94	0.888-0.892	0.92-0.86

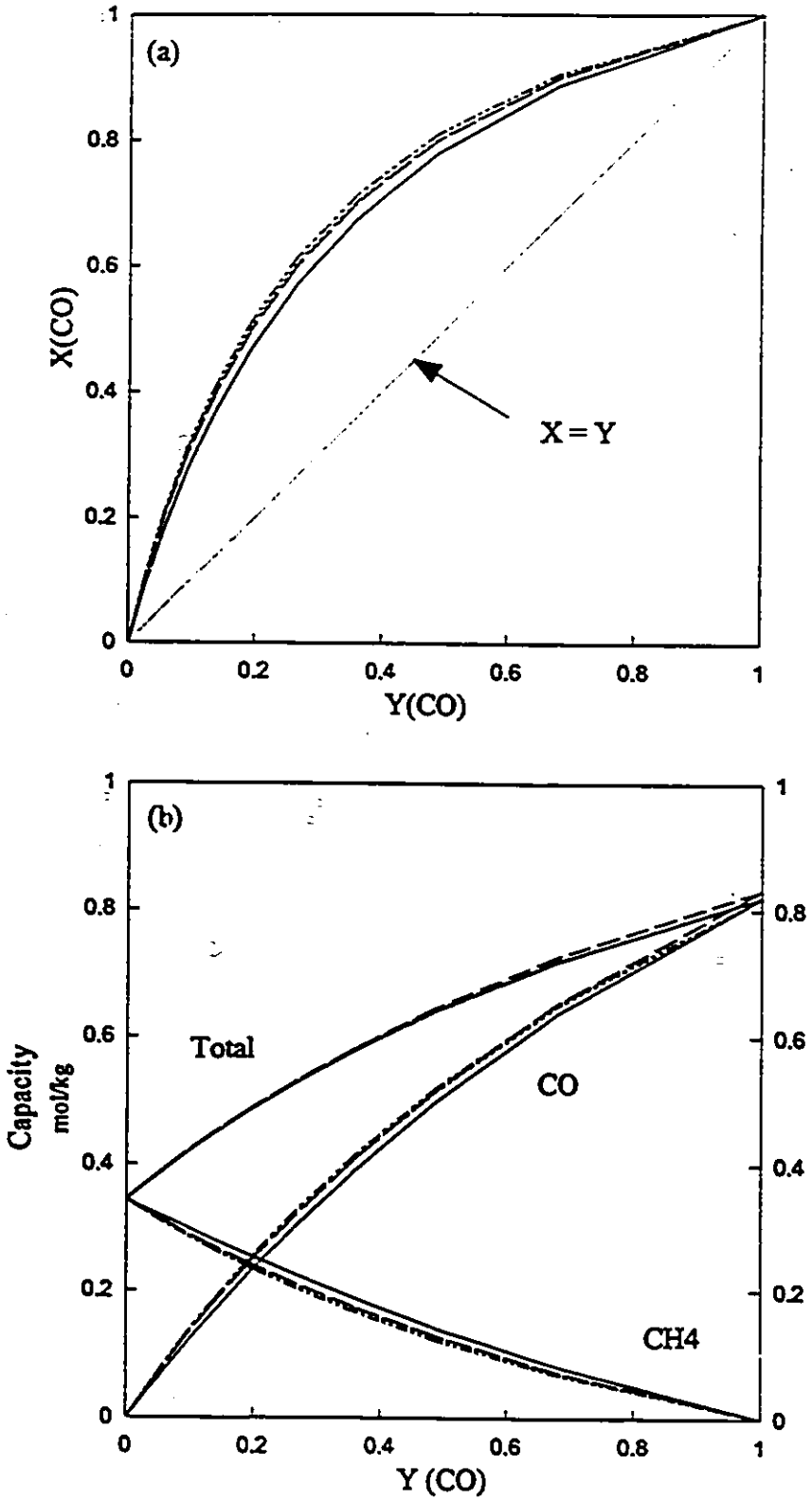

Figure 4.9 Predicted (a) X-Y diagram and (b) binary equilibrium isotherm for CO-CH4 adsorption on zeolite 5A at 22.6-22.8°C and 101.3 kPa total pressure
_____ a-ELM _ _ _ _ FH-VST _ _ _ _ IAST ——— d-ELM

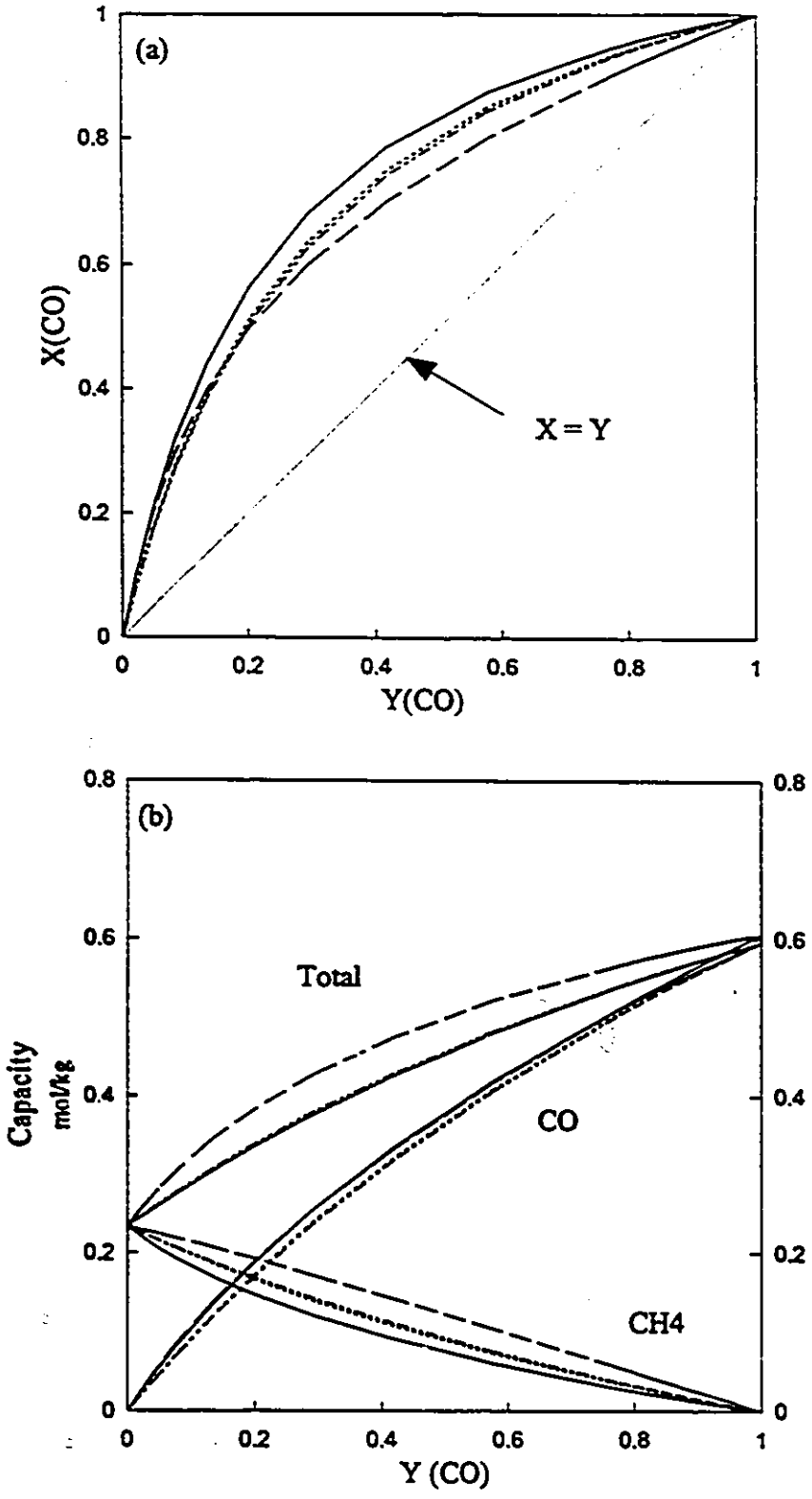

Figure 4.10 Predicted (a) X-Y diagram and (b) binary equilibrium isotherm for CO-CH4 adsorption on zeolite 5A at 40.0-40.1°C and 101.3 kPa total pressure
_____ a-ELM _ _ _ _ FH-VST _ _ _ IAST ——— d-ELM

The total lack of polarity of the CH_4 molecule could be responsible for the relative insensitivity of the separation to the adsorption temperature. Despite its high polarizability, CH_4 does not become sufficiently polarized to compete with the full-fledged polar character of CO. The extremely weak interactions consequently existing between the adsorbate molecules make the adsorbed phase quasi-ideal. In the adsorbed phase there are no strong interactions between the non-polar CH_4 molecules themselves or between the non-polar CH_4 and polar CO molecules. Interactions between adsorbed CO molecules are probably not so intense because of the presence of CH_4 molecules interspersed among the CO molecules acting as a "buffer."

At room temperature, the absence of strong interactions within the adsorbed phase could explain the close agreement between the predictions yielded by the three models, since the ideal adsorbed phase assumption is valid for ELM and IAST. In the case of FH-VST, both gas-vacancy interaction parameters regressed for pure-component adsorption are zero, and thus the hypothesis of negligible interactions between non-polar CH_4 molecules and polar CH_4 molecules appears reasonable. The adsorbate-adsorbent interactions between the CO molecules and the Ca^{2+} cations in the energetically heterogeneous zeolite 5A are much stronger than the adsorbate-adsorbate interactions between polar CO and non-polar CH_4 molecules, and the latter can therefore be considered negligible. The quasi-perfect agreement between IAST and d-ELM at room temperature backs up the validity of the ideal adsorbed phase assumption. The fact that a-ELM predictions are slightly "straying" from the others at room temperature is probably due to the averaging, which "exaggerates" the influence of one species over the other in the adsorbed phase by conferring too much "weight" to non-polar CH_4 and by diminishing the impact of the electrostatic contribution of the polar CO in terms of self-potential. The a-ELM predictions may not be extremely reliable considering that the averaging supplements unfavourably the fact that the Langmuir fits for the CO / 5A experimental isotherms are good, but not perfect.

At 40°C the FH-VST predicted X-Y diagram is more asymmetric than the one corresponding to room temperature binary mixture adsorption. FH-VST predicts lower selectivities than the other models for $Y(CO) > 0.2$, i.e. $X(CO) > 0.5$, and higher

selectivities than either IAST or the d-ELM below Y(CO) = 0.2, approaching the a-ELM estimations in that composition range. This asymmetry could be related to the close-range repulsions between the polar CO molecules adsorbed in higher amounts than CH_4 molecules at X(CO) > 0.5. At these mole fractions of CO in the adsorbed phase, the CH_4 molecules interspersed among the CO molecules cannot play their role of repulsion-attenuating buffers as successfully as they do it when X(CO) < 0.5.

The more pronounced asymmetry in the FH-VST prediction of the XY diagram at 40°C for the CO-CH_4 system compared to the CO-N_2 system could be attributed to the difference in the polarity of the adsorbates and the entailing repulsive interactions in the adsorbed phase. At 40°C the adsorption capacities of zeolite 5A for the components in the CO-CH_4 mixture are lower than those at room temperature, but CO is still better retained than CH_4 because of its polarity. However, a lower fractional coverage by CH_4 when X(CO) > 0.5 means more intense repulsive interactions between the CO molecules adsorbed. When X(CO) < 0.5, repulsive interactions between CO molecules are more easily "dealt with" in the system since the fractional coverage by CH_4 molecules is higher. Thus, the difference in polarity between the adsorbates could be dictating the extent of asymmetry of the X-Y diagram predicted by FH-VST (Figure 4.10).

Methane - Nitrogen / 5A. The phase equilibrium diagrams in Figures 4.11a and 4.12a show that the separation of N_2 from CH_4 cannot be performed with zeolite 5A at either temperature investigated, although the selectivities are slightly higher at 40°C. At both room temperature and 40°C IAST, FH-VST, and d-ELM virtually agree in their estimations of the separation capability of zeolite 5A for this mixture. These models predict that at 40°C the adsorbed phase will be richer in CH_4, whereas at 23°C the adsorbed phase will be richer in N_2, as expected from the experimental pure-component isotherms (Figure 4.1).

At room temperature FH-VST sees the CH_4-N_2 mixture in the adsorbed phase as "ideal" because of the zero and near-zero values of the adsorbate-vacancy interaction parameters for pure-gas adsorption (Table 4.1) and, accordingly, the activity coefficients are approaching unity.

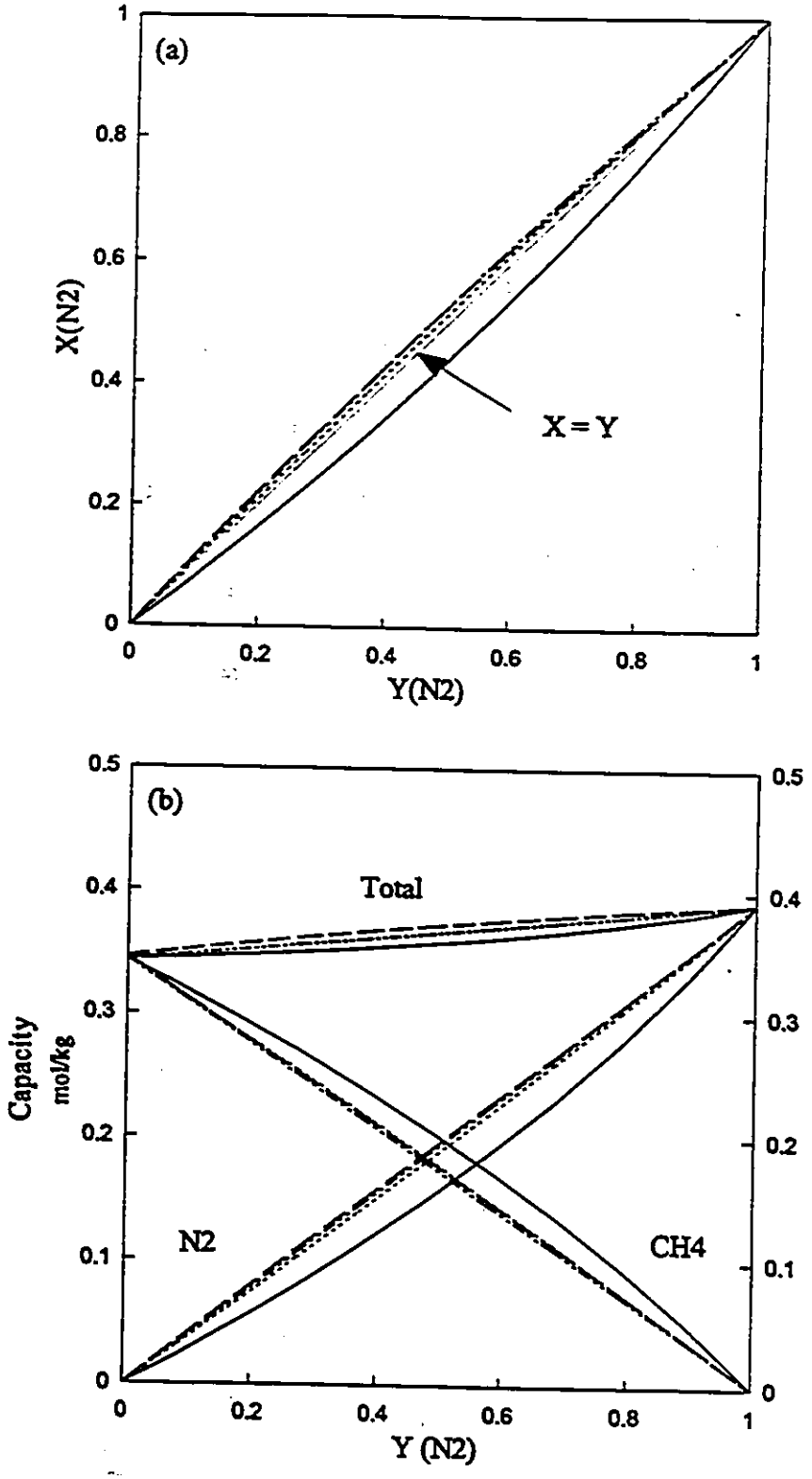

Figure 4.11 Predicted (a) X-Y diagram and (b) binary equilibrium isotherm for CH4-N2 adsorption on zeolite 5A at 22.7-22.8°C and 101.3 kPa total pressure
——— a-ELM _ _ _ _ FH-VST _ _ _ IAST ——— d-ELM

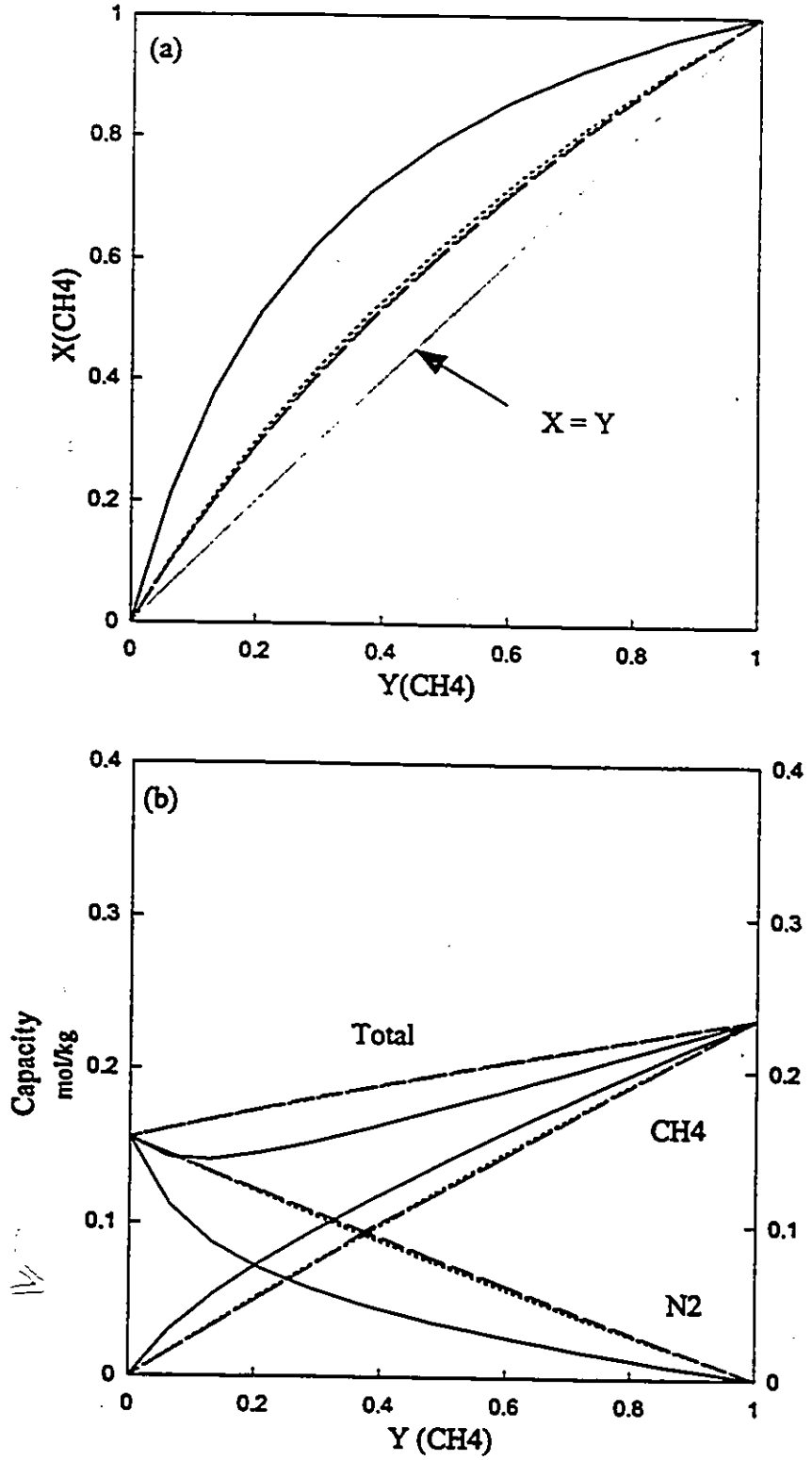

Figure 4.12 Predicted (a) X-Y diagram and (b) binary equilibrium isotherm for CH4-N2 adsorption on zeolite 5A at 39.8-40.1°C and 101.3 kPa total pressure
——— a-ELM _ _ _ _ FH-VST _ _ _ _ IAST ——— d-ELM

The a-ELM predictions lack reliability since they indicate that at room temperature the better adsorbed component is CH_4. Considering the experimental pure-component information available (Figure 4.1), CH_4 is, indeed, better adsorbed than N_2 in zeolite 5A at 40°C. However, the adsorption capacity for CH_4 is lower than for N_2 at room temperature, a fact that a-ELM fails to acknowledge in its binary mixture adsorption prediction. The averaging of the relative contributions of the components in the mixture to the overall adsorption potential leads therefore to unrealistic predictions at room temperature. In the absence of experimental confirmation, the FH-VST and IAST predictions could be perceived as fairly reliable. According to these predictions, it appears that zeolite 5A would be a risky choice for the separation of CH_4-N_2 gas mixtures.

Summary for 5A. As shown by the predicted binary equilibrium isotherms and XY diagrams (Figures 4.7 through 4.12), zeolite 5A appears to perform a good separation of mixtures of components with very different polarities (CO-N_2 and CO-CH_4), but is not suitable for mixtures consisting of nonpolar and quadrupolar species (CH_4-N_2). Comparison with literature data is not really possible because of the different adsorption conditions (temperature and total pressure) reported.

The predicted effect of adsorption temperature is the one expected: the capacity of zeolite 5A for either individual component adsorbed from the mixture and for the total amount adsorbed decreases as the adsorption temperature increases.

4.2.1.2 Binary Mixture Equilibrium Adsorption in Turkish Clinoptilolite

Carbon Monoxide - Nitrogen / Turkish Clinoptilolite. Figures 4.13 and 4.14 show that all models agree on the fact that the polar species (CO) would be the better adsorbed component. IAST and FH-VST predictions are relatively close to one another, while ELM predictions are pessimistic in both the selectivity values and the total amount adsorbed (according to a-ELM, the separation of the mixture is feasible only at room temperature). Possible explanations would be the fact that the Langmuir pure-gas adsorption isotherm fits were not perfect in the pressure range investigated.

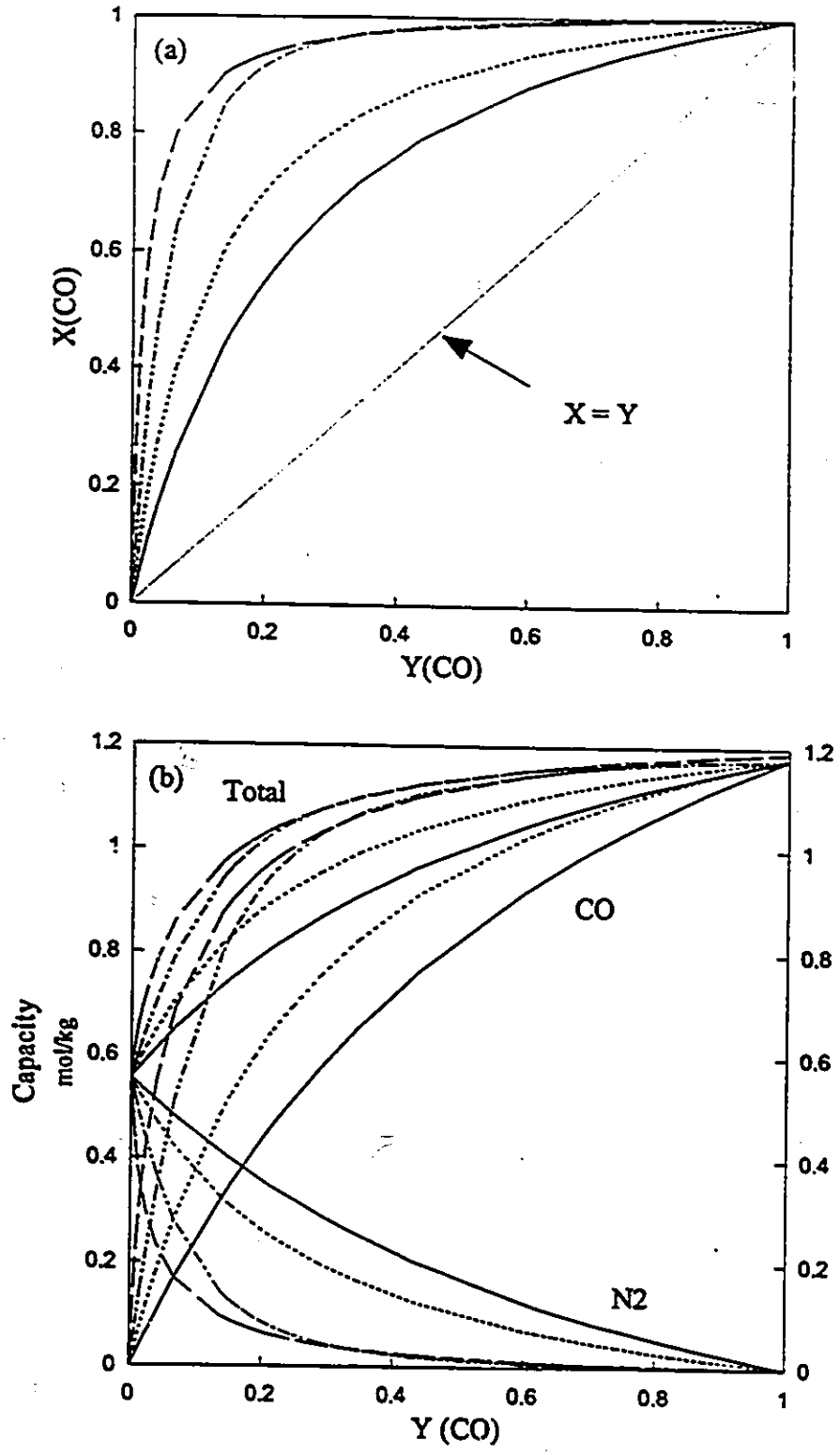

Figure 4.13 Predicted (a) X-Y diagram and (b) binary equilibrium isotherm for CO-N2 adsorption on Turkish clinoptilolite at 22.6-22.8°C and 101.3 kPa total pressure
——— a-ELM _ _ _ _ _ FH-VST _ _ _ _ IAST ——— d-ELM

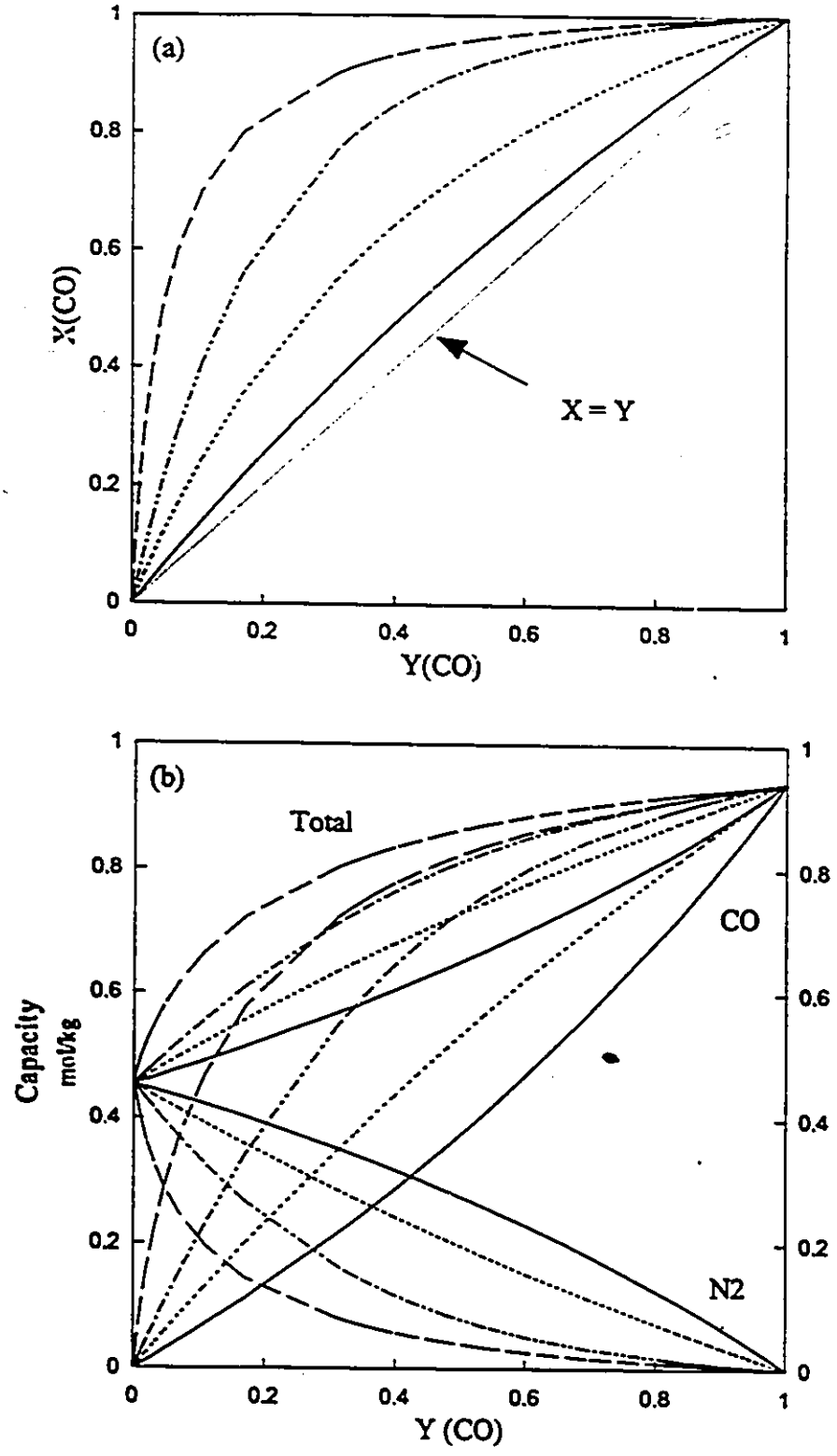

Figure 4.14 Predicted (a) X-Y diagram and (b) binary equilibrium isotherm for CO-N2 adsorption on Turkish clinoptilolite at 40.0°C and 101.3 kPa total pressure
_____a-ELM _ _ _ _ FH-VST _ _ _ _ IAST ——— d-ELM

IAST and FH-VST predictions are closer at room temperature than at 40°C. As illustrated by the stronger curvature of the corresponding binary adsorption isotherms, both IAST and FH-VST perceive the behaviour of the system as being strongly non-ideal at room temperature (potentially true). The strong adsorbate-adsorbent interactions anticipated by IAST and FH-VST in this adsorption system appear logical given the presence of electric moments in the gaseous species involved and the energetic heterogeneity topped by electrical "non-uniformity" (due to the presence of a mixed cation population) of the adsorbent.

FH-VST predicts stronger non-ideal behaviour of the adsorbates in the adsorbed phase at room temperature than at 40°C because of more intense electrostatic interactions at this temperature. The FH-VST equilibrium selectivities are higher at room temperature than at 40°C, as expected from the experimental pure-gas adsorption data available (Figure 4.2): at 101.3 kPa, the difference between the equilibrium adsorption capacities of Turkish clinoptilolite for pure CO and pure N_2 at room temperature is much higher than at 40°C.

Carbon Monoxide - Methane / Turkish Clinoptilolite. Figures 4.15 and 4.16 show that the models appear to follow the same predicting trend as the one followed for the adsorption of CO-N_2 mixture for this adsorbent. The weaker interactions at the higher temperature could be probably associated with the lower partial fractional coverages and the larger difference in polarity between the two gaseous components.

IAST yields higher separation factors than ELM since it predicts higher capacities for CO than ELM. As seen with the CO-N_2 mixture, the IAST predicted selectivities increase with increasing CO content at both temperatures (Table 4.13).

At both temperatures FH-VST predicts the highest equilibrium separation factors. Deviations from ideal behaviour in the adsorbed phase are reflected in the ranges of the γ_v activity-coefficient values (Table 4.14). According to these activity coefficients, both N_2 and CO deviate from ideality but CO is, as expected, the less ideally-behaving species at both temperatures.

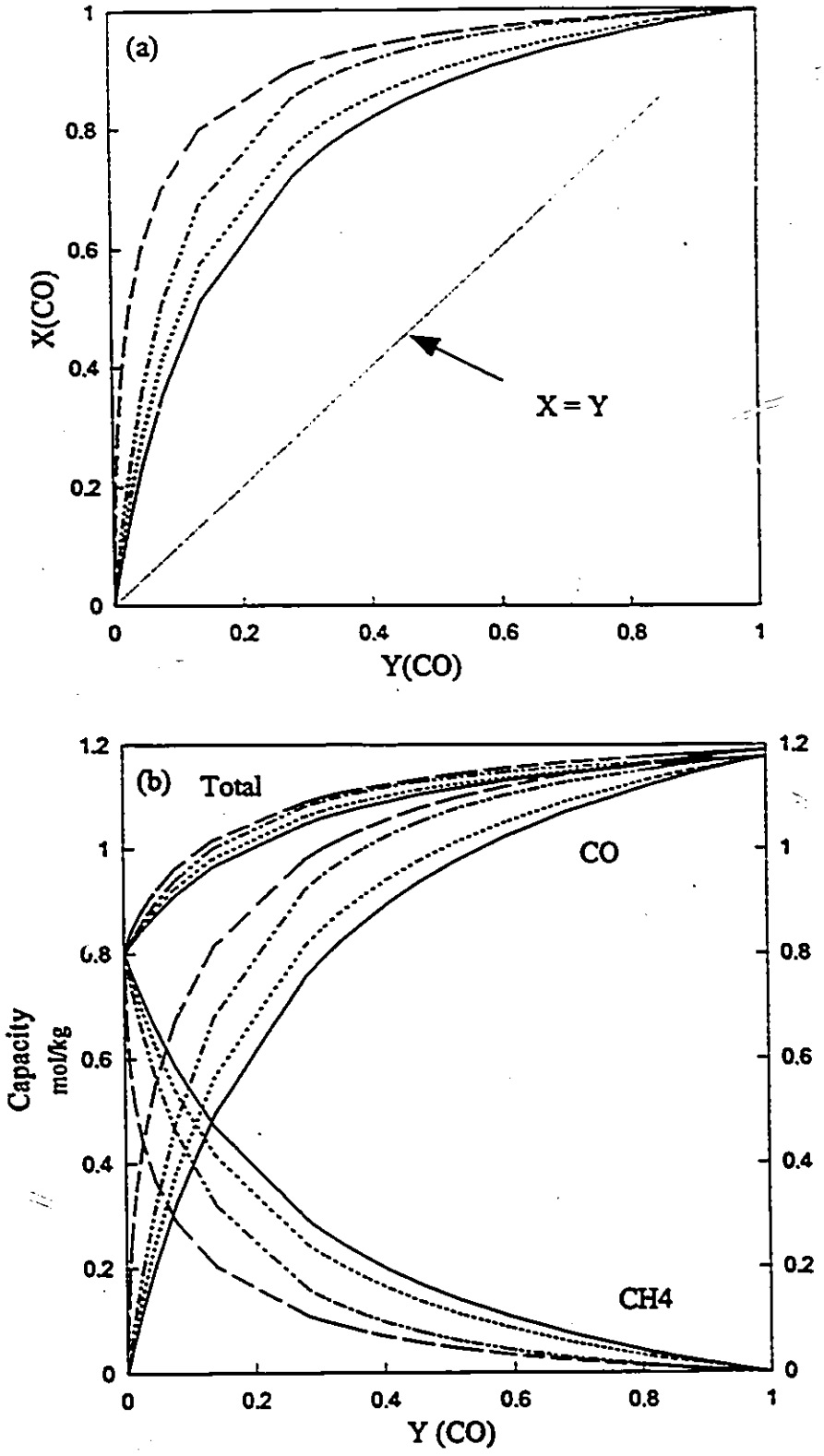

Figure 4.15 Predicted (a) X-Y diagram and (b) binary equilibrium isotherm for CO-CH4 adsorption on Turkish clinoptilolite at 22.8°C and 101.3.kPa total pressure
_____ a-ELM _ _ _ _ _ FH-VST _ _ _ _ IAST ——— d-ELM

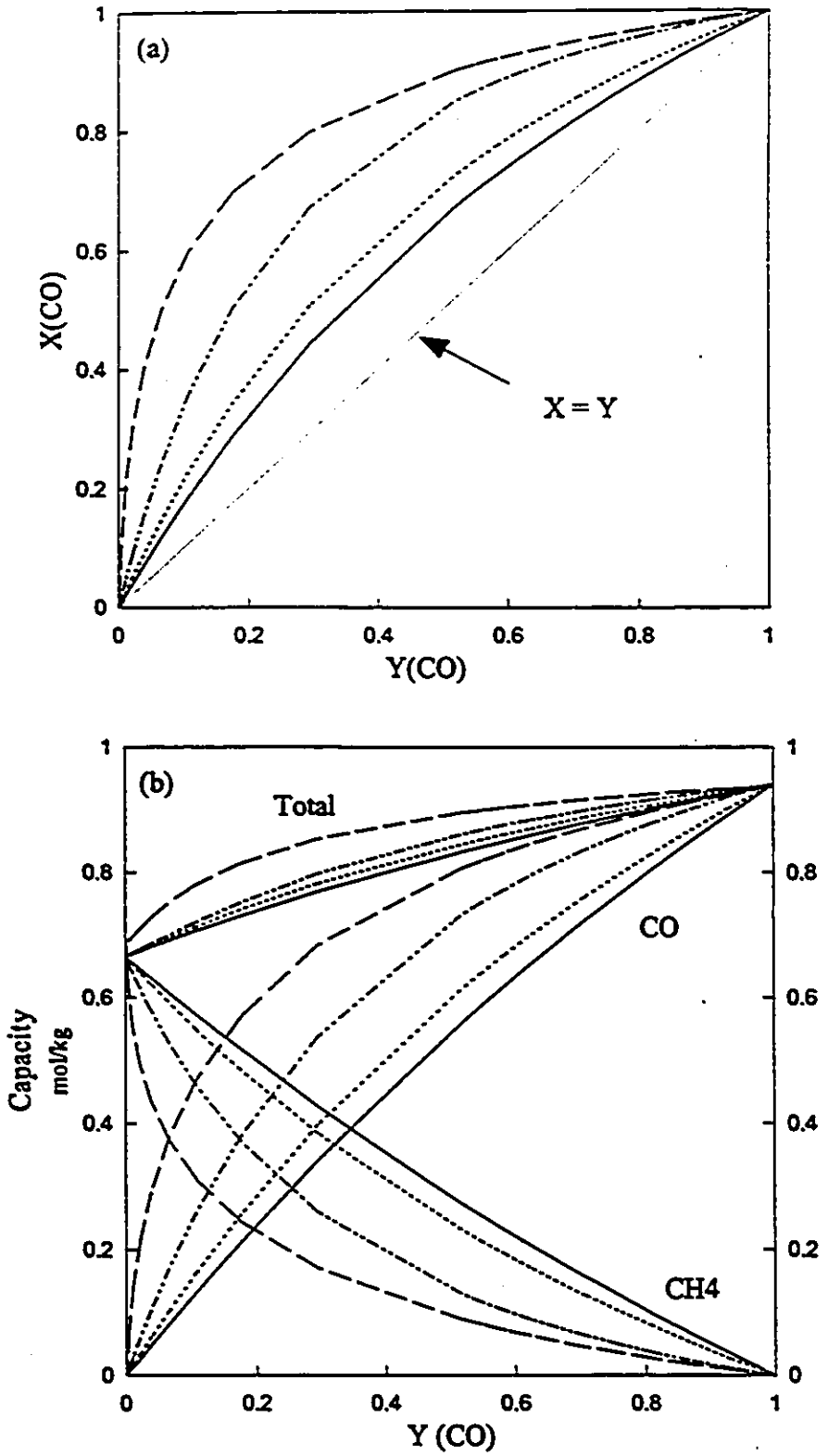

Figure 4.16 Predicted (a) X-Y diagram and (b) binary equilibrium isotherm for CO-CH4 adsorption on Turkish clinoptilolite at 40.0°C and 101.3 kPa total pressure
_____ a-ELM _ _ _ _ _ FH-VST _ _ _ _ IAST ———— d-ELM

Table 4.13 Predicted equilibrium separation factors for Turkish clinoptilolite (TC) at 101.3 kPa total pressure for all the adsorption systems

Binary gas mixture adsorption system (1)-(2)/Adsorbent	Temperature [°C]	Predicted equilibrium separation factors (*azeotrope) a-ELM	d-ELM	IAST	FH-VST
$CO-N_2$ / TC	40.0	1.36	2.72	5.09-14.27	24.11-19.62
	22.6-22.8	4.91	9.48	18.57-144.9	77.13-57.96
$CO-CH_4$ / TC	40.0	1.91	2.47	4.51- 5.68	29.13- 7.46
	22.8	8.54	6.61	11.25-19.48	110.5 -22.38
CH_4-N_2 / TC	40.0	0.71	1.10	1.72- 2.02	2.42-0.43*
	22.6-22.8	0.74	1.11	1.78-2.10	2.04-0.53*

Table 4.14 Ranges of FH-VST predicted vacancy activity coefficient values for binary mixture adsorption systems involving zeolites as adsorbents and N_2, CO, CH_4 binary mixtures (corresponding to 0.1 - 0.9 reference species mole fraction range)

Adsorbent	Gas Mixture	Reference species	Temperature	Range of γ_v values
Zeolite 5A	$CO-N_2$	CO	39.8-40.0	0.9999 - 0.9722
			22.6-22.7	1.0000
	$CO-CH_4$	CO	40.0-40.1	0.9986 - 0.9674
			22.6-22.8	1.0000
	CH_4-N_2	CH_4	39.8-40.1	1.0000 - 0.9980
			22.7-22.8	1.0000
Turkish Clinoptilolite	$CO-N_2$	CO	40.0	0.4276 - 0.3696
			22.6-22.8	0.3653 - 0.2759
	$CO-CH_4$	CO	40.0	0.7203 - 0.3715
			22.8	0.6438 - 0.2690
	CH_4-N_2	CH_4	40.0	0.4479 - 0.7173
			22.6-22.7	0.3844 - 0.6599
Cuban Clinoptilolite	$CO-N_2$	CO	40.0-40.1	0.9219 - 0.7686
	$CO-CH_4$	CO	40.0-40.1	0.7751 - 0.9232
	CH_4-N_2	CH_4	40.0	0.9322 - 0.9329

Methane - Nitrogen / Turkish Clinoptilolite. Figures 4.17 and 4.18 show that according to the selectivities predicted by each model, the separation of quadrupolar N_2 from the non-polar CH_4 is virtually not feasible with Turkish clinoptilolite. The values of

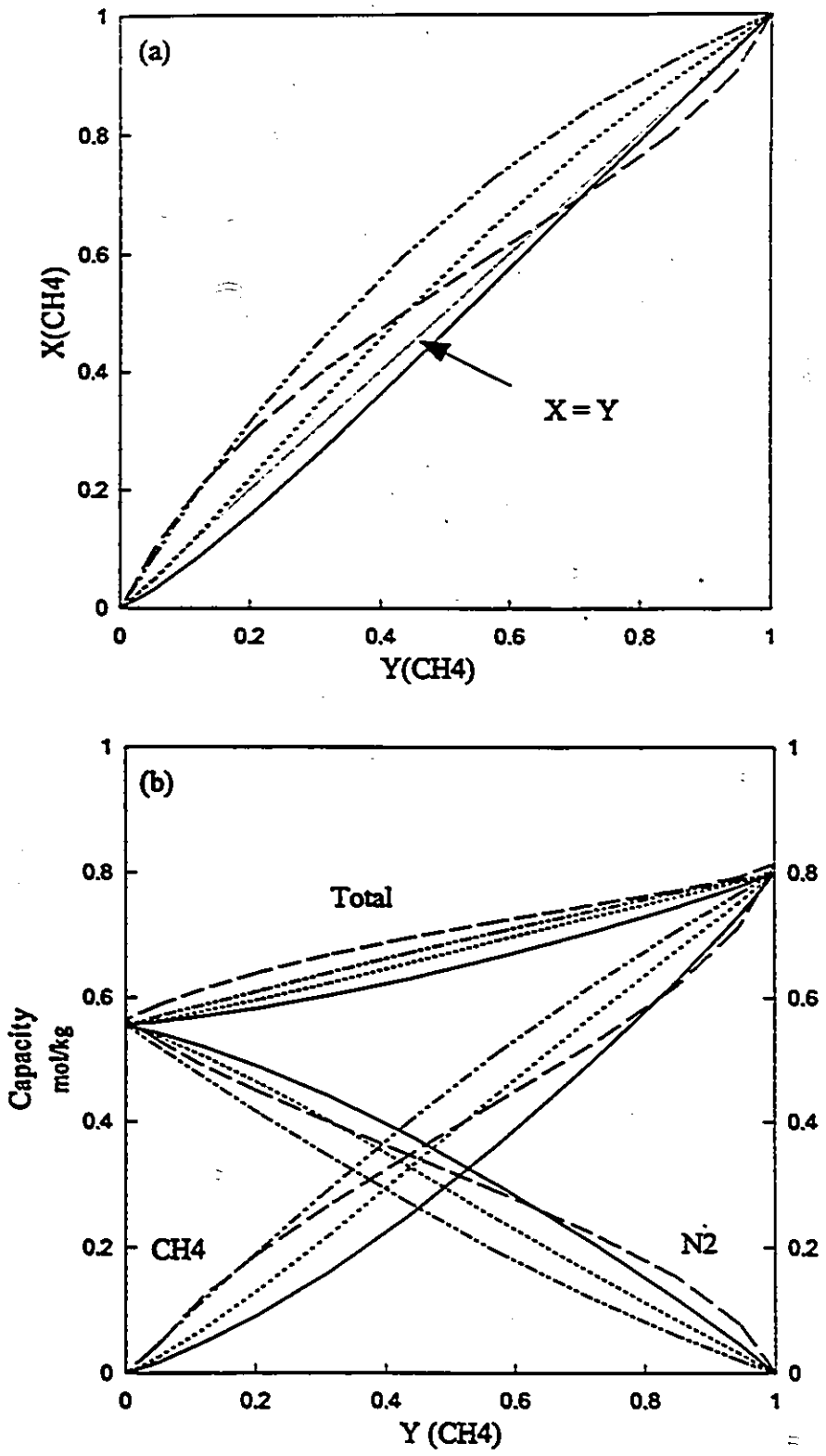

Figure 4.17 Predicted (a) X-Y diagram and (b) binary equilibrium isotherm for CH4-N2 adsorption on Turkish clinoptilolite at 22.6-22.8°C and 101.3 kPa total pressure
_____ a-ELM _ _ _ _ _ FH-VST _ _ _ _ IAST ——— d-ELM

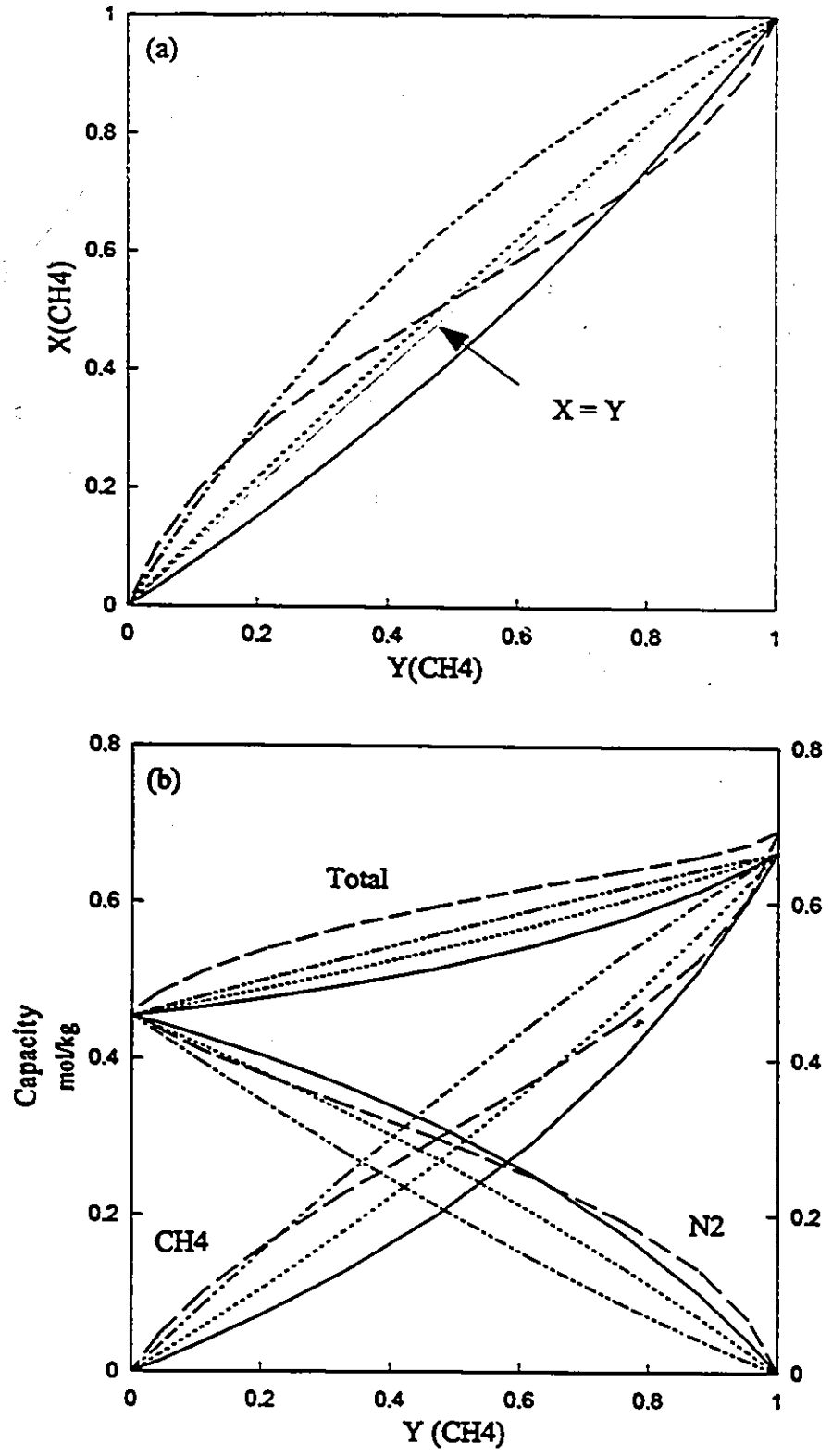

Figure 4.18 Predicted (a) X-Y diagram and (b) binary equilibrium isotherm for CH4-N2 adsorption on Turkish clinoptilolite at 40.0°C and 101.3 kPa total pressure
_____ a-ELM _ _ _ _ _ FH-VST _ _ _ _ IAST ——— d-ELM

the separation factors are very weakly influenced by the change in the adsorption temperature (Table 4.13). The influence of the adsorption temperature appears to be exerted on the total amount adsorbed, with higher amounts adsorbed at room temperature.

As shown in Appendix D, the IAST-predicted equilibrium separation factors increase with increasing partial pressure of CH_4 (the better adsorbed component), with the corresponding range provided in Table 4.13. A small composition dependence of these selectivities is to be expected, according to Myers and Prausnitz (1965).

At room temperature as well as at 40°C, FH-VST predicts the formation of an azeotrope at $Y(CH_4) = 0.64$ and $Y(CH_4) = 0.54$, respectively. This is expected since the FH-VST fits of the experimental adsorption isotherms intersect (Figure 4.2). Although the datapoints measured on each experimental isotherm by Stelmack (1994) do not show a crossover point, Ackley and Yang (1991b) reported a crossover for the same binary system with another clinoptilolite. ELM, known in the literature as the "constant separation factor approximation," yields XY diagrams that are almost symmetric, and cannot predict selectivity reversal and azeotrope formation given the Langmuir assumptions of ideal adsorbed and gas phases. Similarly, IAST is unable to forecast non-ideal behaviour such as azeotrope formation since it was not developed to describe non-ideal adsorption systems.

Summary for Turkish clinoptilolite. All models agree that the separation factors as well as the capacities are higher at the lower temperature for the adsorption systems investigated at 101.3 kPa total pressure (Table 4.13). Even those predicted at 40°C allow a satisfactory separation of these particular gas mixtures.

Binary equilibrium isotherms as well as X-Y diagrams (Figures 4.13 through 4.18) confirm expectations that strong adsorbents such as silica-rich, energetically heterogeneous clinoptilolite will perform excellent separations of gas mixtures consisting of components with widely different polarities ($CO-N_2$ and $CO-CH_4$). In the absence of a polar species in the mixture, the separation becomes difficult (CH_4-N_2).

There is much more obvious disagreement between the a-ELM predictions and the other models (IAST and FH-VST) in the case of Turkish clinoptilolite compared to zeolite 5A; however, the two ELM approaches agree more closely than in the case of

zeolite 5A systems. This result could be attributed to the more diversified surface heterogeneity of clinoptilolite which possesses a mixed cation population (Table 4.4) with 1.46 Ca^{2+} cations and only 0.22 Na^{+} cations per unit cell. Therefore, the presence of over six times more Ca^{2+} cations than Na^{2+} cations could be seen as imparting a much higher surface heterogeneity (divalent cations generate much stronger electric fields) to the Turkish clinoptilolite surface than the surface heterogeneity featured by the Cuban clinoptilolite surface.

A comparison between the number of divalent (2.48) and monovalent (1.56) cations present in a Turkish clinoptilolite unit cell and the number of divalent (1.9) and monovalent (2.52) cations present in a Cuban clinoptilolite unit cell (Table 4.4) enforces the conclusion that the probability of a much more heterogeneous surface (resulting from a larger number of strongly polarizing divalent cations) is higher in Turkish clinoptilolite than in Cuban clinoptilolite. Consequently, the energetic homogeneity and localized adsorption assumptions of the Langmuir model are less likely to be applicable in Turkish clinoptilolite, and their applicability varies with the nature of the gaseous species forming the binary gas mixture.

Even though the Si/Al ratio in zeolite 5A is much lower than in any clinoptilolite and the number of framework charge-balancing cations is accordingly higher, the local electric fields generated by the same type of cation (Ca^{2+}) probably form a more electrically uniform overall field in the zeolite 5A framework. On the scale of adsorbent energetic heterogeneity, a distinction could be made between a "uniform" energetic heterogeneity yielded by a single cation population (generating fairly similar field gradients) and a "non-uniform" energetic heterogeneity given by a mixed cation population, in which the cations bear different charges and generate field gradients that vary in magnitude from location to location.

As mentioned before, FH-VST is the only model which appears to account for the difference in the energetic heterogeneity of aluminosilicate adsorbents through the composition-dependent values of γ_v, the activity coefficient attributed to the vacancy in the vacancy solution. The vacancy can be seen as an unoccupied adsorption site and the variation of its activity coefficient could be related to the variation in the nature, the

valency, and the location of the cations in the micropore. The fact that γ_v does not vary tremendously with the composition of the binary gas mixture adsorbing in zeolite 5A appears to support this idea, as this weak variation would be expected from a zeolite featuring only one type of cation. The weak variation could be attributed to temperature-dependent surface migration of cations from one location to another within the channel network.

4.2.1.3 Binary Mixture Equilibrium Adsorption in Cuban Clinoptilolite

Carbon Monoxide - Nitrogen / Cuban Clinoptilolite. Figure 4.19 shows that ELM and IAST agree that the better adsorbed component in the binary gas mixture is CO (as expected from the pure-gas experimental isotherms - Figure 4.3) and upon the moderate intensity of adsorbent-adsorbate interactions. Because the adsorption capacity of Cuban clinoptilolite for pure CO at 40°C and 101.3 kPa is not much higher than that for pure N_2 at this temperature and pressure, the total amount adsorbed is much lower than in the case of Turkish clinoptilolite at the same temperature and total pressure. The values of the binary interaction parameter and of the activity coefficients corresponding to each adsorption system are listed in Appendix D.

The FH-VST predicted azeotrope occurs at Y(CO) ~ 0.895, above which FH-VST estimates that both species are adsorbed in similar amounts. The close-range repulsions in the adsorbed phase are probably too strong to allow a clear preferential adsorption of quadrupolar N_2 molecules and CO molecules are even less "welcome" with their dipole-quadrupole tandem. Cuban clinoptilolite does not feature the large number of highly polarizing divalent cations which impart a higher degree of energetic heterogeneity on the Turkish clinoptilolite surface (non-uniform field gradients), and therefore it cannot discriminate as well between N_2 and CO which both possess electric moments. As shown in Table 4.14, the range of γ_v values is farther removed from 1 for the CO-N_2 / Turkish clinoptilolite system at 40°C and 101.3 kPa total pressure than for the CO-N_2 / Cuban clinoptilolite system under the same conditions. Although the experimental isotherms did not intersect in the pressure range investigated, according to the values predicted by

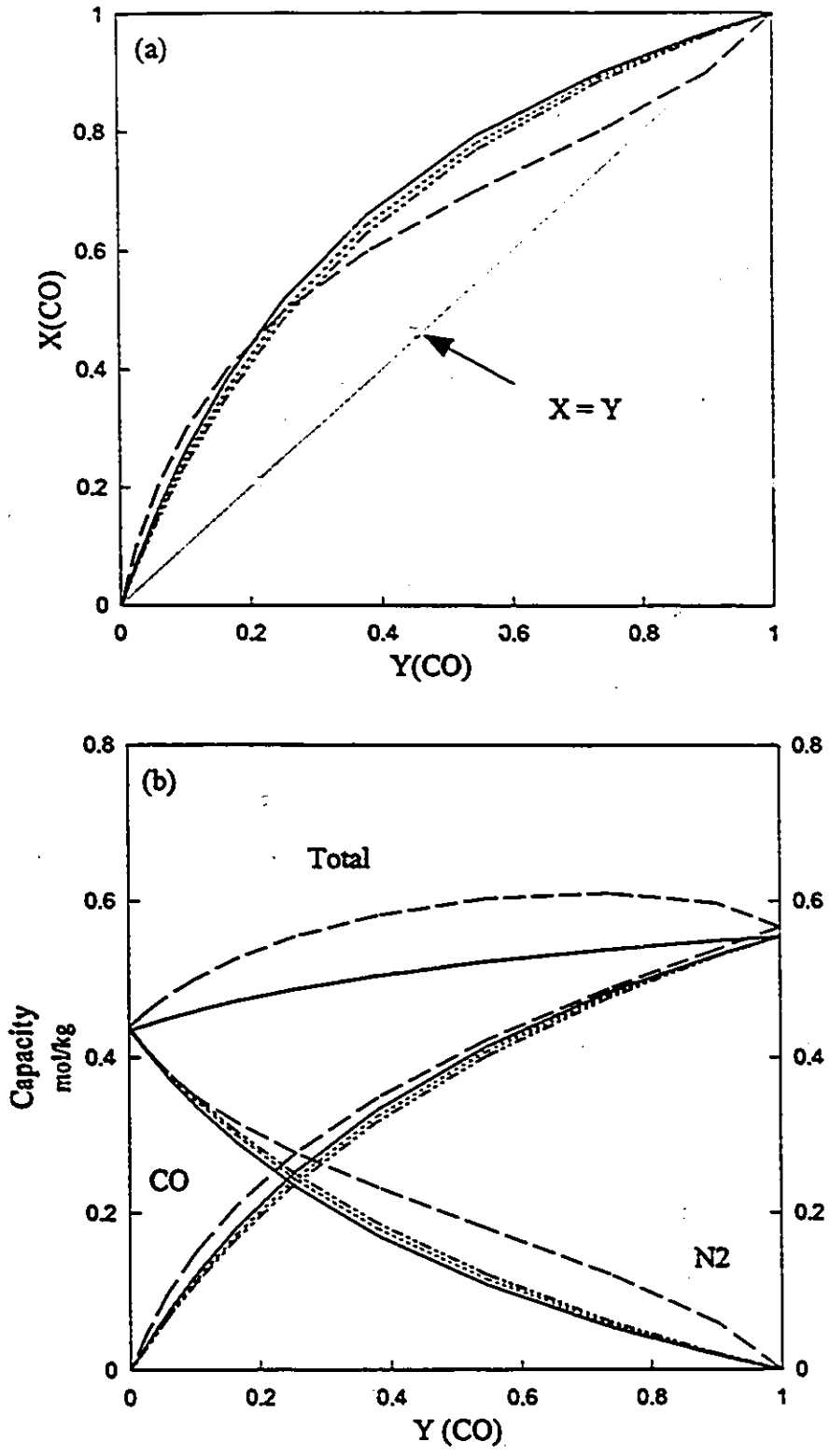

Figure 4.19 Predicted (a) X-Y diagram and (b) binary equilibrium isotherm for CO-N2 adsorption on Cuban clinoptilolite at 40.0-40.1°C and 101.3 kPa total pressure
_____ a-ELM _ _ _ _ _ FH-VST _ _ _ _ IAST ——— d-ELM

FH-VST (which yielded an excellent fit for the pure N_2 isotherm and a good fit for the CO isotherm) for the limiting amount of adsorption and Henry's law constant (Table 4.3) they are expected to do so at much higher pressures where the CO isotherm levels off because of intense close-range repulsions in the adsorbed phase. The predicted equilibrium binary isotherms also prove that only FH-VST forecasts azeotrope formation. As a result, Cuban clinoptilolite is unable to perform the separation of CO-N_2 mixtures at 40°C and 101.3 kPa total pressure unless ELM and IAST predictions are experimentally proven more accurate than the FH-VST predictions, which acccording to the aforementioned, is quite unlikely.

Carbon Monoxide - Methane / Cuban Clinoptilolite. Figure 4.20 illustrates how different predictions can be for a particular adsorption system. The separation of the CO-CH_4 mixture is seen as feasible by a-ELM, d-ELM and IAST. However, a-ELM predicts the preferential adsorption of CH_4 (probably as a result of the averaging of the influence of each gaseous species), unlike the two other models which see CO as the main component of the adsorbed phase. IAST and d-ELM forecast that CO would be better adsorbed, but they are not "equipped" to predict azeotrope formation. As far as a-ELM is concerned, the thermodynamic consistency condition should be applied with caution since the experimental pure-gas equilibrium isotherms were not measured up to the saturation pressure, and the equality of the monolayer volumes in the adsorbed mixture is not easily attainable given the difference in polarity of the gaseous adsorbates and the different affinity of clinoptilolite (irrespective of geographical origin and cation composition) for each of them.

The FH-VST prediction of the separation potential of the system is the most accurate: its prediction of azeotrope formation and selectivity reversal at Y(CO) ~ 0.69 could be foreseen from the intersection of the experimental pure-gas adsorption isotherms at 40°C (Figure 4.3). As soon as the concentration of CO has reached the level at which the close-range repulsions jeopardize the stability of the adsorbed phase, the molecular sieve retains non-polar CH_4 preferentially to attenuate the interactions between the dipolar CO molecules. The isotherm crossover occurs in this adsorption system at a much higher pressure (~75 kPa) than in the case of the adsorption of pure CH_4 and pure N_2 in Turkish

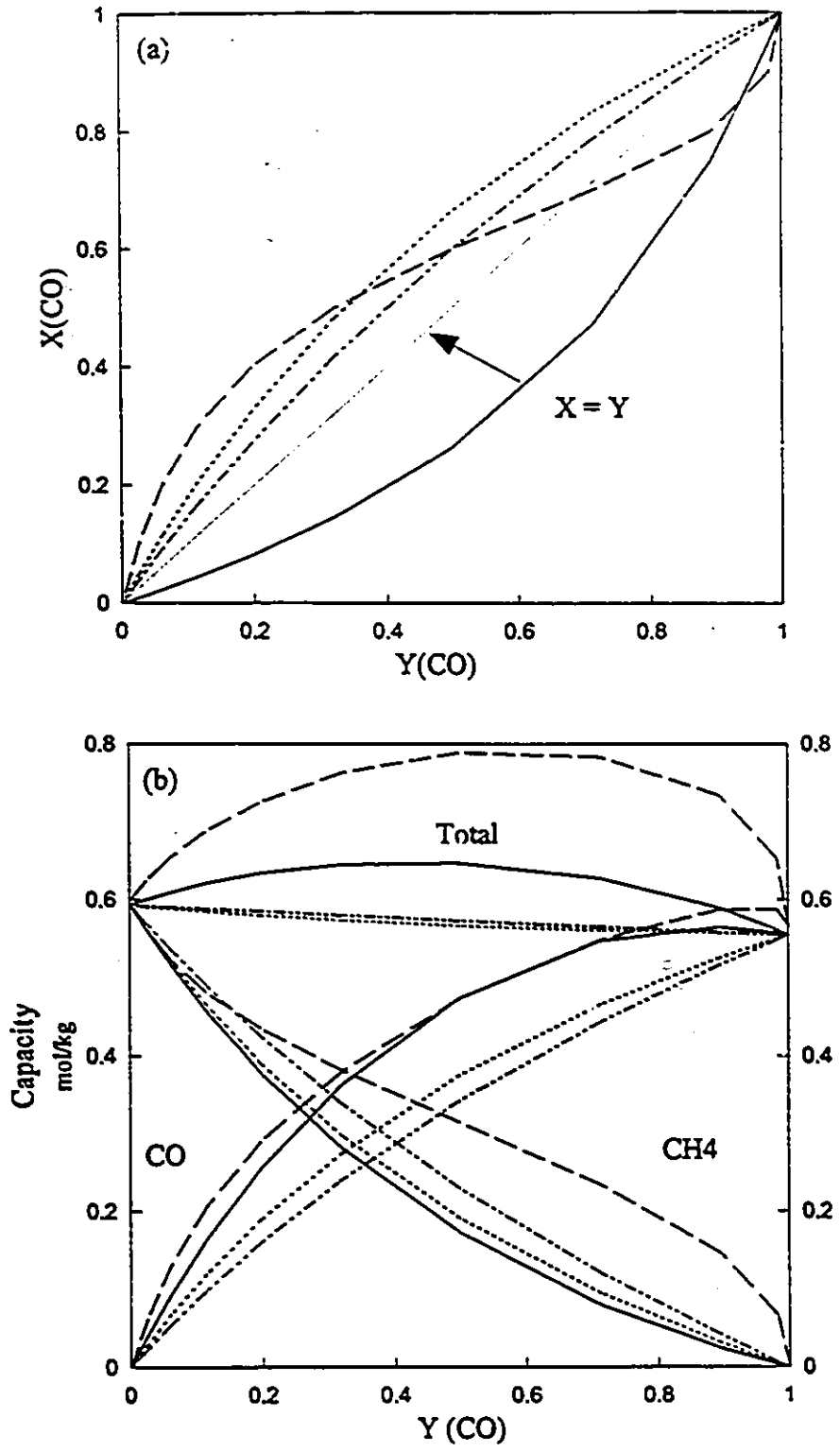

Figure 4.20 Predicted (a) X-Y diagram and (b) binary equilibrium isotherm for CO-CH4 adsorption on Cuban clinoptilolite at 39.9-40.1°C and 101.3 kPa total pressure
_____ a-ELM _ _ _ _ _ FH-VST _ _ _ _ IAST ——— d-ELM

clinoptilolite, as predicted by the FH-VST fits. The experimental backup available for the CO-CH_4 adsorption system give a big boost to the credibility of FH-VST predictions.

Furthermore, Cuban clinoptilolite has almost the same equilibrium adsorption capacity for pure CO and for pure CH_4 at 40°C and 101.3 kPa, which increases the likelihood that the separation of this mixture is not possible using this natural zeolite. The FH-VST binary equilibrium isotherm illustrates well the quasi-equality of the pure-gas adsorption capacities at 40°C and 101.3 kPa total pressure, but it displays however the slight preference of Cuban clinoptilolite for CH_4 under these particular adsorption conditions. As the FH-VST predictions are likely to be the most accurate, it appears that Cuban clinoptilolite would be an uninspired choice for the separation of CO from CH_4 at this total pressure.

FH-VST attributes a larger deviation from ideality to CH_4, as illustrated by the variation of the corresponding activity coefficients with composition (Appendix D). The influence of the strongly polarizing cations in the clinoptilolite framework and of the electric moments present in the CO molecules must be acutely exerted on the otherwise "ideality-abiding" non-polar (but highly polarizable) CH_4 molecules. In this case, the influence of the cations is understandably less felt by the polar-quadrupolar CO molecules of lower polarizability than by the non-polar CH_4 molecules of higher polarizability.

Methane - Nitrogen / Cuban Clinoptilolite. Figure 4.21 shows that at 40°C and 101.3 kPa total pressure Cuban clinoptilolite would not yield too high separation factors upon the adsorption of this binary mixture. The total amount of CH_4-N_2 mixture adsorbed is lower over the entire composition range for Cuban clinoptilolite than for Turkish clinoptilolite.

According to IAST, the interactions in this system are sufficiently weak to be negligible, and the predicted selectivities slightly increase with increasing partial pressure of the preferentially adsorbed component (CH_4), which seems reasonable given the non-polar nature of CH_4 and its high stability in the adsorbed phase compared to that of N_2. The interactions between the charge-compensating cations in Cuban clinoptilolite and the induced dipoles in CH_4 molecules are probably weak enough to approximate the behaviour of the system as ideal.

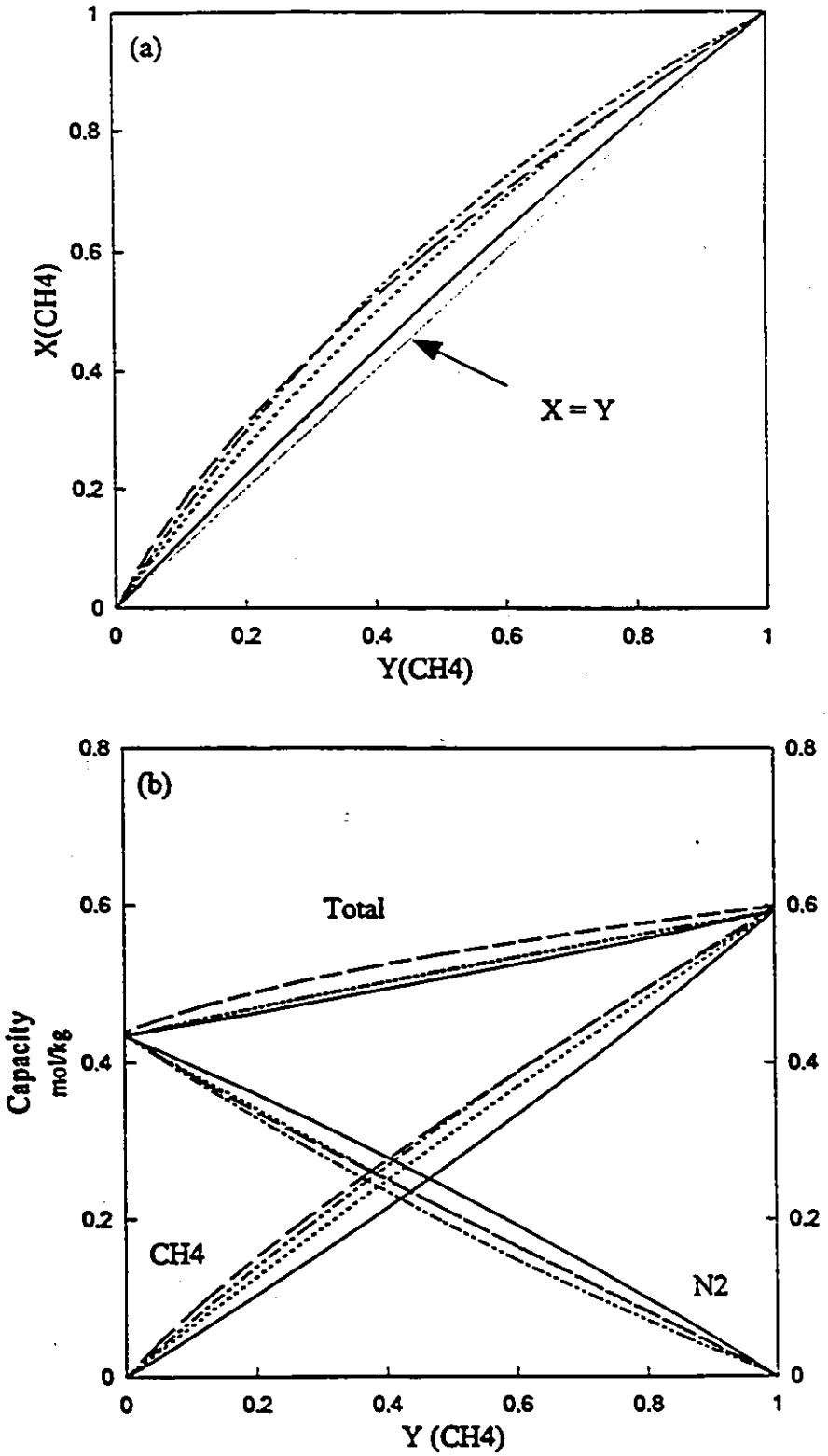

Figure 4.21 Predicted (a) X-Y diagram and (b) binary equilibrium isotherm for CH4-N2 adsorption on Cuban clinoptilolite at 39.9-40.0°C and 101.3 kPa total pressure
_____ a-ELM _ _ _ _ _ FH-VST _ _ _ _ IAST ——— d-ELM

IAST yields selectivities that do not vary much with composition (Table 4.15), which explains the symmetry of the X-Y diagram it predicts.

Table 4.15 Predicted equilibrium separation factors for Cuban clinoptilolite (CC) at 101.3 kPa total pressure for all the adsorption systems.

Binary gas mixture adsorption system (1) - (2) / Adsorbent	Temperature [°C]	Predicted equilibrium separation factors (*azeotrope) a-ELM	d-ELM	IAST	FH-VST
$CO-N_2$ / CC	40.0-40.1	3.18	2.95	2.83-2.73	4.51-0.99*
$CO-CH_4$ / CC	39.9-40.1	0.36	1.98	1.56-1.45	4.30-0.17*
CH_4-N_2 / CC	39.9-40.0	1.15	1.49	1.68-1.75	2.01-1.48

ELM also yields symmetric XY diagrams, with d-ELM predicting slightly higher selectivity values. Unlike the CH_4-N_2 / Turkish clinoptilolite at 40°C and 101.3 kPa total pressure, in which a-ELM forecasts the preferential adsorption of N_2, a-ELM predicts an equilibrium CH_4 selectivity only slightly higher than 1 for the adsorption of the same binary mixture at the same temperature and total pressure in Cuban clinoptilolite. According to a-ELM, the separation of CH_4 from N_2 is impossible, but the averaging of monolayer volumes may not be the most realistic approach for the adsorption of this binary mixture in Cuban clinoptilolite.

FH-VST forecasts a fairly steady deviation from ideality of both components but the predicted activity coefficients associated with CH_4 span slightly lower values than those associated with N_2 (Appendix D). The γ_v values are also fairly constant (about 0.933) which supports the idea of weak adsorbent-adsorbate (gas-vacancy) interactions and the assumption of quasi-ideality for this system.

Summary for Cuban clinoptilolite. According to the overall trend of the predictions, Cuban clinoptilolite appears to have lower selectivity and capacity than Turkish clinoptilolite for the binary gas mixtures investigated at 40°C and 101.3 kPa total pressure. This leads to the conclusion that better adsorptive properties are obtained with natural aluminosilicate molecular sieves which feature strongly polarizing divalent cations

rather than monovalent cations. Divalent cations are therefore extremely important in upgrading the energetic heterogeneity of the adsorbent to enhance its separation potential by increasing its preference for polar adsorbates.

The discrepancy between a-ELM predictions and the other models is observed to a much lower extent in Cuban clinoptilolite adsorption systems at 40°C and 101.3 kPa total pressure than in the Turkish clinoptilolite systems involving the same adsorbates. An explanation of this observation could be provided by the different cation composition (virtually equal number of Na^+ and Ca^{2+} cations) and the higher Si/Al ratio in Cuban clinoptilolite (Table 4.4), which contains only 1.9 divalent cations (Ca^{2+} and Mg^{2+}) per unit cell, a lower number than in Turkish clinoptilolite (2.48 Ca^{2+} and Mg^{2+} cations per unit cell). Considering that the electric fields generated by monovalent atoms are less strong than those generated by the divalent atoms, but that the number of these monovalent atoms is much larger, one could think that the monovalent cations are more uniformly spread within the channel network and that they generate a much more uniform electric field throughout the framework, or a more "uniform" energetic heterogeneity. Given these conditions, the assumptions which constitute the basis of the Langmuir model are more easily justified in Cuban clinoptilolite than in Turkish clinoptilolite, which is why the a-ELM estimations would be in closer agreement with the other models than they are in the case of Turkish clinoptilolite. An exception is the CH_4-CO / Cuban clinoptilolite adsorption system at 40°C (and 101.3 kPa total pressure) which is expected to form an azeotrope (predicted by FH-VST only), for which a-ELM predicts the preferential adsorption of CH_4 instead of that of CO the way IAST and d-ELM anticipate.

The discrepancy between the a-ELM and d-ELM predictions could also be related to the electrical "uniformity" of the polarizing field generated by the cations: the more "uniform" the field, the closer the agreement between the two ELM approaches.

4.2.2 Aluminophosphate Molecular Sieves

With the linear trend of most of the experimental single-component adsorption isotherms in the pressure range investigated, prediction of binary mixture adsorption must

be looked upon with caution. For those aluminophosphate molecular sieves for which pure-gas adsorption data could be correlated with both the Langmuir equation (2.2) and the FH-VST equation (2.5), that is $AlPO_4$-11 and $AlPO_4$-18, all three models (ELM, IAST, FH-VST) were used to obtain binary mixture adsorption information. For the $AlPO_4$-17 binary mixture adsorption sytems only FH-VST predictions were determined because no fit could be obtained with the Langmuir equation for the single-component CO isotherm, which is slightly unfavourable and is well represented by the Freundlich equation (2.4). These FH-VST predicted binary mixture data are questionable in the case of $AlPO_4$-17 because the pure-gas isotherm fits were not perfect over the pressure range investigated for the adsorption of those gaseous species featuring electric moments (CO, N_2). In the case of $AlPO_4$-17, only the pure CH_4 adsorption isotherm could be correlated with both the Langmuir and the FH-VST equation, the latter yielding a better fit.

4.2.2.1 Binary Mixture Equilibrium Adsorption in $AlPO_4$-11

Carbon Monoxide - Nitrogen / $AlPO_4$-11. Figures 4.22 and 4.23 show that the models do not agree upon the adsorptive behaviour of this system when compared to each other, but do forecast for each system similar behaviour at different temperatures. IAST and d-ELM predictions are very similar and estimate that the separation would be feasible through preferential adsorption of CO, while a-ELM predicts the preferential adsorption of N_2. This preference for N_2 could be explained by the less intense close-range repulsions exerted between neighbouring N_2 molecules and the smaller kinetic diameter which allows a larger number of molecules to be accommodated within the micropores. The FH-VST prediction of azeotrope formation at 40°C for high CO partial pressures could be due to the more intense close-range repulsions exerted between the CO molecules when the sieve is confronted with a lower fractional coverage by N_2 molecules (Figure 4.4).

Methane - Carbon Monoxide / $AlPO_4$-11. Figures 4.24 and 4.25 show that IAST, FH-VST, and d-ELM virtually agree in their predictions, according to which the separation of CH_4 from this mixture using $AlPO_4$-11 would be slightly more successful at 40°C. The a-ELM predicted selectivities are the most conservative, probably as a result of

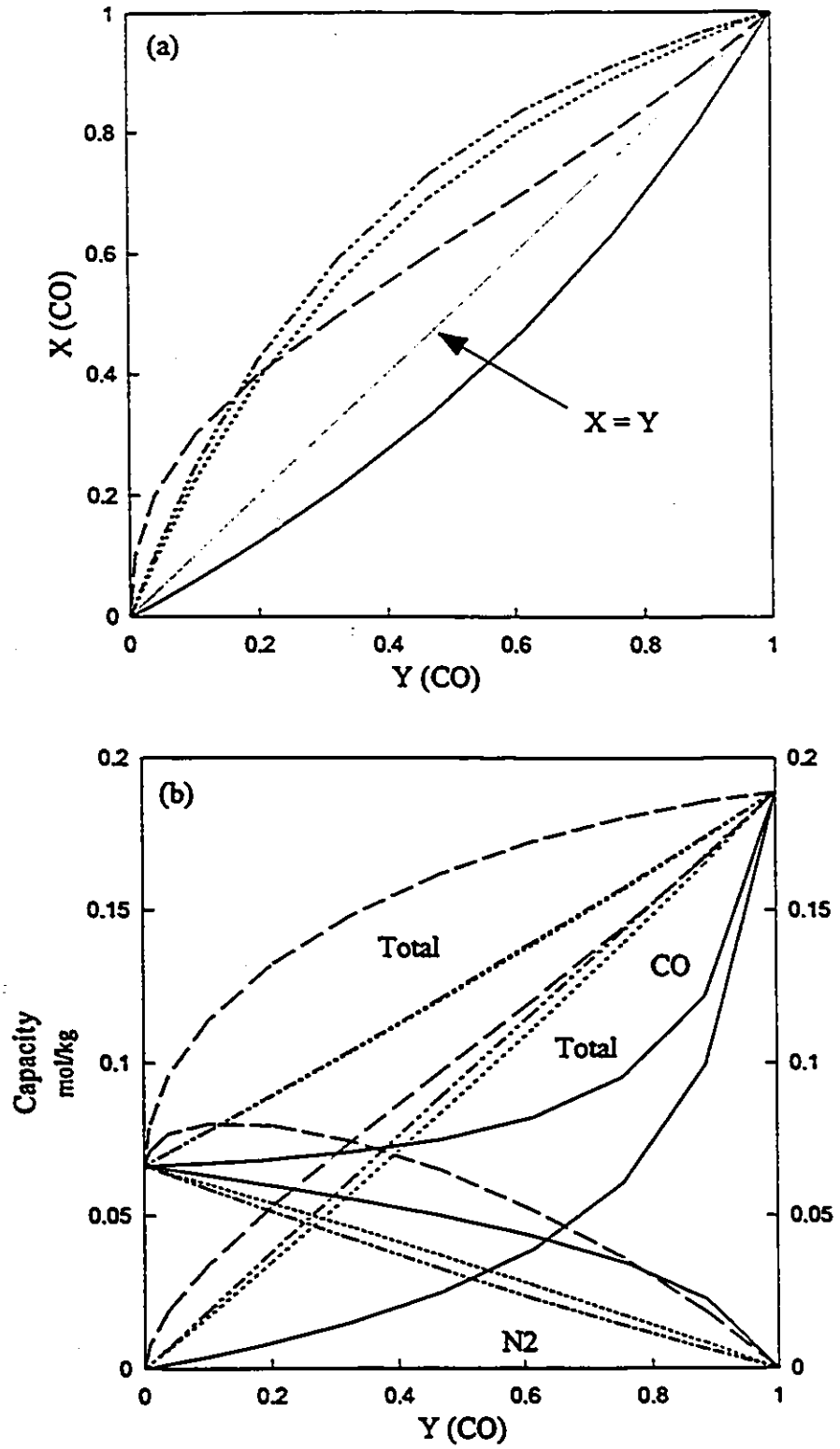

Figure 4.22 Predicted (a) X-Y diagram and (b) binary equilibrium isotherm for CO-N2 adsorption on AlPO4-11 at 22.6-22.8°C and 101.3 kPa total pressure
_____ a-ELM _ _ _ _ _ FH-VST _ _ _ _ IAST ——— d-ELM

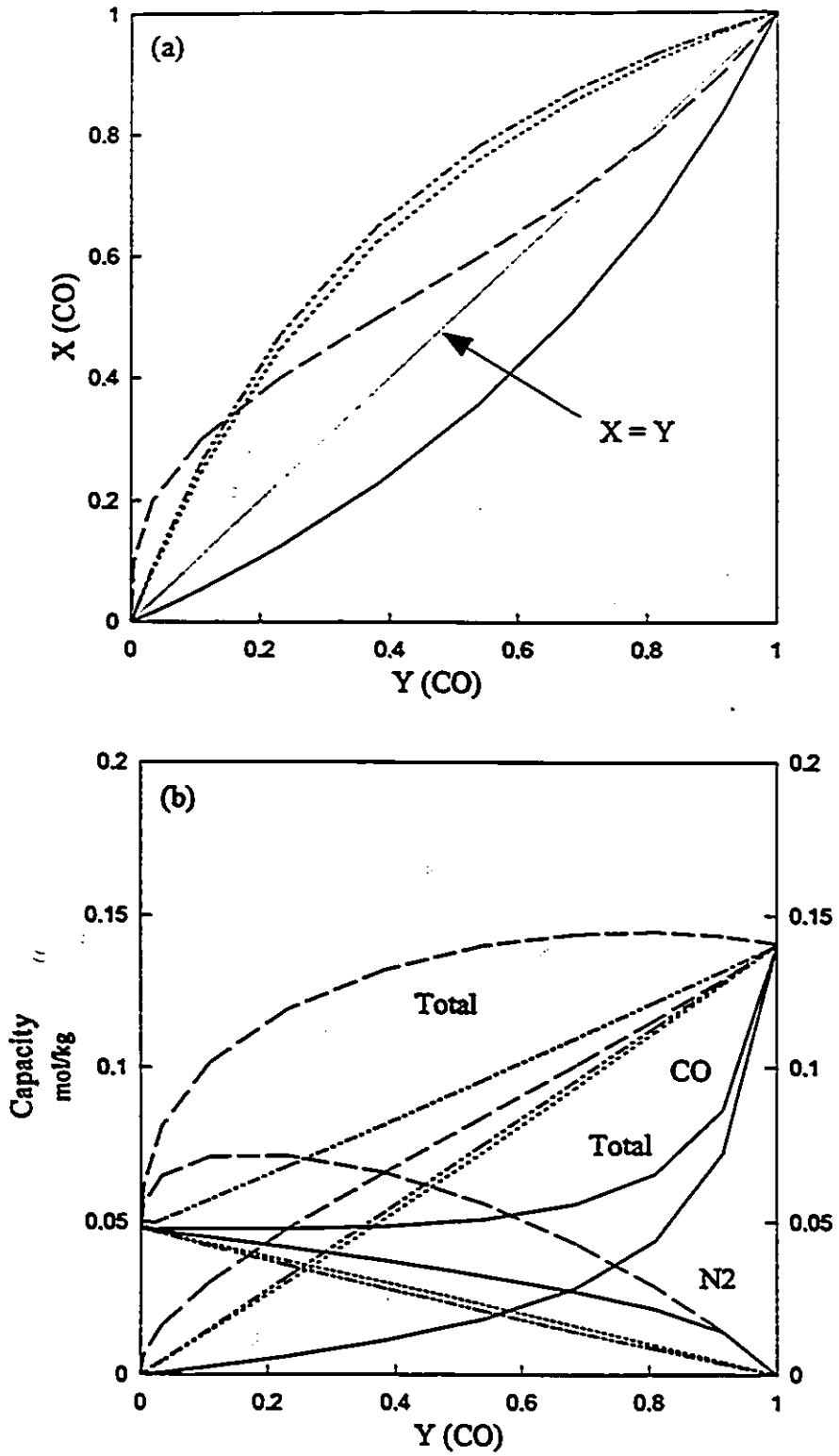

Figure 4.23 Predicted (a) X-Y diagram and (b) binary equilibrium isotherm for CO-N2 adsorption on AlPO4-11 at 40.0°C and 101.3 kPa total pressure
_____ a-ELM _ _ _ _ _ FH-VST _ _ _ IAST ——— d-ELM

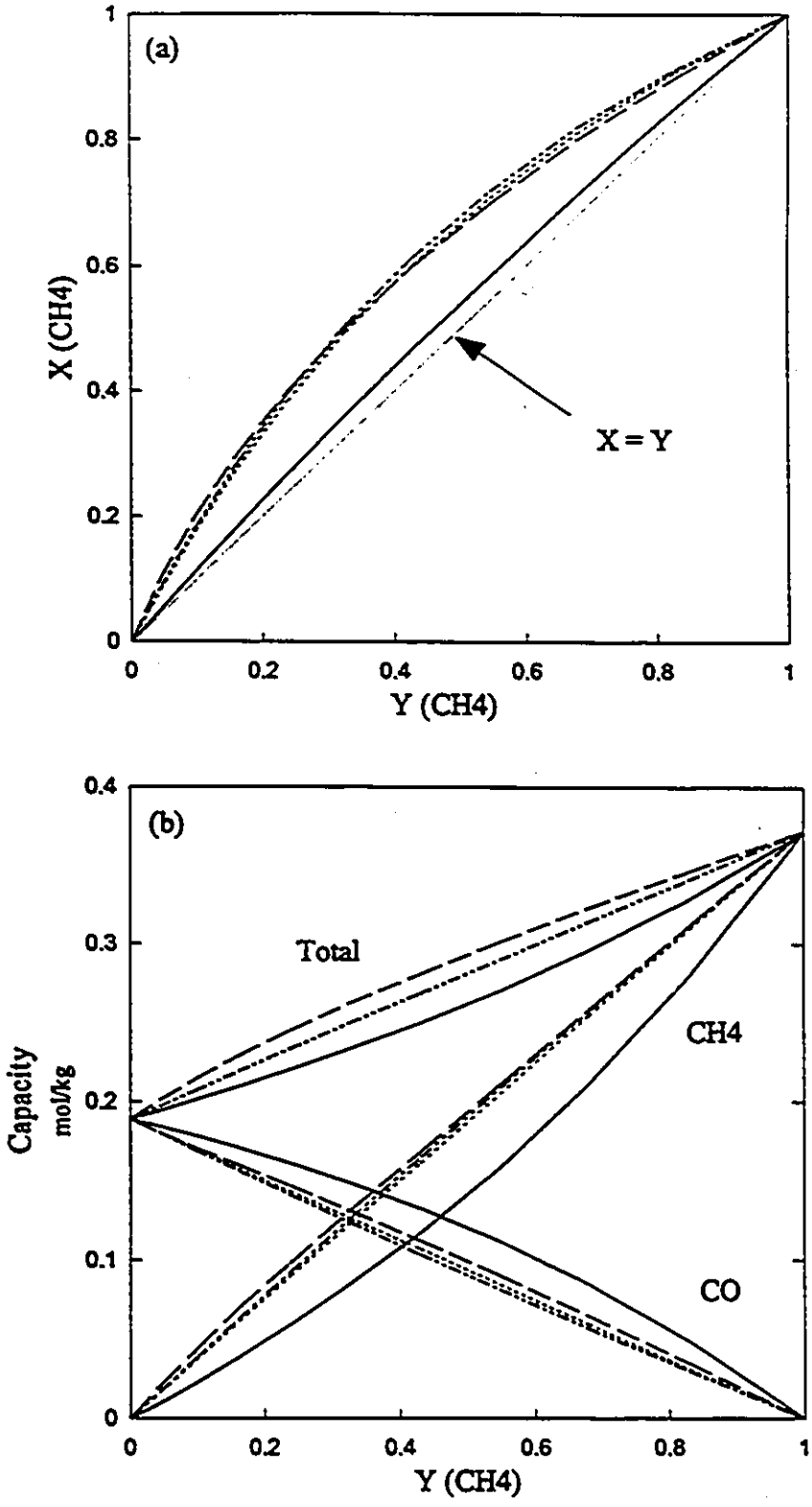

Figure 4.24 Predicted (a) X-Y diagram and (b) binary equilibrium isotherm for CH4-CO adsorption on AlPO4-11 at 22.6-22.8°C and 101.3 kPa total pressure
_____ a-ELM _ _ _ _ _ FH-VST _ _ _ _ IAST ——— d-ELM

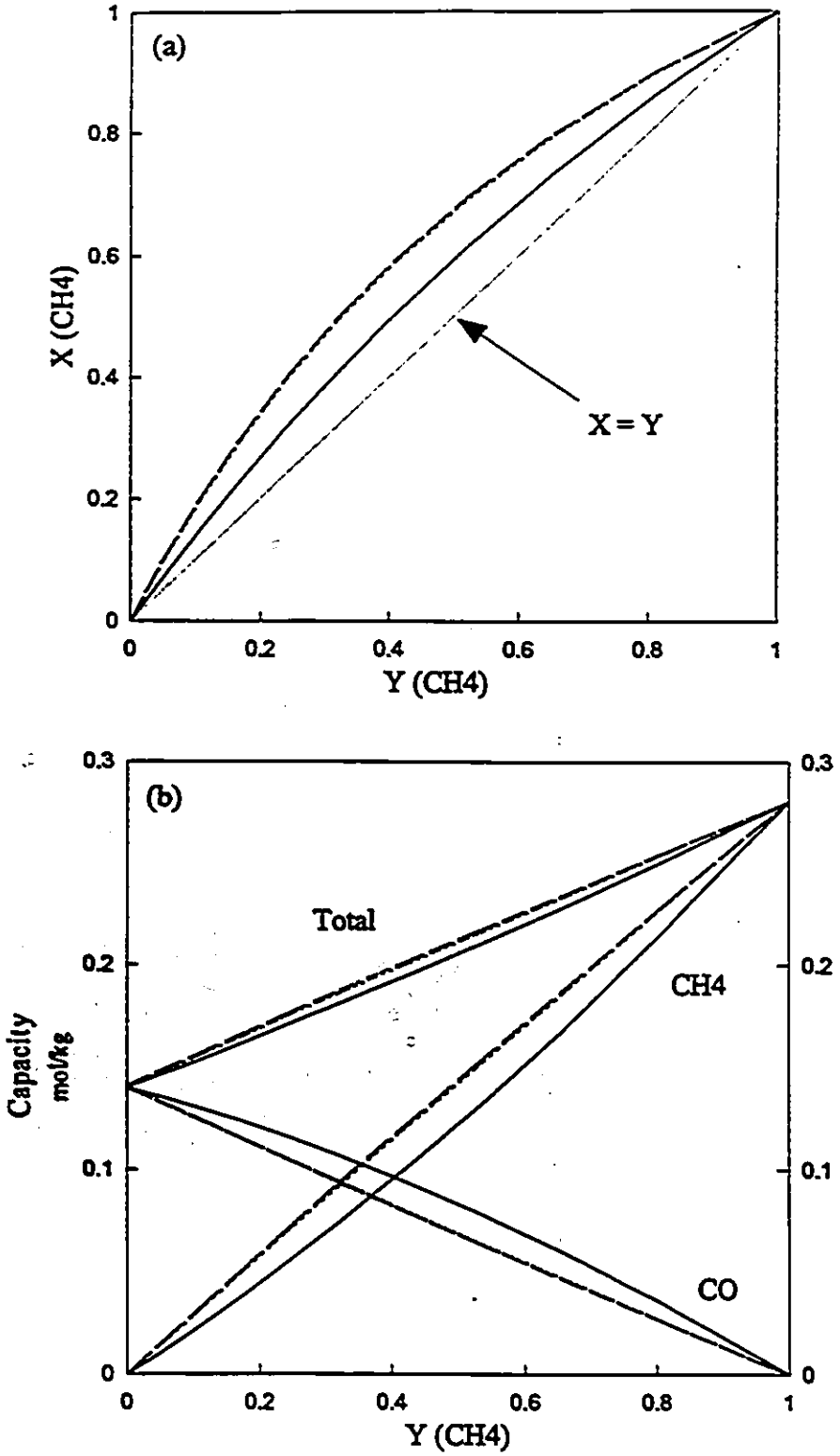

Figure 4.25 Predicted (a) X-Y diagram and (b) binary equilibrium isotherm for CH4-CO adsorption on AlPO4-11 at 40.0°C and 101.3 kPa total pressure
_____ a-ELM _ _ _ _ _ FH-VST _ _ _ _ IAST ——— d-ELM

the averaging effect. Non-ideal behaviour appears to be quite unlikely for this adsorption system at these temperatures and total pressure.

Methane - Nitrogen / $AlPO_4$-11. Figures 4.26 and 4.27 show that a-ELM predicts at both temperatures the preferential adsorption of N_2, undoubtedly the consequence of averaging. FH-VST calculations yield a very asymmetric X-Y diagram, which indicates that the values of the separation factors can become huge at very low partial pressures of CH_4, i.e. $Y(CH_4) < 0.1$, with slightly greater values at room temperature. For $Y(CH_4) > 0.1$, the selectivities are higher at 40°C. Given the much larger capacity of $AlPO_4$-11 for pure CH_4 than for N_2 at 101.3 kPa, the preferential adsorption of CH_4 indicated by IAST, FH-VST, and d-ELM looks reasonable. As expected, the X-Y diagrams yielded by IAST and d-ELM are much more symmetric, predicting similar selectivity values.

Summary for $AlPO_4$-11. The diversity of predictions yielded by each model in the case of binary mixture adsorption in $AlPO_4$-11 makes comprehensive interpretation a difficult task. Theoretical considerations would indicate that steric effects are not likely to be exerted on the adsorbate molecules seeking access to this medium-pore molecular sieve, even though the pore apertures are elliptical (the smaller dimension is larger than the adsorbate molecule with the largest kinetic diameter, CH_4). Equal accessibility is offered to both components in the mixture. However, the fact that all models agree that CH_4 is preferentially adsorbed from its mixtures with CO or N_2 leads to the conclusion that this energetically homogeneous molecular sieve accommodates bulkier non-polar molecules like CH_4 in larger amounts since they present a clear advantage in the absence of close-range repulsions in the adsorbed phase. The molecular-dimension criterion also applies in the case of CO-N_2 mixtures, from which $AlPO_4$-11 preferentially retains the larger molecule (CO), which also has the greatest ability to contribute the self-potential much needed by energetically homogeneous adsorbents.

The relatively narrow selectivity ranges (Table 4.16) upon which the models seem to agree for the adsorption of the CH_4-CO mixture in $AlPO_4$-11 at 40°C and 101.3 kPa total pressure indicate that this molecular sieve might be useful in the bulk separation of this mixture. In Table 4.16, the range-end selectivity values are given for the lowest

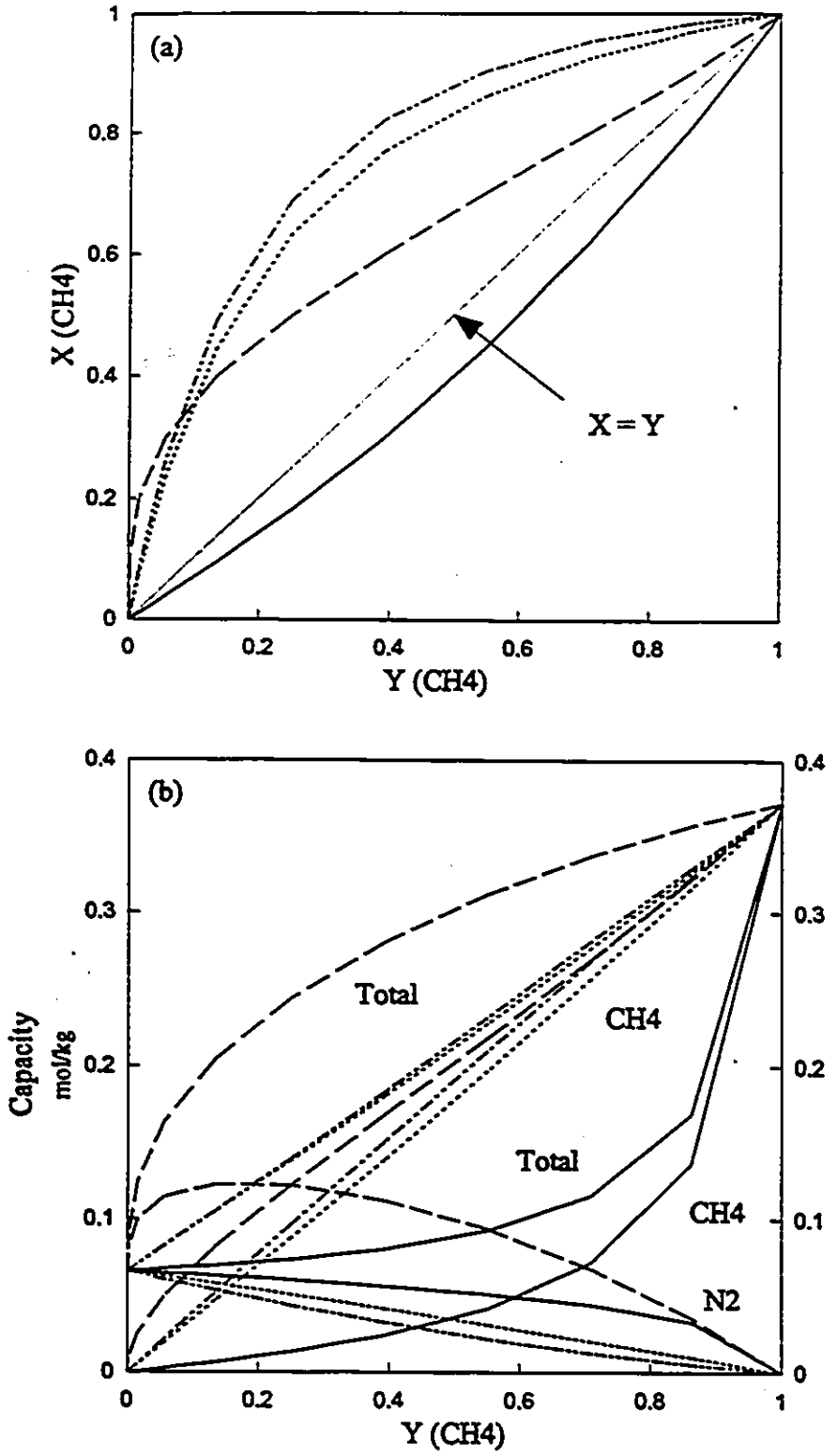

Figure 4.26 Predicted (a) X-Y diagram and (b) binary equilibrium isotherm for CH4-N2 adsorption on AlPO4-11 at 22.6-22.8°C and 101.3 kPa total pressure
_____ a-ELM _ _ _ _ _ FH-VST _ _ _ _ IAST ——— d-ELM

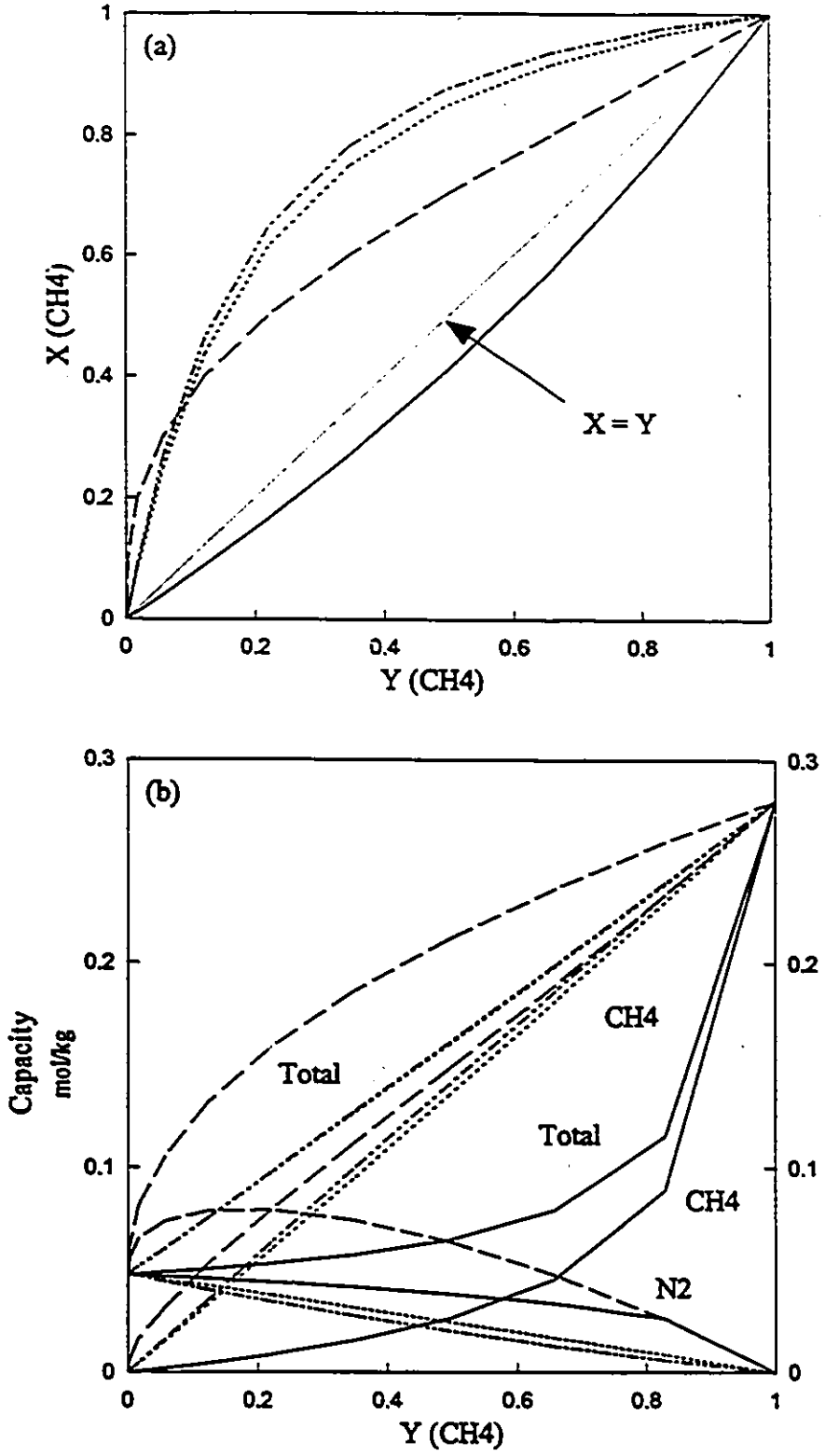

Figure 4.27 Predicted (a) X-Y diagram and (b) binary equilibrium isotherm for CH4-N2 adsorption on AlPO4-11 at 40.0°C and 101.3 kPa total pressure

_____ a-ELM _ _ _ _ _ FH-VST _ _ _ _ IAST ——— d-ELM

mole fraction of the reference species (quoted first in the pair) and the highest mole fraction of the reference species for which FH-VST calculations were performed.

Table 4.16 Predicted equilibrium separation factors for $AlPO_4$-11 (A11), $AlPO_4$-17 (A17), and $AlPO_4$-18 (A18) at 101.3 kPa total pressure for all the adsorption systems.

Binary gas mixture adsorption system	Temperature [°C]	Predicted equilibrium separation factors (*azeotrope) a-ELM	d-ELM	IAST	FH-VST
$CO-N_2$ / A11	40	0.48	2.71	2.89 - 3.23	600.2- 0.84*
	23	0.57	2.57	2.09 - 2.12	66.4 - 1.17
CH_4-CO / A11	40	1.47	2.07	4.51 - 5.68	2.113 - 2.111
	23	1.17	2.02	2.09 - 2.15	2.49 - 1.80
CH_4-N_2 / A11	40	0.70	5.61	6.01 - 7.97	1065 - 1.86
	23	0.66	5.18	5.82 - 9.48	6779 - 1.44
N_2-CO / A17	40	n/a	n/a	n/a	1.28 - 0.85*
CH_4-CO / A17	40	n/a	n/a	n/a	121.01-0.96*
CH_4-N_2 / A17	40	n/a	n/a	n/a	8.34 - 1.69
$CO-N_2$ / A18	40	16.36	4.10	3.97-3.69	91.99-0.0007*
$CO-CH_4$ / A18	40	3.70	1.57	1.48-1.44	21.08-0.0004*
CH_4-N_2 / A18	40	4.43	2.60	2.58 - 2.56	2.86 - 2.25

4.2.2.2 Binary Mixture Equilibrium Adsorption in $AlPO_4$-17

As the pure N_2 and pure CO experimental equilibrium isotherms could not be fitted with the Langmuir equation, no ELM predictions could be determined for the adsorption of the binary gas mixtures investigated in $AlPO_4$-17 at 40°C at 101.3 kPa total pressure. Since these experimental isotherms were slightly unfavourable, graphical integration for the purpose of determining the spreading pressure of each component in the mixture and IAST predictions was not attempted. Despite the imperfect fits yielded by regressing the FH-VST parameters for the adsorption of pure N_2, CO, and CH_4 in $AlPO_4$-17 at 40°C, FH-VST predictions for binary isotherms were obtained.

Nitrogen - Carbon Monoxide / $AlPO_4$-17. According to FH-VST, it would be impossible to separate N_2-CO gas mixtures at 40°C using $AlPO_4$-17 (Figure 4.28) because

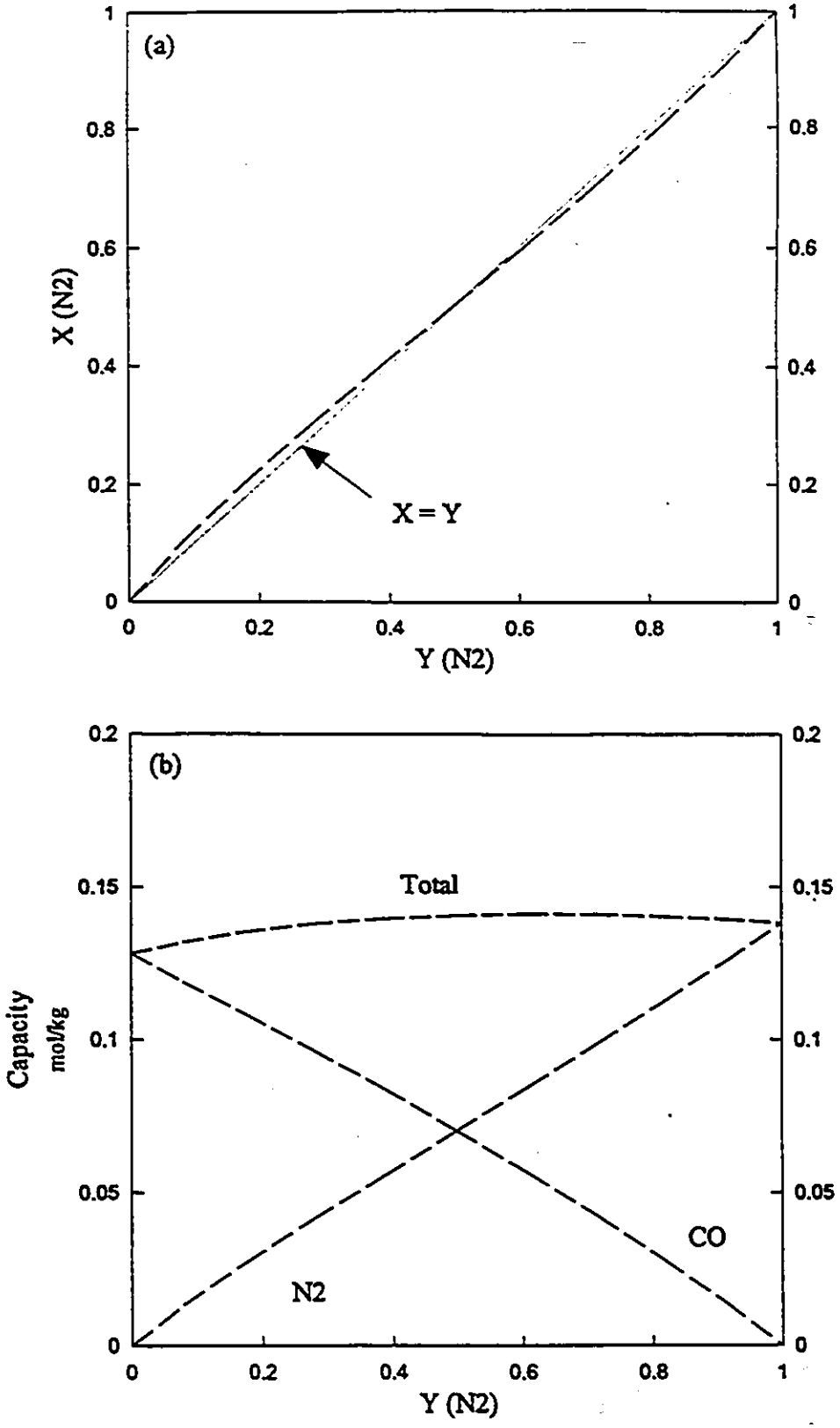

Figure 4.28 FH-VSTpredicted (a) X-Y diagram and (b) binary equilibrium isotherm for N2-CO adsorption on AlPO4-17 at 39.6-40.0°C and 101.3 kPa total pressure

the selectivity values are around unity and because of the anticipated azeotrope. These phenomena should not be surprising considering the similarly low adsorption capacities of $AlPO_4$-17 for pure N_2 and pure CO at 40°C and 101.3 kPa total pressure (Figure 4.5). Furthermore, both gaseous species must overcome sterically unfavourable geometric factors in order to get adsorbed, with CO being more affected.

Methane - Carbon Monoxide / $AlPO_4$-17. Figure 4.29 reveals that the preference of $AlPO_4$-17 for tetrahedral CH_4 molecules is higher at lower CH_4 partial pressures. As the CH_4 partial pressure increases, the values of the separation factor approach unity, indicating that the separation of the CH_4-CO mixture is not feasible when CO is present in low amounts in the mixture. It appears that at low CO partial pressures, similar amounts of CO and CH_4 are adsorbed, despite the considerable steric hindrance encountered by the CO molecules when attempting to enter the $AlPO_4$-17 elliptical pore openings. An explanation would lie in the ability of the polar CO to contribute self-potential to the overall adsorption potential of the system, conjugated with the inability of the energetically homogeneous adsorbent to accommodate too many bulky CH_4 molecules (despite its known preference for non-polar gaseous species).

Methane - Nitrogen / $AlPO_4$-17. $AlPO_4$-17 might be a promising adsorbent for the separation of CH_4-N_2 gas mixtures at 40°C and 101.3 kPa total pressure. Figure 4.30 shows that, according to the FH-VST predicted X-Y diagram, the separation would be efficient at low CH_4 partial pressures. As there is no CO in the system (the adsorbate which encounters most steric hindrance upon adsorption in $AlPO_4$-17), FH-VST does not forecast azeotrope formation and selectivity reversal for this system. $AlPO_4$-17 is known to adsorb pure CH_4 in the largest amounts (compared to N_2 and CO) for pressures below 1000 mm Hg (133.3 kPa). Furthermore, the quadrupole moment in the N_2 molecules cannot generate too strong repulsive interactions which would call for "buffer" non-polar CH_4 molecules and would therefore result in selectivity reversal.

Summary for $AlPO_4$-17. In the event that these predictions are found to be fairly close to the actual experimental behaviour of each adsorption system, then $AlPO_4$-17 could be considered a promising adsorbent for the reputably difficult separation of CH_4-N_2 gas mixtures.

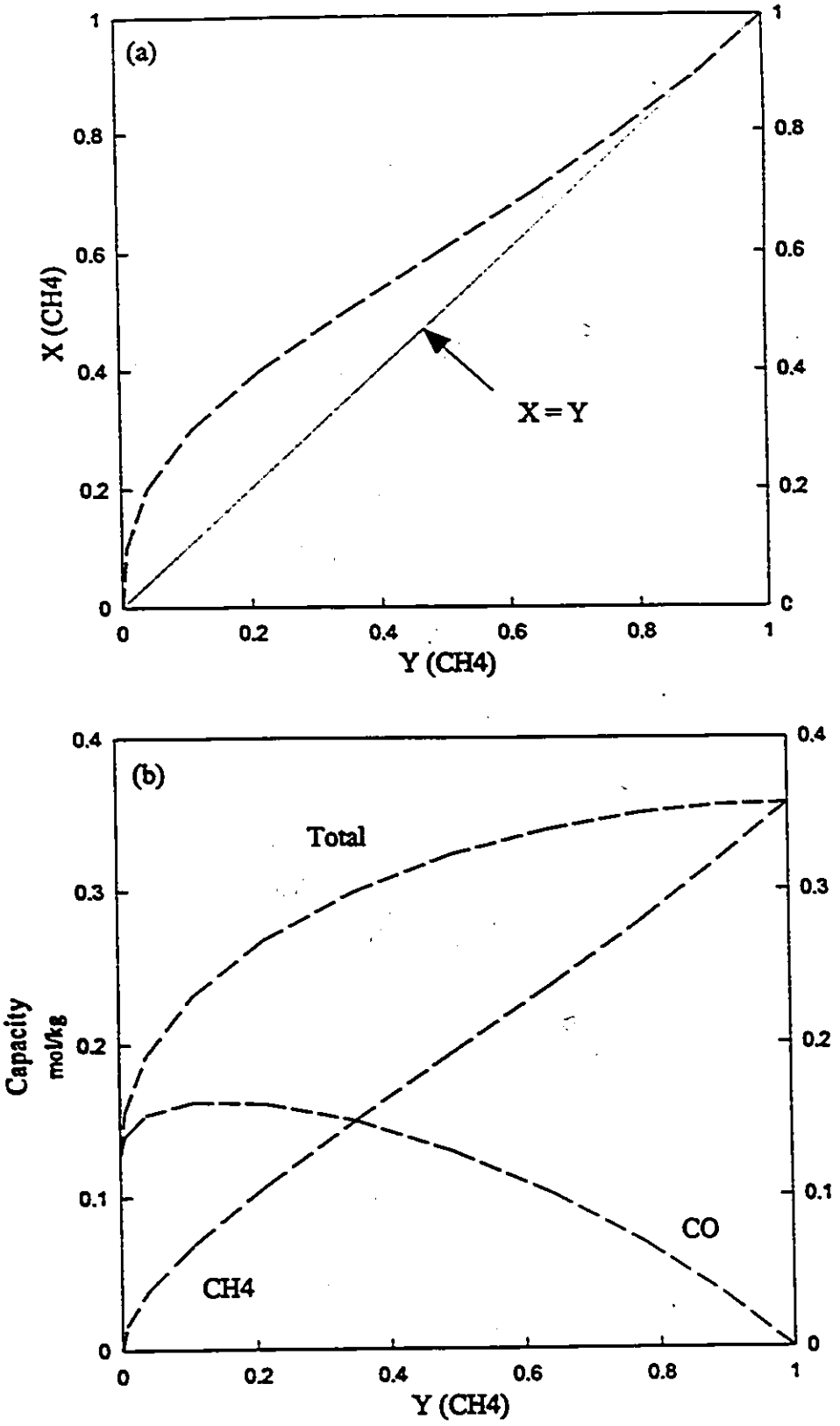

Figure 4.29 FH-VST predicted (a) X-Y diagram and (b) binary equilibrium isotherm for CH4-CO adsorption on AlPO4-17 at 40.0°C and 101.3 kPa total pressure

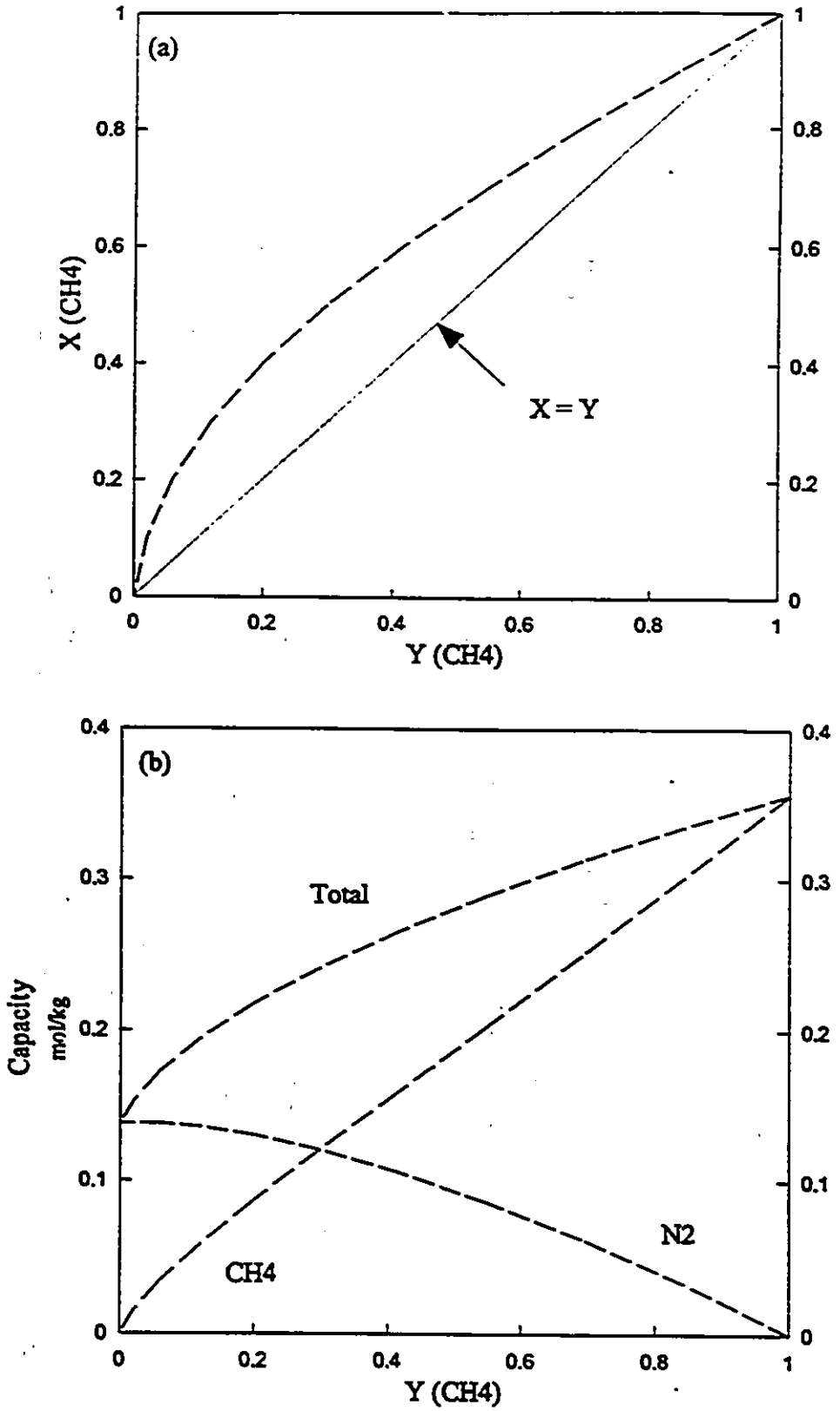

Figure 4.30 FH-VST predicted (a) X-Y diagram and (b) binary equilibrium isotherm for CH4-N2 adsorption on AlPO4-17 at 39.6-40.0°C and 101.3 kPa total pressure

4.2.2.3 Binary Mixture Equilibrium Adsorption in $AlPO_4$-18

Carbon Monoxide - Nitrogen / $AlPO_4$-18. Figure 4.31 illustrates the discrepancy in the predictions yielded by the three models, which agree however upon the nature of the preferentially adsorbed species (CO). The a-ELM binary isotherm features the "hook" previously encountered with aluminosilicate molecular sieves (zeolite 5A) for the same binary gas mixture at the same temperature, which was viewed as an unrealistic displacement of a larger amount of the weakly adsorbed component by a smaller amount of the better adsorbed species (instead of a larger amount of the better adsorbed species). IAST and d-ELM predict virtually linear binary mixture adsorption isotherms.

Just like for the adsorption of this binary gas mixture in $AlPO_4$-17 (Figure 4.28), FH-VST predicts selectivity reversal (Figure 4.31) which translates into a rounded curve for the total amount adsorbed, typical for azeotrope formation with positive deviations from ideality. This seems to enforce the idea that non-ideal behaviour such as azeotropy and selectivity reversal is very likely in small-pore aluminophosphate molecular sieves which feature similar capacities for the components of the binary gas mixture and considerable steric hindrance upon adsorption in the micropores.

The adsorption of a polar adsorbate can constitute both a benefit and a disadvantage for an energetically homogeneous aluminophosphate adsorbent. The dipole and quadrupole moments of CO molecules impart a certain degree of energetic heterogeneity to the adsorbent surface once they get adsorbed and become "part and parcel" of the adsorbent. Consequently, the benefit of CO adsorption in $AlPO_4$'s lies in the fact that the adsorbed CO molecules contribute self-potential to the total adsorption potential, a contribution much greater than that of adsorbed quadrupolar N_2 molecules. However, as the CO partial pressure increases in the adsorbed phase, the same electric moments of the CO molecules become responsible for more intense close-range repulsions, thus threatening the stability of the adsorbed phase (a drawback of the adsorption of polar gases). The energetically homogeneous adsorbent thereby faces a conflicting situation in which the tendency to retain the adsorbate which can pay a large contribution in self-potential (CO) must oppose the tendency to ensure the stability of the

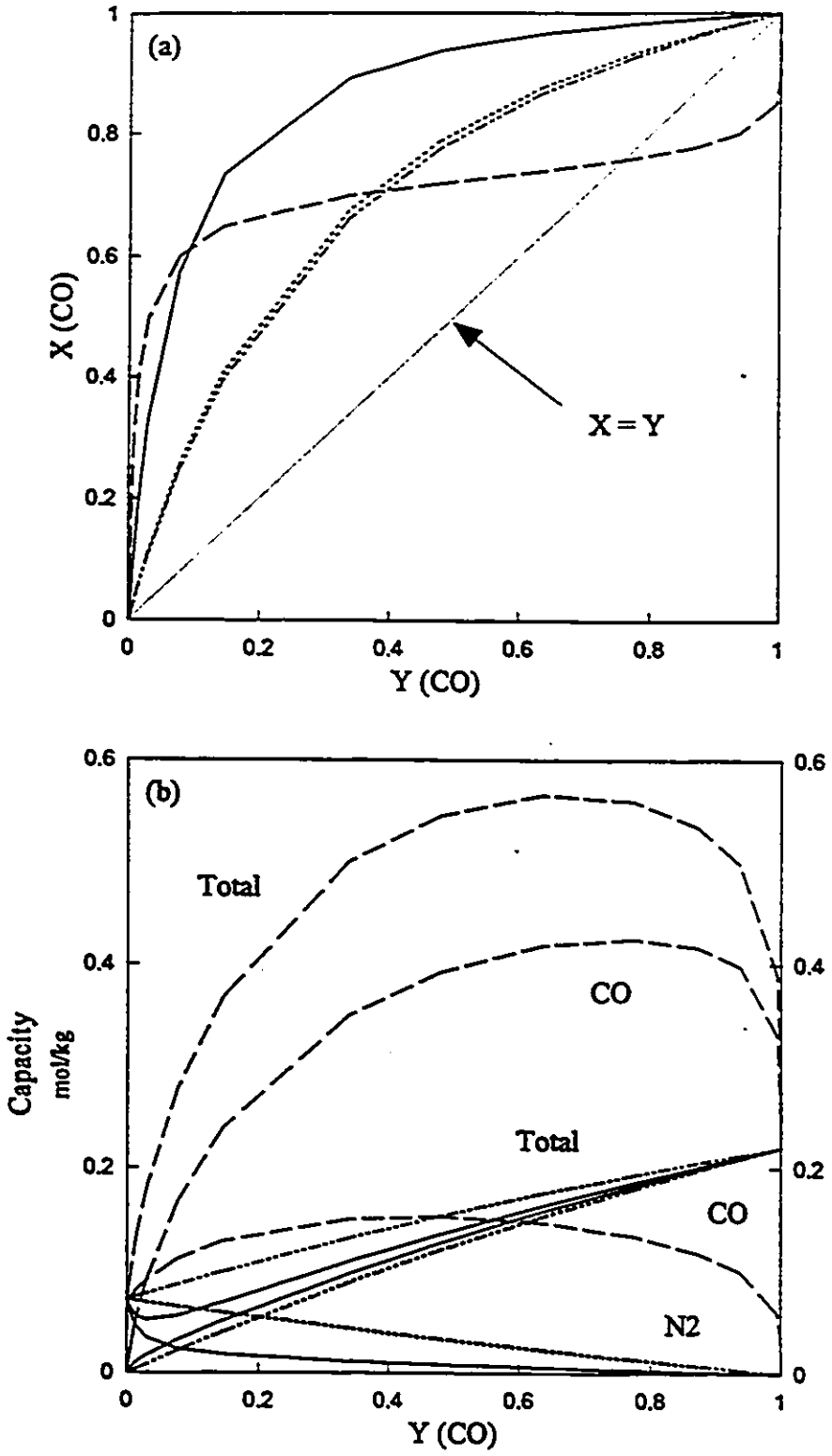

Figure 4.31 Predicted (a) X-Y diagram and (b) binary equilibrium isotherm for CO-N2 adsorption on AlPO4-18 at 40.1°C and 101.3 kPa total pressure
_____ a-ELM _ _ _ _ _ FH-VST _ _ _ _ IAST ——— d-ELM

adsorbed phase by restricting the access of the major self-potential contributor (CO).

Carbon Monoxide - Methane / $AlPO_4$-18. The models predict virtually similar trends for the adsorption of this binary gas mixture (Figure 4.32) as for the CO-N_2 gas mixture (Figure 4.31), with the FH-VST predicted azeotrope formation seen again as a response to the threat brought to the stability of the adsorbed phase by the close-range repulsions between the polar CO molecules adsorbed. The a-ELM "hook" is less clear: given the fairly similar kinetic diameters of CO and CH_4, the displacement of a certain number of CH_4 molecules is seen as feasible by only a slightly lower number of CO molecules. IAST (just like its "shadow" d-ELM) remains as insensitive to potential interactions as its name indicates ("linear" binary isotherms), forecasting values of the separation factor that are lower than those predicted by a-ELM, but close to those predicted by d-ELM. The prediction by FH-VST of azeotrope formation and selectivity reversal is reflected in the binary adsorption isotherm (Figure 4.32b) by the rounded curve indicating the total amount adsorbed, this type of curve being characteristic for azeotropes with positive deviations from ideality. The hypothesis regarding the relationship between azeotrope formation and steric hindrance can be again considered for this adsorption system.

Methane - Nitrogen / $AlPO_4$-18. Figure 4.33 shows that from the adsorption point of view this is a "normally-behaving" system in which the intensity of interactions in the adsorbed phase is seen moderate by all models except a-ELM, which predicts a slightly curvier binary isotherm. All models agree that CH_4 would be the preferentially adsorbed species, with similar selectivity values forecast by IAST, d-ELM, and FH-VST and a slightly more "optimistic" value of the separation factor produced by a-ELM. The selectivity values higher than 2 predicted by the models would make $AlPO_4$-18 a potential adsorbent for CH_4-N_2 mixtures (Table 4.16).

Summary for $AlPO_4$-18. Data on single-component equilibrium adsorption indicates that $AlPO_4$-18 has the highest capacity for CO, compared to the other two gases, at 101.3 kPa and 40°C, but it is not much higher than that for CH_4 at the same pressure and temperature. IAST and d-ELM reflect this relative difference in pure-gas capacities by predicting that the feasibility of the separation is higher if the relative ratio of the

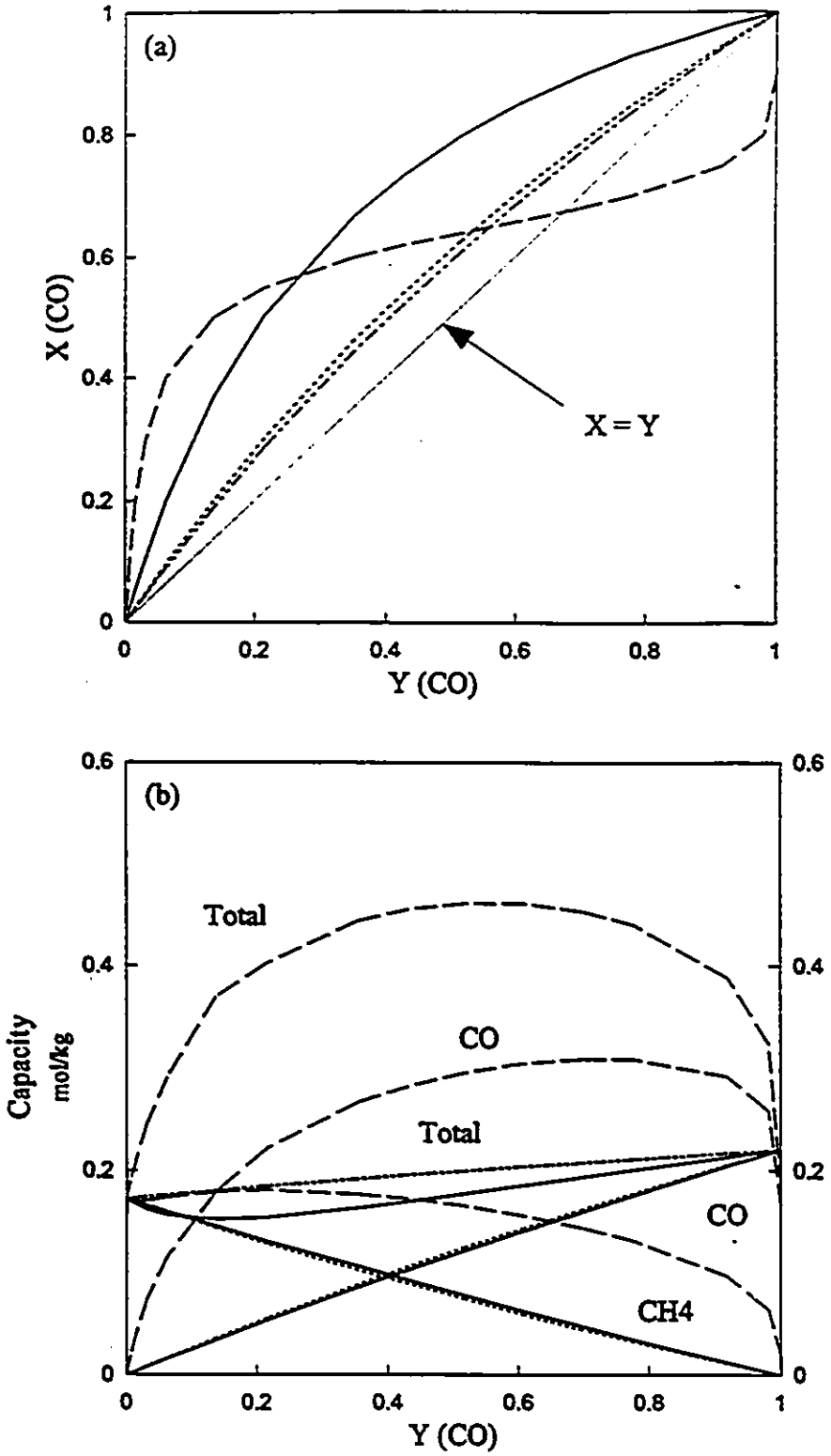

Figure 4.32 Predicted (a) X-Y diagram and (b) binary equilibrium isotherm for CO-CH4 adsorption on AlPO4-18 at 40.0-40.1°C and 101.3 kPa total pressure
_____ a-ELM _ _ _ _ _ FH-VST _ _ _ _ IAST ——— d-ELM

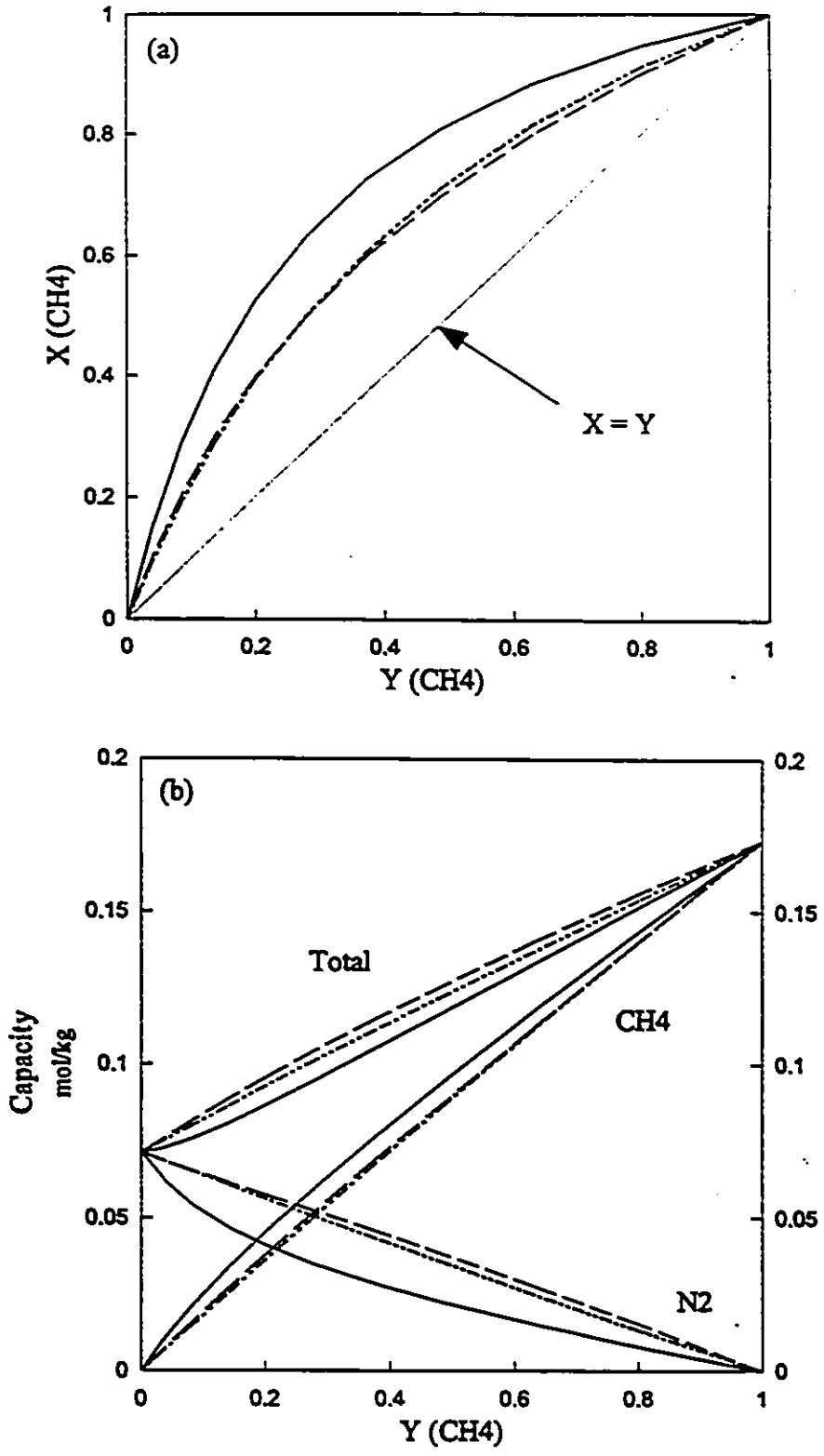

Figure 4.33 Predicted (a) X-Y diagram and (b) binary equilibrium isotherm for CH4-N2 adsorption on AlPO4-18 at 40.0-40.1°C and 101.3 kPa total pressure
_____ a-ELM _ _ _ _ _ FH-VST _ _ _ IAST ——— d-ELM

single-component capacity is high. Thus, the separation would be more successful for CH_4-N_2 gas mixtures at 40°C and 101.3 kPa total pressure than for the CO-CH_4 gas mixture because of the close values of the pure-gas adsorption capacities of $AlPO_4$-18 for CO and CH_4 (at 40°C and 101. 3 kPa).

It appears that ultimately the ratio of the single-component monolayer volumes is responsible for the FH-VST predictions of nonideality. For $AlPO_4$-17 the influence of this ratio is visible in the difference in pure-gas adsorption capacities between CH_4 and the two other adsorbates which feature similar capacities. In the case of $AlPO_4$-18, the influence of this ratio is visible from the shape of the experimental isotherms and the associated FH-VST fits (Figure 4.5): the FH-VST fit of the curvier pure CO isotherm will very likely intersect the linear FH-VST fits of the pure CH_4 and pure N_2 isotherms at some higher pressure, the "crossover" being lower for the CO-CH_4 pair than for the CO-N_2 pair because the ratio between the single-component monolayer volumes is lower.

4.2.3 Final Overview of Binary Gas Mixture Adsorption

The reliability of the information provided by the application of each of the three theories chosen (ELM, IAST, and the FH-VST for mixtures) is a result of the accuracy of the pure gas adsorption isotherm fits since no binary mixture adsorption data are available to confirm predictions. The greater the accuracy of the fits of the single-component adsorption isotherms, the higher the reliability of the binary gas mixture adsorption predictions. Collection of experimental binary adsorption data would be necessary for a final say on the predictive ability of each model.

Irrespective of the model chosen, the accuracy of the predictions may be affected by the experimental errors associated with the pure isotherm measurements.

An interesting observation is that whenever FH-VST predicts non-ideal behaviour, the IAST-predicted selectivity values decrease with increasing content of the better adsorbed component in the gas phase, which is opposite to the trend anticipated when the FH-VST does not predict azeotrope formation or selectivity reversal (slight increase in selectivity values with increasing content of the better retained species).

Another observation is that the IAST-predicted equilibrium separation factors appear to increase with increasing mole fraction of the better adsorbed component whenever this species is non-polar but very polarizable (e.g. CH_4), and therefore does not generate a close-range repulsion problem in the adsorbed phase. An explanation would lie with the use of the Langmuir pure-component adsorption fits to obtain IAST binary mixture adsorption predictions. All the Langmuir fits overestimate the adsorption capacity in the middle of the pressure range over which the experimental isotherm was determined, and underestimate the capacity of the adsorbent at the ends of this pressure range. When extrapolating the Langmuir fit for the lesser adsorbed component, the portion of the Langmuir fit which overestimates the adsorption capacity for the preferentially retained species corresponds to the portion of the Langmuir fit which underestimates the adsorption capacity for the lesser adsorbed species. Thus, the resulting values for the IAST predicted separation factors are higher if the chosen total pressure is found in the pressure range in which the overestimation of the capacity for one species corresponds to the underestimation of the capacity for the other species.

When the a-ELM equation (2.9) is applied, the constant selectivity value characteristic to ELM (irrespective of the approach) is affected only by the ratio of the Langmuir constants (B_i/B_j) regressed from the respective pure-gas adsorption experimental isotherms. The influence of the Langmuir constants is obvious in the variation of the capacities of the adsorbent for the components and the mixture. When the d-ELM equation (2.7) is applied, the constant selectivity value obtained is influenced by both the ratio of the Langmuir constants (B_i/B_j) and the ratio of the monolayer volumes of the pure species (v_{mi}/v_{mj}), and the effects of the Langmuir constants on the capacities of the adsorbents for the components and the mixture are tuned down by the effects of the monolayer volume of each pure species. Several adsorption systems among the ones investigated in this study (CH_4-N_2 / 5A, CH_4-N_2 / Turkish clinoptilolite, CO-N_2 / $AlPO_4$-11 at room temperature, as well as CH_4-N_2 / Turkish clinoptilolite, CH_4-CO / Cuban clinoptilolite, and CO - N_2 / $AlPO_4$-11 at 40°C) show that, as a result of the averaging of the monolayer volumes, when all the other models (IAST, FH-VST, d-ELM) predict equilibrium separation factors between 1 and 3, a-ELM predicts a value lower than 1;

vice-versa, when the other three models predict equilibrium selectivities lower than 1, a-ELM yields a value slightly higher than 1.

As far as ELM predictions are concerned, if the pure-component adsorption isotherms are not determined up to the saturation pressure, the applicability of the thermodynamic consistency condition that distinguishes a-ELM from d-ELM should be looked upon with caution.

IAST predictions may be very sensitive to the difference in the spreading pressures of the two components, which can be very high if the adsorption capacities of the molecular sieve for the two components are widely different (e.g. mixtures of polar and non-polar or weakly polar gases, such as CO-N_2 and CO-CH_4). As Myers and Prausnitz emphasized (1965), the accuracy of the fit in the low-pressure range is very important for reliable mixture predictions. IAST predicted equilibrium selectivities may increase or decrease with increasing partial pressure of the better adsorbed component of the mixture. The increase in selectivity with increasing content of the better adsorbed species appears to be encountered when the better adsorbed component is non-polar and there are no close-range repulsive interactions in the adsorbed phase.

Given its accountability of non-ideality through the Flory-Huggins activity coefficients and the excellent fitting capability proven with the pure-gas adsorption experimental data in the case of the aluminosilicate molecular sieves, FH-VST is likely to provide more realistic values for the amounts adsorbed from binary mixture adsorption systems in which the gaseous species possess electric moments and in which intense adsorbate-adsorbate and adsorbent-adsorbate interactions are likely to be exerted. The fitting capability of FH-VST may be questioned to a certain degree when it comes to adsorption systems involving small-pore aluminophosphate molecular sieve $AlPO_4$-17, especially when the adsorption systems involve "capsular" adsorbate molecules such as N_2 and CO. The slightly unfavourable isotherms, accurately fitted with the Freundlich equation but less well correlated by FH-VST, attest to the importance of the part played by steric effects during the adsorption - diffusion process.

The FH-VST predicted equilibrium separation factors have been found to increase as the partial pressure of the better adsorbed component decreases, irrespective of

the nature of the adsorbent (aluminosilicate or aluminophosphate) in the adsorption system. This observation appears to prove by itself that FH-VST accounts, indeed, for the adsorbent-adsorbate interactions, in the sense that it identifies (without being able to discriminate, however) close-range repulsion interactions as well as electrostatic interactions. For the adsorption systems involving aluminophosphate molecular sieves as adsorbents, IAST predicted selectivities were found to increase with increasing partial pressure of the better retained species, which could somewhat indicate the acknowledgment of a volume-filling mechanism dominant when adsorbent-adsorbate interactions are negligible enough to be ignored. The opposite is true with FH-VST predicted selectivities, despite the unity value of all the activity coefficients and the zero value of the binary interaction parameter. This observation seems to emphasize the contrast between IAST and FH-VST regarding the ability to recognize not only interactions but also physical restrictions (pore volume) related to adsorption mechanisms in energetically homogeneous adsorbents (volume filling) in which adsorbent-adsorbate electrostatic interactions are not dominant.

The composition-dependent γ_v values attributed to the activity coefficient of the vacancy in the vacancy solution reflect to a certain extent the degree of energetic heterogeneity of the adsorbent. It seems that the lower the degree of energetic heterogeneity in an aluminosilicate molecular sieve (i.e. the higher the Si/Al ratio), the closer to unity the γ_v values corresponding to the composition of the adsorbed phase (vacancy solution). Considering that the activity coefficient indicates the deviation from ideality, this interpretation relates the γ_v values and the intensity of the adsorbate-adsorbent interactions (the degree of energetic heterogeneity of the adsorbent): the weaker these interactions, the closer to unity the γ_v values are. Supporting this observation are the γ_v values equal to unity, associated with the activity of energetically homogeneous adsorbents such as the aluminophosphate molecular sieves.

According to the data in Table 4.14, given any of the three binary gas mixtures at a certain temperature (and 101.3 kPa total pressure), the FH-VST predicted γ_v ranges feature the lowest values in the case of Turkish clinoptilolite (an observation which is in agreement with the fact that the adsorbent-adsorbate interactions are expected to be the

most intense for this adsorbent), and the highest for zeolite 5A which features homogeneous cation population and therefore a lower degree of energetic heterogeneity (more "uniform" field gradients). Cuban clinoptilolite features a higher Si/Al ratio than Turkish clinoptilolite as well as mixed cation population with a larger content of monovalent cations than Turkish clinoptilolite, which would be responsible for generating a less intense and more uniform electric field in the zeolitic framework. It is not surprising therefore that the γ_v values associated with each binary gas mixture span over intermediate ranges, corresponding to a degree of energetic "non-uniformity" somehow lower than those associated with Turkish clinoptilolite but higher than those representing zeolite 5A (Appendix D). In view of the above, agreement between IAST and FH-VST predictions should be expected, in the case of aluminosilicate molecular sieves, whenever the range of γ_v values approaches unity. Discrepancies between the two models become more and more accentuated as γ_1 and γ_2 take lower and lower values, and tend to disappear as γ_1 and γ_2 approach unity very closely.

In general, for the zeolite adsorption systems investigated the γ_v values decrease with increasing coverage by the better adsorbed gas in the binary mixture, thus reflecting the tendency of the adsorbed phase to deviate from ideal behaviour as the intensity of adsorbate-adsorbate interactions (of the close-range repulsion type) increases. Two of the three exceptions encountered (CH_4-N_2 / Turkish clinoptilolite at both temperatures) could be explained by the predicted azeotrope formation for the CH_4-N_2 / Turkish clinoptilolite system; the third exception (CO-N_2 / 5A at room temperature) could be ignored given the minute variation of γ_v (Appendix D). In the adsorbed phase, the adsorbent-adsorbate interactions are more intense at low partial pressures of the more polar species (corresponding to high partial pressures of the less polar component) because of the field gradient - quadrupole interactions (which are quantified by FH-VST through γ_v values lower than 1). However, as soon as the number of less polar molecules in the adsorbed phase is higher than that of quadrupolar N_2 molecules, the adsorbent-adsorbate interactions become less intense – a fact illustrated by FH-VST through γ_v values that increase toward unity. The less polar molecules serve as "buffer" when interspersed among the more polar molecules.

The three models tend to disagree in their predictions of the equilibria of CH_4, CO, and N_2 binary mixture adsorption in the aluminophosphate molecular sieves investigated. Allowance must be made for ELM, the "constant separation factor approximation", which was developed with the Langmuir assumptions in mind, and is therefore unable to predict composition-dependent separation factors or non-idealities such as azeotropes. The only systems in which the models tend to agree to a certain extent are CH_4-CO / $AlPO_4$-11 (at both room temperature and 40°C) and CH_4-N_2 / $AlPO_4$-18 at 40°C.

If FH-VST accounts indeed for the degree of energetic heterogeneity of the adsorbent, that is if its predictions regarding mixture adsorption in aluminophosphate molecular sieves are proven right by experimental binary equilibrium information, then it appears that energetic heterogeneity is a basic ingredient in the adsorptive separation recipe. For zeolite adsorption systems, azeotrope formation and selectivity reversal appear to be the standard response whenever the stability of the adsorbed phase is jeopardized by too intense adsorbate-adsorbate interactions such as close-range repulsions. In the absence of adsorbent energetic heterogeneity (the case of aluminophosphate molecular sieves), adsorption systems are more likely to feature azeotropy and selectivity reversal because of the extra free energy possessed by molecules which are not strongly held on the surface of the adsorbent, that is they have not reduced enough their free energy by giving off heat of adsorption. Steric effects must also be considered when investigating the likelihood of non-ideal behaviour for a certain adsorption system.

The estimated equilibrium separation factors were encouraging especially for CH_4-CO / $AlPO_4$-11 and CH_4-N_2 / $AlPO_4$-18 at 40°C, as for these systems FH-VST did not predict azeotrope formation and selectivity reversal. Although FH-VST forecasts the possibility of separating the CH_4-N_2 gas mixture at 40°C using $AlPO_4$-17, these predictions are questionable given the imperfect FH-VST fits for the pure CO and pure N_2 adsorption isotherms. Measurement of experimental binary equilibrium isotherms is necessary to decide upon the reliability of $AlPO_4$-11 and $AlPO_4$-18 predictions yielded by all the models used. Further investigation of pure-gas adsorptive behaviour of $AlPO_4$-17 should be

carried out to determine which are the factors that lead to unfavourable single-component equilibrium isotherms describing adsorption in this small-pore aluminophosphate molecular sieve.

Table 4.16 shows that azeotrope formation and selectivity reversal are predicted by FH-VST to occur only when CO is part of the mixture and only at 40°C. This implies that the probability that these phenomena occur in binary mixture adsorption systems is higher at a higher temperature. Azeotrope formation could be related to steric hindrance, but it could also be interpreted in terms of the free energy that molecules possess at a higher temperature when confined in the adsorbed phase on the surface of an energetically homogeneous adsorbent. Since the adsorbed molecules (especially those which feature electric moments) are denied the possibility to interact with the aluminophosphate framework the way they would when adsorbed in an energetically heterogeneous zeolite, they have much more free energy to use in interactions with either neighbouring molecules or with molecules in the gas phase. If these interactions occur predominantly with molecules in the gas phase, they can lead to an equalization of the composition of the adsorbed phase and the gas phase, i.e. azeotrope formation. The molecules cannot, however, engage in interactions with molecules in the gas phase unless they possess a certain "threshold" energy. This "threshold" energy would probably be attained only under certain circumstances such as increased freedom of translation, rotation, and vibration (due to increased temperature), or as a result of the growing intensity of close-range repulsions or electrostatic interactions (dipole-dipole, dipole-induced dipole, dipole-quadrupole, quadrupole-quadrupole, induced dipole - induced dipole, etc.).

Selectivity reversal occurs probably as a palleative for too intense adsorbate-adsorbate repulsive interactions: the species possessing the smaller electric moment is preferentially adsorbed in an attempt to maintain stability in the adsorbed phase. The fact that azeotrope formation and selectivity reversal are predicted to occur at higher CO partial pressures backs up the hypothesis.

CHAPTER 5

CONCLUSIONS

1. Physical adsorption is governed by the energetic heterogeneity of the adsorbent in systems including aluminosilicate molecular sieves, and by steric effects in energetically homogeneous aluminophosphate molecular sieves.
2. Adsorption capacities are higher in aluminosilicate molecular sieves than in aluminophosphate molecular sieves.
3. Zeolites with a low Si/Al ratio and high content of strongly polarizing divalent cations are better adsorbents of polar gases than zeolites with predominantly monovalent cations.
4. In the pressure range investigated (<120 kPa) equilibrium adsorption capacities for CO are highest in Turkish clinoptilolite among the aluminosilicate molecular sieves, and in $AlPO_4$-18 among the aluminophosphate molecular sieves. At 101.3 kPa CH_4 is preferentially retained by Cuban clinoptilolite among the aluminosilicate molecular sieves and by $AlPO_4$-17 among the aluminophosphate molecular sieves. N_2 is adsorbed in relatively low amounts compared to the other two adsorbates in all the microporous materials investigated, except in $AlPO_4$-17.
5. Adsorption of CO in $AlPO_4$-17 and $AlPO_4$-18 and of CH_4 in $AlPO_4$-18 features hysteresis. This means that, if these adsorbents are used, the temperature-swing cycle has to be incorporated in pressure-swing adsorptive separation units.
6. For the pressure range investigated (< 123 kPa), the Flory-Huggins form of the Vacancy Solution Theory (FH-VST) proves to be an excellent fitting tool for the

extrapolation of pure-gas adsorption isotherms of N_2, CO, and CH_4 in aluminosilicate and aluminophosphate molecular sieves alike. Experiments carried out at large superatmospheric pressure ranges would confirm or invalidate its predictive capabilities.

7. The Langmuir equation also provides excellent fits for the pure N_2 and CH_4 adsorption isotherms in zeolite 5A, clinoptilolite, $AlPO_4$-11 and $AlPO_4$-18, but is less accurate in the case of the more rectangular CO adsorption isotherms in zeolite 5A and clinoptilolite.
8. Modelling of the binary mixture adsorption isotherms reveals that aluminosilicate molecular sieves are a good choice for the separation of mixtures involving polar and non-polar (or weakly polar) components, and their performance is usually directly related to their Si/Al ratio and their cation composition. The energetically homogeneous aluminophosphate molecular sieves are more suitable for the separation of gas mixtures involving non-polar adsorbates (CH_4) and adsorbates with very small electric moments (N_2).
9. The Ideal Adsorbed Solution Theory (IAST) virtually ignores all interactions occurring in an adsorption system, and its reliability is therefore questionable in systems with intense adsorbate-adsorbate and adsorbent-adsorbate interactions.
10. The Extended Langmuir Model in its averaging version (a-ELM) should be used with caution to describe the behaviour of those binary gas mixture systems involving zeolites, because the intensity of the interactions of the adsorbing molecules with the zeolitic framework appears to be too high for the averaging of the influence of one species over the other in the adsorbed phase to reflect reality truthfully. This approach should also be avoided in the case of linear isotherms which have not been determined up to the saturation pressure (e.g. N_2, CO, and CH_4 in $AlPO_4$-11 and $AlPO_4$-18).
11. FH-VST appears to be the most reliable model given its accountability of the non-idealities in the adsorption system through the Flory-Huggins activity coefficients. Its prediction of azeotrope formation with selectivity reversal is confirmed by the crossover of the pure CH_4 and the pure CO experimental isotherms

describing adsorption in Cuban clinoptilolite. It appears that FH-VST will predict azeotropy and selectivity reversal in aluminosilicate or aluminophosphate systems whenever the single-component equilibrium capacities are very similar at the pressure for which the predictions are determined.

12. The influence of the adsorption temperature on binary mixture equilibrium is acknowledged by all models through a decrease in individual adsorption capacities and total amount adsorbed with an increase in temperature.
13. Zeolite 5A and Turkish clinoptilolite appear to be suitable adsorbents for the separation of binary mixtures containing polar gases such as CO, while the aluminophosphate molecular sieves investigated seem to be more adequate for the separation of binary mixtures containing non-polar species such as CH_4.
14. Promising adsorbents for ultra-purification processes are those which have such a high affinity for a certain adsorbate that they will adsorb it even when present in the most minute trace amounts (e.g. CO in Turkish clinoptilolite). Zeolite 5A and clinoptilolite appear to be promising adsorbents for purification processes, while $AlPO_4$-11, $AlPO_4$-17, and $AlPO_4$-18 seem to have potential for bulk separation processes.
15. According to model predictions, $AlPO_4$-17 and $AlPO_4$-18 appear to have the potential to separate CH_4-N_2 mixtures.

CHAPTER 6

RECOMMENDATIONS

1. Equilibrium adsorption isotherms should be evaluated at higher pressures and at various temperatures (including room temperature), especially for the adsorption systems involving Cuban clinoptilolite, $AlPO_4$-11, $AlPO_4$-17, $AlPO_4$-18, about which data is scarce in the literature.
2. Desorption isotherms should be determined for all the systems, especially in the case of aluminophosphate molecular sieves to assess their suitability as industrial adsorbents.
3. Experimental binary isotherms should be determined for all the adsorption systems for which predictions have been made to verify the applicability and accuracy of each model.
4. Single-component experimental isotherms should be determined for the adsorption of ethylene, n-butane and i-butane in $AlPO_4$-11, $AlPO_4$-17, and $AlPO_4$-18 to assess the presence of the molecular sieving effect exerted by these aluminophosphate adsorbents. Measurement of binary isotherms for the adsorption of C_2H_4-N_2 and C_2H_4-CO mixtures should be carried out to assess the potential of $AlPO_4$-11, $AlPO_4$-17, and $AlPO_4$-18 for the separation of light paraffins from CO and N_2 gases. Predictions of the potential of these adsorbents for the separation of these gaseous mixtures should be made to verify the applicability of the mixture adsorption models to systems involving insaturated hydrocarbons.

5. Adsorption and diffusion studies should be carried out on the pelletized form of the aluminophosphate molecular sieves investigated to determine the contribution of different types of mass transfer to overall adsorption.
6. Equilibrium single-component and binary mixture isotherms should be determined for the adsorption of other adsorbates such as CO_2, NO, NO_2, H_2S, SO_2, NH_3, H_2, O_2, C_2H_6, C_2H_4, and other light hydrocarbons, especially for those adsorbents whose adsorptive behaviour has been less comprehensively investigated (e.g. Cuban clinoptilolite, $AlPO_4$-11, $AlPO_4$-17, and $AlPO_4$-18).
7. Ion-exchange studies on Cuban clinoptilolite could provide additional information regarding the possibility of tailoring natural zeolites to suit the requirements of certain industrial applications and to reduce the impediment represented by impurities and defects normally encountered in natural zeolites.
8. Diffusion studies should also be undertaken for Cuban clinoptilolite to better understand the mechanisms leading to the difference in adsorption capacity with respect to Turkish clinoptilolite.
9. Adsorption and desorption studies should be carried out in silicon-substituted aluminophosphate molecular sieves (SAPO's) to confirm the benefits of the presence of the silicon atom in the framework from the point of view of adsorbent energetic heterogeneity (and implicitly adsorptive properties) as well as from the point of view of framework rigidity translated into minimal hysteresis, improved mechanical resistance, and resistance to attrition.

REFERENCES

1. Ackley, M. W. and R. T. Yang, "Diffusion in Ion-Exchanged Clinoptilolites", *AIChE J.*, 37(11), 1645-1656 (1991a).

2. Ackley, M. W. and R. T. Yang, "Adsorption Characteristics of high-exchange clinoptilolites", *Ind. Eng. Chem. Res.*, 30(12), 2523-2530 (1991b).

3. Apolonatos, G., *Gas Adsorption With Molecular Sieve Zeolites*, M. A. Sc. Thesis Diss., Department of Chemical Engineering, University of Ottawa, 1994.

4. Barrer, R. M., *Zeolites and Clay Minerals as Sorbents and Molecular Sieves*, Academic Press, London, 1978.

5. Bennett, J. M., W. J. Dytrych, J. J. Pluth, J. W. Richardson, Jr., and J. V. Smith, "Structural features of aluminophosphate materials with Al/P = 1", *Zeolites*, 6, 349-359 (1986).

6. Breck, D. W., *Zeolite Molecular Sieves: Structure, Chemistry and Use*, John Wiley & Sons Inc., New York, 1974.

7. Broughton, D.B., "Adsorption Isotherms for Binary Gas Mixtures", *Ind. Eng. Chem.*, 40(8), 1506-1508 (1948).

8. Cochran, T. W., R. L. Kabel, and R. P. Danner, "Vacancy Solution Theory of Adsorption Using Flory-Huggins Activity Coefficient Equations", *AIChE J.*, 31(2), 268-277 (1985a).

9. Cochran, T. W., R. L. Kabel, and R. P. Danner, "The Vacancy Solution Model of Adsorption -- Improvements and Recommendations", *AIChE J.*, 31(12), 2075-2082 (1985b).

10. Danner, R.P. and L.A. Wenzel, "Adsorption of Carbon Monoxide-Nitrogen, Carbon Monoxide-Oxygen, and Oxygen-Nitrogen Mixtures on Synthetic Zeolites", *AIChE J.*, 15(4), 515-520 (1969).

11. Davis, M. E., "Zeolites and Molecular Sieves: Not Just Ordinary Catalysts", *Ind. Eng. Chem. Res.*, 30, 1675-1683 (1991).

12. Dubinin, M. M., "Investigation of the Adsorption Properties and Secondary Porous Structure of Adsorbents Exhibiting A Molecular Sieve Action. Report 8: Improvement of the Method of Calculation of the Volumes of Large Cavities of

Dehydrated Crystals of Type X Synthetic Zeolites on the Basis of X-ray Diffracion Data", *Physical Chemistry*, 195-200 (1964).

13. Esenli, F. and I. Kumbasar, "Thermal behavior of heulandites and clinoptilolites of Western Anatolia" in *Zeolites and Related Microporous Materials: State of the Art 1994*, J. Weitkamp *et al.* (eds.), Studies in Surface Science and Catalysis, Vol. 87A, Elsevier, Amsterdam, 645-651, 1994.

14. Frankiewicz, T. C. and R. G. Donnelly, "Methane/Nitrogen Gas Separation over the Zeolite Clinoptilolite by the Selective Adsorption of Nitrogen", in *Industrial Gas Separations*, Whyte, T. E., Jr., *et al.* (eds.), American Chemical Society, Washington, D.C., 1983.

15. Graham, D., "Adsorption Equilibria" in *Adsorption, Ion Exchange and Dialysis*, AIChE Chemical Engineering Progress Symposium Series, 55(24), 17-23 (1959).

16. Grillet, Y., P. L. Llewellyn, H. Reichert, J. P. Coulomb, N. Pellenq, and J. Rouquerol, "Confinement in micropores and enthalpies of physisorption" in *Characterization of Porous Solids III*, J. Rouquerol *et al.* (eds.), Studies in Surface Science and Catalysis Vol. 87, Elsevier, Amsterdam, 525-534, 1994.

17. Hansley, P. L. and R. A. Sheppard, "Distribution and Properties of Clinoptilolite-Bearing Tuffs in the Upper Jurassic Morrison Formation on the Ute Mountain Ute Reservation, Southwestern Colorado and Northwestern New Mexico", *U.S. Geological Survey Bulletin*, **2061-A** (1993).

18. Haq, N., and D. M. Ruthven, "A Chromatographic Study of Sorption and Diffusion in 5A Zeolite", *J. Coll. Interface Sci.*, **112**(1), 164-169 (1986).

19. Iijima, A., "Composition and Origin of Clinoptilolite in the Nakanosawa Tuff of Rumoi, Hokkaido", *Molecular Sieve Zeolites - I*, American Chemical Society, 334-341 (1971).

20. Innes, W. B. and H. H. Rowley, "Adsorption Isotherms of Mixed Vapors of Carbon Tetrachloride and Methanol On Activated Charcoal at 25°C", *J. Phys. Coll. Chem.*, **51**, 1154-1171 (1947).

21. Innes, W. B., R. B. Olney, and H. H. Rowley, "Adsorption Isotherms of Mixed Vapors of Benzene and Methanol On Activated Charcoal at 25°C", *J. Phys. Coll. Chem.*, 55, 1324-1334 (1951).

22. Kärger, J. and D. M. Ruthven, *Diffusion in Zeolites and Other Microporous Solids*, John Wiley & Sons, Inc., New York, 1992.

23. Kemball, C., E. C. Rideal, and E. A. Guggenheim, "Thermodynamics of Monolayers", *Trans. Faraday Soc.*, 44, 948-954 (1948).

24. Koyama, K. and Y. Takeuchi, "Clinoptilolite: the distribution of potassium atoms and its role in thermal stability", *Zeitschrift für Kristallographie*, 145(8), 216-239 (1977).

25. Langmuir, I., "Adsorption of Gases on Plain Surfaces of Glass, Mica, and Platinum", *J. Am. Chem. Soc.*, 40, 1361-1403 (1918).

26. Lederman, Peter B. and Brymer William, "The Adsorption of Nitrogen-Methane on Molecular Sieves", *AIChE J.*, 10(1), 30-34 (1964).

27. Lillerud, K. P. and D. Akporiaye, "Systematic Relationships Between the Structures of CHA, AEI and KFI" in *Zeolites and Related Microporous Materials: State of the Art 1994*, J. Weitkamp *et al.* (eds.), Studies in Surface Science and Catalysis Vol. 84, Elsevier, Amsterdam, 543-550, 1994.

28. Loughlin, K. F. and D. M. Ruthven, "The Sorption and Diffusion of Ethane in Type A Zeolites", *Chem. Eng. Sci.*, 27, 1401-1408 (1972).

29. Malla, P. B. and S. Komarneni, "Synthesis and Water Sorption Properties of Aluminophosphate ($AlPO_4$) and Silicoaluminophosphate (SAPO) Molecular Sieves" in *Mat. Res. Soc. Symp. Proc.*, 233, 237-242 (1991).

30. Markham, E.C. and A.F. Benton, "The Adsorption of Gas Mixtures by Silica", *J. Am. Chem. Soc.*, 53, 497-507 (1931).

31. Martens, J. A. and P. A. Jacobs, "Crystalline Microporous Phosphates: a Family of Versatile Catalysts and Adsorbents" in *Advanced Zeolite Science and Applications*, Studies in Surface Science and Catalysis, Vol. 85, Elsevier, Amsterdam, p. 653-685, 1994.

32. Meier, W. M., "Zeolite Structures: Some Common Misconceptions and Pitfalls" in *Zeolites – Synthesis, Structure, Technology and Application*, B. Drzaj, S. Hocevar, and S. Pejovnik (eds.), Studies in Surface Science and Catalysis, Vol. 24, Elsevier, Amsterdam, 217-218 (1985).

33. Meier, W. M. and D. H. Olson, *Atlas of Zeolite Structure Types*, 3rd rev. ed., Butterworth-Heinemann, London, 1992.

34. Micromeritics Instrument Corporation, *Instruction Manual for Accusorb 2100E Physical Adsorption Analyzer and Including Chemisorption Option*, Norcross, Georgia (1986).

35. Myers, A.L. and J. M. Prausnitz, "Thermodynamics of Mixed-Gas Adsorption", *AIChE J.*, **11**(1), 121-127 (1965).

36. Noll, K. E., V. Gounaris, and W.-S. Hou, *Adsorption Technology for Air and Water Pollution Control*, Lewis Publishers, Inc., Chelsea (Michigan), 1992.

37. Oberholtzer, J. E. and L. B. Rogers, "Effects of Micropores on Peak Shape and Retention Volume in Gas-Solid Chromatography, *Anal. Chem.*, **41**(12), 1590-1594 (1969).

38. Peeters, M. P. J., J. H. C. van Hooff, R. A. Sheldon, V. L. Zholobenko, L. M. Kustov, and V. B. Kazanski, "Spectroscopic Investigation of the Redox Properties of CoAPO Molecular Sieves" in *Proceedings from the 9th International Conference*, Vol. I, Montreal, 1992, Eds. R. von Ballmoos *et al.*, Butterworth-Heinemann, Guildford, p. 651-658, 1993.

39. Pluth, J. J. and J. V. Smith, "Four- and Six-coordinated Al and an Encapsulated Isopropylamine Species in 7 $AlPO_4.2(C_3H_7NH_2).2H_2O$", *Acta Cryst.*, **C43**, 866-870 (1987).

40. Rabo, J. A., "New Applications of Nonclassical Molecular Sieve Catalysts" in *Zeolite Microporous Solids: Synthesis, Structure, and Reactivity*, NATO ASI Series C - Mathematical and Physical Sciences, **352**, Kluwer Academic Publishers, Dordrecht, 1992.

41. Reichert, H., W. Schmidt, Y. Grillet, P. Llewellyn, J. Rouquerol, and K. Unger, "Investigation on the Adsorption of N_2, Ar, CO and CH_4 on Aluminophosphates" in *Characterization of Porous Solids III*, J. Rouquerol *et al.* (eds.), Studies in Surface Science and Catalysis Vol. 87, Elsevier, Amsterdam, 1994.

42. Rudolf, P. R. and C. E. Crowder, "Structure refinement and water location in the very large-pore molecular sieve VPI-5 by X-ray Rietveld techniques", *Zeolites*, **10**, 163 (1990).

43. Ruthven, D. M., "Sorption of Oxygen, Nitrogen, Carbon Monoxide, Methane, and Binary Mixtures of these Gases in 5A Molecular Sieve", *AIChE J.*, **22**(4), 753-759 (1976).

44. Ruthven, D. M., *Principles of Adsorption and Adsorption Processes*, John Wiley & Sons, New York, 1984.

45. Ruthven, D. M. and R.I. Derrah, "Transition State Theory of Zeolitic Diffusion - Diffusion of CH_4 and CF_4 in 5A Zeolite", *J. Chem. Soc. Faraday Trans. 1*, **68**, 2332-2343 (1972).

46. Ruthven, D. M. and R. I. Derrah, "Diffusion of Monatomic and Diatomic Gases in 4A and 5A Zeolites", *J.Chem.Soc., Faraday Trans. 1*, 71, 2031-2044 (1975).

47. Ruthven, D. M., K. F. Loughlin, and R. I. Derrah, "Sorption and Diffusion of Light Hydrocarbons and Other Simple Nonpolar Molecules in Type A Zeolites", *Adv. Chem.*, 121, 330-344 (1973).

48. Shah, D. B. and D. M. Ruthven, "Measurement of Zeolitic Diffusivities and Equilibrium Isotherms by Chromatography", *AIChE J.*, 23(6), 804-809 (1977).

49. Sievers, W. and A. Mersmann, "Correlation of Single and Prediction of Multicomponent Adsorption Equilibria at High Pore Filling Degrees" in *Characterization of Porous Solids III*, J. Rouquerol *et al.* (eds.), Studies in Surface Science and Catalysis Vol. 87, Elsevier, Amsterdam, 99-108, 1994.

50. Simmen A., L. B. McCusker, Ch. Baerlocher, and W. M. Meier, "The structure determination and Rietveld refinement of the aluminophosphate $AlPO_4$-18", *Zeolites*, 11, 654-661 (1991).

51. Sirkecioglu, A., Y. Altav, and A. Erdem-Senatalar, "Adsorption of H_2S and SO_2 on Bigadic clinoptilolite", *Sep. Sci. Tech.*, 30(13), 2747-2762 (1995).

52. Stelmack, P. *Adsorption of N_2, CO, CH_4, and Binary Mixtures of these Gases in Zeolite 5A, Clinoptilolite, and $AlPO_4$-11 Molecular Sieves*, B.A.Sc. Thesis, University of Ottawa, Ottawa, 1994.

53. Suzuki, M., *Adsorption Engineering*, Kodansha Ltd., Tokyo, and Elsevier Science Publishers B.V., Amsterdam, 1990.

54. Szostak, R., *Handbook of Molecular Sieves*, Van Nostrand Reinhold, New York, 1992.

55. Theocharis, C. R. and M. R. Gelsthorpe, "Modified Aluminophosphate Microporous Solids" in *Characterization of Porous Solids*, K. K. Unger *et al.* (eds.), Elsevier Science Publishers B.V., Amsterdam, 1988.

56. Tezel, F.H. and G. Apolonatos, "Chromatographic study of adsorption for N_2, CO and CH_4 in molecular sieve zeolites", *Gas Sep. Purif.*, 7(1), 11-17 (1993).

57. Triebe, R. W., *Separation and Purification of Gases with Molecular Sieves*, M. A. Sc. Thesis Diss., Department of Chemical Engineering, University of Ottawa, 1994.

58. Triebe, R. W. and F. H. Tezel, "Adsorption of nitrogen, carbon monoxide, carbon dioxide and nitric oxide on molecular sieves", *Gas Sep. Purif.*, 9(4), 223-230 (1995).

59. Triebe, R. W., F. H. Tezel and K. C. Khulbe, "Adsorption of methane, ethane, and ethylene on molecular sieve zeolites", accepted for publication in *Gas Sep. Purif.*

60. U.S. Environmental Protection Agency, "Optimization of Ammonia Removal by Ion Exchange Using Clinoptilolite", U.S. Government Printing Office, Washington, D.C., 1971.

61. Valenzuela, D. P. and A. L. Myers, *Adsorption Equilibrium Data Handbook*, Prentice-Hall Advanced Reference Series, Prentice-Hall, Englewood Cliffs, New Jersey, 1989.

62. Werner, L., J. Caro, G. Finger, and J. Kornatowski, "Optical Second Harmonic Generation (SHG) on *p*-Nitroaniline in Large Crystals on $AlPO_4$-5 and ZSM-5", *Zeolites*, **12**, 658-663 (1992).

63. Wilson S. T., B. M. Lok, C. A. Messina, and E. M. Flanigen, "Synthesis of $AlPO_4$ Molecular Sieves" in *Proceedings of the Sixth International Zeolite Conference*, D. Olson and A. Bisio (eds.), Butterworth & Co (Publishers) Ltd., Guildford, 1984.

64. Wilson, S. T., "Synthesis of $AlPO_4$-Based Molecular Sieves" in *Introduction to Zeolite Science and Practice*, Studies in Surface Science and Catalysis, Vol. 58, H. van Bekkum, E. M. Flanigen, and J. C. Hansen (eds.), Elsevier, Amsterdam, 137-151 (1991).

65. Yang, R. T., *Gas Separation by Adsorption Processes*, Butterworth Publishers, Mass., U.S.A., 1987.

66. Yeh, Y. T. and R. T. Yang, "Diffusion in Zeolites Containing Mixed Cations", *AIChE J.*, **35**(10), 1659-1666 (1989).

67. Zeldowitsh, J., "On the Theory of the Freundlich Adsorption Isotherm", *Acta Physicochim. U.R.S.S.*, **1**(6), 961-973 (1935).

APPENDIX A

Calculation of Experimental Pure-Component Adsorption Data

Calculation of Experimental Pure-Component Adsorption Volumetric Data

The determination of an equilibrium adsorption isotherm through the static volumetric method is performed by contacting a known quantity of adsorbent with a known quantity of adsorbate which is incrementally admitted into the volumetric apparatus. In order to obtain the necessary equilibrium information, the ideal gas law is applied and therefore the pressure, temperature, and volume of the gas in each section of the apparatus must be known or measured. Once this information is known, a material balance can be written for the static volumetric system considering the total amount of adsorbent involved (Micromeritics, 1986):

$$n_{di} = n_{de} + n_{se} + n_{ie} + n_{ae} \qquad (A.1)$$

For the first datapoint on the equilibrium adsorption isotherm, the material balance is written as:

$$\frac{P_1 V_d}{T_d} = \frac{P_2 V_d}{T_d} + \frac{P_2 V_s}{T_s} + \frac{P_2 V_i}{T_i} + \frac{760}{273} V_a \qquad (A.2)$$

where $T_i = (T_d + T_s) / 2$. In this case the pressure P_1 is the pressure of the gas admitted into the distributing manifold system prior to opening the valve isolating the sample from the rest of the volumetric apparatus. For subsequent datapoints on the equilibrium adsorption isotherm, the pressure P_1 is the equilibrium pressure reached after contacting the adsorbate and the adsorbent and equilibrating the two phases of the adsorption system (the pressure P_2 measured for the previous datapoint), i.e. $P_1(n) = P_2\ (n\text{-}1)$. The expression of the material balance becomes:

$$\frac{P_1 V_d}{T_d} + \frac{P_e V_s}{T_s} + \frac{P_e V_i}{T_i} = \frac{P_2 V_d}{T_d} + \frac{P_2 V_s}{T_s} + \frac{P_2 V_i}{T_i} + \frac{760}{273} V_a \qquad (A.3)$$

The volume of gas adsorbed at STP conditions (273 K and 101.325 kPa) can be calculated by rearranging equation (A3):

$$V_a = \frac{273}{760}\left[\frac{(P_1 - P_2)V_d}{T_d} + \frac{(P_c - P_2)V_s}{T_s} + \frac{(P_c - P_2)V_i}{T_i}\right] \qquad (A.4)$$

or

$$V_a = \frac{273}{760}\left[\frac{(P_1 - P_2)V_d}{T_d} + (P_c - P_2)\left(\frac{V_s}{T_s} + \frac{V_i}{T_i}\right)\right] \qquad (A.5)$$

Since V_d/T_d , V_s/T_s, and V_i/T_i are constant during the measurement of the equilibrium adsorption isotherm, the amount of gas adsorbed by the entire amount of sample is a function only of P_1, P_2, and P_c. The values of V_d, V_i, and T_d are provided by the manufacturer as 31.49 ml, 3.65 ml, and 307.2 K, respectively (Micromeritics, 1986).

The equilibrium adsorption capacity of an adsorbent for an adsorbate (the volume of gas adsorbed per unit mass adsorbent) results then from:

$$q = \frac{V_a}{W_s} = \frac{273}{760}\left[\frac{(P_1 - P_2)V_d}{T_d W_s} + (P_c - P_2)\left(\frac{V_s}{T_s W_s} + \frac{V_i}{T_i W_s}\right)\right] \qquad (A.6)$$

The equilibrium adsorption isotherm describing the behaviour of an adsorption system over a specific pressure range is obtained by plotting q vs. P_2.

The dead-space volume V_s results from a material balance analogous to the one used in determining the equilibrium adsorption capacity for the first equilibrium pressure determined for the isotherm, assuming that helium is not adsorbed. Thus:

$$\frac{H_1 V_d}{T_d} = \frac{H_2 V_d}{T_d} + \frac{H_2 V_s}{T_s} + \frac{H_2 V_i}{T_i} \qquad (A.7)$$

where H_1 represents the pressure of helium admitted into the distributing manifold system prior to opening the valve isolating the adsorbent sample from the rest of the volumetric apparatus, and H_2 represents the pressure of the non-adsorbing helium after being released

onto the adsorbent sample and after having filled all the void space available in the micropores and/or macropores. Therefore:

$$V_s = \left[\frac{V_d(H_1-H_2)}{T_d} - \frac{V_iH_2}{T_i}\right]\frac{T_s}{H_2} \qquad (A.8)$$

APPENDIX B

Flory-Huggins Vacancy Solution Theory Equations for the Prediction of Binary Adsorption Isotherms

Equations for the Prediction by FH-VST for Mixtures of Binary Equilibrium Adsorption Data

The system of equations solved iteratively according to the procedure indicated by Cochran *et al.* (1985a) is provided below. The principal equation is that for the distribution of gas species *i* between the adsorbed and gas phases:

$$y_i \phi_i P = \gamma_i^s x_i \frac{n_m n_i^\infty}{n_m^\infty b_i} \left[\frac{\exp \alpha_{rv}}{1 + \alpha_{rv}} \right] \exp\left(\left[\left(\frac{n_i^\infty - n_m^\infty}{n_m} \right) - 1 \right] \ln(\gamma_v^s x_v^s) \right) \qquad \text{(B.1)}$$

The two equilibrium equations resulting in the case of a binary mixture can be summed to eliminate y_i and obtain a simpler solution for n_m.

The activity coefficient of a component in the adsorbed phase, γ_i^s, during gas mixture adsorption is a function of the mole fractions of the adsorbed vacancy soluion, x_i^s and x_v^s. The experimental mole fraction, x_i, is on a vacancy-free basis. The equations relating the two mole fractions are:

$$x_i^s = \frac{n_m x_i}{n_m^\infty} \qquad \text{(B.2)} \qquad \text{and} \qquad x_v^s = 1 - \frac{n_m}{n_m^\infty} \qquad \text{(B.3)}$$

where the limiting amount adsorbed of the gas mixture, n_m^∞, is a function of the experimental mole fractions only:

$$n_m^\infty = \Sigma x_i n_i^\infty \qquad i = 1, \ldots N \qquad \text{(B.4)}$$

The total amount adsorbed of the gas mixture is the sum of the amounts of individual components adsorbed:

$$n_m = \Sigma n_i \qquad i = 1, \ldots N \qquad \text{(B.5)}$$

which means that the amounts of individual components adsorbed are calculated as

$$n_i = x_i n_m \qquad \text{(B.6)}$$

The total limiting amount of adsorption is calculated similarly using the following equation:

$$n_m^{\infty} = x_i n_i^{\infty} \tag{B.7}$$

The Flory-Huggins activity coefficient of a component in a multicomponent vacancy solution is given by:

$$\ln\gamma_i^s = -\ln\Sigma\frac{x_j^s}{\alpha_{ij}+1} + \left[1 - \left(\Sigma\frac{x_j^s}{\alpha_{ij}+1}\right)^{-1}\right] \qquad j = 1, \ldots M \tag{B.8}$$

The binary parameter, α_{ij}, is defined in terms of the gas-vacancy interaction parameters regressed from pure-component adsorption data:

$$\alpha_{ij} = \frac{\alpha_{iv}+1}{\alpha_{jv}+1} - 1 \tag{B.9}$$

a definition which leads to the obvious conclusion that $\alpha_{ii} = 0$.

In the case of binary mixture adsorption, the equations yielding the values of the Flory-Huggins activity coefficients are:

$$\ln\gamma_1^s = -\ln\left(x_1^s + \frac{x_2^s}{1+\alpha_{12}} + \frac{x_v^s}{1+\alpha_{1v}}\right) + \left[1 - \left(x_1^s + \frac{x_2^s}{1+\alpha_{12}} + \frac{x_v^s}{1+\alpha_{1v}}\right)^{-1}\right] \tag{B.10}$$

$$\ln\gamma_2^s = -\ln\left[(1+\alpha_{12})x_1^s + x_2^s + \frac{x_v^s}{1+\alpha_{2v}}\right] + \left[1 - \left((1+\alpha_{12})x_1^s + x_2^s + \frac{x_v^s}{1+\alpha_{2v}}\right)^{-1}\right] \tag{B.11}$$

$$\ln\gamma_v = -\ln\left[(1+\alpha_{1v})x_1^s + (1+\alpha_{2v})x_2^s + x_v^s\right] + \left[1 - \left((1+\alpha_{1v})x_1^s + (1+\alpha_{2v})x_2^s + x_v^s\right)^{-1}\right] \tag{B.12}$$

The other equations added to the system are:

$$\Sigma y_i = 1 \qquad i = 1, \ldots N \tag{B.13}$$

$$\Sigma x_i = 1 \qquad i = 1, \ldots N \tag{B.14}$$

$$x_1^s + x_2^s + x_v^s = \tag{B.15}$$

All these equations are solved simultaneously after selecting the composition of the adsorbed phase, x_i, and the total pressure of the gas mixture (101.3 kPa in this study).

APPENDIX C

Experimental and Predicted Pure-Component Adsorption Data

N2 / 5A ADSORPTION ISOTHERM at 22.7°C

Flory-Huggins Vacancy Solution Theory

Parameter	estimates	Asymptotic standard error	Asymptotic 95% confidence interval lower limit	upper limit
ninf [mol/kg]	1.6650457	0.9956749	-0.894381	4.2244725
b1 [mol/kg*Pa]	5.06E-06	1.62E-07	4.64E-06	5.48E-06
alfa1v	-0.010772	41.838894	-107.5595	107.537

p {exp} [Pa]	v {exp} [m3 STP/kg]	n {exp} [mol/kg]	theta {VST}	P {VST} [Pa]	n {VST} [mol/kg]	p {exp} [mm Hg]	v {exp} [cc STP/g]	Square deviation
0	0	0	0	0	0	0	0	0
5122.245	0.000562	0.02508	0.01532	5122.245	0.02552	38.42	0.562	1.95E-07
10884.438	0.001217	0.05430	0.03201	10884.438	0.05330	81.64	1.217	9.96E-07
25421.909	0.002709	0.12087	0.07170	25421.909	0.11939	190.68	2.709	2.20E-06
36026.370	0.003762	0.16785	0.09866	36026.370	0.16427	270.22	3.762	1.28E-05
57475.273	0.005507	0.24571	0.14867	57475.273	0.24754	431.1	5.507	3.34E-06
76380.385	0.007007	0.31263	0.18835	76380.385	0.31362	572.9	7.007	9.70E-07
91725.789	0.008102	0.36149	0.21795	91725.789	0.36289	688	8.102	1.97E-06
113657.319	0.009605	0.42855	0.25668	113657.319	0.42739	852.5	9.605	1.35E-06
		At 1 atm:	0.23539	101325.000	0.39193			
							Standard deviation:	0.00184

N2 / 5A ADSORPTION ISOTHERM at 22.7°C

Langmuir Theory

B [1/Pa] = 3.13E-06 vm [m3/kg]= 0.03644 nm [mol/kg]= 1.626029

p {exp} [Pa]	v {exp} [m3 STP/kg]	n {exp} [mol/kg]	p/v [Pa/m3]	Langmuir v [m3 STP/kg]	Langmuir n [mol/kg]	p {exp} [mm Hg]	v {exp} [cc STP/g]	Square deviation
0	0	0		0	0	0	0	0
5122.245	0.000562	0.02508	9114316	0.000576	0.02568	38.42	0.562	3.64E-07
10884.438	0.001217	0.05430	8943663	0.001202	0.05361	81.64	1.217	4.72E-07
25421.909	0.002709	0.12087	9384241	0.002688	0.11994	190.68	2.709	8.68E-07
36026.370	0.003762	0.16785	9576388	0.003696	0.16489	270.22	3.762	8.74E-06
57475.273	0.005507	0.24571	1.04E+07	0.005560	0.24809	431.1	5.507	5.66E-06
76380.385	0.007007	0.31263	1.09E+07	0.007036	0.31394	572.9	7.007	1.69E-06
91725.789	0.008102	0.36149	1.13E+07	0.008134	0.36293	688	8.102	2.07E-06
113657.319	0.009605	0.42855	1.18E+07	0.009569	0.42692	852.5	9.605	2.65E-06
101325.000				0.008780	0.39176			
							Standard deviation:	0.00179

N2 / 5A ADSORPTION ISOTHERM at 39.8°C

Flory-Huggins Vacancy Solution Theory

Parameter	estimates	Asymptotic standard error	Asymptotic 95% confidence interval lower limit	upper limit
ninf [mol/kg]	2.5947941	1.4503008	-2.020788	7.2103766
b1 [mol/kg*Pa]	1.23E-05	4.65E-07	1.08E-05	1.37E-05
alfa1v	1.6362931	2.121495	-5.115365	8.387951

p {exp} [Pa]	v {exp} [m3 STP/kg]	n {exp} [mol/kg]	theta {VST}	P {VST} [Pa]	n {VST} [mol/kg]	p {exp} [mm Hg]	v {exp} [cc STP/g]	Square deviation
0	0	0	0	0	0	0	0	0
4955.592	0.001235	0.05510	0.02165	4955.592	0.05618	37.17	1.235	1.16E-06
13953.519	0.003181	0.14193	0.05450	13953.519	0.14141	104.66	3.181	2.69E-07
27920.370	0.005579	0.24892	0.09558	27920.370	0.24802	209.42	5.579	8.09E-07
52227.705	0.00877	0.39130	0.15130	52227.705	0.39260	391.74	8.77	1.69E-06
76540.372	0.011389	0.50815	0.19557	76540.372	0.50747	574.1	11.389	4.61E-07
99965.112	0.013459	0.60051	0.23147	99965.112	0.60062	749.8	13.459	1.39E-08
		At 1 atm:	0.23340	101325.000	0.60563			
						Standard deviation:		0.0009390

N2 / 5A ADSORPTION ISOTHERM at 39.8°C

Langmuir Theory

B [1/Pa] = 4.51E-07 vm [m3/kg]= 0.07967 nm [mol/kg]= 3.5547698

p {exp} [Pa]	v {exp} [m3 STP/kg]	n {exp} [mol/kg]	p/v [Pa/m3]	Langmuir v [m3 STP/kg]	Langmuir n [mol/kg]	p {exp} [mm Hg]	v {exp} [cc STP/g]	Square deviation
0	0	0		0	0	0	0	0
8693.952	0.000273	0.01218	3.18E+07	0.000311	0.01387	65.21	0.273	2.87E-06
26949.784	0.00094	0.04194	2.87E+07	0.000956	0.04266	202.14	0.94	5.16E-07
42345.851	0.001509	0.06733	2.81E+07	0.001492	0.06657	317.62	1.509	5.69E-07
55862.072	0.001967	0.08776	2.84E+07	0.001957	0.08730	419	1.967	2.13E-07
74300.556	0.00261	0.11645	2.85E+07	0.002582	0.11518	557.3	2.61	1.61E-06
94978.855	0.003267	0.14577	2.91E+07	0.003271	0.14592	712.4	3.267	2.47E-08
109004.368	0.003697	0.16495	2.95E+07	0.003731	0.16646	817.6	3.697	2.28E-06
101325.000				0.003480	0.15525			
						Standard deviation:		0.00116

CH4 / 5A ADSORPTION ISOTHERM at 22.8°C

Flory-Huggins Vacancy Solution Theory

Parameter	values	Asymptotic standard error	Asymptotic 95% confidence interval lower limit	upper limit
ninf [mol/kg]	1.2641213	2.50466	0.9544431	1.5738
b1 [mol/kg*Pa]	4.70E-06	1.33E-07	4.33E-06	4.33E-06
alfa1v	0	0	0	0

p {exp} [Pa]	v {exp} [m3 STP/kg]	n {exp} [mol/kg]	theta {VST}	P {VST} [Pa]	n {VST} [mol/kg]	p {exp} mm Hg]	v {exp} [cc STP/g]	Square deviation
0	0	0	0	0	0	0	0	0
5128.912	0.000542	0.02418	0.01871	5128.912	0.02365	38.47	0.542	2.79E-07
20956.943	0.002092	0.09334	0.07229	20956.943	0.09138	157.2	2.092	3.85E-06
38610.158	0.003486	0.15554	0.12553	38610.158	0.15869	289.6	3.486	9.93E-06
56835.326	0.004968	0.22166	0.17445	56835.326	0.22053	426.3	4.968	1.29E-06
80980.007	0.006453	0.28792	0.23141	80980.007	0.29253	607.4	6.453	2.13E-05
102258.257	0.007860	0.35069	0.27547	102258.257	0.34822	767	7.86	6.11E-06
		At 1 atm:	0.27364	101325.000	0.34591			
						Standard deviation:		0.0029236

CH4 / 5A ADSORPTION ISOTHERM at 22.8°C

Langmuir Theory

B [1/Pa] = 4.00E-06 vm [m3/kg]= 0.02673 nm [mol/kg]= 1.19249

p {exp} [Pa]	v {exp} [m3 STP/kg]	n {exp} [mol/kg]	p/v [Pa/m3]	Langmuir v [m3 STP/kg]	Langmuir n [mol/kg]	p {exp} mm Hg]	v {exp} [cc STP/g]	Square deviation
0	0	0		0	0	0	0	0
5128.9	0.000542	0.02418	9.46E+06	0.000537	0.02396	38.47	0.542	4.94E-08
20956.9	0.002092	0.09334	1.00E+07	0.002066	0.09219	157.2	2.092	1.33E-06
38610.2	0.003486	0.15554	1.11E+07	0.003574	0.15946	289.6	3.486	1.54E-05
56835.3	0.004968	0.22166	1.14E+07	0.004949	0.22079	426.3	4.968	7.55E-07
80980.0	0.006453	0.28792	1.25E+07	0.006537	0.29165	607.4	6.453	1.39E-05
102258.3	0.00786	0.35069	1.30E+07	0.007756	0.34604	767	7.860	2.16E-05
101325				0.007705	0.34379			
						Standard deviation:		0.0032576

CH4 / 5A ADSORPTION ISOTHERM at 40.1°C

Flory-Huggins Vacancy Solution Theory

Parameter	values	Asymptotic standard error	Asymptotic 95% confidence interval lower limit	upper limit
ninf [mol/kg]	2.3706831	0.00000	2.37068	2.37068
b1 [mol/kg*Pa]	2.72E-06	1.87E-06	-1.20E-06	9.20E-06
alfa1v	-0.715019	0.02215	-0.7719622	-0.6581

p {exp} [Pa]	v {exp} [m3 STP/kg]	n {exp} [mol/kg]	theta {VST}	P {VST} [Pa]	n {VST} [mol/kg]	p {exp} mm Hg	v {exp} [cc STP/g]	Square deviation
0	0	0	0	0	0	0	0	0
6874.1013	0.000416	0.01856	0.00778	6874.101	0.01845	51.56	0.416	1.21E-08
17126.591	0.001022	0.04560	0.01906	17126.591	0.04518	128.5	1.022	1.75E-07
29518.906	0.001722	0.07683	0.03218	29518.906	0.07630	221.4	1.722	2.85E-07
43587.082	0.002455	0.10954	0.04646	43587.082	0.11014	326.9	2.455	3.68E-07
59528.438	0.003288	0.14670	0.06189	59528.438	0.14673	446.5	3.288	9.16E-10
80086.747	0.004287	0.19128	0.08073	80086.747	0.19139	600.7	4.287	1.23E-08
103058.191	0.005340	0.23826	0.10049	103058.191	0.23822	773	5.34	1.28E-09
		At 1 atm:	0.09904	101325.000	0.23479			
							Standard deviation:	0.0003775

CH4 / 5A ADSORPTION ISOTHERM at 40.1°C

Langmuir Theory

B [1/Pa] = 1.80E-06 vm [m3/kg]= 0.03403 nm [mol/kg]= 1.51822

p {exp} [Pa]	v {exp} [m3 STP/kg]	n {exp} [mol/kg]	p/v [Pa/m3]	Langmuir v [m³ STP/kg]	Langmuir n [mol/kg]	p {exp} mm Hg	v {exp} [cc STP/g]	Square deviation
0	0	0		0	0	0	0	0
6874.101	0.000416	0.01856	1.65E+07	0.000416	0.01856	51.56	0.416	1.34E-11
17126.591	0.001022	0.04560	1.68E+07	0.001018	0.04541	128.5	1.022	3.69E-08
29518.906	0.001722	0.07683	1.71E+07	0.001717	0.07660	221.4	1.722	5.16E-08
43587.082	0.002455	0.10954	1.78E+07	0.002476	0.11046	326.9	2.455	8.47E-07
59528.438	0.003288	0.14670	1.81E+07	0.003293	0.14694	446.5	3.288	5.85E-08
80086.747	0.004287	0.19128	1.87E+07	0.004288	0.19130	600.7	4.287	4.99E-10
103058.191	0.00534	0.23826	1.93E+07	0.005325	0.23758	773	5.340	4.57E-07
101325.000				0.005249	0.23420			
							Standard deviation:	0.0004919

CO / 5A ADSORPTION ISOTHERM at 22.6°C

Flory-Huggins Vacancy Solution Theory

Parameter	estimates	Asymptotic standard error	Asymptotic 95% confidence interval lower limit	upper limit
ninf [mol/kg]	1.4659641	0.0537566	1.3277803	1.60415
b1 [mol/kg*Pa]	1.90E-05	8.02E-07	1.69E-05	2.11E-05
alfa1v	0	0	0	0

p {exp} [Pa]	v {exp} [m3 STP/kg]	n {exp} [mol/kg]	theta {VST}	P {VST} [Pa]	n {VST} [mol/kg]	p {exp} [mm Hg]	v {exp} [cc STP/g]	Square deviation
0	0	0	0	0	0	0	0	0
3913.012	0.001819	0.08116	0.04827	3913.012	0.07076	29.35	1.819	1.08E-04
11643.042	0.004577	0.20421	0.13112	11643.042	0.19221	87.33	4.577	1.44E-04
25277.921	0.008026	0.35810	0.24677	25277.921	0.36176	189.6	8.026	1.34E-05
41143.283	0.011229	0.50101	0.34778	41141.283	0.50983	308.6	11.229	7.78E-05
64381.372	0.014601	0.65146	0.45487	64381.372	0.66683	482.9	14.601	2.36E-04
85926.266	0.01717	0.76608	0.52689	85926.266	0.7724	644.5	17.17	3.99E-05
104831.378	0.019083	0.85144	0.57604	104831.378	0.84445	786.3	19.083	4.88E-05
		At 1 atm:	0.56771	101325.000	0.83224			
							Standard deviation:	0.0105535

CO / 5A ADSORPTION ISOTHERM at 22.6°C

Langmuir Theory

B [1/Pa] = 0.0000148 vm [m3/kg]= 0.03065 nm [mol/kg]= 1.367377

p {exp} [Pa]	v {exp} [m3 STP/kg]	n {exp} [mol/kg]	p/v [Pa/m3]	Langmuir v [m3 STP/kg]	Langmuir n [mol/kg]	p {exp} [mm Hg]	v {exp} [cc STP/g]	Square deviation
0	0	0		0	0	0	0	0
3913.012	0.001819	0.08116	2151188	0.001679	0.07493	29.35	1.819	3.88E-05
11643.042	0.004577	0.20421	2543815	0.004509	0.20118	87.33	4.577	9.19E-06
25277.921	0.008026	0.35810	3149504	0.008351	0.37259	189.6	8.026	2.10E-04
41143.283	0.011229	0.50101	3664020	0.011607	0.51787	308.6	11.229	2.84E-04
64381.372	0.014601	0.65146	4409381	0.014962	0.66757	482.9	14.601	2.59E-04
85926.266	0.01717	0.76608	5004442	0.017165	0.76584	644.5	17.170	5.80E-08
104831.378	0.019083	0.85144	5493443	0.018644	0.83183	786.3	19.083	3.84E-04
101325				0.018394	0.82071			
							Standard deviation:	0.1678438

CO / 5A ADSORPTION ISOTHERM at 40.0°C

Flory-Huggins Vacancy Solution Theory

Parameter	estimates	Asymptotic standard error	Asymptotic 95% confidence interval lower limit	upper limit
ninf [mol/kg]	2.5947941	1.4503008	-2.020788	7.21038
b1 [mol/kg*Pa]	1.23E-05	4.65E-07	1.08E-05	1.37E-05
alfa1v	1.6362931	2.121495	-5.115365	8.38795

p {exp} [Pa]	v {exp} [m3 STP/kg]	n {exp} [mol/kg]	theta {VST}	P {VST} [Pa]	n {VST} [mol/kg]	p {exp} [mm Hg]	v {exp} [cc STP/g]	Square deviation
0	0	0	0	0	0	0	0	0
4955.592	0.001235	0.05510	0.02165	4955.592	0.05618	37.17	1.235	1.16E-06
13953.519	0.003181	0.14193	0.05450	13953.519	0.14141	104.66	3.181	2.69E-07
27920.370	0.005579	0.24892	0.09558	27920.370	0.24802	209.42	5.579	8.09E-07
52227.705	0.008770	0.39130	0.15130	52227.705	0.3926	391.74	8.77	1.69E-06
76540.372	0.011389	0.50815	0.19557	76540.372	0.50747	574.1	11.389	4.61E-07
99965.112	0.013459	0.60051	0.23147	99965.112	0.60062	749.8	13.459	1.39E-08
		At 1 atm:	0.23340	101325.000	0.60563			
						Standard deviation:		0.00093895

CO / 5A ADSORPTION ISOTHERM at 40.0°C

Langmuir Theory

B [1/Pa] = 9.19E-06 vm [m3/kg]= 0.02771 nm [mol/kg]= 1.236152

p {exp} [Pa]	v {exp} [m3 STP/kg]	n {exp} [mol/kg]	p/v [Pa/m3]	Langmuir v [m3 STP/kg]	Langmuir n [mol/kg]	p {exp} [mm Hg]	v {exp} [cc STP/g]	Square deviation
0	0	0		0	0	0	0	0
4955.592	0.001235	0.05510	4012625	0.001207	0.05385	37.17	1.235	1.56E-06
13953.519	0.003181	0.14193	4386520	0.003149	0.14052	104.66	3.181	1.98E-06
27920.370	0.005579	0.24892	5004547	0.005658	0.25245	209.42	5.579	1.25E-05
52227.705	0.00877	0.39130	5955268	0.008986	0.40095	391.74	8.770	9.32E-05
76540.372	0.011389	0.50815	6720552	0.011442	0.51051	574.1	11.389	5.59E-06
99965.112	0.013459	0.60051	7427380	0.013267	0.59194	749.8	13.459	7.35E-05
101325.000				0.013360	0.59611			
						Standard deviation:		0.0061356

N2 / TURKISH CLINOPTILOLITE ADSORPTION ISOTHERM at 22.7°C

Flory-Huggins Vacancy Solution Theory

Parameter	estimates	Asymptotic standard error	Asymptotic 95% confidence interval lower limit	upper limit
ninf [mol/kg]	0.8204479	0.0463	0.6212207	1.01968
b1 [mol/kg*Pa]	0.0065092	0.00123	0.0012295	0.01179
alfa1v	7.1046088	0.27702	0.6212207	1.01968

p {exp} [Pa]	v {exp} [m3 STP/kg]	n {exp} [mol/kg]	theta {VST}	P {VST} [Pa]	n {VST} [mol/kg]	p {exp} [mm Hg]	v {exp} [cc STP/g]	Square deviation
0	0	0	0	0	0	0	0	0
4043.667	0.004673	0.20850	0.25181	4043.667	0.2066	30.33	4.673	3.61E-06
19929.028	0.007905	0.35270	0.42897	19929.028	0.35194	149.48	7.905	5.72E-07
52235.704	0.010559	0.47112	0.57783	52235.704	0.47408	391.8	10.559	8.80E-06
81366.641	0.011966	0.53389	0.65184	81366.641	0.5348	610.3	11.966	8.28E-07
108831.049	0.01289	0.57512	0.69974	108831.049	0.5741	816.3	12.89	1.03E-06
		At 1 atm:	0.68811	101325.000	0.56456			
							Standard deviation:	0.0019268

N2 / TURKISH CLINOPTILOLITE ADSORPTION ISOTHERM at 22.7°C

Langmuir Theory

B [1/Pa] = 0.0000775 vm [m3/kg] 0.01404 nm [mol/kg]= 0.62622

p {exp} [Pa]	v {exp} [m3 STP/kg]	n {exp} [mol/kg]	p/v [Pa/m3]	Langmuir v [m3 STP/kg]	Langmuir n [mol/kg]	p {exp} [mm Hg]	v {exp} [cc STP/g]	Square deviation
0	0	0		0	0	0	0	0
4043.667	0.004673	0.20850	865326	0.003350	0.14946	30.33	4.673	3.49E-03
19929.028	0.007905	0.35270	2521066	0.008521	0.38016	149.48	7.905	7.54E-04
52235.704	0.010559	0.47112	4947031	0.011256	0.50221	391.8	10.559	9.67E-04
81366.641	0.011966	0.53389	6799820	0.012115	0.54053	610.3	11.966	4.41E-05
108831.049	0.01289	0.57512	8443060	0.012548	0.55986	816.3	12.89	2.33E-04
101325.000				0.012450	0.55550			
							Standard deviation:	0.03702

N2 / TURKISH CLINOPTILOLITE ADSORPTION ISOTHERM at 40.0°C

Flory-Huggins Vacancy Solution Theory

Parameter	estimates	Asymptotic standard error	Asymptotic 95% confidence interval lower limit	upper limit
ninf [mol/kg]	0.7305716	0.02935	0.6042967	0.85685
bl [mol/kg*Pa]	0.0030581	0.00037	0.0014794	0.00464
alfa1v	6.8065758	0.12772	6.2570145	7.35614

p {exp} [Pa]	v {exp} [m3 STP/kg]	n {exp} [mol/kg]	theta {VST}	P {VST} [Pa]	n {VST} [mol/kg]	p {exp} [mm Hg]	v {exp} [cc STP/g]	Square deviation
0	0	0	0	0	0	0	0	0
5828.854	0.003998	0.17838	0.25051	5828.854	0.18302	43.72	3.998	2.15E-05
23316.749	0.006578	0.29349	0.40110	23316.749	0.29303	174.89	6.578	2.17E-07
56342.033	0.008706	0.38844	0.53222	56342.033	0.38882	422.6	8.706	1.47E-07
87472.806	0.009892	0.44136	0.60501	87472.806	0.44200	656.1	9.892	4.19E-07
111924.128	0.010576	0.47187	0.64644	111924.128	0.47227	839.5	10.576	1.57E-07
		At 1 atm:	0.62973	101325.000	0.46006			
						Standard deviation:		0.00237

N2 / TURKISH CLINOPTILOLITE ADSORPTION ISOTHERM at 40.0°C

Langmuir Theory

B [1/Pa] = 0.000063 vm [m3/kg] 0.01179 nm [mol/kg]= 0.52589

p {exp} [Pa]	v {exp} [m3 STP/kg]	n {exp} [mol/kg]	p/v [Pa/m3]	Langmuir v [m3 STP/kg]	Langmuir n [mol/kg]	p {exp} [mm Hg]	v {exp} [cc STP/g]	Square deviation
0	0	0		0	0	0	0	0
5828.854	0.003998	0.17838	4012625	0.003167	0.14130	43.72	3.998	1.37E-03
23316.749	0.006578	0.29349	4386520	0.007014	0.31296	174.89	6.578	3.79E-04
56342.033	0.008706	0.38844	5004547	0.009197	0.41035	422.6	8.706	4.80E-04
87472.806	0.009892	0.44136	5955268	0.009977	0.44516	656.1	9.892	1.44E-05
111924.128	0.010576	0.47187	6720552	0.010323	0.46060	839.5	10.576	1.27E-04
101325.000				0.010191	0.45470			
						Standard deviation:		0.02437

CH4 / TURKISH CLINOPTILOLITE ADSORPTION ISOTHERM at 22.8°C

Flory-Huggins Vacancy Solution Theory

Parameter	estimates	Asymptotic standard error	Asymptotic 95% confidence interval lower limit	upper limit
ninf [mol/kg]	1.0829027	0.14796	0.6119882	1.55382
bl [mol/kg*Pa]	0.00011	0.00005	-6.61E-05	0.00028
alfa1v	1.9705939	2.57236	-6.215953	10.1571

p {exp} [Pa]	v {exp} [m3STP/kg]	n {exp} [mol/kg]	theta {VST}	P {VST} [Pa]	n {VST} [mol/kg]	p {exp} [mm Hg]	v {exp} [cc STP/g]	Square deviation
0	0	0	0	0	0	0	0	0
3925.0105	0.004963	0.22144	0.18407	3925.010	0.19933	29.44	4.963	4.89E-04
13788.199	0.009253	0.41285	0.36879	13788.199	0.39936	103.42	9.253	1.82E-04
27668.391	0.012055	0.53786	0.50209	27668.391	0.54372	207.53	12.055	3.43E-05
52835.655	0.015131	0.67511	0.63230	52835.655	0.68472	396.3	15.131	9.24E-05
77153.655	0.017350	0.77411	0.70443	77153.655	0.76283	578.7	17.35	1.27E-04
101005.026	0.018136	0.80918	0.75157	101005.026	0.81387	757.6	18.136	2.20E-05
		At 1 atm:	0.75209	101325.000	0.81444			
						Standard deviation:		0.0137586

CH4 / TURKISH CLINOPTILOLITE ADSORPTION ISOTHERM at 22.8°C

Langmuir Theory

B [1/Pa] = 0.0000576 vm [m3/kg]= 0.02099 m [mol/kg]= 0.93664

p {exp} [Pa]	v {exp} [m3 STP/kg]	n {exp} [mol/kg]	p/v [Pa/m3]	Langmuir v [m3 STP/kg]	Langmuir n [mol/kg]	p {exp} [mm Hg]	v {exp} [cc STP/g]	Square deviation
0	0	0		0	0	0	0	0
3925.011	0.004693	0.20939	836354	0.003869	0.17264	0.1726	4.693	1.35E-03
13788.199	0.009253	0.41285	1490133	0.009290	0.41449	0.4145	9.253	2.72E-06
27668.391	0.012055	0.53786	2295180	0.012897	0.57541	0.5754	12.055	1.41E-03
52835.655	0.015131	0.67511	3491881	0.015799	0.70491	0.7049	15.131	8.88E-04
77153.655	0.01735	0.77411	4446897	0.017135	0.76453	0.7645	17.350	9.19E-05
101005.026	0.018136	0.80918	5569311	0.017912	0.7992	0.7992	18.136	9.96E-05
101325				0.017921	0.79958			
						Standard deviation:		0.02772

CH4 / TURKISH CLINOPTILOLITE ADSORPTION ISOTHERM at 40.0°C

Flory-Huggins Vacancy Solution Theory

Parameter	estimates	Asymptotic standard error	Asymptotic 95% confidence interval lower limit	upper limit
ninf [mol/kg]	1.1901889	0.63481	-1.541203	3.92158
b1 [mol/kg*Pa]	5.60E-05	9.38E-06	1.57E-05	9.64E-05
alfa1v	2.193935	3.71029	-13.77033	18.1582

p {exp} [Pa]	v {exp} [m3 STP/kg]	n {exp} [mol/kg]	theta {VST}	P {VST} [Pa]	n {VST} [mol/kg]	p {exp} [mm Hg]	v {exp} [cc STP/g]	Square deviation
0	0	0	0	0	0	0	0	0
3529.043	0.003957	0.17655	0.10053	3529.043	0.11964	26.47	3.957	3.24E-03
18107.844	0.007072	0.31554	0.27271	18107.844	0.32457	135.82	7.072	8.17E-05
41076.622	0.010657	0.47549	0.40716	41076.622	0.48460	308.1	10.657	8.31E-05
69087.651	0.013697	0.61113	0.50623	69087.651	0.60251	518.2	13.697	7.43E-05
99031.855	0.015349	0.68483	0.57765	99031.855	0.68751	742.8	15.349	7.18E-06
		At 1 atm:	0.58220	101325.000	0.69292			
						Standard deviation:		0.0295158

CH4 / TURKISH CLINOPTILOLITE ADSORPTION ISOTHERM at 40.0°C

Langmuir Theory

B [1/Pa] = 0.000045 vm [m3/kg]= 0.31819 nm [mol/kg]= 0.8115

p {exp} [Pa]	v {exp} [m3 STP/kg]	n {exp} [mol/kg]	p/v [Pa/m3]	Langmuir v [m3 STP/kg]	Langmuir n [mol/kg]	p {exp} [mm Hg]	v {exp} [cc STP/g]	Square deviation
0	0	0		0	0	0	0	0
3529.043	0.003957	0.17655	891848	0.002492	0.11118	26.47	3.957	4.27E-03
18107.844	0.007072	0.31554	2560498	0.008165	0.36429	135.82	7.072	2.38E-03
41076.622	0.010657	0.47549	3854426	0.011801	0.52654	308.1	10.657	2.61E-03
69087.651	0.013697	0.61113	5043999	0.013760	0.61395	518.2	13.697	7.98E-06
99031.855	0.015349	0.68483	6452007	0.014854	0.66273	742.8	15.349	4.88E-04
101325.000				0.014916	0.66549			
						Standard deviation:		0.04938

CO / TURKISH CLINOPTILOLITE ADSORPTION ISOTHERM at 22.8°C

Flory-Huggins Vacancy Solution Theory

Parameter	estimates	Asymptotic standard error	Asymptotic 95% confidence interval lower limit	upper limit
ninf [mol/kg]	1.25	0.13873	0.6530988	1.8469
b1 [mol/kg*Pa]	1.9	1.51952	-4.638049	8.43805
alfa1v	9.9	12.71443	-44.8064	64.6064

p {exp} [Pa]	v {exp} [m3 STP/kg]	n {exp} [mol/kg]	theta {VST}	P {VST} [Pa]	n {VST} [mol/kg]	p {exp} [mm Hg]	v {exp} [cc STP/g]	Square deviation
0	0		0	0	0	0	0	0
305.308	0.005470	0.24406	0.26439	305.308	0.33049	2.29	5.47	1.08E-04
6510.131	0.018207	0.81235	0.65200	6510.131	0.81500	48.83	18.207	1.44E-04
33994.538	0.023934	1.06788	0.87805	33994.538	1.09756	254.98	23.934	1.34E-05
63848.082	0.026380	1.17701	0.92790	63848.082	1.15988	478.9	26.38	7.78E-05
96765.375	0.026402	1.17799	0.95026	96765.375	1.18783	725.8	26.402	2.36E-04
		At 1 atm:	0.95231	101325.000	1.19039			
							Standard deviation:	0.04676817

CO / TURKISH CLINOPTILOLITE ADSORPTION ISOTHERM at 22.8°C

Langmuir Theory

B [1/Pa] = 0.0003807 vm [m3/kg]= 0.02709 nm [mol/kg]= 1.20884

p {exp} [Pa]	v {exp} [m3 STP/kg]	n {exp} [mol/kg]	p/v [Pa/m3]	Langmuir v [m3 STP/kg]	Langmuir n [mol/kg]	p {exp} [mm Hg]	v {exp} [cc STP/g]	Square deviation
0	0	0		0	0	0	0	0
305.308	0.00547	0.24406	55815	0.002822	0.12589	2.29	5.470	1.40E-02
6510.131	0.018207	0.81235	357562	0.019305	0.86134	48.83	18.207	2.40E-03
33994.538	0.023934	1.06788	1420345	0.025150	1.12214	254.98	23.934	2.94E-03
63848.082	0.02638	1.17701	2420322	0.026023	1.16108	478.9	26.380	2.54E-04
96765.375	0.026402	1.17799	3665077	0.026377	1.17689	725.8	26.402	1.20E-06
101325.000				0.026409	1.17830			
							Standard deviation:	0.069936

CO / TURKISH CLINOPTILOLITE ADSORPTION ISOTHERM at 40.0°C

Flory-Huggins Vacancy Solution Theory

Parameter	estimates	Asymptotic standard error	Asymptotic 95% confidence interval lower limit	upper limit
ninf [mol/kg]	1.0400051	0.05443	0.8058083	1.2742
b1 [mol/kg*Pa]	0.0269982	0.00679	-0.002228	0.05622
alfa1v	6.5990727	2.26710	-3.155597	16.3537

p {exp} [Pa]	v {exp} [m3 STP/kg]	n {exp} [mol/kg]	theta {VST}	P {VST} [Pa]	n {VST} [mol/kg]	p1 {exp} [mm Hg]	v1 {exp} [cc STP/g]	Square deviation
0	0	0	0	0	0	0	0	0
1698.527	0.006687	0.29836	0.32686	1698.527	0.33993	12.74	6.687	1.73E-03
16144.006	0.013615	0.60747	0.66133	16144.006	0.68779	121.09	13.615	6.45E-03
42325.852	0.018375	0.81985	0.80906	42325.852	0.84142	317.47	18.375	4.66E-04
70594.194	0.020406	0.91047	0.86922	70594.194	0.90399	529.5	20.406	4.19E-05
100898.368	0.021014	0.93759	0.90209	100898.368	0.93818	756.8	21.014	3.45E-07
		At 1 atm:	0.90244	101325.000	0.93854			
						Standard deviation:		0.0466038

CO / TURKISH CLINOPTILOLITE ADSORPTION ISOTHERM at 40.0°C

Langmuir Theory

B [1/Pa] = 0.000086 vm [m3/kg]= 0.02353 nm [mol/kg]= 1.04989

p {exp} [Pa]	v {exp} [m3 STP/kg]	n {exp} [mol/kg]	p/v [Pa/m3]	Langmuir v [m3 STP/kg]	Langmuir n [mol/kg]	p {exp} [mm Hg]	v {exp} [cc STP/g]	Square deviation
0	0	0		0	0	0	0	0
1698.527	0.006687	0.29836	254004	0.002998	0.13377	12.74	6.687	2.71E-02
16144.006	0.013615	0.60747	1185751	0.013676	0.61021	121.09	13.615	7.51E-06
42325.852	0.018375	0.81985	2303448	0.018458	0.82355	317.47	18.375	1.37E-05
70594.194	0.020406	0.91047	3459482	0.020202	0.90137	529.5	20.406	8.28E-05
100898.368	0.021014	0.93759	4801483	0.021099	0.94136	756.8	21.014	1.42E-05
101325.000				0 021108	0.94177			
						Standard deviation:		0.0824744

N2 / CUBAN CLINOPTILOLITE ADSORPTION ISOTHERM at 40.0°C

Flory-Huggins Vacancy Solution Theory

Parameter	estimates	Asymptotic standard error	Asymptotic 95% confidence interval lower limit	upper limit
ninf [mol/kg]	2.3900492	0.32922247	1.6308535	3.14924
bl [mol/kg*Pa]	1.30E-05	2.03E-06	8.32E-06	1.77E-05
alfa1v	2.6986245	1.03854502	0.3037123	5.09354

p {exp} [Pa]	v {exp} [m3 STP/kg]	n {exp} [mol/kg]	theta {VST}	P {VST} [Pa]	n {VST} [mol/kg]	p {exp} [mm Hg]	v {exp} [cc STP/g]	Square deviation
0	0	0	0	0	0	0	0	0
7474.0520	0.001952	0.08708	0.03180	7474.052	0.07600	56.06	1.9517	1.23E-04
15889.360	0.003221	0.14373	0.05691	15889.360	0.13601	119.18	3.2214	5.96E-05
27092.438	0.004510	0.20122	0.08264	27092.438	0.19752	203.21	4.5100	1.37E-05
39790.061	0.005662	0.25262	0.10610	39790.061	0.25359	298.45	5.6620	9.27E-07
52982.309	0.006750	0.30115	0.12660	52982.309	0.30258	397.40	6.7496	2.05E-06
66607.855	0.007663	0.34192	0.14501	66607.855	0.34657	499.60	7.6634	2.16E-05
80140.076	0.008571	0.38239	0.16128	80140.076	0.38547	601.10	8.5705	9.49E-06
93605.635	0.009403	0.41954	0.17597	93605.635	0.42057	702.10	9.4030	1.06E-06
107204.516	0.010178	0.45412	0.1895806	107204.516	0.45311	804.10	10.1780	1.02E-06
120723.405	0.010885	0.48566	0.2021235	120723.405	0.48309	905.50	10.8850	6.64E-06
		At 1 atm:	0.1838287	101325.000	0.43936			
						Standard deviation:		0.0069110

N2 / CUBAN CLINOPTILOLITE ADSORPTION ISOTHERM at 40.0°C

Langmuir Theory

B [1/Pa] = 1.48E-05 vm [m3/kg]= 0.01623 nm [mol/kg]= 0.72425

p {exp} [Pa]	v {exp} [m3 STP/kg]	n {exp} [mol/kg]	p/v [Pa/m3]	Langmuir v [m3 STP/kg]	Langmuir n [mol/kg]	p {exp} [mm Hg]	v {exp} [cc STP/g]	Square deviation
0	0	0		0	0	0	0	0
7474.052	0.001952	0.08708	85828	0.001618	0.07221	56.06	1.9517	2.21E-04
15889.360	0.003221	0.14373	110549	0.003093	0.13802	119.18	3.2214	3.26E-05
27092.438	0.004510	0.20123	134637	0.004650	0.20746	203.21	4.5100	3.89E-05
39790.061	0.005662	0.25263	157506	0.006021	0.26863	298.45	5.6620	2.56E-04
52982.309	0.006750	0.30115	175934	0.007139	0.31852	397.4	6.7496	3.02E-04
66607.855	0.007663	0.34192	194804	0.008063	0.35975	499.6	7.6634	3.18E-04
80140.076	0.008571	0.38240	209573	0.008812	0.39316	601.1	8.5705	1.16E-04
93605.635	0.009420	0.42031	222706	0.009432	0.42083	702.1	9.4203	2.74E-07
107204.516	0.010178	0.45413	236068	0.009961	0.44445	804.1	10.1782	9.35E-05
120723.405	0.010885	0.48567	248570	0.010412	0.46455	905.5	10.8852	4.46E-04
101325				0.009743	0.43471			
						Standard deviation:		0.0142361

CH4 / CUBAN CLINOPTILOLITE ADSORPTION ISOTHERM at 40.0°C

Flory-Huggins Vacancy Solution Theory

Parameter	estimates	Asymptotic standard error	Asymptotic 95% confidence interval lower limit	upper limit
ninf [mol/kg]	4.0459297	0.2203	3.5379080	4.55395
b1 [mol/kg*Pa]	2.05E-05	3.00E-06	1.36E-05	2.74E-05
alfa1v	3.302105	0.79842	1.4609232	5.14329

p {exp} [Pa]	v {exp} [m3 STP/kg]	n {exp} [mol/kg]	theta {VST}	P {VST} [Pa]	n {VST} [mol/kg]	p {exp} [mm Hg]	v {exp} [cc STP/g]	Square deviation
0	0	0	0	0	0	0	0	0
6427.471	0.002503	0.11169	0.02476	6427.471	0.10017	48.21	2.5032	1.33E-04
14425.480	0.004298	0.19175	0.04539	14425.480	0.18364	108.20	4.2977	6.58E-05
25385.912	0.006128	0.27342	0.06636	25385.912	0.26850	190.41	6.1281	2.42E-05
38116.865	0.007774	0.34687	0.08544	38116.865	0.34570	285.90	7.7742	1.37E-06
51229.120	0.009391	0.41902	0.10170	51229.120	0.41148	384.25	9.3914	5.69E-05
65207.970	0.010623	0.47396	0.11660	65207.970	0.47177	489.10	10.6227	4.80E-06
79206.819	0.011673	0.52083	0.12976	79206.819	0.52502	594.10	11.6733	1.75E-05
92712.375	0.012782	0.57029	0.14122	92712.375	0.57135	695.40	12.7818	1.12E-06
106444.579	0.013742	0.61311	0.15188	106444.579	0.61450	798.40	13.7415	1.93E-06
119883.474	0.014717	0.65665	0.16154	119883.474	0.65360	899.20	14.7174	9.35E-06
		At 1 atm:	0.14801	101325.000	0.59883			
							Standard deviation:	0.0059221

CH4 / CUBAN CLINOPTILOLITE ADSORPTION ISOTHERM at 40.0°C

Langmuir Theory

B [1/Pa] =	1.48E-05	vm [m3/kg]	0.01623	nm [mol/kg]=	0.72425

p {exp} [Pa]	v {exp} [m3 STP/kg]	n {exp} [mol/kg]	p/v [Pa/m3]	Langmuir v [m3 STP/kg]	Langmuir n [mol/kg]	p {exp} [mm Hg]	v {exp} [cc STP/g]	Square deviation
0	0	0		0	0	0	0	0
6427.471	0.002503	0.11169	57549	0.002074	0.09253	48.21	2.5032	3.67E-04
14425.480	0.004298	0.19175	75230	0.004145	0.18492	108.2	4.2977	4.67E-05
25385.912	0.006128	0.27342	92846	0.006341	0.28293	190.41	6.1281	9.05E-05
38116.865	0.007774	0.34687	109889	0.008268	0.36888	285.9	7.7742	4.85E-04
51229.120	0.009391	0.41902	122259	0.009785	0.43657	384.25	9.3914	3.08E-04
65211.970	0.010621	0.47387	137615	0.011048	0.49295	489.13	10.6207	3.64E-04
79210.819	0.011670	0.52069	152125	0.012056	0.53793	594.13	11.6702	2.97E-04
92705.709	0.012783	0.57034	162545	0.012852	0.57341	695.35	12.7828	9.44E-06
106440.579	0.013743	0.61318	173587	0.013527	0.60356	798.37	13.7431	9.26E-05
119876.808	0.014721	0.65683	182507	0.014088	0.62857	899.15	14.7215	7.99E-04
101325				0.013289	0.59294			
							Standard deviation:	0.01782

CO / CUBAN CLINOPTILOLITE ADSORPTION ISOTHERM at 40.0°C

Flory-Huggins Vacancy Solution Theory

Parameter	estimates	Asymptotic standard error	Asymptotic 95% confidence interval lower limit	upper limit
ninf [mol/kg]	0.9387339	0.8367592	-2.6659	4.53906
b1 [mol/kg*Pa]	5.31E-05	2.20E-05	-4.15E-05	1.48E-04
alfa1v	2.2843351	7.8407174	-31.45192	36.0206

p {exp} [Pa]	v {exp} [m3 STP/kg]	n {exp} [mol/kg]	theta {VST}	P {VST} [Pa]	n {VST} [mol/kg]	p {exp} [mm Hg]	v {exp} [cc STP/g]	Square deviation
0	0	0	0	0	0	0	0	0
6418.139	0.004308	0.19223	0.16329	6418.139	0.15329	48.14	4.30847	1.52E-03
25325.917	0.008009	0.35736	0.34395	25325.917	0.32288	189.96	8.00932	1.19E-03
59461.776	0.009966	0.44466	0.49901	59461.776	0.46843	446.00	9.96599	5.65E-04
85326.316	0.012097	0.53972	0.57002	85326.316	0.53510	640.00	12.0965	2.13E-05
110230.934	0.013069	0.58311	0.62031	110230.934	0.58231	826.80	13.069	6.32E-07
		At 1 atm:	0.60386	101325.000	0.56686			
							Standard deviation:	0.02869126

CO / CUBAN CLINOPTILOLITE ADSORPTION ISOTHERM at 40.0°C

Langmuir Theory

B [1/Pa] = 0.0000472 vm [m3/kg] 0.01505 nm [mol/kg]= 0.67128

p {exp} [Pa]	v {exp} [m3 STP/kg]	n {exp} [mol/kg]	p/v [Pa/m3]	Langmuir v [m3 STP/kg]	Langmuir n [mol/kg]	p {exp} [mm Hg]	v {exp} [cc STP/g]	Square deviation
0	0	0		0	0	0	0	0
6418.139	0.004308	0.19223	33387	0.003496	0.15598	48.14	4.30847	1.31E-03
25325.917	0.008009	0.35736	70870	0.008189	0.36538	189.96	8.00932	6.44E-05
59461.776	0.009966	0.44466	133725	0.011091	0.49483	446.00	9.96599	2.52E-03
85326.316	0.012097	0.53972	158094	0.012051	0.53767	640.00	12.0965	4.18E-06
110230.934	0.013069	0.58311	189041	0.012618	0.56299	826.80	13.069	4.05E-04
101325				0.012442	0.55512			
							Standard deviation:	0.0328061

N2 / AlPO4-11 ADSORPTION ISOTHERM at 22.6°C

Flory-Huggins Vacancy Solution Theory

Parameter	estimates	Asymptotic standard error	Asymptotic 95% confidence interval lower limit	upper limit
ninf [mol/kg]	0.2319197	0.02983	0.1491081	0.31473
b1 [mol/kg*Pa]	9.03E-07	4E-08	7.88E-07	1E-06
alfa1v	0	0	0	0

p {exp} [Pa]	v {exp} [m3 STP/kg]	n {exp} [mol/kg]	theta {VST}	P {VST} [Pa]	n {VST} [mol/kg]	p {exp} [mm Hg]	v {exp} [cc STP/g]	Square deviation
0	0	0	0	0	0	0	0	0
12145.668	0.000208	0.00928	0.04515	12145.668	0.01047	91.1	0.208	1.42E-06
27680.390	0.000468	0.02088	0.09728	27680.390	0.02256	207.62	0.468	2.82E-06
46849.480	0.000803	0.03583	0.15426	46849.480	0.03578	351.4	0.803	2.77E-09
68701.016	0.001125	0.05019	0.20859	67701.016	0.04838	515.3	1.125	3.31E-06
90272.576	0.001359	0.06064	0.26005	90272.576	0.06031	677.1	1.359	1.05E-07
109297.678	0.001540	0.06871	0.29850	109297.678	0.06923	819.8	1.54	2.67E-07
		At 1 atm:	0.28288	101325.000	0.06561			
						Standard deviation:		0.0012587

N2 / AlPO4-11 ADSORPTION ISOTHERM at 22.6°C

Langmuir Theory

B [1/Pa] = 2.92E-06 vm [m3/kg] 0.0065 nm [mol/kg]= 2.90E-01

p {exp} [Pa]	v {exp} [m3 STP/kg]	n {exp} [mol/kg]	p/n [Pa kg/mol]	Langmuir v [m3 STP/kg]	Langmuir n [mol/kg]	p {exp} [mm Hg]	v {exp} [cc STP/g]	Square deviation
0	0	0		0	0	0	0	0
12145.668	0.000208	0.00928	1308738	0.000223	0.00994	91.1	0.208	4.37E-07
27680.390	0.000468	0.02088	1325626	0.000486	0.02170	207.62	0.468	6.79E-07
46849.480	0.000803	0.03583	1307627	0.000783	0.03493	351.4	0.803	8.14E-07
68701.016	0.001125	0.05019	1368690	0.001087	0.04849	515.3	1.125	2.90E-06
90272.576	0.001359	0.06064	1488782	0.001357	0.06054	677.1	1.359	9.34E-09
109297.678	0.001540	0.06871	1590687	0.001574	0.07021	819.8	1.54	2.24E-06
101325				0.001485	0.06626			
						Standard deviation:		0.0011901

N2 / AlPO4-11 ADSORPTION ISOTHERM at 40.0°C

Flory-Huggins Vacancy Solution Theory

Parameter	estimates	Asymptotic standard error	Asymptotic 95% confidence interval lower limit	upper limit
ninf [mol/kg]	0.3024951	0.08768	0.0234685	0.58152
bl [mol/kg*P	5.60E-07	2.54E-08	4.79E-07	6.41E-07
alfalv	0	0	0	0

p {exp} [Pa]	v {exp} [m3 STP/kg]	n {exp} [mol/kg]	theta {VST}	P {VST} [Pa]	n {VST} [mol/kg]	p {exp} [mm Hg]	v {exp} [cc STP/g]	Square deviation
0	0	0	0	0	0	0	0	0
11799.030	0.000145	0.00647	0.02138	11799.030	0.00647	88.5	0.145	1.11E-11
33199.936	0.000378	0.01687	0.05790	33199.936	0.01752	249.02	0.378	4.23E-07
57395.280	0.000649	0.02896	0.09605	57395.280	0.02905	430.5	0.649	9.50E-09
77900.260	0.000875	0.03904	0.12604	77900.260	0.03813	584.3	0.875	8.36E-07
99498.484	0.001044	0.04658	0.15555	99498.484	0.04705	746.3	1.044	2.22E-07
		At 1 atm:	0.15795	101325.000	0.04778			
							Standard deviation:	0.0006148

N2 / AlPO4-11 ADSORPTION ISOTHERM at 40.0°C

Langmuir Theory

B [1/Pa] = 1.62E-06 vm [m3/kg] 0.0076 nm [mol/kg]= 0.3391

p {exp} [Pa]	v {exp} [m3 STP/kg]	n {exp} [mol/kg]	p/n [Pa kg/mol]	Langmuir v [m3 STP/kg]	Langmuir n [mol/kg]	p {exp} [mm Hg]	v {exp} [cc STP/g]	Square deviation
0	0	0		0	0	0	0	0
11799.030	0.000145	0.00647	1823782	0.000143	0.00637	88.5	0.145	9.01E-09
33199.936	0.000378	0.01687	1968521	0.000389	0.01735	249.02	0.378	2.30E-07
57395.280	0.000649	0.02896	1982102	0.000648	0.02891	430.5	0.649	2.32E-09
77900.260	0.000875	0.03904	1995379	0.000853	0.03808	584.3	0.875	9.28E-07
99498.484	0.001044	0.04658	2136046	0.001057	0.04717	746.3	1.044	3.42E-07
101325				0.001074	0.04791			
							Standard deviation:	0.0006148

CH4 / AlPO4-11 ADSORPTION ISOTHERM at 22.8°C

Flory-Huggins Vacancy Solution Theory

Parameter	estimates	Asymptotic standard error	Asymptotic 95% confidence interval lower limit	upper limit
ninf [mol/kg]	2.3039946	0.1622335	1.8535682	2.75442
b1 [mol/kg*Pa]	4.38E-06	5.02E-08	4.24E-06	4.52E-06
alfa1v	0	0	0	0

p {exp} [Pa]	v {exp} [m3 STP/kg]	n {exp} [mol/kg]	theta {VST}	P {VST} [Pa]	n {VST} [mol/kg]	p {exp} [mm Hg]	v {exp} [cc STP/g]	Square deviation
0	0	0	0	0	0	0	0	0
9911.185	0.000968	0.04319	0.01851	9911.185	0.04264	74.34	0.968	3.06E-07
22087.517	0.002068	0.09227	0.04032	22087.517	0.09291	165.67	2.068	4.06E-07
40943.299	0.00369	0.16464	0.07226	40943.299	0.16649	307.1	3.69	3.42E-06
58275.207	0.005208	0.23237	0.09980	58275.207	0.22993	437.1	5.208	5.94E-06
79340.141	0.006758	0.30153	0.13114	79340.141	0.30214	595.1	6.758	3.83E-07
102351.582	0.008414	0.37541	0.16298	102351.582	0.37549	767.7	8.414	6.92E-09
		At 1 atm:	0.16161	101325.000	0.37234			
						Standard deviation:		0.0014465

CH4 / AlPO4-11 ADSORPTION ISOTHERM at 22.8°C

Langmuir Theory

B [1/Pa] = 1.94E-06 vm [m3/kg]= 0.05074 nm [mol/kg]= 2.26401

p {exp} [Pa]	v {exp} [m3 STP/kg]	n {exp} [mol/kg]	p/n [Pa kg/mol]	Langmuir v [m3 STP/kg]	Langmuir n [mol/kg]	p {exp} [mm Hg]	v {exp} [cc STP/g]	Square deviation
0	0	0		0	0	0	0	0
9911.185	0.000968	0.0432	229480	0.0009574	0.0427	74.34	0.968	2.25E-07
22087.517	0.002068	0.0923	239382	0.0020852	0.0930	165.67	2.068	5.90E-07
40943.299	0.00369	0.1646	248686	0.0037343	0.1666	307.1	3.69	3.91E-06
58275.207	0.005208	0.2324	250788	0.0051546	0.2300	437.1	5.208	5.69E-06
79340.141	0.006758	0.3015	263129	0.0067692	0.3020	595.1	6.758	2.51E-07
102351.582	0.008414	0.3754	272638	0.0084073	0.3751	767.7	8.414	9.07E-08
101325				0.0083368	0.3720			
						Standard deviation:		0.0014667

CH4 / AlPO4-11 ADSORPTION ISOTHERM at 40.0°C

Flory-Huggins Vacancy Solution Theory

Parameter	estimates	Asymptotic standard error	Asymptotic 95% confidence interval lower limit	upper limit
ninf [mol/kg]	2.5116517	5.7806955	-15.88541	20.9087
b1 [mol/kg*Pa]	3.11E-06	5.79E-08	2.93E-06	3.30E-06
alfa1v	0	1.65E+16	-5.24E+16	5.24E+16

p {exp} [Pa]	v {exp} [m3 STP/kg]	n {exp} [mol/kg]	theta {VST}	P {VST} [Pa]	n {VST} [mol/kg]	p {exp} [mm Hg]	v {exp} [cc STP/g]	Square deviation
0	0	0	0	0	0	0	0	0
9153.914	0.000625	0.02789	0.01122	9153.914	0.02818	68.66	0.625	8.44E-08
23363.412	0.001571	0.07009	0.02814	23363.412	0.07068	175.24	1.571	3.47E-07
40263.355	0.002690	0.12002	0.04753	40263.355	0.11938	302	2.69	4.08E-07
60834.997	0.003959	0.17664	0.07011	60834.997	0.17610	456.3	3.959	2.91E-07
82966.510	0.005230	0.23335	0.09324	82966.510	0.23419	622.3	5.23	7.11E-07
105617.980	0.006521	0.29095	0.11575	105617.980	0.29073	792.2	6.521	4.85E-08
		At 1 atm:	0.11157	101325.000	0.28023			
							Standard deviation:	0.0006148

CH4 / AlPO4-11 ADSORPTION ISOTHERM at 40.0°C

Langmuir Theory

B [1/Pa] = 1.14E-06 vm [m3/kg]= 0.06075 nm [mol/kg]= 2.71045

p {exp} [Pa]	v {exp} [m3 STP/kg]	n {exp} [mol/kg]	p/n [Pa kg/mol]	Langmuir v [m3 STP/kg]	Langmuir n [mol/kg]	p {exp} [mm Hg]	v {exp} [cc STP/g]	Square deviation
0	0	0		0	0	0	0	0
9153.914	0.000625	0.02789	328263	0.000628	0.02800	68.66	0.625	1.35E-08
23363.412	0.001571	0.07009	333315	0.001577	0.07034	175.24	1.571	6.14E-08
40263.355	0.002690	0.12002	335469	0.002667	0.11899	302	2.69	1.06E-06
60834.997	0.003959	0.17664	344400	0.003941	0.17584	456.3	3.959	6.40E-07
82966.510	0.005230	0.23335	355546	0.005251	0.23428	622.3	5.23	8.69E-07
105617.980	0.006521	0.29095	363010	0.006530	0.29137	792.2	6.521	1.75E-07
101325				0.006292	0.28075			
							Standard deviation:	0.0007513

CO / AlPO4-11 ADSORPTION ISOTHERM at 22.6°C

Flory-Huggins Vacancy Solution Theory

Parameter	estimates	Asymptotic standard error	Asymptotic 95% confidence interval lower limit	upper limit
ninf [mol/kg]	1.270189	8.291E-02	1.04001	1.50037
b1 [mol/kg*Pa]	2.19E-06	2.12E-08	2.13E-06	2.25E-06
alfa1v	0	0	0	0

p {exp} [Pa]	v {exp} [m3 STP/kg]	n {exp} [mol/kg]	theta {VST}	P {VST} [Pa]	n {VST} [mol/kg]	p {exp} [mm Hg]	v {exp} [cc STP/g]	Square deviation
0	0	0	0	0	0	0	0	0
6482.134	0.000300	0.01339	0.01105	6482.134	0.01404	48.62	0.3	4.27E-07
16999.935	0.000808	0.03605	0.02848	16999.935	0.03617	127.51	0.808	1.41E-08
33931.876	0.001566	0.06987	0.05527	33931.876	0.07020	254.51	1.566	1.11E-07
54555.513	0.002440	0.10887	0.08598	54555.513	0.10920	409.2	2.44	1.14E-07
77566.954	0.003379	0.15076	0.11796	77566.954	0.14983	581.8	3.379	8.64E-07
101898.286	0.004245	0.18940	0.14943	101898.286	0.18981	764.3	4.245	1.67E-07
		At 1 atm:	0.14872	101325.000	0.18890			
						Standard deviation:		0.0005825

CO / AlPO4-11 ADSORPTION ISOTHERM at 22.6°C

Langmuir Theory

B [1/Pa] = 1.65E-06 vm [m3/kg]= 0.02955 nm [mol/kg]= 1.31854

p {exp} [Pa]	v {exp} [m3 STP/kg]	n {exp} [mol/kg]	p/n [Pa kg/mol]	Langmuir v [m3 STP/kg]	Langmuir n [mol/kg]	p {exp} [mm Hg]	v {exp} [cc STP/g]	Square deviation
0	0	0		0	0	0	0	0
6482.134	0.000300	0.01339	484274	0.000313	0.01397	48.62	0.3	3.47E-07
16999.935	0.000808	0.03605	471553	0.000808	0.03603	127.51	0.808	4.64E-10
33931.876	0.001566	0.06987	485636	0.001569	0.07001	254.51	1.566	1.92E-08
54555.513	0.002440	0.10887	501122	0.002444	0.10904	409.2	2.44	3.08E-08
77566.954	0.003379	0.15076	514497	0.003358	0.14981	581.8	3.379	9.06E-07
101898.286	0.004245	0.18940	538002	0.004259	0.19003	764.3	4.245	3.97E-07
101325				0.004239	0.18912			
						Standard deviation:		0.0005832

CO / AlPO4-11 ADSORPTION ISOTHERM at 40.0°C

Flory-Huggins Vacancy Solution Theory

Parameter	estimates	Asymptotic standard error	Asymptotic 95% confidence interval lower limit	upper limit
ninf [mol/kg]	2.5765486	0.2412881	1.9066344	3.24646
b1 [mol/kg*Pa]	1.47E-06	6.860E-09	1.49E-06	1.42E-05
alfa1v	0	0	0	0

p {exp} [Pa]	v {exp} [m3 STP/kg]	n {exp} [mol/kg]	theta {VST}	P {VST} [Pa]	n {VST} [mol/kg]	p {exp} [mm Hg]	v {exp} [cc STP/g]	Square deviation
0	0	0	0	0	0	0	0	0
6411.473	0.000215	0.00959	0.00365	6411.473	0.00940	48.09	0.215	3.59E-08
17607.885	0.000583	0.02601	0.00996	17607.885	0.02566	132.07	0.583	1.23E-07
33745.225	0.001093	0.04877	0.01891	33745.225	0.04873	253.11	1.093	1.12E-09
57368.615	0.001827	0.08152	0.03173	57368.615	0.08177	430.3	1.827	6.27E-08
81246.651	0.002559	0.11418	0.04436	81246.651	0.11429	609.4	2.559	1.30E-08
102418.243	0.003193	0.14246	0.05528	102418.243	0.14243	768.2	3.193	1.42E-09
		At 1 atm:	0.05472	101325.000	0.14099			
						Standard deviation:		0.000218

CO / AlPO4-11 ADSORPTION ISOTHERM at 40.0°C

Langmuir Theory

B [1/Pa] = 7.76E-07 vm [m3/kg]= 0.04314 nm [mol/kg]= 1.92467

p {exp} [Pa]	v {exp} [m3 STP/kg]	n {exp} [mol/kg]	p/n [Pa kg/mol]	Langmuir v [m3 STP/kg]	Langmuir n [mol/kg]	p {exp} [mm Hg]	v {exp} [cc STP/g]	Square deviation
0	0	0		0	0	0	0	0
6411.473	0.000215	0.00959	668365	0.000214	0.00953	48.09	0.215	3.84E-09
17607.885	0.000583	0.02601	676914	0.000582	0.02595	132.07	0.583	3.82E-09
33745.225	0.001093	0.04877	691969	0.001101	0.04913	253.11	1.093	1.29E-07
57368.615	0.001827	0.08152	703769	0.001839	0.08205	430.3	1.827	2.86E-07
81246.651	0.002559	0.11418	711590	0.002559	0.11418	609.4	2.559	5.67E-14
102418.243	0.003193	0.14246	718908	0.003177	0.14174	768.2	3.193	5.28E-07
101325				0.003145	0.14033			
						Standard deviation:		0.0004359

N2 / AlPO4-17 ADSORPTION ISOTHERM at 39.6°C

Flory-Huggins Vacancy Solution Theory

Parameter	estimates	Asymptotic standard error	Asymptotic 95% confidence interval lower limit	upper limit
ninf [mol/kg]	2.069951	2.1501322	-3.014345	7.1542
b1 [mol/kg*Pa]	2.00E-06	8.53E-07	-1.80E-08	4E-06
alfa1v	2.1881487	31.166962	-71.5106	75.887

p {exp} [Pa]	v {exp} [m3 STP/kg]	n {exp} [mol/kg]	theta {VST}	P {VST} [Pa]	n {VST} [mol/kg]	p {exp} [mm Hg]	v {exp} [cc STP/g]	Square deviation
0	0	0	0	0	0	0	0	0
11071.089	0.000305	0.01363	0.01010	11071.089	0.02091	83.04	0.3054	5.30E-05
19690.381	0.000558	0.02492	0.01726	19690.381	0.03574	147.69	0.5585	1.17E-04
30870.794	0.000899	0.04011	0.02585	30870.794	0.05350	231.55	0.8989	1.79E-04
43333.769	0.001217	0.05429	0.03464	43333.769	0.07171	325.03	1.2168	3.03E-04
56102.053	0.001666	0.07435	0.04298	56102.053	0.08897	420.8	1.6665	2.14E-04
69274.303	0.002063	0.09204	0.05099	69274.303	0.10555	519.6	2.0628	1.83E-04
82513.214	0.002481	0.11072	0.05854	82513.214	0.12118	618.9	2.4814	1.10E-04
95778.789	0.002918	0.13021	0.06568	95778.789	0.13595	718.4	2.9184	3.30E-05
108964.372	0.003445	0.15373	0.07240	108964.372	0.14987	817.3	3.4454	1.49E-05
122363.270	0.003860	0.17221	0.07891	122363.270	0.16333	917.8	3.8598	7.89E-05
		At 1 atm:	0.06855	101325.000	0.14189			
						Standard deviation:		0.011951

N2 / AlPO4-17 ADSORPTION ISOTHERM at 39.6°C

Langmuir and Freundlich Theories

B [1/Pa] =	4.82E-07	vm [m3/kg]=	0.060001	nm [mol/kg]=	2.67708
		k =	7.40E-07	n =	0.94923

p {exp} [Pa]	n {exp} [mol/kg]	p/n [Pa kg/mol]	Langmuir n [mol/kg]	Freundlich n [mol/kg]	p {exp} [mm Hg]	v {exp} [cc STP/g]	Square deviation {Langmuir}	Square deviation {Freundlich}
0	0		0	0	0	0		
11071.089	0.01363	812553	0.01422	0.01348	83.04	0.3054	3.56E-07	2.22E-08
19690.381	0.02492	790207	0.02519	0.02472	147.69	0.5585	7.35E-08	4.03E-08
30870.794	0.04011	769745	0.03928	0.03970	231.55	0.8989	6.78E-07	1.68E-07
43333.769	0.05429	798164	0.05482	0.05674	325.03	1.2168	2.75E-07	6.00E-06
56102.053	0.07435	754516	0.07054	0.07448	420.8	1.6665	1.45E-05	1.60E-08
69274.303	0.09204	752683	0.08657	0.09301	519.6	2.0628	2.99E-05	9.53E-07
82513.214	0.11072	745271	0.10248	0.11183	618.9	2.4814	6.78E-05	1.24E-06
95778.789	0.13021	735573	0.11823	0.13085	718.4	2.9184	1.44E-04	4.07E-07
108964.372	0.15373	708816	0.13369	0.14989	817.3	3.4454	4.01E-04	1.47E-05
122363.270	0.17221	710533	0.14921	0.16937	917.8	3.8598	5.29E-04	8.08E-06
101325			0.12475	0.13884				
					Standard deviations:		0.011488	0.001875

CH4 / AlPO4-17 ADSORPTION ISOTHERM at 40.0°C

Flory-Huggins Vacancy Solution Theory

Parameter	estimates	Asymptotic standard error	Asymptotic 95% confidence interval lower limit	upper limit
ninf [mol/kg]	4.1225671	0.2005952	3.6599892	4.5851
b1 [mol/kg*Pa]	3.853E-06	1.7210E-08	3.81E-05	3.89E-06
alfa1v	0	0	0	0

p {exp} [Pa]	v {exp} [m3 STP/kg]	n {exp} [mol/kg]	theta {VST}	P {VST} [Pa]	n {VST} [mol/kg]	p {exp} [mm Hg]	v {exp} [cc STP/g]	Square deviation
0	0	0	0	0	0	0	0	0
10204.494	0.000873	0.03893	0.00945	10204.494	0.03895	76.54	0.8725	2.48E-10
18611.803	0.001599	0.07135	0.01710	18611.803	0.07049	139.6	1.5991	7.45E-07
29580.234	0.002505	0.11175	0.02690	29580.234	0.11091	221.87	2.5047	7.19E-07
44543.003	0.003683	0.16431	0.03997	44543.003	0.16476	334.1	3.6827	2.04E-07
55995.395	0.004599	0.20518	0.04973	55995.395	0.20502	420	4.5986	2.48E-08
68407.707	0.005555	0.24785	0.06009	68407.707	0.24774	513.1	5.5550	1.34E-08
81313.313	0.006536	0.29161	0.07063	81313.313	0.29117	609.9	6.5357	1.88E-07
94498.895	0.007477	0.33362	0.08115	94498.895	0.33456	708.8	7.4773	8.80E-07
107764.470	0.008427	0.37599	0.09150	107764.470	0.37722	808.3	8.4270	1.51E-06
121190.033	0.0094294	0.42072	0.10174	121190.033	0.41944	909	9.4294	1.64E-06
		At 1 atm:	0.08651	101325.000	0.3566			
						Standard deviation:		0.0008114

CH4/ AlPO4-17 ADSORPTION ISOTHERM at 40.0°C

Langmuir and Freundlich Theories

B [1/Pa] =	9.99E-07	vm [m3/kg]=	0.0868945	nm [mol/kg]=	3.87702
		k =	5.75E-06	n =	1.04389

p {exp} [Pa]	n {exp} [mol/kg]	p/n [Pa kg/mol]	Langmuir n [mol/kg]	Freundlich n [mol/kg]	p {exp} [mm Hg]	v {exp} [cc STP/g]	Square deviation {Langmuir}	Square deviation {Freundlich}
0	0		0	0	0	0		
10204.494	0.03893	262119	0.03913	0.03977	76.54	0.8725	4.05E-08	7.08E-07
18611.803	0.07135	260858	0.07078	0.07073	139.6	1.5991	3.19E-07	3.82E-07
29580.234	0.11175	264690	0.11130	0.11024	221.87	2.5047	2.06E-07	2.28E-06
44543.003	0.16431	271085	0.16520	0.16318	334.1	3.6827	7.88E-07	1.29E-06
55995.395	0.20518	272911	0.20543	0.20317	420	4.5986	6.11E-08	4.04E-06
68407.707	0.24785	276003	0.24805	0.24612	513.1	5.5550	3.86E-08	2.98E-06
81313.313	0.29161	278847	0.29133	0.29044	609.9	6.5357	7.71E-08	1.36E-06
94498.895	0.33362	283255	0.33449	0.33541	708.8	7.4773	7.66E-07	3.21E-06
107764.470	0.37599	286613	0.37688	0.38039	808.3	8.4270	7.93E-07	1.93E-05
121190.033	0.42072	288056	0.41877	0.42567	909	9.4294	3.81E-06	2.45E-05
101325			0.35643	0.35859				
					Standard deviations:		0.00088	0.0025845

CO / AlPO4-17 ADSORPTION ISOTHERM at 40.0°C

Flory-Huggins Vacancy Solution Theory

Parameter	estimates	Asymptotic standard error	Asymptotic 95% confidence interval lower limit	upper limit
ninf [mol/kg]	0.6675282	5.37314	-13.14436	14.479
b1 [mol/kg*Pa]	1.563E-06	0.00000	0.00000	0.00000
alfa1v	-4.58E-05	127982.76	-328985.4	328985

p {exp} [Pa]	v {exp} [m3 STP/kg]	n {exp} [mol/kg]	theta {VST}	P {VST} [Pa]	n {VST} [mol/kg]	p {exp} [mm Hg]	v {exp} [cc STP/g]	Square deviation
0	0	0	0	0	0	0	0	0
7502.050	0.000182	0.00813	0.01726	7502.050	0.01152	56.27	0.18219	1.15E-05
18110.511	0.000492	0.02197	0.04067	18110.511	0.02715	135.84	0.49232	2.69E-05
43123.120	0.001130	0.05040	0.09170	43123.120	0.06121	323.45	1.12953	1.17E-04
63421.451	0.001679	0.07490	0.12928	63421.451	0.08630	475.7	1.67869	1.30E-04
79820.102	0.002176	0.09707	0.15744	79820.102	0.10510	598.7	2.17565	6.44E-05
94658.882	0.002571	0.11471	0.18140	94658.882	0.12109	710	2.5709	4.07E-05
108471.079	0.003024	0.13493	0.20251	108471.079	0.13518	813.6	3.02413	6.33E-08
122056.628	0.003481	0.15530	0.22224	122056.628	0.14835	915.5	3.48073	4.83E-05
		At 1 atm:	0.19173	101325.000	0.12798			
						Standard deviation:		0.0079166

CO/ AlPO4-17 ADSORPTION ISOTHERM at 40.0°C

Langmuir and Freundlich Theories

B [1/Pa] = -8.92E-07 nm [mol/kg] = -1.279563 k = 7.81E-07 n = 0.9606953

N.B. Since the Langmuir parameters have negative values, they are void of physical significance and should be seen only as fitting parameters.

p {exp} [Pa]	n {exp} [mol/kg]	p/n [Pa kg/mol]	Langmuir n [mol/kg]	Freundlich n [mol/kg]	p {exp} [mm Hg]	v {exp} [cc STP/g]	Square deviation {Langmuir}	Square deviation {Freundlich}
0	0		0	0	0	0		
7502.050	0.00825	909022	0.00862	0.00844	56.27	0.185	1.37E-07	3.59E-03
18110.511	0.02230	812098	0.02102	0.02113	135.84	0.4998	1.65E-06	1.37E-06
43123.120	0.05116	842830	0.05121	0.05213	323.45	1.1467	1.87E-09	9.26E-07
63421.451	0.07604	834050	0.07676	0.07788	475.7	1.7043	5.15E-07	3.40E-06
79820.102	0.09855	809935	0.09813	0.09895	598.7	2.2088	1.80E-07	1.57E-07
94658.882	0.11646	812836	0.11805	0.11816	710	2.6101	2.55E-06	2.92E-06
108471.079	0.13699	791846	0.13712	0.13616	813.6	3.0702	1.91E-08	6.77E-07
122056.628	0.15767	774139	0.15640	0.15396	915.5	3.5338	1.62E-06	1.38E-05
101325.000			0.12719	0.12684				
					Standard deviations:		0.00098	0.0018225

N2 / AlPO4-18 ADSORPTION ISOTHERM at 40.1°C

Flory-Huggins Vacancy Solution Theory

Parameter	estimates	Asymptotic standard error	Asymptotic 95% confidence interval lower limit	upper limit
ninf [mol/kg]	4.0747326	1.8239901	-0.131437	8.2809
b1 [mol/kg*Pa]	7.1700E-07	5.60E-09	7.04E-07	7E-07
alfa1v	0	0	0	0

p {exp} [Pa]	v {exp} [m3 STP/kg]	n {exp} [mol/kg]	theta {VST}	P {VST} [Pa]	n {VST} [mol/kg]	p {exp} [mm Hg]	v {exp} [cc STP/g]	Square deviation
0	0	0	0	0	0	0	0	0
11472.390	0.000181	0.00808	0.00201	11472.390	0.00821	86.05	0.1812	1.58E-08
19715.712	0.000319	0.01423	0.00346	19715.712	0.01409	147.88	0.3189	2.00E-08
30778.802	0.000501	0.02236	0.00539	30778.802	0.02195	230.86	0.5011	1.66E-07
43044.460	0.000693	0.03091	0.00752	43044.460	0.03063	322.86	0.6929	8.07E-08
55915.401	0.000893	0.03986	0.00974	55915.401	0.03970	419.4	0.8935	2.67E-08
69114.316	0.001089	0.04859	0.01202	69114.316	0.04896	518.4	1.0891	1.34E-07
82326.563	0.001292	0.05764	0.01428	82326.563	0.05819	617.5	1.2920	2.93E-07
95552.141	0.001509	0.06731	0.01654	95552.141	0.06738	716.7	1.5087	4.18E-09
108857.714	0.001720	0.07674	0.01879	108857.714	0.07658	816.5	1.7200	2.46E-08
122189.951	0.001926	0.08592	0.02105	122189.951	0.08577	916.5	1.9258	2.47E-08
		At 1 atm:	0.01752	101325.000	0.07138			
							Standard deviation:	0.000296

N2 / AlPO4-18 ADSORPTION ISOTHERM at 40.1°C

Langmuir Theory

B [1/Pa] = 2.15E-07 vm [m3/kg]= 0.0750323 nm [mol/kg]= 3.34775

p {exp} [Pa]	v {exp} [m3 STP/kg]	n {exp} [mol/kg]	p/n [Pa kg/mol]	Langmuir v [m3 STP/kg]	Langmuir n [mol/kg]	p {exp} [mm Hg]	v {exp} [cc STP/g]	Square deviation
0	0	0		0	0	0	0	0
11472.390	0.000181	0.00808	1419246	0.000185	0.00824	86.05	0.1812	2.31E-08
19715.712	0.000319	0.01423	1385624	0.000317	0.01413	147.88	0.3189	1.02E-08
30778.802	0.000501	0.02236	1376725	0.000493	0.02200	230.86	0.5011	1.25E-07
43044.460	0.000693	0.03091	1392351	0.000688	0.03069	322.86	0.6929	4.99E-08
55915.401	0.000893	0.03986	1402647	0.000891	0.03976	419.4	0.8935	1.09E-08
69114.316	0.001089	0.04859	1422300	0.001098	0.04901	518.4	1.0891	1.72E-07
82326.563	0.001292	0.05764	1428181	0.001305	0.05821	617.5	1.2920	3.24E-07
95552.141	0.001509	0.06731	1419512	0.001510	0.06738	716.7	1.5087	4.04E-09
108857.714	0.001720	0.07674	1418511	0.001716	0.07654	816.5	1.7200	3.85E-08
122189.951	0.001926	0.08592	1422083	0.001920	0.08568	916.5	1.9258	5.95E-08
101325				0.001599	0.07136			
							Standard deviation:	0.000301

CH4 / AlPO4-18 ADSORPTION ISOTHERM at 40.0°C

Flory-Huggins Vacancy Solution Theory

Parameter	estimates	Asymptotic standard error	Asymptotic 95% confidence interval lower limit	upper limit
ninf [mol/kg]	2.4393007	0.3606148	1.6077135	3.27089
bl [mol/kg*Pa]	1.843E-06	2.0140E-08	1.80E-06	1.8896E-06
alfalv	0	0	0	0

p {exp} [Pa]	v {exp} [m3 STP/kg]	n {exp} [mol/kg]	theta {VST}	P {VST} [Pa]	n {VST} [mol/kg]	p {exp} [mm Hg]	v {exp} [cc STP/g]	Square deviation
0	0	0	0	0	0	0	0	0
9992.512	0.000416	0.01854	0.00749	9992.512	0.01828	74.95	0.41563	7.10E-08
18373.156	0.000760	0.03393	0.01369	18373.156	0.03340	137.81	0.76036	2.78E-07
29241.595	0.001207	0.05383	0.02162	29241.595	0.05273	219.33	1.20655	1.22E-06
41481.922	0.001668	0.07441	0.03039	41481.922	0.07413	311.14	1.66783	8.20E-08
54582.178	0.002168	0.09671	0.03961	54582.178	0.09661	409.4	2.16762	1.06E-08
67461.118	0.002659	0.11865	0.04850	67461.118	0.11830	506	2.65935	1.24E-07
80660.033	0.003136	0.13991	0.05744	80660.033	0.14012	605	3.13586	4.12E-08
93965.605	0.003601	0.16069	0.06629	93965.605	0.16170	704.8	3.60139	1.03E-06
107297.842	0.004064	0.18131	0.07499	107297.842	0.18292	804.8	4.06363	2.60E-06
120390.099	0.004598	0.20514	0.08338	120390.099	0.20338	903	4.59765	3.08E-06
		At 1 atm:	0.07111	101325.000	0.17346			
						Standard deviation:		0.00097

CH4 / AlPO4-18 ADSORPTION ISOTHERM at 40.0°C

Langmuir Theory

B [1/Pa] = 9.52E-07 vm [m3/kg]= 0.0441178 nm [mol/kg]= 1.96843

p {exp} [Pa]	v {exp} [m3 STP/kg]	n {exp} [mol/kg]	p/n [Pa kg/mol]	Langmuir v [m3 STP/kg]	Langmuir n [mol/kg]	p {exp} [mm Hg]	v {exp} [cc STP/g]	Square deviation
0	0	0		0	0	0	0	0
11472.390	0.000181	0.00808	1419246	0.000416	0.01855	74.95	0.4156	2.02E-12
19715.712	0.000319	0.01423	1385624	0.000758	0.03383	137.81	0.7604	8.50E-09
30778.802	0.000501	0.02236	1376725	0.001195	0.05330	219.33	1.2066	2.80E-07
43044.460	0.000693	0.03091	1392351	0.001676	0.07477	311.14	1.6678	1.27E-07
55915.401	0.000893	0.03986	1402647	0.002179	0.09722	409.4	2.1676	2.53E-07
69114.316	0.001089	0.04859	1422300	0.002662	0.11877	506	2.6593	1.39E-08
82326.563	0.001292	0.05764	1428181	0.003146	0.14035	605	3.1359	1.92E-07
95552.141	0.001509	0.06731	1419512	0.003622	0.16160	704.8	3.6014	8.44E-07
108857.714	0.001720	0.07674	1418511	0.004088	0.18241	804.8	4.0636	1.21E-06
122189.951	0.001926	0.08592	1422083	0.004536	0.20238	903	4.5977	7.61E-06
101325				0.003881	0.17315			
						Standard deviation:		0.00108

CO / AlPO4-18 ADSORPTION ISOTHERM at 40.1°C

Flory-Huggins Vacancy Solution Theory

Parameter	estimates	Asymptotic standard error	Asymptotic 95% confidence interval lower limit	upper limit
ninf [mol/kg]	0.7092515	0.09207	0.4915388	0.92696
bl [mol/kg*Pa]	3.125E-06	1.761E-07	2.709E-06	3.5419E-06
alfalv	0	0	0	0

p {exp} [Pa]	v {exp} [m3 STP/kg]	n {exp} [mol/kg]	theta {VST}	P {VST} [Pa]	n {VST} [mol/kg]	p {exp} [mm Hg]	v {exp} [cc STP/g]	Square deviation
0	0	0	0	0	0	0	0	0
10539.133	0.000277	0.01237	0.04438	10539.133	0.03148	79.05	0.2771	3.65E-04
23810.042	0.001328	0.05924	0.09496	23810.042	0.06735	178.59	1.3278	6.57E-05
37707.565	0.002276	0.10155	0.14249	37707.565	0.10106	282.83	2.2759	2.38E-07
51622.421	0.003059	0.13647	0.18532	51622.421	0.13144	387.2	3.0586	2.53E-05
65807.921	0.003664	0.16347	0.22480	65807.921	0.15944	493.6	3.6638	1.62E-05
79846.766	0.004170	0.18604	0.26028	79846.766	0.18460	598.9	4.1697	2.08E-06
93672.296	0.004616	0.20594	0.29217	93672.296	0.20723	702.6	4.6156	1.66E-06
107204.516	0.005067	0.22606	0.32084	107204.516	0.22756	804.1	5.0667	2.23E-06
120616.747	0.005513	0.24596	0.34705	120616.747	0.24615	904.7	5.5127	3.34E-08
		At 1 atm:	0.30868	101325.000	0.21893			
							Standard deviation:	0.00774

CO / AlPO4-18 ADSORPTION ISOTHERM at 40.1°C

Langmuir Theory

B [1/Pa] = 5.08E-06 vm [m3/kg]= 0.0144503 nm [mol/kg]= 0.64474

p {exp} [Pa]	v {exp} [m3 STP/kg]	n {exp} [mol/kg]	p/n [Pa kg/mol]	Langmuir v [m3 STP/kg]	Langmuir n [mol/kg]	p {exp} [mm Hg]	v {exp} [cc STP/g]	Square deviation
0	0	0		0	0	0	0	0
10539.133	0.000277	0.01237	852294	0.000734	0.03276	79.05	0.2771	4.16E-04
23810.042	0.001328	0.05924	401900	0.001559	0.06956	178.59	1.3278	1.06E-04
37707.565	0.002276	0.10155	371333	0.002323	0.10363	282.83	2.2759	4.33E-06
51622.421	0.003059	0.13647	378275	0.003002	0.13393	387.2	3.0586	6.47E-06
65807.921	0.003664	0.16347	402569	0.003620	0.16151	493.6	3.6638	3.85E-06
79846.766	0.004170	0.18604	429188	0.004169	0.18602	598.9	4.1697	3.97E-10
93672.296	0.004616	0.20594	454863	0.004658	0.20785	702.6	4.6156	3.66E-06
107204.516	0.005067	0.22606	474224	0.005094	0.22729	804.1	5.0667	1.50E-06
120616.747	0.005513	0.24596	490385	0.005489	0.24492	904.7	5.5127	1.08E-06
101325				0.004910	0.21906			
							Standard deviation:	0.00824

APPENDIX D

Predicted Binary Mixture Adsorption Data

N2 - CO / 5A at 22.6-22.7°C and 101.3 kPa total pressure

Flory-Huggins Vacancy Solution Theory Binary Prediction

Binary Parameter: a12 = -0.010772

x1 (N2)	y1 (N2)	x2 (CO)	y2 (CO)	gamma1	gamma2	gammav	n1 [mol/kg]	n2 [mol/kg]	nt [mol/kg]	alpha21 CO/N2
0	0	1	1	—	—	—	0	0.832	0.832	------
0.1	0.2822	0.9	0.7178	0.9999473	0.9999985	0.9999999	0.075	0.678	0.753	3.538
0.2	0.472	0.8	0.528	0.9999517	0.9999995	0.9999995	0.137	0.549	0.686	3.576
0.3	0.6071	0.7	0.3929	0.999955	0.9999991	0.9999991	0.189	0.44	0.629	3.605
0.4	0.7076	0.6	0.2924	0.9999577	0.9999987	0.9999987	0.232	0.348	0.58	3.63
0.5	0.785	0.5	0.215	0.9999598	0.9999983	0.9999983	0.269	0.268	0.537	3.651
0.6	0.8462	0.4	0.1538	0.9999615	0.9999979	0.9999979	0.3	0.2	0.5	3.668
0.701	0.8962	0.299	0.1038	0.9999629	0.9999976	0.9999976	0.328	0.14	0.468	3.684
0.8	0.9367	0.2	0.0633	0.999964	0.9999973	0.9999973	0.352	0.088	0.44	3.698
0.9	0.9709	0.1	0.0377	0.9999649	0.999997	0.999997	0.373	0.041	0.414	2.862
1	1	0	0	----	----	----	0.392	0	0.392	----

N2 - CO / 5A at 39.8-40.0°C and 101.3 kPa total pressure

Flory-Huggins Vacancy Solution Theory Binary Prediction

Binary Parameter: a12 = -0.62068

x1 (N2)	y1 (N2)	x2 (CO)	y2 (CO)	gamma1	gamma2	gammav	n1 [mol/kg	n2 [mol/kg	nt [mol/kg	alpha21 CO/N2
0	0	1	1	———	———	———	0	0.606	0.606	------
0.1	0.3711	0.9	0.6289	0.9721839	0.7141904	0.9721839	0.049	0.444	0.493	5.311
0.2	0.589	0.8	0.411	0.983512	0.6682966	0.983512	0.082	0.326	0.408	5.731
0.3	0.7232	0.7	0.2768	0.9903567	0.6317497	0.9903567	0.103	0.241	0.344	6.097
0.4	0.8104	0 6	0.1896	0.9944711	0.6028105	0.9944711	0.118	0.177	0.296	6.41
0.5	0.8697	0.5	0.1303	0.9969396	0.5797308	0.9969396	0.129	0.129	0.258	6.677
0.6	0.912	0.4	0.088	0.998408	0.5610894	0.998408	0.137	0.091	0.228	6.906
0.7	0.9431	0.3	0.0569	0.9992593	0.5458142	0.9992593	0.143	0.061	0.205	7.103
0.8	0.9668	0.2	0.0332	0.9997235	0.5331161	0.9997235	0.148	0.037	0.185	7.274
0.9	0.9853	0.1	0.0147	0.9999412	0.5224164	0.9999412	0.152	0.017	0.169	7.424
1	1	0	0	———	------	———	0.155	0	0.155	----

CH4 - CO / 5A at 22.6-22.8°C and 101.3 kPa total pressure

Flory-Huggins Vacancy Solution Theory Binary Prediction

Binary Parameter: a12 = 2.0927

x1 (CH4)	y1 (CH4)	x2 (CO)	y2 (CO)	gamma1	gamma2	gammav	n1 [mol/kg]	n2 [mol/kg]	nt [mol/kg]	alpha21 CO/CH4
0	0	1	1	—	—	—	0	0.832	0.832	———
0.1	0.1332	0.9	0.8668	0.4987	0.9952	0.9952	0.088	0.792	0.879	1.383
0.2	0.3731	0.8	0.6269	0.51362	0.98792	0.98792	0.169	0.678	0.847	2.38
0.3	0.592	0.7	0.408	0.53479	0.98398	0.98398	0.227	0.529	0.756	3.386
0.4	0.7384	0.6	0.2616	0.53919	0.98309	0.98309	0.263	0.394	0.657	4.235
0.5	0.831	0.5	0.169	0.5365	0.98364	0.98364	0.286	0.286	0.573	4.916
0.6	0.8913	0.4	0.1087	0.53122	0.98468	0.98468	0.303	0.202	0.505	5.468
0.7	0.9325	0.3	0.0675	0.52522	0.98582	0.98582	0.316	0.136	0.452	5.925
0.8	0.9619	0.2	0.0381	0.51926	0.98692	0.98692	0.327	0.082	0.409	6.311
0.9	0.9836	0.1	0.0164	0.51365	0.98791	0.98791	0.337	0.037	0.374	6.644
1	1	0	0	—	—	—	0.346	0	0.346	———

CH4 - CO / 5A at 40.0-40.1°C and 101.3 kPa total pressure

Flory-Huggins Vacancy Solution Theory Binary Prediction

Binary Parameter: a12 = -0.6207

x1 (CH4)	y1 (CH4)	x2 (CO)	y2 (CO)	gamma1	gamma2	gammav	n1 [mol/kg	n2 [mol/kg	nt [mol/kg	alpha21 CO/CH4
0	0	1	1	—	—	—	0	0.606	0.606	———
0.01	0.0242	0.99	0.9758	0.45895	0.76629	0.95525	0.006	0.597	0.603	2.459
0.02	0.0482	0.98	0.9518	0.45983	0.76245	0.95666	0.012	0.587	0.599	2.481
0.03	0.0719	0.97	0.9281	0.46183	0.75857	0.95806	0.018	0.578	0.596	2.504
0.04	0.0952	0.96	0.9048	0.46383	0.75466	0.95737	0.024	0.568	0.592	2.526
0.05	0.1183	0.95	0.8817	0.46584	0.75072	0.9608	0.029	0.558	0.588	2.549
0.06	0.1411	0.94	0.8589	0.46786	0.74675	0.96215	0.035	0.549	0.584	2.573
0.07	0.1635	0.93	0.8365	0.4699	0.74274	0.96348	0.041	0.539	0.58	2.597
0.08	0.1856	0.92	0.8144	0.47194	0.73871	0.96479	0.046	0.53	0.576	2.621
0.09	0.2074	0.91	0.7926	0.47398	0.73465	0.96608	0.051	0.52	0.571	2.646
0.1	0.2289	0.9	0.7711	0.47604	0.73057	0.95735	0.057	0.51	0.567	2.671
0.2	0.424	0.8	0.576	0.49679	0.68883	0.97883	0.104	0.418	0.522	2.945
0.3	0.5823	0.7	0.4177	0.51726	0.64698	0.98773	0.143	0.333	0.475	3.253
0.4	0.7051	0.6	0.2847	0.53659	0.60722	0.99392	0.172	0.257	0.429	3.715
0.5	0.7972	0.5	0.2028	0.55415	0.57114	0.99767	0.193	0.193	0.385	3.93
0.6	0.865	0.4	0.135	0.56964	0.53948	0.99952	0.207	0.138	0.346	4.273
0.7	0.9149	0.3	0.0851	0.58308	0.51226	1	0.218	0.093	0.311	4.606
0.8	0.9517	0.2	0.0483	0.59466	0.48902	0.99958	0.225	0.056	0.281	4.923
0.9	0.9792	0.1	0.0208	0.60466	0.4692	0.99859	0.23	0.026	0.256	5.224
1	1	0	0	—	—	—	0.235	0	0.235	———

N2 - CH4 / 5A at 22.7-22.8°C and 101.3 kPa total pressure

Flory-Huggins Vacancy Solution Theory Binary Prediction

Binary Parameter: a12 = -0.010772

x1 (N2)	y1 (N2)	x2 (CH4)	y2 (CH4)	gamma1	gamma2	gammav	n1 [mol/kg]	n2 [mol/kg]	nt [mol/kg]	alpha12 N2/CH4
0	0	1	1	———	———	———	0	0.346	0.346	———
0.1	0.0868	0.9	0.9132	0.99994465	0.99999996	0.99999996	0.035	0.316	0.351	1.169
0.2	0.1778	0.8	0.8222	0.99994756	0.99999984	0.99999984	0.071	0.285	0.357	1.156
0.3	0.2727	0.7	0.7273	0.99995031	0.99999964	0.99999964	0.109	0.253	0.362	1.143
0.4	0.3707	0.6	0.6293	0.99995291	0.99999938	0.99999938	0.147	0.22	0.367	1.132
0.5	0.4716	0.5	0.5284	0.99995537	0.99999906	0.99999906	0.186	0.186	0.372	1.121
0.601	0.5757	0.399	0.4243	0.99995771	0.99999869	0.99999869	0.226	0.15	0.376	1.11
0.701	0.6805	0.299	0.3195	0.99995990	0.99999827	0.99999827	0.267	0.114	0.38	1.101
0.801	0.7866	0.199	0.2134	0.99996196	0.99999780	0.99999780	0.308	0.077	0.385	1.092
0.9	0.8927	0.0999	0.1073	0.99996389	0.99999731	0.99999731	0.35	0.039	0.388	1.083
1	1	0	0	———	———	———	0.392	0	0.392	———

N2 - CH4 / 5A at 39.8-40.1°C and 101.3 kPa total pressure

Flory-Huggins Vacancy Solution Theory Binary Prediction

Binary Parameter: a12 = 2.5089997

x1 (N2)	y1 (N2)	x2 (CH4)	y2 (CH4)	gamma1	gamma2	gammav	n1 [mol/kg	n2 [mol/kg	nt [mol/kg	alpha21 CH4/N2
0	0	1	1	———	———	———	0	0.235	0.235	———
0.1	0.1488	0.9	0.8512	0.9980212	0.6087543	0.9980212	0.022	0.201	0.224	1.573
0.2	0.2839	0.8	0.7161	0.9986009	0.604589	0.9986009	0.043	0.172	0.214	1.586
0.3	0.4065	0.7	0.5935	0.9990403	0.6008083	0.9990403	0.062	0.144	0.205	1.598
0.4	0.5175	0.6	0.4825	0.9993671	0.5973816	0.9993671	0.079	0.118	0.197	1.609
0.5	0.6181	0.5	0.3819	0.9996046	0.594277	0.9996045	0.094	0.097	0.189	1.619
0.6	0.7094	0.4	0.2906	0.9997718	0.5914634	0.9997718	0.109	0.072	0.181	1.628
0.7	0.7924	0.3	0.2076	0.999884	0.5889114	0.999884	0.122	0.052	0.174	1.636
0.8	0.868	0.2	0.132	0.9999533	0.5865938	0.9999533	0.134	0.033	0.167	1.643
0.9	0.9369	0.1	0.0631	0.9999894	0.5844862	0.9999894	0.145	0.016	0.161	1.65
1	1	0	0	———	———	———	0.155	0	0.155	———

N2 - CO / Turkish clinoptilolite at 22.6-22.8°C and 101.3 kPa total pressure

Flory-Huggins Vacancy Solution Theory Binary Prediction

Binary Parameter: a12 = -0.172804

x1 (N2)	y1 (N2)	x2 (CO)	y2 (CO)	gamma1	gamma2	gammav	n1 [mol/kg]	n2 [mol/kg]	nt [mol/kg]	alpha21 CO/N2
0	0	1	1	—	—	—	0	1.19	1.19	———
0.001	0.0688	0.999	0.9312	0.9903812	0.9988603	0.2375025	0.001	1.185	1.186	73.77
0.002	0.1272	0.998	0.8728	0.990769	0.9987112	0.238143	0.002	1.18	1.182	72.72
0.003	0.1776	0.997	0.8224	0.9911365	0.9985583	0.2387631	0.004	1.175	1.178	71.79
0.004	0.2218	0.996	0.7782	0.991486	0.9984019	0.2393655	0.005	1.17	1.174	70.96
0.005	0.2608	0.995	0.7392	0.9918194	0.998242	0.2399524	0.006	1.165	1.171	70.21
0.006	0.2956	0.994	0.7044	0.9921381	0.9980787	0.2405254	0.007	1.16	1.167	69.53
0.007	0.3269	0.993	0.6731	0.9924435	0.9979122	0.2410859	0.008	1.156	1.164	68.9
0.008	0.3552	0.992	0.6448	0.9927366	0.9977425	0.2416351	0.009	1.151	1.16	68.32
0.009	0.3811	0.991	0.6189	0.9930182	0.9975699	0.242174	0.01	1.147	1.157	67.79
0.01	0.4047	0.99	0.5953	0.9932892	0.9973943	0.2427033	0.012	1.142	1.154	67.29
0.02	0.5654	0.98	0.4346	0.99553	0.9954958	0.2475944	0.022	1.102	1.124	63.75
0.03	0.6559	0.97	0.3441	0.9971392	0.993384	0.2519724	0.033	1.066	1.099	61.63
0.04	0.715	0.96	0.285	0.9982966	0.9911074	0.2560011	0.043	1.033	1.076	60.21
0.05	0.7571	0.95	0.2429	0.9991034	0.9887014	0.2597637	0.053	1.002	1.055	59.22
0.06	0.7887	0.94	0.2113	0.9996262	0.986193	0.2633102	0.062	0.974	1.036	58.49
0.07	0.8135	0.93	0.1865	0.9999129	0.983604	0.2666743	0.071	0.947	1.018	57.96
0.08	0.8335	0.92	0.1665	0.99999998	0.9809518	0.2698799	0.08	0.921	1.001	57.56
0.09	0.8499	0.91	0.1501	0.9999162	0.9782511	0.2729451	0.089	0.897	0.986	57.26
0.1	0.8637	0.9	0.1363	0.9996852	0.9755141	0.2758839	0.097	0.874	0.971	57.04
0.2	0.9345	0.8	0.0655	0.9924453	0.9478426	0.3001398	0.172	0.687	0.859	57.05
0.3	0.9617	0.7	0.0383	0.9814848	0.922277	0.3180632	0.235	0.549	0.784	58.61
0.4	0.9759	0.6	0.0241	0.9701739	0.9001633	0.3318281	0.292	0.438	0.73	60.73
0.5	0.9844	0.5	0.0156	0.9577482	0.8816523	0.3425467	0.344	0.344	0.687	63.23
0.6	0.99	0.4	0.01	0.9507849	0.8665523	0.3508886	0.392	0.261	0.653	66.06
0.7	0.9939	0.3	0.0061	0.9433863	0.8545953	0.3572883	0.438	0.188	0.626	69.26
0.8	0.9966	0.2	0.0034	0.937625	0.8455265	0.3620389	0.482	0.12	0.602	72.91
0.9	0.9986	0.1	0.0014	0.93349	0.8391319	0.3653409	0.524	0.058	0.582	77.13
1	1	0	0	—	—	—	0.565	0	0.565	—

N2 - CO / Turkish clinoptilolite at 40.0°C and 101.3 kPa total pressure

Flory-Huggins Vacancy Solution Theory Binary Prediction

Binary Parameter: a12 = 0.0273064

x1 (N2)	y1 (N2)	x2 (CO)	y2 (CO)	gamma1	gamma2	gammav	n1 [mol/kg]	n2 [mol/kg]	nt [mol/kg]	alpha21 CO/N2
0	0	1	1	———	———	———	0	0.939	0.939	———
0.001	0.0222	0.999	0.9778	0.9929017	0.9958256	0.3389395	0.001	0.936	0.937	22.72
0.002	0.0434	0.998	0.9566	0.9927104	0.9956797	0.3393867	0.002	0.933	0.935	22.64
0.003	0.0636	0.997	0.9364	0.9925194	0.9955334	0.3398279	0.003	0.93	0.933	22.56
0.004	0.0828	0.996	0.9172	0.9923285	0.9953866	0.3402635	0.004	0.927	0.931	22.49
0.005	0.1012	0.995	0.8988	0.9921378	0.9952395	0.3406936	0.005	0.924	0.929	22.42
0.006	0.1189	0.994	0.8811	0.9919472	0.9950919	0.3411185	0.006	0.921	0.927	22.35
0.007	0.1357	0.993	0.8643	0.9917568	0.994744	0.3415684	0.006	0.918	0.925	22.28
0.008	0.152	0.992	0.848	0.9915664	0.9947957	0.3419535	0.007	0.916	0.923	22.22
0.009	0.1675	0.991	0.8325	0.9913762	0.994647	0.342364	0.008	0.913	0.921	22.16
0.01	0.1825	0.99	0.8175	0.991186	0.994498	0.34277	0.009	0.91	0.92	22.1
0.02	0.3059	0.98	0.6941	0.9892889	0.9929901	0.3466155	0.018	0.884	0.903	21.59
0.03	0.3962	0.97	0.6038	0.9873985	0.9914563	0.3501406	0.027	0.86	0.887	21.22
0.04	0.4657	0.96	0.5343	0.9855159	0.9899043	0.353414	0.035	0.838	0.873	20.92
0.05	0.5212	0.95	0.4788	0.9836431	0.9883407	0.3564803	0.043	0.817	0.86	20.68
0.06	0.5667	0.94	0.4333	0.9817824	0.9867709	0.3593706	0.051	0.796	0.847	20.49
0.07	0.6048	0.93	0.3952	0.9799361	0.9851996	0.3621079	0.058	0.777	0.835	20.33
0.08	0.6372	0.92	0.3628	0.9781062	0.9836307	0.3647098	0.066	0.758	0.824	20.2
0.09	0.6652	0.91	0.3348	0.9762948	0.9820674	0.3671905	0.073	0.74	0.814	20.09
0.1	0.6896	0.9	0.3104	0.9745033	0.9805126	0.3695611	0.08	0.723	0.804	19.99
0.2	0.8306	0.8	0.1694	0.9579215	0.9658223	0.3887509	0.144	0.578	0.722	19.62
0.3	0.8943	0.7	0.1057	0.9440806	0.9532875	0.4023366	0.199	0.464	0.663	19.74
0.4	0.9305	0.6	0.0695	0.9330301	0.9431632	0.4121958	0.247	0.37	0.617	20.09
0.5	0.9537	0.5	0.0463	0.9246299	0.9354136	0.4192537	0.29	0.29	0.579	20.61
0.6	0.9696	0.4	0.0304	0.9187053	0.929924	0.4240447	0.329	0.219	0.548	21.26
0.7	0.9809	0.3	0.0191	0.9150915	0.926567	0.4268998	0.365	0.156	0.521	22.05
0.8	0.9892	0.2	0.0108	0.9136448	0.9252212	0.4280296	0.398	0.1	0.498	22.99
0.9	0.9954	0.1	0.0046	0.9142397	0.9257748	0.4275659	0.43	0.048	0.478	24.11
1	1	0	0	———	———	———	0.46	0	0.46	———

CH4 - CO / Turkish clinoptilolite at 22.8°C and 101.3 kPa total pressure

Flory-Huggins Vacancy Solution Theory Binary Prediction

Binary Parameter: a12 = -0.7275

x1 (CH4)	y1 (CH4)	x2 (CO)	y2 (CO)	gamma1	gamma2	gammav	n1 [mol/kg]	n2 [mol/kg]	nt [mol/kg]	alpha21 CO/CH4
0	0	1	1	—	—	—	0	1.19	1.19	———
0.001	0.0221	0.999	0.9779	0.58305	0.99893	0.23717	0.001	1.188	1.189	22.59
0.002	0.0433	0.998	0.9567	0.5837	0.99886	0.23751	0.002	1.185	1.188	22.57
0.003	0.0635	0.997	0.9365	0.58435	0.99878	0.23784	0.004	1.183	1.187	22.55
0.004	0.083	0.585	0.9987	0.585	0.9987	0.23817	0.005	1.181	1.185	12.16
0.005	0.1017	0.995	0.8983	0.58564	0.99862	0.2385	0.006	1.178	1.184	22.52
0.006	0.1196	0.994	0.8804	0.58628	0.99854	0.23883	0.007	1.176	1.183	22.5
0.007	0.1368	0.993	0.8632	0.58692	0.99845	0.23917	0.008	1.173	1.182	22.49
0.008	0.1534	0.992	0.8466	0.58756	0.99837	0.2395	0.009	1.171	1.181	22.48
0.009	0.1694	0.991	0.8306	0.58819	0.99828	0.23982	0.011	1.169	1.179	22.46
0.01	0.1849	0.99	0.8151	0.58883	0.99819	0.24015	0.012	1.166	1.178	22.45
0.02	0.3135	0.98	0.6865	0.59511	0.99715	0.24342	0.023	1.143	1.167	22.38
0.03	0.4088	0.97	0.5912	0.60128	0.9959	0.24665	0.035	1.121	1.156	22.36
0.04	0.4826	0.96	0.5174	0.60736	0.99445	0.24986	0.046	1.099	1.145	22.39
0.05	0.5415	0.95	0.4585	0.61338	0.9928	0.25306	0.057	1.078	1.135	22.44
0.06	0.5897	0.94	0.4103	0.61933	0.99096	0.25625	0.068	1.058	1.125	22.52
0.07	0.63	0.93	0.37	0.62523	0.98893	0.25943	0.078	1.038	1.116	22.62
0.08	0.6641	0.92	0.3359	0.63108	0.98671	0.26261	0.089	1.019	1.107	22.74
0.09	0.6934	0.91	0.3066	0.6369	0.9843	0.2658	0.099	1	1.098	22.87
0.1	0.7189	0.9	0.2811	0.64267	0.98171	0.26899	0.109	0.981	1.09	23.02
0.2	0.8622	0.8	0.1378	0.69892	0.94612	0.30145	0.203	0.814	1.017	25.02
0.3	0.9228	0.7	0.0772	0.75323	0.89361	0.3357	0.288	0.673	0.961	27.89
0.4	0.9549	0.6	0.0451	0.80596	0.82475	0.37264	0.366	0.55	0.916	31.73
0.5	0.9737	0.5	0.0263	0.85687	0.73987	0.41326	0.44	0.44	0.881	36.96
0.6	0.9852	0.4	0.0148	0.90501	0.63948	0.45878	0.512	0.341	0.853	44.42
0.7	0.9924	0.3	0.0076	0.94831	0.52495	0.51079	0.582	0.249	0.832	55.76
0.8	0.9967	0.2	0.0033	0.98261	0.39948	0.57157	0.654	0.163	0.817	74.62
0.9	0.999	0.1	0.001	0.99975	0.26971	0.64382	0.73	0.081	0.811	110.5
1	1	0	0	—	—	—	0.814	0	0.814	———

CH4 - CO / Turkish clinoptilolite at 40.0°C and 101.3 kPa total pressure

Flory-Huggins Vacancy Solution Theory Binary Prediction

Binary Parameter: a12 = -0.5797

x1 (CH4)	y1 (CH4)	x2 (CO)	y2 (CO)	gamma1	gamma2	gammav	n1 [mol/kg]	n2 [mol/kg]	nt [mol/kg]	alpha21 CO/CH4
0	0	1	1	—	—	—	0	0.939	0.939	——
0.01	0.0701	0.99	0.9299	0.79318	0.99492	0.34159	0.009	0.925	0.934	7.462
0.02	0.1338	0.98	0.8662	0.79775	0.99274	0.34475	0.019	0.912	0.93	7.567
0.03	0.1918	0.97	0.8082	0.80233	0.99243	0.34795	0.028	0.898	0.926	7.673
0.04	0.2448	0.96	0.7552	0.80692	0.99097	0.35119	0.037	0.885	0.922	7.779
0.05	0.2933	0.95	0.7067	0.81152	0.98937	0.35448	0.046	0.872	0.918	7.886
0.06	0.3378	0.94	0.6622	0.81612	0.98763	0.35781	0.055	0.859	0.913	7.993
0.07	0.3788	0.93	0.6212	0.82073	0.98574	0.36118	0.064	0.846	0.909	8.101
0.08	0.4165	0.92	0.5835	0.82532	0.9837	0.36459	0.072	0.832	0.905	8.209
0.09	0.4513	0.91	0.5487	0.82991	0.98152	0.36804	0.081	0.82	0.901	8.318
0.1	0.4836	0.9	0.5164	0.83449	0.97918	0.37152	0.09	0.807	0.896	8.428
0.2	0.7057	0.8	0.2943	0.87893	0.94735	0.40822	0.171	0.683	0.854	9.591
0.3	0.824	0.7	0.176	0.91916	0.9002	0.44777	0.244	0.57	0.815	10.93
0.4	0.893	0.6	0.107	0.953	0.83887	0.48959	0.312	0.468	0.78	12.52
0.5	0.9353	0.5	0.0647	0.97869	0.76553	0.53325	0.375	0.375	0.751	14.45
0.6	0.962	0.4	0.038	0.99477	0.68299	0.57838	0.436	0.291	0.727	16.86
0.7	0.9789	0.3	0.0211	0.99998	0.59438	0.6247	0.496	0.213	0.709	19.9
0.8	0.9896	0.2	0.0104	0.99314	0.50283	0.67202	0.557	0.139	0.697	23.85
0.9	0.9962	0.1	0.0038	0.97296	0.41127	0.72027	0.622	0.069	0.691	29.13
1	1	0	0	—	—	—	0.693	0	0.693	——

N2 - CH4 / Turkish clinoptilolite at 22.6-22.8°C and 101.3 kPa total pressure

Flory-Huggins Vacancy Solution Theory Binary Prediction

Binary Parameter: a12 = 2.0352313

x1 (N2)	y1 (N2)	x2 (CH4)	y2 (CH4)	gamma1	gamma2	gammav	n1 [mol/kg]	n2 [mol/kg]	nt [mol/kg]	alpha12 N2/CH4
0	0	1	1	------	------	------	0	0.814	0.814	------
0.1	0.0556	0.9	0.9444	0.3847126	0.999891	0.6599056	0.079	0.714	0.793	0.53
0.2	0.1529	0.8	0.8471	0.5004276	0.9924613	0.5997398	0.154	0.618	0.772	0.722
0.3	0.2822	0.7	0.7178	0.6004281	0.9726312	0.5502398	0.225	0.524	0.749	0.918
0.4	0.4252	0.6	0.5748	0.6828347	0.9474885	0.5096418	0.289	0.434	0.723	1.11
0.5	0.5646	0.5	0.4354	0.7492096	0.9208347	0.4761044	0.348	0.348	0.696	1.297
0.6	0.6894	0.4	0.3106	0.8023306	0.8944641	0.4479955	0.401	0.267	0.668	1.48
0.7	0.795	0.3	0.205	0.8449835	0.8690656	0.4239881	0.448	0.192	0.64	1.662
0.8	0.8808	0.2	0.1192	0.8795089	0.8447641	0.4030446	0.491	0.123	0.613	1.846
0.9	0.9483	0.1	0.0517	0.9077188	0.8214146	0.3843645	0.529	0.048	0.588	2.037
1	1	0	0	------	------	------	0.565	0	0.565	------

N2 - CH4 / Turkish clinoptilolite at 40.0°C and 101.3 kPa total pressure

Flory-Huggins Vacancy Solution Theory Binary Prediction

Binary Parameter: a12 = 1.4441874

x1 (N2)	y1 (N2)	x2 (CH4)	y2 (CH4)	gamma1	gamma2	gammav	n1 [mol/kg	n2 [mol/kg	nt [mol/kg	alpha21 CH4/N2
0	0	1	1	------	------	------	0	0.693	0.693	------
0.1	0.0458	0.9	0.9542	0.3949409	0.9746009	0.7172994	0.068	0.608	0.675	0.432
0.2	0.1247	0.8	0.8753	0.4871647	0.9941064	0.6684189	0.132	0.527	0.659	0.57
0.3	0.2384	0.7	0.7616	0.573248	0.9999915	0.6240506	0.192	0.449	0.641	0.731
0.4	0.3786	0.6	0.6214	0.6493181	0.9961954	0.5848485	0.248	0.372	0.62	0.914
0.5	0.5288	0.5	0.4712	0.7141005	0.9861901	0.5507186	0.298	0.298	0.596	1.122
0.6	0.6712	0.4	0.3288	0.7683757	0.9724698	0.5209778	0.341	0.227	0.569	1.361
0.7	0.793	0.3	0.207	0.8139423	0.9564748	0.4946414	0.378	0.162	0.54	1.642
0.8	0.8882	0.2	0.1118	0.852793	0.9387793	0.4706428	0.409	0.102	0.512	1.985
0.9	0.9561	0.1	0.0439	0.8866557	0.9193211	0.4479453	0.436	0.048	0.485	2.421
1	1	0	0	------	------	------	0.46	0	0.46	------

N2 - CO / Cuban clinoptilolite at 40.0–40.1°C and 101.3 kPa total pressure

Flory-Huggins Vacancy Solution Theory Binary Prediction

Binary Parameter: a12 = 0.1261

x1 (N2)	y1 (N2)	x2 (CO)	y2 (CO)	gamma1	gamma2	gammav	n1 [mol/kg]	n2 [mol/kg]	nt [mol/kg]	alpha21 CO/N2
0	0	1	1	------	------	------	0	0.567	0.567	------
0.1	0.099	0.9	0.901	0.8711551	0.9275981	0.7685715	0.06	0.538	0.597	0.989
0.2	0.2647	0.8	0.7353	0.8442095	0.9068882	0.78901	0.122	0.488	0.61	1.44
0.3	0.4545	0.7	0.5455	0.8097262	0.8793908	0.8125449	0.181	0.422	0.603	1.944
0.4	0.6198	0.6	0.3802	0.7697292	0.8463278	0.8370308	0.233	0.349	0.582	2.446
0.5	0.7454	0.5	0.2546	0.7282002	0.8108673	0.8599428	0.277	0.277	0.555	2.928
0.6	0.8352	0.4	0.1648	0.6884265	0.7759473	0.8799164	0.316	0.211	0.527	3.378
0.7	0.8984	0.3	0.1016	0.6521615	0.7433544	0.8966773	0.35	0.15	0.501	3.79
0.8	0.9434	0.2	0.0566	0.6199712	0.7138512	0.9105076	0.382	0.095	0.477	4.167
0.9	0.9759	0.1	0.0241	0.5917663	0.6875708	0.9218673	0.411	0.046	0.457	4.509
1	1	0	0	------	------	------	0.439	0	0.439	----

CH4 - CO / Cuban clinoptilolite at 39.9-40.1°C and 101.3 kPa total pressure

Flory-Huggins Vacancy Solution Theory Binary Prediction

Binary Parameter: a12 = 0.3099

x1 (CH4)	y1 (CH4)	x2 (CO)	y2 (CO)	gamma1	gamma2	gammav	n1 [mol/kg]	n2 [mol/kg]	nt [mol/kg]	alpha21 CO/CH4
0	0	1	1	———	———	———	0	0.567	0.567	———
0.1	0.0189	0.9	0.9811	0.7672786	0.9212799	0.7751129	0.065	0.588	0.653	0.173
0.2	0.1076	0.8	0.8924	0.7428984	0.906125	0.7897126	0.147	0.588	0.735	0.482
0.3	0.2875	0.7	0.7125	0.7126595	0.8863194	0.8069298	0.235	0.549	0.784	0.942
0.4	0.5017	0.6	0.4983	0.6699611	0.8565834	0.8298033	0.316	0.474	0.789	1.51
0.5	0.68	0.5	0.32	0.6202459	0.8195041	0.8546311	0.382	0.382	0.763	2.125
0.6	0.8039	0.4	0.1961	0.5716692	0.7808146	0.8772659	0.435	0.29	0.726	2.733
0.7	0.8852	0.3	0.1148	0.52866	0.7445462	0.8960931	0.482	0.206	0.688	3.303
0.8	0.9387	0.2	0.0613	0.4922395	0.712332	0.911188	0.523	0.131	0.654	3.827
0.9	0.9748	0.1	0.0252	0.4618764	0.6843921	0.9231837	0.562	0.062	0.624	4.302
1	1	0	0	———	———	———	0.599	0	0.599	———

N2 - CH4 / Cuban clinoptilolite at 39.9-40.0°C and 101.3 kPa total pressure

Flory-Huggins Vacancy Solution Theory Binary Prediction

Binary Parameter: a12 = -0.1403

x1 (N2)	y1 (N2)	x2 (CH4	y2 (CH4)	gamma1	gamma2	gammav	n1 [mol/kg]	n2 [mol/kg]	nt [mol/kg]	alpha21 CH4/N2
0	0	1	1	——	——	——	0	0.599	0.599	——
0.1	0.141	0.9	0.859	0.5626467	0.4362569	0.9328819	0.058	0.526	0.584	1.478
0.2	0.275	0.8	0.725	0.5622508	0.4358663	0.9330267	0.114	0.455	0.569	1.517
0.3	0.4009	0.7	0.5991	0.5618532	0.435474	0.9331721	0.166	0.387	0.553	1.562
0.4	0.518	0.6	0.482	0.561514	0.4361393	0.9332959	0.215	0.322	0.537	1.612
0.5	0.6254	0.5	0.3746	0.5613112	0.4349393	0.93337	0.26	0.26	0.521	1.669
0.6	0.7225	0.4	0.2775	0.5613457	0.4349734	0.9333574	0.303	0.202	0.504	1.735
0.7	0.8088	0.3	0.1912	0.5617484	0.4353706	0.9332103	0.341	0.146	0.488	1.812
0.8	0.8839	0.2	0.1161	0.5626901	0.4362997	0.932866	0.377	0.094	0.471	1.903
0.9	0.9477	0.1	0.0523	0.5643964	0.437985	0.9322402	0.409	0.045	0.455	2.012
1	1	0	0	——	——	——	0.439	0	0.439	——

N2 - CO / AlPO4-11 at 22.6-22.8°C and 101.3 kPa total pressure

Flory-Huggins Vacancy Solution Theory Binary Prediction

Binary Parameter: a12 = 0

x1 (N2)	y1 (N2)	x2 (CO)	y2 (CO)	gamma1	gamma2	gammav	n1 [mol/kg]	n2 [mol/kg]	nt [mol/kg]	alpha21 CO/N2
0	0	1	1	—	—	—	0	0.1889	0.1889	——
0.1	0.1148	0.9	0.8852	1	1	1	0.0186	0.1671	0.1857	1.168
0.2	0.2442	0.8	0.7558	1	1	1	0.0361	0.1443	0.1804	1.292
0.3	0.3851	0.7	0.6149	1	1	1	0.0518	0.1208	0.1726	1.461
0.4	0.5316	0.6	0.4684	1	1	1	0.0648	0.0972	0.162	1.702
0.5	0.6738	0.5	0.3262	1	1	1	0.0742	0.0742	0.1484	2.066
0.6	0.7998	0.4	0.2002	1	1	1	0.0793	0.0529	0.1322	2.664
0.7	0.8982	0.3	0.1018	1	1	1	0.0799	0.0343	0.1142	3.782
0.8	0.9622	0.2	0.0378	1	1	1	0.0766	0.0192	0.0958	6.356
0.9	0.9927	0.1	0.0073	1	1	1	0.0708	0.0079	0.0786	15.01
0.99	0.9998	0.01	0.0002	1	1	1	0.0659	0.0007	0.0665	66.4
1	1	0	0	—	—	—	0.0646	0	0.0646	——

N2 - CO / AlPO4-11 at 40.0°C and 101.3 kPa total pressure

Flory-Huggins Vacancy Solution Theory Binary Prediction

Binary Parameter: a12 = 0

x1 (N2)	y1 (N2)	x2 (CO)	y2 (CO)	gamma1	gamma2	gammav	n1 [mol/kg 5	n2 [mol/kg 5	nt [mol/kg 5	alpha21 CO/N2
0	0	1	1	—	—	—	0	0.141	0.141	——
0.1	0.0852	0.9	0.9148	1	1	1	0.0143	0.1291	0.1434	0.838
0.2	0.1897	0.8	0.8103	1	1	1	0.0289	0.1158	0.1447	0.937
0.3	0.3155	0.7	0.6845	1	1	1	0.0432	0.1009	0.1441	1.076
0.4	0.4611	0.6	0.5389	1	1	1	0.0561	0.0842	0.1404	1.283
0.5	0.6181	0.5	0.3819	1	1	1	0.0662	0.0662	0.1324	1.618
0.6	0.7694	0.4	0.2306	1	1	1	0.0716	0.0477	0.1193	2.224
0.7	0.8918	0.3	0.1082	1	1	1	0.0711	0.0305	0.1016	3.531
0.8	0.9673	0.2	0.0327	1	1	1	0.065	0.0162	0.0812	7.394
0.9	0.9963	0.1	0.0037	1	1	1	0.0555	0.0062	0.0616	29.56
0.99	1	0.01	2E-05	1	1	1	0.0481	0.0005	0.0486	600.2
1	1	0	0	—	—	—	0.0478	0	0.0478	——

CH4 - CO / AlPO4-11 at 22.6-22.8°C and 101.3 kPa total pressure

Flory-Huggins Vacancy Solution Theory Binary Prediction

Binary Parameter: a12 = 0

x1 (CH4)	y1 (CH4)	x2 (CO)	y2 (CO)	gamma1	gamma2	gammav	n1 [mol/kg]	n2 [mol/kg]	nt [mol/kg]	alpha21 CO/CH4
0	0	1	1	—	—	—	0	0.1889	0.1889	——
0.1	0.0427	0.9	0.9573	1	1	1	0.0201	0.1808	0.2009	2.489
0.2	0.0961	0.8	0.9039	1	1	1	0.0428	0.1714	0.2142	2.35
0.3	0.1608	0.7	0.8392	1	1	1	0.0697	0.1603	0.229	2.237
0.4	0.2373	0.6	0.7627	1	1	1	0.098	0.147	0.245	2.142
0.5	0.3265	0.5	0.6735	1	1	1	0.1312	0.1312	0.2624	2.063
0.6	0.4292	0.4	0.5708	1	1	1	0.1687	0.1125	0.2812	1.995
0.7	0.5466	0.3	0.4534	1	1	1	0.211	0.0904	0.3015	1.936
0.8	0.6797	0.2	0.3203	1	1	1	0.2587	0.0647	0.3234	1.885
0.9	0.8303	0.1	0.1697	1	1	1	0.3122	0.0347	0.3469	1.84
0.99	0.9821	0.01	0.0179	1	1	1	0.366	0.0037	0.3697	1.804
1	1	0	0	—	—	—	0.3723	0	0.3723	——

CH4 - CO / AlPO4-11 at 40.0°C and 101.3 kPa total pressure

Flory-Huggins Vacancy Solution Theory Binary Prediction

Binary Parameter: a12 = 0

x1 (CH4)	y1 (CH4)	x2 (CO)	y2 (CO)	gamma1	gamma2	gammav	n1 [mol/kg]	n2 [mol/kg]	nt [mol/kg]	alpha21 CO/CH4
0	0	1	1	—	—	—	0	0.141	0.141	——
0.1	0.0499	0.9	0.9501	1	1	1	0.0148	0.1335	0.1484	2.114
0.2	0.1058	0.8	0.8942	1	1	1	0.0313	0.1253	0.1566	2.114
0.3	0.1686	0.7	0.8314	1	1	1	0.0497	0.116	0.1657	2.113
0.4	0.2398	0.6	0.7602	1	1	1	0.0704	0.1056	0.176	2.113
0.5	0.3213	0.5	0.6787	1	1	1	0.0938	0.0938	0.1876	2.113
0.6	0.4152	0.4	0.5848	1	1	1	0.1206	0.0804	0.2009	2.112
0.7	0.5249	0.3	0.4751	1	1	1	0.1514	0.0649	0.2162	2.112
0.8	0.6545	0.2	0.3455	1	1	1	0.1873	0.0468	0.2341	2.112
0.9	0.81	0.1	0.19	1	1	1	0.2296	0.0255	0.2551	2.111
0.99	0.9791	0.01	0.0209	1	1	1	0.2747	0.0028	0.2775	2.111
1	1	0	0	—	—	—	0.2802	0	0.2802	——

N2 - CH4 / AlPO4-11 at 22.6-22.8°C and 101.3 kPa total pressure

Flory-Huggins Vacancy Solution Theory Binary Prediction

Binary Parameter: a12 = 0

x1 (N2)	y1 (N2)	x2 (CH4)	y2 (CH4)	gamma1	gamma2	gammav	n1 [mol/kg]	n2 [mol/kg]	nt [mol/kg]	alpha12 N2/CH4
0	0	1	1	----	----	----	0	0.3723	0.3723	----
0.1	0.1382	0.9	0.8618	1	1	1	0.0358	0.3219	0.3577	1.444
0.2	0.2902	0.8	0.7098	1	1	1	0.0676	0.2703	0.3379	1.635
0.3	0.4499	0.7	0.5501	1	1	1	0.0937	0.2186	0.3123	1.908
0.4	0.6074	0.6	0.3926	1	1	1	0.1124	0.1685	0.2809	2.321
0.5	0.7501	0.5	0.2499	1	1	1	0.1222	0.1222	0.2444	3.002
0.6	0.8652	0.4	0.1348	1	1	1	0.1227	0.0818	0.2045	4.279
0.7	0.9441	0.3	0.0559	1	1	1	0.1145	0.0491	0.1636	7.234
0.8	0.9857	0.2	0.0143	1	1	1	0.0996	0.0249	0.1244	17.2
0.9	0.9988	0.1	0.0012	1	1	1	0.0811	0.009	0.0901	96.24
0.99	1	0.01	1E-06	1	1	1	0.0665	0.0007	0.0672	6779
1	1	0	0	----	----	----	0.0646	0	0.0646	----

N2 - CH4 / AlPO4-11 at 40.0°C and 101.3 kPa total pressure

Flory-Huggins Vacancy Solution Theory Binary Prediction

Binary Parameter: a12 = 0

x1 (N2)	y1 (N2)	x2 (CH4)	y2 (CH4)	gamma1	gamma2	gammav	n1 [mol/kg 5	n2 [mol/kg 5	nt [mol/kg 5	alpha21 CH4/N2
0	0	1	1	----	----	----	0	0.2802	0.2802	----
0.1	0.1715	0.9	0.8285	1	1	1	0.026	0.2341	0.2601	1.863
0.2	0.3421	0.8	0.6579	1	1	1	0.0475	0.1899	0.2374	2.08
0.3	0.5052	0.7	0.4948	1	1	1	0.0638	0.1488	0.2126	2.382
0.4	0.6535	0.6	0.3465	1	1	1	0.0744	0.1117	0.1861	2.829
0.5	0.7798	0.5	0.2202	1	1	1	0.0794	0.0794	0.1588	3.542
0.6	0.8785	0.4	0.1215	1	1	1	0.0789	0.0526	0.1315	4.82
0.7	0.9436	0.3	0.0564	1	1	1	0.0738	0.0316	0.1054	7.174
0.8	0.9842	0.2	0.0158	1	1	1	0.0652	0.0163	0.0816	15.52
0.9	0.9981	0.1	0.0019	1	1	1	0.0552	0.0061	0.0614	59.62
0.99	1	0.01	9E-06	1	1	1	0.0481	0.0005	0.0486	1065
1	1	0	0	----	----	----	0.0461	0	0.0461	----

N2 - CO / AlPO4-17 at 39.6-40.0°C and 101.3 kPa total pressure

Flory-Huggins Vacancy Solution Theory Binary Prediction

Binary Parameter: a12 = 5.0E-05

x1 (N2)	y1 (N2)	x2 (CO)	y2 (CO)	gamma1	gamma2	gammav	n1 [mol/kg]	n2 [mol/kg]	nt [mol/kg]	alpha21 CO/N2
0	0	1	1	——	——	——	0	0.128	0.128	——
0.1	0.0798	0.9	0.9202	1	1	1	0.0132	0.1187	0.1319	1.282
0.2	0.1736	0.8	0.8264	1	1	1	0.0271	0.1082	0.1353	1.19
0.3	0.2772	0.7	0.7228	1	1	1	0.0414	0.0965	0.1379	1.117
0.4	0.3866	0.6	0.6134	1	1	1	0.0559	0.0838	0.1397	1.058
0.5	0.4979	0.5	0.5021	1	1	1	0.0704	0.0704	0.1409	1.008
0.6	0.6081	0.4	0.3919	1	1	1	0.0848	0.0565	0.1413	0.967
0.7	0.7147	0.3	0.2853	1	1	1	0.0988	0.0424	0.1412	0.931
0.8	0.8162	0.2	0.1838	1	1	1	0.1125	0.0281	0.1406	0.901
0.9	0.9114	0.1	0.0886	1	1	1	0.1256	0.014	0.1396	0.874
0.999	0.9991	0.001	0.0009	1	1	1	0.1381	0.0001	0.1382	0.852
1	1	0	0	——	——	——	0.1382	0	0.1382	——

CH4 - CO / AlPO4-17 at 40.0°C and 101.3 kPa total pressure

Flory-Huggins Vacancy Solution Theory Binary Prediction

Binary Parameter: a12 = 4.6E-05

x1 (CH4)	y1 (CH4)	x2 (CO)	y2 (CO)	gamma1	gamma2	gammav	n1 [mol/kg]	n2 [mol/kg]	nt [mol/kg]	alpha21 CO/CH4
0	0	1	1	——	——	——	0	0.128	0.128	——
0.001	8.3E-06	0.999	1	1	1	1	0.0001	0.128	0.1282	121
0.1	0.0068	0.9	0.9932	1	1	1	0.0155	0.1396	0.1551	16.17
0.2	0.0388	0.8	0.9612	1	1	1	0.0384	0.1537	0.1921	6.194
0.3	0.1083	0.7	0.8917	1	1	1	0.0694	0.162	0.2315	3.528
0.4	0.2152	0.6	0.7848	1	1	1	0.1073	0.161	0.2683	2.431
0.5	0.3492	0.5	0.6508	1	1	1	0.1497	0.1497	0.2995	1.864
0.6	0.4956	0.4	0.5044	1	1	1	0.194	0.1293	0.3234	1.527
0.7	0.641	0.3	0.359	1	1	1	0.2379	0.102	0.3399	1.307
0.8	0.776	0.2	0.224	1	1	1	0.28	0.07	0.3501	1.154
0.9	0.8961	0.1	0.1039	1	1	1	0.3197	0.0355	0.3552	1.043
0.999	0.999	0.001	0.001	1	1	1	0.3563	0.0004	0.3566	0.96
1	1	0	0	——	——	——	0.3566	0	0.3566	——

N2 - CH4 / AlPO4-17 at 39.6-40.0°C and 101.3 kPa total pressure

Flory-Huggins Vacancy Solution Theory Binary Prediction

Binary Parameter: a12 = 4.5E-06

x1 (N2)	y1 (N2)	x2 (CH4	y2 (CH4)	gamma1	gamma2	gammav	n1 [mol/kg]	n2 [mol/kg]	nt [mol/kg]	alpha21 CH4/N2
0	0	1	1	——	——	——	0	0.3566	0.3566	——
0.1	0.1578	0.9	0.8422	1	1	1	0.0335	0.3019	0.3354	1.686
0.2	0.3098	0.8	0.6902	1	1	1	0.0626	0.2505	0.3131	1.796
0.3	0.4531	0.7	0.5469	1	1	1	0.0869	0.2029	0.2898	1.933
0.4	0.5846	0.6	0.4154	1	1	1	0.1064	0.1595	0.2659	2.111
0.5	0.7013	0.5	0.2987	1	1	1	0.1209	0.1209	0.2417	2.348
0.6	0.8007	0.4	0.1993	1	1	1	0.1307	0.0871	0.2178	2.679
0.7	0.8808	0.3	0.1192	1	1	1	0.1363	0.0584	0.1946	3.168
0.8	0.9405	0.2	0.0595	1	1	1	0.1384	0.0346	0.1729	3.951
0.9	0.9797	0.1	0.0203	1	1	1	0.1383	0.0154	0.1536	5.358
0.999	0.9999	0.001	0.0001	1	1	1	0.1382	0.0001	0.1383	8.345
1	1	0	0	——	——	——	0.1382	0	0.1382	——

N2 - CO / AlPO4-18 at 40.1°C and 101.3 kPa total pressure

Flory-Huggins Vacancy Solution Theory Binary Prediction

Binary Parameter: a12 = 0

x1 (N2)	y1 (N2)	x2 (CO)	y2 (CO)	gamma1	gamma2	gammav	n1 [mol/kg]	n2 [mol/kg]	nt [mol/kg]	alpha21 CO/N2
0	0	1	1	———	———	———	0	0.2189	0.2189	———
0.1	8.3E-05	0.9	0.9999	1	1	1	0.0274	0.2467	0.2741	0.001
0.15	5.9E-03	0.85	0.9941	1	1	1	0.0583	0.3304	0.3887	0.034
0.2	0.0643	0.8	0.9357	1	1	1	0.0997	0.3989	0.4986	0.275
0.22	0.1278	0.78	0.8722	1	1	1	0.1177	0.4173	0.535	0.519
0.24	0.2276	0.76	0.7724	1	1	1	0.1344	0.4256	0.56	0.933
0.26	0.3651	0.74	0.6349	1	1	1	0.1472	0.4188	0.566	1.637
0.28	0.5225	0.72	0.4775	1	1	1	0.1527	0.3927	0.5453	2.814
0.3	0.6632	0.7	0.3368	1	1	1	0.15	0.3499	0.4999	4.595
0.35	0.8552	0.65	0.1448	1	1	1	0.1287	0.2391	0.3678	10.97
0.4	0.9242	0.6	0.0758	1	1	1	0.1106	0.1659	0.2764	18.29
0.5	0.9708	0.5	0.0292	1	1	1	0.09	0.09	0.18	33.2
0.6	0.9861	0.4	0.0139	1	1	1	0.08	0.0534	0.1334	47.41
0.7	0.993	0.3	0.007	1	1	1	0.075	0.0321	0.1071	60.53
0.8	0.9966	0.2	0.0034	1	1	1	0.0725	0.0181	0.0906	72.45
0.9	0.9987	0.1	0.0013	1	1	1	0.0715	0.0079	0.0794	83.22
0.99	0.9999	0.01	0.0001	1	1	1	0.0714	0.0007	0.0721	91.99
1	1	0	0	———	———	———	0.0714	0	0.0714	———

CH4 - CO / AlPO4-18 at 40.0-40.1°C and 101.3 kPa total pressure

Flory-Huggins Vacancy Solution Theory Binary Prediction

Binary Parameter: a12 = 0

x1 (CH4)	y1 (CH4)	x2 (CO)	y2 (CO)	gamma1	gamma2	gammav	n1 [mol/kg]	n2 [mol/kg]	nt [mol/kg]	alpha21 CO/CH4
0	0	1	1	——	——	——	0	0.2189	0.2189	——
0.1	4.9E-05	0.9	1	1	1	1	0.0186	0.1673	0.1858	0.000
0.2	0.0195	0.8	0.9805	1	1	1	0.0647	0.2587	0.3234	0.079
0.25	0.082	0.75	0.918	1	1	1	0.0973	0.292	0.3894	0.268
0.3	0.2234	0.7	0.7766	1	1	1	0.1324	0.3089	0.4414	0.671
0.32	0.3036	0.68	0.6964	1	1	1	0.1455	0.3091	0.4546	0.926
0.34	0.3924	0.66	0.6076	1	1	1	0.157	0.3047	0.4617	1.254
0.36	0.4836	0.64	0.5164	1	1	1	0.1663	0.2957	0.4621	1.665
0.38	0.5701	0.62	0.4299	1	1	1	0.1733	0.2827	0.4559	2.164
0.4	0.6466	0.6	0.3534	1	1	1	0.1778	0.2666	0.4444	2.745
0.45	0.7845	0.55	0.2155	1	1	1	0.1814	0.2217	0.4031	4.45
0.5	0.8632	0.5	0.1368	1	1	1	0.1799	0.1799	0.3697	6.311
0.6	0.9373	0.4	0.0627	1	1	1	0.1746	0.1164	0.2911	9.974
0.7	0.9688	0.3	0.0312	1	1	1	0.1714	0.0735	0.2449	13.31
0.8	0.9849	0.2	0.0151	1	1	1	0.1705	0.0426	0.2132	16.29
0.9	0.9942	0.1	0.0058	1	1	1	0.1714	0.019	0.1904	18.94
0.99	0.9995	0.01	0.0005	1	1	1	0.1732	0.0017	0.175	21.08
1	1	0	0	——	——	——	0.1735	0	0.1735	——

N2 - CH4 / AlPO4-18 at 40.0-40.1°C and 101.3 kPa total pressure

Flory-Huggins Vacancy Solution Theory Binary Prediction

Binary Parameter: a12 = 0

x1 (N2)	y1 (N2)	x2 (CH4	y2 (CH4)	gamma1	gamma2	gammav	n1 [mol/kg]	n2 [mol/kg]	nt [mol/kg]	alpha21 CH4/N2
0	0	1	1	——	——	——	0	0.1735	0.1735	——
0.1	0.1997	0.9	0.8003	1	1	1	0.0156	0.1405	0.1561	2.246
0.2	0.3692	0.8	0.6308	1	1	1	0.0281	0.1123	0.1404	2.341
0.3	0.5098	0.7	0.4902	1	1	1	0.038	0.0886	0.1266	2.427
0.4	0.6255	0.6	0.3745	1	1	1	0.0459	0.0688	0.1147	2.505
0.5	0.7205	0.5	0.2795	1	1	1	0.0523	0.0523	0.1045	2.577
0.6	0.7986	0.4	0.2014	1	1	1	0.0575	0.0383	0.0958	2.644
0.7	0.8632	0.3	0.1368	1	1	1	0.0618	0.0265	0.0883	2.705
0.8	0.917	0.2	0.083	1	1	1	0.0655	0.0164	0.0818	2.762
0.9	0.962	0.1	0.038	1	1	1	0.0686	0.0076	0.0762	2.815
0.99	0.9965	0.01	0.0035	1	1	1	0.0711	0.0007	0.0718	2.859
1	1	0	0	——	——	——	0.0714	0	0.0714	——

Extended Langmuir Model for N2-CO / 5A at 22.6-22.7°C and 101325 Pa total pressure

Averaging approach

y1 (N2)	P1 (N2) [Pa]	P2 (CO) [Pa]	x1 (N2)	x2 (CO)	vm [m3 STP/kg]	v1 (N2) [m3 STP/kg]	v2 (CO) [m3 STP/kg]	vt [m3 STP/kg]	n1 (N2) [mol/kg]	n2 (CO) [mol/kg]	nt [mol/kg]	alpha21 CO/N2
0	0	101325	0	1	0.0306466	0	0.0183944	0.0183944	0	0.8207	0.8207	.....
0.2822	28590.450	72734.550	0.0767	0.9233	0.0310253	0.0012821	0.0154277	0.0167098	0.0572	0.6883	0.7455	4.73
0.472	47825.244	53499.756	0.159	0.8410	0.0314416	0.0024249	0.0128306	0.0152555	0.1082	0.5725	0.6807	4.73
0.6071	61514.307	39810.693	0.2462	0.7538	0.031896	0.003448	0.0105547	0.0140026	0.1538	0.4709	0.6248	4.73
0.7076	71696.908	29628.092	0.3385	0.6615	0.0323905	0.0043729	0.0085473	0.0129202	0.1951	0.3814	0.5765	4.73
0.785	79537.094	21787.906	0.4356	0.5644	0.0329283	0.005219	0.0067622	0.0119812	0.2329	0.3017	0.5346	4.73
0.8462	85742.655	15582.345	0.5378	0.4622	0.0335134	0.006003	0.0051602	0.0111632	0.2678	0.2302	0.4981	4.73
0.8962	90811.431	10513.569	0.6462	0.3538	0.0341575	0.0067466	0.0036945	0.0104411	0.301	0.1648	0.4659	4.73
0.9367	94908.846	6416.154	0.7577	0.2423	0.0348467	0.0074406	0.0023792	0.0098198	0.332	0.1062	0.4381	4.73
0.9709	98379.163	2945.837	0.8759	0.1241	0.0356081	0.0081176	0.0011497	0.0092673	0.3622	0.0513	0.4135	4.73
1	101325	0	1	0	0.0364437	0.0087804	0	0.0087804	0.3918	0	0.3918	.....

Direct approach

y1 (N2)	P1 (N2) [Pa]	P2 (CO) [Pa]	x1 (N2)	x2 (CO)	v1 (N2) [m3 STP/kg]	v2 (CO) [m3 STP/kg]	vt [m3 STP/kg]	n1 (N2) [mol/kg]	n2 (CO) [mol/kg]	nt [mol/kg]	alpha21 CO/N2
0	0	101325	0	1	0	0.0183944	0.0183944	0	0.8207	0.8207	.....
0.2822	28590.45	72734.55	0.0899	0.9101	0.001506	0.0152394	0.0167454	0.0671947	0.6799	0.7471	3.98
0.472	47825.244	53499.756	0.1835	0.8165	0.0028107	0.0125062	0.0153169	0.1254058	0.558	0.6834	3.98
0.6071	61514.307	39810.693	0.2798	0.7202	0.0039396	0.0101412	0.0140808	0.175774	0.4525	0.6283	3.98
0.7076	71696.908	29628.092	0.3783	0.6217	0.0049201	0.0080871	0.0130072	0.2195221	0.3608	0.5803	3.98
0.785	79537.094	21787.906	0.4786	0.5214	0.0057762	0.0062937	0.0120699	0.2577187	0.2808	0.5385	3.98
0.8462	85742.655	15582.345	0.5804	0.4196	0.0065279	0.0047188	0.0112467	0.2912605	0.2105	0.5018	3.98
0.8962	90811.431	10513.569	0.6847	0.3153	0.0071982	0.0033147	0.0105129	0.3211637	0.1479	0.4691	3.98
0.9367	94908.846	6416.1543	0.7881	0.2119	0.0077816	0.0020925	0.0098741	0.3471957	0.0934	0.4406	3.98
0.9709	98379.163	2945.8369	0.8936	0.1064	0.0083081	0.0009895	0.0092976	0.3706857	0.0441	0.4148	3.98
1	101325	0	1	0	0.0087804	0	0.0087804	0.3917604	0	0.3918	.....

Extended Langmuir Model for N2-CO / 5A at 39.8-40.0°C and 101325 Pa total pressure

Averaging approach

y1 (N2)	P1 (N2) [Pa]	P2 (CO) [Pa]	x1 (N2)	x2 (CO)	vm [m3 STP/kg]	v1 (N2) [m3 STP/kg]	v2 (CO) [m3 STP/kg]	vt [m3 STP/kg]	n1 (N2) [mol/kg]	n2 (CO) [mol/kg]	nt [mol/kg]	alpha21 CO/N2
0	0	101325	0	1	0.0277055	0	0.0133604	0.0133604	0	0.5961	0.5961	-------
0.3711	37601.698	63723.302	0.0281	0.9719	0.0282232	0.0002984	0.0103147	0.0106131	0.0133	0.4602	0.4735	20.39
0.5890	59676.103	41648.897	0.0656	0.9344	0.0289449	0.0005522	0.0078603	0.0084125	0.0246	0.3507	0.3753	20.39
0.7232	73280.835	28044.165	0.1136	0.8864	0.0299222	0.0007656	0.0059755	0.0067411	0.0342	0.2666	0.3008	20.39
0.8104	82111.071	19213.929	0.1732	0.8268	0.0312351	0.0009525	0.0045454	0.0054979	0.0425	0.2028	0.2453	20.39
0.8697	88127.325	13197.675	0.2467	0.7533	0.0330176	0.0011295	0.0034498	0.0045793	0.0504	0.1539	0.2043	20.39
0.9120	92405.036	8919.964	0.3369	0.6631	0.0355068	0.001316	0.0025909	0.0039069	0.0587	0.1156	0.1743	20.39
0.9431	95559.520	5765.480	0.4483	0.5517	0.0391559	0.0015386	0.0018932	0.0034318	0.0686	0.0845	0.1531	20.39
0.9668	97958.493	3366.507	0.5879	0.4121	0.0449386	0.0018455	0.0012934	0.0031389	0.0823	0.0577	0.1401	20.39
0.9853	99830.959	1494.041	0.7662	0.2338	0.0553812	0.0023536	0.0007184	0.0030719	0.105	0.0321	0.1371	20.39
1	101325	0	1	0	0.0796721	0.0034795	0	0.0034795	0.1552	0	0.1552	-------

Direct approach

y1(N2)	P1 (N2) [Pa]	P2 (CO) [Pa]	x1 (N2)	x2 (CO)	v1 (N2) [m3 STP/kg]	v2 (CO) [m3 STP/kg]	vt [m3 STP/kg]	n1(N2) [mol/kg]	n2 (CO) [mol/kg]	nt [mol/kg]	alpha21 (CO/N2)
0	0	101325	0	1	0	0.0133604	0.0133604	0	0.5961	0.5961	-------
0.3711	37601.698	63723.30	0.0768	0.9232	0.0008425	0.0101255	0.010968	0.0375892	0.4518	0.4894	7.09
0.5890	59676.103	41648.90	0.1681	0.8319	0.0015201	0.0075237	0.0090438	0.0678215	0.3357	0.4035	7.09
0.7232	73280.835	28044.17	0.2692	0.7308	0.0020386	0.0055328	0.0075714	0.0909559	0.2469	0.3378	7.09
0.8104	82111.071	19213.93	0.376	0.6240	0.0024295	0.0040318	0.0064613	0.1083978	0.1799	0.2883	7.09
0.8697	88127.325	13197.68	0.4849	0.5151	0.0027256	0.0028948	0.0056204	0.1216096	0.1292	0.2508	7.09
0.9120	92405.036	8919.964	0.5936	0.4064	0.002953	0.0020216	0.0049746	0.1317558	0.0902	0.222	7.09
0.9431	95559.52	5765.480	0.7003	0.2997	0.0031306	0.0013396	0.0044702	0.1396813	0.0598	0.1994	7.09
0.9668	97958.493	3366.507	0.804	0.1960	0.0032718	0.0007974	0.0040693	0.1459808	0.0356	0.1816	7.09
0.9853	99830.959	1494.041	0.904	0.0960	0.0033859	0.0003594	0.0037453	0.1510711	0.016	0.1671	7.09
1	101325	0	1	0.0000	0.0034795	0	0.0034795	0.1552469	0	0.1552	-------

Extended Langmuir Model for CH4-CO / 5A at 22.6-22.8°C and 101325 Pa total pressure

Averaging approach

y1 (CH4)	P1 (CH4) [Pa]	P2 (CO) [Pa]	x1 (CH4)	x2 (CO)	vm [m3 STP/kg]	v1 (CH4) [m3 STP/kg]	v2 (CO) [m3 STP/kg]	vt [m3 STP/kg]	n1 (CH4) [mol/kg]	n2 (CO) [mol/kg]	nt [mol/kg]	alpha21 CO/CH4
0	0	101325	0	1	0.0306466	0	0.0183944	0.0183944	0	0.8207	0.8207	-------
0.1332	13492.615	87832.385	0.0398	0.9602	0.0304688	0.0006978	0.0168349	0.0175327	0.0311	0.7511	0.7823	3.71
0.3731	37800.512	63524.488	0.1383	0.8617	0.0300372	0.0021695	0.013512	0.0156815	0.0968	0.6029	0.6997	3.71
0.592	59985.653	41339.347	0.2814	0.7186	0.0294322	0.0038105	0.0097324	0.0135429	0.17	0.4342	0.6043	3.71
0.7384	74822.428	26502.572	0.4324	0.5676	0.0288192	0.0050955	0.0066891	0.0117847	0.2274	0.2985	0.5258	3.71
0.831	84198.93	17126.07	0.5702	0.4298	0.0282817	0.0059861	0.0045125	0.0104986	0.2671	0.2013	0.4684	3.71
0.8913	90314.084	11010.916	0.6888	0.3112	0.027835	0.0065937	0.0029794	0.0095731	0.2942	0.1329	0.4271	3.71
0.9325	94490.016	6834.9843	0.7886	0.2114	0.0274698	0.0070161	0.0018809	0.008897	0.313	0.0839	0.397	3.71
0.9619	97464.112	3860.8878	0.872	0.1280	0.0271719	0.0073176	0.0010743	0.0083919	0.3265	0.0479	0.3744	3.71
0.9836	99658.286	1666.7142	0.9416	0.0584	0.026928	0.0075389	0.0004673	0.0080062	0.3364	0.0208	0.3572	3.71
1	101325	0	1	0	0.026727	0.0077054	0	0.0077054	0.3438	0	0.3438	-------

Direct approach

y1 (CH4)	P1 (CH4) [Pa]	P2 (CO) [Pa]	x1 (CH4)	x2 (CO)	v1 (CH4) [m3 STP/kg]	v2 (CO) [m3 STP/kg]	vt [m3 STP/kg]	n1 (CH4) [mol/kg]	n2 (CO) [mol/kg]	nt [mol/kg]	alpha21 CO/CH4
0	0	101325	0	1	0	0.0183944	0.0183944	0	0.8207	0.8207	-------
0.1332	13492.615	87832.385	0.0349	0.9651	0.0006121	0.0169332	0.0175453	0.0273105	0.7555	0.7828	4.25
0.3731	37800.512	63524.488	0.1228	0.8772	0.0019304	0.0137861	0.0157165	0.086129	0.6151	0.7012	4.25
0.592	59985.653	41339.347	0.2545	0.7455	0.0034603	0.010134	0.0135943	0.1543884	0.4522	0.6065	4.25
0.7384	74822.428	26502.572	0.3992	0.6008	0.0047256	0.0071133	0.0118389	0.2108459	0.3174	0.5282	4.25
0.831	84198.93	17126.070	0.5364	0.4636	0.005657	0.0048898	0.0105469	0.2524027	0.2182	0.4706	4.25
0.8913	90314.084	11010.916	0.6587	0.3413	0.0063313	0.0032803	0.0096116	0.2824854	0.1464	0.4288	4.25
0.9325	94490.016	6834.984	0.7649	0.2351	0.0068264	0.0020984	0.0089248	0.3045748	0.0936	0.3982	4.25
0.9619	97464.112	3860.888	0.8559	0.1441	0.0071978	0.0012117	0.0084095	0.3211479	0.0541	0.3752	4.25
0.9836	99658.286	1666.714	0.9336	0.0664	0.0074826	0.0005318	0.0080144	0.3338553	0.0237	0.3576	4.25
1	101325	0	1	0	0.0077054	0	0.0077054	0.343795	0	0.3438	-------

Extended Langmuir Model for CH4-CO / 5A at 40.0-40.1°C and 101325 Pa total pressure

Averaging approach

y1 (CH4)	P1 (CH4) [Pa]	P2 (CO) [Pa]	x1 (CH4)	x2 (CO)	vm [m3 STP/kg]	v1 (CH4) [m3 STP/kg]	v2 (CO) [m3 STP/kg]	vt [m3 STP/kg]	n1 (CH4) [mol/kg]	n2 (CO) [mol/kg]	nt [mol/kg]	alpha21 CO/CH
0	0	101325	0	1	0.0277055	0	0.0133604	0.0133604	0	0.5961	0.5961	.....
0.0242	2455.874	98869.126	0.0048	0.9952	0.0277305	0.0000641	0.0131721	0.0132361	0.0029	0.5877	0.5906	5.11
0.0482	4883.325	96441.675	0.0098	0.9902	0.0277562	0.0001287	0.0129823	0.0131111	0.0057	0.5792	0.585	5.11
0.0719	7281.585	94043.415	0.0149	0.9851	0.0277826	0.000194	0.0127912	0.0129852	0.0087	0.5707	0.5794	5.11
0.0952	9649.906	91675.094	0.0202	0.9798	0.0278099	0.0002597	0.0125988	0.0128585	0.0116	0.5621	0.5737	5.11
0.1183	11987.562	89337.438	0.0256	0.9744	0.027838	0.000326	0.0124051	0.0127311	0.0145	0.5535	0.568	5.11
0.1411	14293.845	87031.155	0.0312	0.9688	0.0278669	0.0003927	0.0122104	0.0126032	0.0175	0.5448	0.5623	5.11
0.1635	16568.074	84756.926	0.0369	0.9631	0.0278966	0.00046	0.0120147	0.0124746	0.0205	0.5361	0.5566	5.11
0.1856	18809.599	82515.401	0.0427	0.9573	0.0279273	0.0005276	0.011818	0.0123456	0.0235	0.5273	0.5508	5.11
0.2074	21017.795	80307.205	0.0488	0.9512	0.0279588	0.0005956	0.0116206	0.0122162	0.0266	0.5185	0.5451	5.11
0.2289	23192.072	78132.928	0.0549	0.9451	0.0279912	0.000664	0.0114224	0.0120864	0.0296	0.5096	0.5393	5.11
0.424	42966.434	58358.566	0.126	0.874	0.0283697	0.0013597	0.0094301	0.0107898	0.0607	0.4207	0.4814	5.11
0.5823	59005.584	42319.416	0.2145	0.7855	0.0288554	0.0020499	0.0075069	0.0095568	0.0915	0.3349	0.4264	5.11
0.7051	71442.158	29882.842	0.3189	0.6811	0.0294504	0.002699	0.0057645	0.0084636	0.1204	0.2572	0.3776	5.11
0.7972	80772.416	20552.584	0.4349	0.5651	0.030141	0.0032845	0.0042674	0.0075519	0.1465	0.1904	0.3369	5.11
0.865	87649.431	13675.569	0.5566	0.4434	0.0309009	0.0037987	0.0030264	0.0068251	0.1695	0.135	0.3045	5.11
0.9149	92698.830	8626.170	0.6779	0.3221	0.0316977	0.0042446	0.0020168	0.0062614	0.1894	0.09	0.2794	5.11
0.9517	96428.460	4896.540	0.7941	0.2059	0.0325005	0.0046296	0.0012004	0.0058299	0.2066	0.0536	0.2601	5.11
0.9792	99214.904	2110.096	0.902	0.098	0.0332835	0.004962	0.0005389	0.0055008	0.2214	0.024	0.2454	5.11
1	101325	0	1	0	0.0340275	0.0052491	0	0.0052491	0.2342	0	0.2342	.....

Extended Langmuir Model for CH4-CO / 5A at 40.0-40.1°C and 101325 Pa total pressure

Direct approach

y1 (CH4)	P1 (CH4) [Pa]	P2 (CO) [Pa]	x1 (CH4)	x2 (CO)	v1 (CH4) [m3 STP/kg]	v2 (CO) [m3 STP/kg]	vt [m3 STP/kg]	n1 (CH4) [mol/kg]	n2 (CO) [mol/kg]	nt [mol/kg]	alpha21 CO/CH4
0	0	101325	0	1	0	0.0133604	0.0133604	0	0.5961	0.5961	.....
0.0242	2455.8738	98869.126	0.0059	0.9941	0.0000786	0.0131602	0.0132389	0.0035082	0.5872	0.5907	4.16
0.0482	4883.3249	96441.675	0.012	0.9880	0.0001578	0.0129586	0.0131165	0.0070418	0.5782	0.5852	4.16
0.0719	7281.5853	94043.415	0.0183	0.9817	0.0002376	0.0127557	0.0129933	0.0105993	0.5691	0.5797	4.16
0.0952	9649.9063	91675.094	0.0247	0.9753	0.0003178	0.0125515	0.0128693	0.0141789	0.56	0.5742	4.16
0.1183	11987.562	89337.438	0.0313	0.9687	0.0003985	0.0123461	0.0127446	0.0177789	0.5509	0.5686	4.16
0.1411	14293.845	87031.155	0.038	0.9620	0.0004796	0.0121397	0.0126193	0.0213973	0.5416	0.563	4.16
0.1635	16568.074	84756.926	0.0449	0.9551	0.000561	0.0119324	0.0124934	0.0250322	0.5324	0.5574	4.16
0.1856	18809.599	82515.401	0.052	0.9480	0.0006428	0.0117242	0.012367	0.0286816	0.5231	0.5518	4.16
0.2074	21017.795	80307.205	0.0592	0.9408	0.0007249	0.0115153	0.0122402	0.0323433	0.5138	0.5461	4.16
0.2289	23192.072	78132.928	0.0666	0.9334	0.0008072	0.0113058	0.012113	0.0360151	0.5044	0.5405	4.16
0.424	42966.434	58358.566	0.1504	0.8496	0.0016309	0.0092093	0.0108402	0.072766	0.4109	0.4837	4.16
0.5823	59005.584	42319.416	0.2511	0.7489	0.0024173	0.0072078	0.009625	0.1078526	0.3216	0.4294	4.16
0.7051	71442.158	29882.842	0.3651	0.6349	0.0031185	0.005423	0.0085415	0.1391389	0.242	0.3811	4.16
0.7972	80772.416	20552.584	0.4859	0.5141	0.003708	0.0039226	0.0076306	0.165441	0.175	0.3405	4.16
0.865	87649.431	13675.569	0.6065	0.3935	0.004183	0.0027134	0.0068965	0.1866369	0.1211	0.3077	4.16
0.9149	92698.83	8626.1701	0.721	0.2790	0.0045565	0.0017628	0.0063193	0.2033007	0.0787	0.282	4.16
0.9517	96428.46	4896.5397	0.8257	0.1743	0.0048471	0.0010233	0.0058704	0.2162646	0.0457	0.2619	4.16
0.9792	99214.904	2110.0962	0.9188	0.0812	0.0050729	0.0004485	0.0055214	0.2263394	0.02	0.2464	4.16
1	101325	0	1	0	0.0052491	0	0.0052491	0.2342022	0	0.2342	.....

Extended Langmuir Model for N2-CH4 / 5A at 22.7-22.8°C and 101325 Pa total pressure

Averaging approach

y1 (N2)	P1 (N2) [Pa]	P2 (CH4) [Pa]	x1 (N2)	x2 (CH4)	vm [m3 STP/kg]	v1 (N2) [m3 STP/kg]	v2 (CH4) [m3 STP/kg]	vt [m3 STP/kg]	n1 (N2) [mol/kg]	n2 (CH4) [mol/kg]	nt [mol/kg]	alpha21 CH4/N2
0	0	101325	0	1	0.026727	0	0.0077054	0.0077054	0	0.3438	0.3438	.....
0.0868	8793.520	92531.480	0.0693	0.9307	0.0272302	0.0005367	0.0072082	0.0077449	0.0239	0.3216	0.3456	1.28
0.1778	18020.316	83304.684	0.1449	0.8551	0.0278013	0.0011294	0.0066636	0.007793	0.0504	0.2973	0.3477	1.28
0.2727	27628.425	73696.575	0.2271	0.7729	0.0284492	0.0017827	0.0060687	0.0078514	0.0795	0.2708	0.3503	1.28
0.3707	37565.827	63759.173	0.3158	0.6842	0.0291847	0.0025021	0.0054199	0.007922	0.1116	0.2418	0.3535	1.28
0.4716	47781.045	53543.955	0.4115	0.5885	0.0300207	0.0032949	0.0047123	0.0080071	0.147	0.2102	0.3573	1.28
0.5757	58329.097	42995.903	0.5153	0.4847	0.0309836	0.0041792	0.0039316	0.0081109	0.1865	0.1754	0.3619	1.28
0.6805	68951.912	32373.088	0.6253	0.3747	0.0320746	0.0051493	0.0030854	0.0082347	0.2297	0.1377	0.3674	1.28
0.7866	79706.120	21618.880	0.7429	0.2571	0.033328	0.0062281	0.0021559	0.008384	0.2779	0.0962	0.3741	1.28
0.8927	90449.526	10875.474	0.867	0.1330	0.0347624	0.0074234	0.0011391	0.0085625	0.3312	0.0508	0.382	1.28
1	101325	0	1	0	0.0364437	0.0087804	0	0.0087804	0.3918	0	0.3918	.....

Direct approach

y1 (N2)	P1 (N2) [Pa]	P2 (CH4) [Pa]	x1 (N2)	x2 (CH4)	v1 (N2) [m3 STP/kg]	v2 (CH4) [m3 STP/kg]	vt [m3 STP/kg]	n1 (N2) [mol/kg]	n2 (CH4) [mol/kg]	nt [mol/kg]	alpha21 CH4/N2
0	0	101325	0	1	0	0.0077054	0.0077054	0	0.3438	0.3438	.....
0.0868	8793.5195	92531.48	0.0922	0.9078	0.0007183	0.007075	0.0077933	0.032051	0.3157	0.3477	0.94
0.1778	18020.316	83304.684	0.1877	0.8123	0.0014806	0.0064061	0.0078867	0.0660586	0.2858	0.3519	0.94
0.2727	27628.425	73696.575	0.286	0.7140	0.0022836	0.0057014	0.007985	0.1018895	0.2544	0.3563	0.94
0.3707	37565.827	63759.173	0.3863	0.6137	0.0031244	0.0049635	0.0080879	0.1394051	0.2215	0.3609	0.94
0.4716	47781.045	53543.955	0.4881	0.5119	0.0039998	0.0041953	0.0081951	0.1784627	0.1872	0.3656	0.94
0.5757	58329.097	42995.903	0.5917	0.4083	0.0049157	0.0033915	0.0083072	0.2193277	0.1513	0.3706	0.94
0.6805	68951.912	32373.088	0.6947	0.3053	0.0058507	0.002571	0.0084217	0.2610429	0.1147	0.3758	0.94
0.7866	79706.12	21618.88	0.7975	0.2025	0.0068103	0.0017289	0.0085392	0.3038587	0.0771	0.381	0.94
0.8927	90449.526	10875.474	0.8988	0.1012	0.0077824	0.0008758	0.0086582	0.3472312	0.0391	0.3863	0.94
1	101325	0	1	0	0.0087804	0	0.0087804	0.3917604	0	0.3918	.....

Extended Langmuir Model for N2-CH4 / 5A at 39.8-40.1°C and 101325 Pa total pressure

Averaging approach

y1 (N2)	P1 (N2) [Pa]	P2 (CH4) [Pa]	x1 (N2)	x2 (CH4)	vm [m3 STP/kg]	v1 (N2) [m3 STP/kg]	v2 (CH4) [m3 STP/kg]	vt [m3 STP/kg]	n1 (N2) [mol/kg]	n2 (CH4) [mol/kg]	nt [mol/kg]	alpha21 CH4/N2
0	0	101325	0	1	0.0340275	0	0.0052491	0.0052491	0	0.2342	0.2342	.....
0.1488	15072.560	86252.440	0.0419	0.9581	0.0348647	0.0002038	0.0046584	0.0048622	0.0091	0.2078	0.2169	3.99
0.2839	28767.693	72557.307	0.0903	0.9097	0.0358839	0.0004068	0.0040984	0.0045053	0.0182	0.1829	0.201	3.99
0.4065	41185.107	60139.893	0.1464	0.8536	0.0371419	0.0006118	0.0035684	0.0041803	0.0273	0.1592	0.1865	3.99
0.5175	52435.635	48889.365	0.2117	0.7883	0.0387238	0.0008232	0.0030657	0.003889	0.0367	0.1368	0.1735	3.99
0.6181	62632.014	38692.986	0.2884	0.7116	0.0407624	0.0010481	0.0025861	0.0036341	0.0468	0.1154	0.1621	3.99
0.7094	71883.003	29441.997	0.3794	0.6206	0.0434771	0.0012977	0.002123	0.0034207	0.0579	0.0947	0.1526	3.99
0.7924	80290.013	21034.987	0.4887	0.5113	0.0472577	0.0015922	0.0016661	0.0032583	0.071	0.0743	0.1454	3.99
0.868	87945.513	13379.487	0.622	0.3780	0.0528678	0.00197	0.001197	0.003167	0.0879	0.0534	0.1413	3.99
0.9369	94932.557	6392.443	0.7881	0.2119	0.0620352	0.0025176	0.0006771	0.0031947	0.1123	0.0302	0.1425	3.99
1	101325	0	1	0	0.0796721	0.0034795	0	0.0034795	0.1552	0	0.1552	.....

Direct approach

y1 (N2)	P1 (N2) [Pa]	P2 (CH4) [Pa]	x1 (N2)	x2 (CH4)	v1 (N2) [m3 STP/kg]	v2 (CH4) [m3 STP/kg]	vt [m3 STP/kg]	n1 (N2) [mol/kg]	n2 (CH4) [mol/kg]	nt [mol/kg]	alpha21 CH4/N2
0	0	101325	0	1	0	0.0052491	0.0052491	0	0.2342	0.2342	.....
0.1488	15072.560	86252.440	0.0929	0.9071	0.0004658	0.0045465	0.0050122	0.0207806	0.2029	0.2236	1.71
0.2839	28767.693	72557.307	0.1886	0.8114	0.0009033	0.0038864	0.0047897	0.0403032	0.1734	0.2137	1.71
0.4065	41185.107	60139.893	0.2865	0.7135	0.0013124	0.0032692	0.0045816	0.0585578	0.1459	0.2044	1.71
0.5175	52435.635	48889.365	0.386	0.6140	0.0016938	0.0026939	0.0043877	0.0755722	0.1202	0.1958	1.71
0.6181	62632.014	38692.986	0.4869	0.5131	0.0020485	0.0021588	0.0042073	0.0913989	0.0963	0.1877	1.71
0.7094	71883.003	29441.997	0.5887	0.4113	0.0023781	0.0016615	0.0040397	0.1061054	0.0741	0.1802	1.71
0.7924	80290.013	21034.987	0.6911	0.3089	0.0026843	0.0011996	0.0038839	0.1197667	0.0535	0.1733	1.71
0.868	87945.513	13379.487	0.794	0.2060	0.0029688	0.0007704	0.0037392	0.1324602	0.0344	0.1668	1.71
0.9369	94932.557	6392.443	0.897	0.1030	0.0032333	0.0003714	0.0036047	0.1442625	0.0166	0.1608	1.71
1	101325	0	1	0	0.0034795	0	0.0034795	0.1552469	0	0.1552	.....

Extended Langmuir Model for N2-CO / Turkish clinoptilolite at 22.6-22.8°C and 101325 Pa total pressure

Averaging approach

y1 (N2)	P1 (N2) [Pa]	P2 (CO) [Pa]	x1 (N2)	x2 (CO)	vm [m3 STP/kg]	v1 (N2) [m3 STP/kg]	v2 (CO) [m3 STP/kg]	vt [m3 STP/kg]	n1 (N2) [mol/kg]	n2 (CO) [mol/kg]	nt [mol/kg]	alpha21 CO/N2
0	0	101325	0	1	0.0270933	0	0.0264088	0.0264088	0	1.1783	1.1783	.....
0.0688	6967.3836	94357.616	0.0148	0.9852	0.026725	0.0003853	0.0256264	0.0260117	0.0172	1.1434	1.1606	4.91
0.1272	12888.158	88436.842	0.0288	0.9712	0.0263859	0.0007391	0.0249071	0.0256462	0.033	1.1113	1.1443	4.91
0.1776	18000.346	83324.654	0.0421	0.9579	0.0260713	0.0010663	0.024241	0.0253073	0.0476	1.0816	1.1291	4.91
0.2218	22471.918	78853.082	0.0548	0.9452	0.025778	0.0013706	0.0236206	0.0249912	0.0612	1.0539	1.115	4.91
0.2608	26425.432	74899.568	0.067	0.9330	0.025503	0.0016552	0.02304	0.0246951	0.0738	1.028	1.1018	4.91
0.2956	29952.786	71372.214	0.0787	0.9213	0.0252444	0.0019222	0.0224944	0.0244166	0.0858	1.0036	1.0894	4.91
0.3269	33124.476	68200.524	0.09	0.9100	0.0250001	0.0021737	0.02198	0.0241537	0.097	0.9807	1.0777	4.91
0.3552	35995.645	65329.355	0.1009	0.8991	0.0247688	0.0024113	0.0214934	0.0239047	0.1076	0.959	1.0666	4.91
0.3811	38610.141	62714.859	0.1114	0.8886	0.0245492	0.0026365	0.0210319	0.0236684	0.1176	0.9384	1.056	4.91
0.4047	41003.343	60321.657	0.1216	0.8784	0.0243401	0.0028503	0.0205932	0.0234435	0.1272	0.9188	1.046	4.91
0.5654	57290.206	44034.794	0.2094	0.7906	0.0226751	0.004535	0.0171191	0.0216541	0.2023	0.7638	0.9662	4.91
0.6559	66457.676	34867.324	0.2796	0.7204	0.0215006	0.0057019	0.014692	0.0203939	0.2544	0.6555	0.9099	4.91
0.715	72448.68	28876.32	0.3381	0.6619	0.0206098	0.006573	0.0128666	0.0194396	0.2933	0.5741	0.8673	4.91
0.7571	76712.075	24612.925	0.3882	0.6118	0.0199039	0.0072539	0.0114303	0.0186842	0.3237	0.51	0.8336	4.91
0.7887	79919.464	21405.536	0.4319	0.5681	0.0193273	0.0078033	0.0102645	0.0180678	0.3482	0.458	0.8061	4.91
0.8135	82429.086	18895.914	0.4704	0.5296	0.0188456	0.0082572	0.0092962	0.0175534	0.3684	0.4148	0.7832	4.91
0.8335	84451.14	16873.86	0.5047	0.4953	0.0184361	0.0086391	0.0084775	0.0171166	0.3855	0.3782	0.7637	4.91
0.8499	86117.82	15207.18	0.5355	0.4645	0.0180832	0.0089653	0.0077751	0.0167404	0.4	0.3469	0.7469	4.91
0.8637	87516.779	13808.221	0.5634	0.4366	0.0177756	0.0092472	0.0071655	0.0164126	0.4126	0.3197	0.7323	4.91
0.9345	94686.279	6638.7208	0.7439	0.2561	0.016012	0.0108148	0.0037239	0.0145387	0.4825	0.1662	0.6487	4.91
0.9617	97445.292	3879.7079	0.8364	0.1636	0.0152363	0.011474	0.0022436	0.0137175	0.5119	0.1001	0.612	4.91
0.9759	98882.826	2442.1737	0.8918	0.1082	0.0148073	0.0118293	0.0014348	0.0132642	0.5278	0.064	0.5918	4.91
0.9844	99747.466	1577.534	0.9279	0.0721	0.0145404	0.0120468	0.0009357	0.0129825	0.5375	0.0417	0.5792	4.91
0.99	100312.66	1012.3442	0.9528	0.0472	0.0143622	0.0121904	0.0006042	0.0127946	0.5439	0.027	0.5709	4.91
0.9939	100701.87	623.13355	0.9705	0.0295	0.0142377	0.01229	0.0003735	0.0126635	0.5483	0.0167	0.565	4.91
0.9966	100978.75	346.25083	0.9834	0.0166	0.0141482	0.0123611	0.0002082	0.0125692	0.5515	0.0093	0.5608	4.91
0.9986	101179.24	145.75804	0.993	0.0070	0.014083	0.0124127	0.0000878	0.0125005	0.5538	0.0039	0.5577	4.91
1	101325	0	1	0.0000	0.0140353	0.0124503	0	0.0124503	0.5555	0	0.5555	.....

Extended Langmuir Model for N2-CO / Turkish clinoptilolite at 22.6-22.8°C and 101325 Pa total pressure

Direct approach

y1 (N2)	P1 (N2) [Pa]	P2 (CO) [Pa]	x1 (N2)	x2 (CO)	v1 (N2) [m3 STP/kg]	v2 (CO) [m3 STP/kg]	vt [m3 STP/kg]	n1 (N2) [mol/kg]	n2 (CO) [mol/kg]	nt [mol/kg]	alpha21 CO/N2
0	0	101325	0	1	0	0.0264088	0.0264088	0	1.1783	1.1783	-------
0.0688	6967.3836	94357.616	0.0077	0.9923	0.0002023	0.0259796	0.0261819	0.0090282	1.1591	1.1682	9.48
0.1272	12888.158	88436.842	0.0151	0.9849	0.0003931	0.0255749	0.025968	0.0175407	1.1411	1.1586	9.48
0.1776	18000.346	83324.654	0.0223	0.9777	0.000574	0.0251912	0.0257653	0.0256114	1.124	1.1496	9.48
0.2218	22471.918	78853.082	0.0292	0.9708	0.0007463	0.0248259	0.0255721	0.0332968	1.1077	1.141	9.48
0.2608	26425.432	74899.568	0.0359	0.9641	0.0009109	0.0244767	0.0253876	0.0406417	1.0921	1.1327	9.48
0.2956	29952.786	71372.214	0.0424	0.9576	0.0010687	0.024142	0.0252107	0.0476823	1.0772	1.1248	9.48
0.3269	33124.476	68200.524	0.0487	0.9513	0.0012203	0.0238203	0.0250406	0.0544484	1.0628	1.1173	9.48
0.3552	35995.645	65329.355	0.0549	0.9451	0.0013664	0.0235105	0.0248769	0.0609649	1.049	1.1099	9.48
0.3811	38610.141	62714.859	0.061	0.9390	0.0015073	0.0232116	0.0247189	0.067253	1.0356	1.1029	9.48
0.4047	41003.343	60321.657	0.0669	0.9331	0.0016435	0.0229226	0.0245662	0.0733309	1.0228	1.0961	9.48
0.5654	57290.206	44034.794	0.1207	0.8793	0.002807	0.0204547	0.0232617	0.1252431	0.9126	1.0379	9.48
0.6559	66457.676	34867.324	0.1674	0.8326	0.0037221	0.0185137	0.0222358	0.1660718	0.826	0.9921	9.48
0.715	72448.68	28876.32	0.2093	0.7907	0.0044762	0.0169142	0.0213904	0.1997174	0.7547	0.9544	9.48
0.7571	76712.075	24612.925	0.2474	0.7526	0.0051151	0.015559	0.0206741	0.2282228	0.6942	0.9224	9.48
0.7887	79919.464	21405.536	0.2825	0.7175	0.0056667	0.014389	0.0200557	0.2528333	0.642	0.8948	9.48
0.8135	82429.086	18895.914	0.3151	0.6849	0.0061496	0.0133648	0.0195143	0.2743785	0.5963	0.8707	9.48
0.8335	84451.14	16873.86	0.3455	0.6545	0.0065769	0.0124583	0.0190352	0.2934452	0.5559	0.8493	9.48
0.8499	86117.82	15207.18	0.374	0.6260	0.0069584	0.0116491	0.0186075	0.3104662	0.5198	0.8302	9.48
0.8637	87516.779	13808.221	0.4007	0.5993	0.0073014	0.0109215	0.0182229	0.3257714	0.4873	0.8131	9.48
0.9345	94686.279	6638.7208	0.6007	0.3993	0.0094797	0.0063012	0.0157808	0.4229598	0.2811	0.7041	9.48
0.9617	97445.292	3879.7079	0.726	0.2740	0.0105695	0.0039895	0.014559	0.4715843	0.178	0.6496	9.48
0.9759	98882.826	2442.1737	0.8103	0.1897	0.0112126	0.0026254	0.013838	0.5002789	0.1171	0.6174	9.48
0.9844	99747.466	1577.534	0.8696	0.1304	0.0116284	0.0017435	0.0133719	0.5188287	0.0778	0.5966	9.48
0.99	100312.66	1012.3442	0.9127	0.0873	0.011913	0.0011398	0.0130528	0.531528	0.0509	0.5824	9.48
0.9939	100701.87	623.13355	0.9446	0.0554	0.0121153	0.0007107	0.012826	0.540553	0.0317	0.5723	9.48
0.9966	100978.75	346.25083	0.9685	0.0315	0.0122624	0.0003986	0.012661	0.547118	0.0178	0.5649	9.48
0.9986	101179.24	145.75804	0.9865	0.0135	0.0123707	0.000169	0.0125396	0.5519492	0.0075	0.5595	9.48
1	101325	0	1	0.0000	0.0124503	0	0.0124503	0.555503	0	0.5555	-------

Extended Langmuir Model for N2-CO / Turkish clinoptilolite at 40.0°C and 101325 Pa total pressure

Averaging approach

y1 (N2)	P1 (N2) [Pa]	P2 (CO) [Pa]	x1 (N2)	x2 (CO)	vm [m3 STP/kg]	v1 (N2) [m3 STP/kg]	v2 (CO) [m3 STP/kg]	vt [m3 STP/kg]	n1 (N2) [mol/kg]	n2 (CO) [mol/kg]	nt [mol/kg]	alpha21 CO/N2
0	0.000	101325.000	0	1	0.023531	0	0.0211077	0.0211077	0	0.9418	0.9418	-------
0.0222	2253.163	99071.837	0.0164	0.9836	0.0231526	0.0003404	0.0204151	0.0207555	0.0152	0.9109	0.9261	1.36
0.0434	4397.576	96927.424	0.0322	0.9678	0.0227995	0.0006577	0.0197693	0.020427	0.0293	0.8821	0.9114	1.36
0.0636	6441.681	94883.319	0.0474	0.9526	0.0224693	0.0009541	0.0191655	0.0201196	0.0426	0.8551	0.8977	1.36
0.0828	8393.023	92931.977	0.0621	0.9379	0.0221596	0.0012317	0.0185997	0.0198314	0.055	0.8299	0.8848	1.36
0.1012	10258.367	91066.633	0.0763	0.9237	0.0218685	0.0014924	0.0180681	0.0195605	0.0666	0.8062	0.8727	1.36
0.1189	12043.798	89281.202	0.09	0.9100	0.0215942	0.0017377	0.0175676	0.0193053	0.0775	0.7838	0.8614	1.36
0.1357	13754.810	87570.190	0.1033	0.8967	0.0213354	0.001969	0.0170955	0.0190645	0.0878	0.7628	0.8506	1.36
0.1520	15396.381	85928.619	0.1161	0.8839	0.0210906	0.0021874	0.0166493	0.0188367	0.0976	0.7429	0.8404	1.36
0.1675	16973.028	84351.972	0.1286	0.8714	0.0208587	0.0023942	0.0162268	0.018621	0.1068	0.724	0.8308	1.36
0.1825	18488 865	82836.135	0.1406	0.8594	0.0206387	0.0025901	0.0158261	0.0184163	0.1156	0.7061	0.8217	1.36
0.3059	30994.683	70330.317	0.2442	0.7558	0.0189255	0.0041085	0.0127141	0.0168226	0.1833	0.5673	0.7506	1.36
0.3962	40144.552	61180.448	0.3248	0.6752	0.017777	0.0051178	0.0106368	0.0157546	0.2283	0.4746	0.7029	1.36
0.4657	47189.064	54135.936	0.3899	0.6101	0.0169467	0.0058422	0.0091404	0.0149826	0.2607	0.4078	0.6685	1.36
0.5212	52811.306	48513.694	0.4439	0.5561	0.0163149	0.00639	0.0080054	0.0143954	0.2851	0.3572	0.6423	1.36
0.5667	57420.518	43904.482	0.4895	0.5105	0.0158162	0.0068201	0.0071118	0.0139319	0.3043	0.3173	0.6216	1.36
0.6048	61278.836	40046.164	0.5288	0.4712	0.0154114	0.0071677	0.0063881	0.0135558	0.3198	0.285	0.6048	1.36
0.6372	64562.935	36762.065	0.5629	0.4371	0.0150755	0.0074548	0.0057889	0.0132438	0.3326	0.2583	0.5909	1.36
0.6652	67396.757	33928.243	0.5929	0.4071	0.0147919	0.0076964	0.0052839	0.0129803	0.3434	0.2358	0.5791	1.36
0.6896	69870.120	31454.880	0.6196	0.3804	0.0145489	0.0079027	0.0048519	0.0127546	0.3526	0.2165	0.5691	1.36
0.8306	84164.143	17160.857	0.7824	0.2176	0.0132225	0.009016	0.0025071	0.011523	0.4023	0.1119	0.5141	1.36
0.8943	90612.539	10712.461	0.8612	0.1388	0.0126643	0.009477	0.001528	0.011005	0.4228	0.0682	0.491	1.36
0.9305	94285.531	7039.469	0.9076	0.0924	0.0123566	0.009729	0.0009906	0.0107196	0.4341	0.0442	0.4783	1.36
0.9537	96635.350	4689.650	0.9379	0.0621	0.0121635	0.0098862	0.0006543	0.0105405	0.4411	0.0292	0.4703	1.36
0.9696	98244.316	3080.684	0.959	0.0410	0.012033	0.0099921	0.0004273	0.0104194	0.4458	0.0191	0.4649	1.36
0.9809	99393.362	1931.638	0.9742	0.0258	0.0119405	0.0100669	0.0002668	0.0103337	0.4492	0.0119	0.4611	1.36
0.9892	100235.210	1089.790	0.9854	0.0146	0.0118732	0.0101213	0.0001501	0.0102713	0.4516	0.0067	0.4583	1.36
0.9954	100860.152	464.848	0.9938	0.0062	0.0118235	0.0101614	0.0000639	0.0102252	0.4534	0.0028	0.4562	1.36
1.0000	101325.000	0.000	1	0.0000	0.0117867	0.0101911	0	0.0101911	0.4547	0	0.4547	------

Extended Langmuir Model for N2-CO / Turkish clinoptilolite at 40.0°C and 101325 Pa total pressure

Direct approach

y1(N2)	P1 (N2) [Pa]	P2 (CO) [Pa]	x1 (N2)	x2 (CO)	v1 (N2) [m3 STP/kg]	v2 (CO) [m3 STP/kg]	vt [m3 STP/kg]	n1(N2) [mol/kg]	n2 (CO) [mol/kg]	nt [mol/kg]	alpha21 (CO/N2)
0	0	101325	0	1	0	0.0211077	0.0211077	0	0.9418	0.9418	-------
0.0222	2253.163	99071.837	0.0083	0.9917	0.0001733	0.0207487	0.0209221	0.007733	0.9258	0.9335	2.72
0.0434	4397.5759	96927.424	0.0164	0.9836	0.00034	0.0204035	0.0207435	0.0151699	0.9104	0.9255	2.72
0.0636	6441.6811	94883.319	0.0243	0.9757	0.0005005	0.0200711	0.0205716	0.0223302	0.8955	0.9179	2.72
0.0828	8393.0233	92931.977	0.0321	0.9679	0.0006552	0.0197508	0.0204059	0.0292313	0.8812	0.9105	2.72
0.1012	10258.367	91066.633	0.0397	0.9603	0.0008044	0.0194417	0.0202461	0.0358893	0.8674	0.9033	2.72
0.1189	12043.798	89281.202	0.0472	0.9528	0.0009485	0.0191432	0.0200917	0.0423185	0.8541	0.8964	2.72
0.1357	13754.81	87570.19	0.0545	0.9455	0.0010877	0.0188548	0.0199425	0.0485324	0.8413	0.8898	2.72
0.1520	15396.381	85928.619	0.0617	0.9383	0.0012225	0.0185758	0.0197982	0.054543	0.8288	0.8833	2.72
0.1675	16973.028	84351.972	0.0688	0.9312	0.0013529	0.0183057	0.0196585	0.0603616	0.8168	0.8771	2.72
0.1825	18488.865	82836.135	0.0758	0.9242	0.0014792	0.018044	0.0195232	0.0659986	0.8051	0.8711	2.72
0.3059	30994.683	70330.317	0.1393	0.8607	0.0025588	0.015808	0.0183668	0.1141652	0.7053	0.8195	2.72
0.3962	40144.552	61180.448	0.1942	0.8058	0.0033932	0.0140797	0.0174729	0.1513973	0.6282	0.7796	2.72
0.4657	47189.064	54135.936	0.2425	0.7575	0.0040633	0.0126917	0.0167551	0.181296	0.5663	0.7476	2.72
0.5212	52811.306	48513.694	0.2856	0.7144	0.0046164	0.0115462	0.0161626	0.2059738	0.5152	0.7211	2.72
0.5667	57420.518	43904.482	0.3245	0.6755	0.0050825	0.0105808	0.0156633	0.2267705	0.4721	0.6989	2.72
0.6048	61278.836	40046.164	0.3598	0.6402	0.0054818	0.0097537	0.0152356	0.2445862	0.4352	0.6798	2.72
0.6372	64562.935	36762.065	0.3921	0.6079	0.0058285	0.0090358	0.0148643	0.2600522	0.4032	0.6632	2.72
0.6652	67396.757	33928.243	0.4218	0.5782	0.0061327	0.0084056	0.0145383	0.273627	0.375	0.6487	2.72
0.6896	69870.12	31454.88	0.4493	0.5507	0.0064023	0.0078474	0.0142496	0.285653	0.3501	0.6358	2.72
0.8306	84164.143	17160.857	0.643	0.3570	0.0080369	0.0044616	0.0124986	0.3585876	0.1991	0.5577	2.72
0.8943	90612.539	10712.461	0.7565	0.2435	0.0088203	0.0028391	0.0116594	0.3935406	0.1267	0.5202	2.72
0.9305	94285.531	7039.4693	0.8311	0.1689	0.0092803	0.0018865	0.0111667	0.4140619	0.0842	0.4982	2.72
0.9537	96635.35	4689.6503	0.8833	0.1167	0.0095799	0.0012658	0.0108457	0.4274325	0.0565	0.4839	2.72
0.9696	98244.316	3080.6843	0.9213	0.0787	0.0097876	0.0008356	0.0106232	0.436699	0.0373	0.474	2.72
0.9809	99393.362	1931.6375	0.9497	0.0503	0.0099372	0.0005258	0.010463	0.443373	0.0235	0.4668	2.72
0.9892	100235.21	1089.7899	0.9712	0.0288	0.0100475	0.0002974	0.0103449	0.4482929	0.0133	0.4616	2.72
0.9954	100860.15	464.84769	0.9876	0.0124	0.0101297	0.0001271	0.0102568	0.4519617	0.0057	0.4576	2.72
1.0000	101325	0	1	0.0000	0.0101911	0	0.0101911	0.4546999	0	0.4547	-------

Extended Langmuir Model for CH4-CO / Turkish clinoptilolite at 22.6-22.8°C and 101325 Pa total pressure

Averaging approach

y1 (CH4)	P1 (CH4) [Pa]	P2 (CO) [Pa]	x1 (CH4)	x2 (CO)	vm [m3 STP/kg]	v1 (CH4) [m3 STP/kg]	v2 (CO) [m3 STP/kg]	vt [m3 STP/kg]	n1 (CH4) [mol/kg]	n2 (CO) [mol/kg]	nt [mol/kg]	alpha21 CO/CH
0	0	101325	0	1	0.0270933	0	0.0264088	0.0264088	0	1.1783	1.1783	.....
0.0221	2240.393	99084.607	0.0034	0.9966	0.0270665	0.0000899	0.0262801	0.0263699	0.004	1.1726	1.1766	6.61
0.0433	4384.4422	96940.558	0.0068	0.9932	0.02704	0.0001789	0.0261526	0.0263314	0.008	1.1669	1.1748	6.61
0.0635	6438.5543	94886.446	0.0102	0.9898	0.0270136	0.000267	0.0260262	0.0262932	0.0119	1.1612	1.1731	6.61
0.083	8408.5605	92916.439	0.0135	0.9865	0.0269875	0.0003544	0.0259009	0.0262553	0.0158	1.1556	1.1714	6.61
0.1017	10299.784	91025.216	0.0168	0.9832	0.0269615	0.000441	0.0257767	0.0262178	0.0197	1.1501	1.1698	6.61
0.1196	12117.091	89207.909	0.0201	0.9799	0.0269358	0.0005269	0.0256536	0.0261805	0.0235	1.1446	1.1681	6.61
0.1368	13864.944	87460.056	0.0234	0.9766	0.0269103	0.000612	0.0255315	0.0261436	0.0273	1.1392	1.1665	6.61
0.1534	15547.443	85777.557	0.0267	0.9733	0.0268849	0.0006964	0.0254104	0.0261069	0.0311	1.1338	1.1648	6.61
0.1694	17168.358	84156.642	0.0299	0.9701	0.0268598	0.0007801	0.0252903	0.0260705	0.0348	1.1284	1.1632	6.61
0.1849	18731.168	82593.832	0.0332	0.9668	0.0268348	0.0008632	0.0251712	0.0260344	0.0385	1.1231	1.1616	6.61
0.3135	31767.359	69557.641	0.0646	0.9354	0.0265941	0.0016593	0.0240275	0.0256868	0.074	1.072	1.1461	6.61
0.4088	41425.938	59899.062	0.0947	0.9053	0.0263679	0.0024011	0.0229601	0.0253611	0.1071	1.0244	1.1316	6.61
0.4826	48898.989	52426.011	0.1236	0.8764	0.0261539	0.0030968	0.0219571	0.0250539	0.1382	0.9797	1.1178	6.61
0.5415	54868.378	46456.622	0.1515	0.8485	0.0259506	0.0037522	0.0210105	0.0247628	0.1674	0.9374	1.1049	6.61
0.5897	59754.816	41570.184	0.1785	0.8215	0.0257569	0.0043719	0.0201141	0.0244861	0.1951	0.8974	1.0925	6.61
0.63	63833.125	37491.875	0.2047	0.7953	0.0255718	0.0049593	0.0192631	0.0242224	0.2213	0.8595	1.0807	6.61
0.6641	67291.023	34033.977	0.2302	0.7698	0.0253948	0.005517	0.0184537	0.0239707	0.2462	0.8234	1.0695	6.61
0.6934	70261.426	31063.574	0.2549	0.7451	0.0252251	0.0060477	0.0176824	0.0237301	0.2698	0.7889	1.0588	6.61
0.7189	72841.272	28483.728	0.2789	0.7211	0.0250623	0.0065531	0.0169466	0.0234997	0.2924	0.7561	1.0485	6.61
0.8622	87361.168	13963.832	0.4861	0.5139	0.0237396	0.0105233	0.011124	0.0216473	0.4695	0.4963	0.9658	6.61
0.9228	93501.197	7823.8028	0.6438	0.3562	0.0228234	0.0131234	0.0072622	0.0203856	0.5855	0.324	0.9096	6.61
0.9549	96750.515	4574.4853	0.7618	0.2382	0.0221824	0.0148655	0.0046482	0.0195137	0.6633	0.2074	0.8707	6.61
0.9737	98655.979	2669.0211	0.8482	0.1518	0.0217354	0.0160412	0.00287	0.0189112	0.7157	0.1281	0.8438	6.61
0.9852	99826.919	1498.081	0.9097	0.0903	0.0214283	0.0168297	0.0016703	0.0185	0.7509	0.0745	0.8254	6.61
0.9924	100552.13	772.87164	0.9516	0.0484	0.0212238	0.0173458	0.0008817	0.0182275	0.7739	0.0393	0.8133	6.61
0.9967	100986.66	338.3414	0.9783	0.0217	0.0210956	0.0176658	0.0003914	0.0180572	0.7882	0.0175	0.8057	6.61
0.999	101223.22	101.77792	0.9934	0.0066	0.0210239	0.0178434	0.0001187	0.0179621	0.7961	0.0053	0.8014	6.61
1	101325	0	1	0	0.0209926	0.0179207	0	0.0179207	0.7996	0	0.7996	.....

Extended Langmuir Model for CH4-CO / Turkish clinoptilolite at 22.6-22.8°C and 101325 Pa total pressure

Direct approach

y1 (CH4)	P1 (CH4) [Pa]	P2 (CO) [Pa]	x1 (CH4)	x2 (CO)	v1 (CH4) [m3 STP/kg]	v2 (CO) [m3 STP/kg]	vt [m3 STP/kg]	n1 (CH4) [mol/kg]	n2 (CO) [mol/kg]	nt [mol/kg]	alpha21 CO/CH4
0	0	101325	0	1	0	0.0264088	0.0264088	0	1.1783	1.1783	.....
0.0221	2240.393	99084.607	0.0026	0.9974	0.0000697	0.0263061	0.0263758	0.0031093	1.1737	1.1768	8.54
0.0433	4384.4422	96940.558	0.0053	0.9947	0.000.389	0.0262042	0.026343	0.0061954	1.1692	1.1754	8.54
0.0635	6438.5543	94886.446	0.0079	0.9921	0.0002075	0.026103	0.0263105	0.009259	1.1647	1.1739	8.54
0.083	8408.5605	92916.439	0.0105	0.9895	0.0002757	0.0260025	0.0262782	0.0123008	1.1602	1.1725	8.54
0.1017	10299.784	91025.216	0.0131	0.9869	0.0003434	0.0259028	0.0262462	0.0153215	1.1557	1.171	8.54
0.1196	12117.091	89207.909	0.0157	0.9843	0.0004106	0.0258037	0.0262143	0.0183217	1.1513	1.1696	8.54
0.1368	13864.944	87460.056	0.0182	0.9792	0.0004774	0.0257052	0.0261827	0.021302	1.1469	1.1682	8.54
0.1534	15547.443	85777.557	0.0208	0.9767	0.0005438	0.0256074	0.0261512	0.0242628	1.1425	1.1668	8.54
0.1694	17168.358	84156.642	0.0233	0.9767	0.0006097	0.0255103	0.02612	0.0272048	1.1382	1.1654	8.54
0.1849	18731.168	82593.832	0.0259	0.9741	0.0006753	0.0254137	0.026089	0.0301283	1.1339	1.164	8.54
0.3135	31767.359	69557.641	0.0508	0.9492	0.0013098	0.0244786	0.0257884	0.0584403	1.0922	1.1506	8.54
0.4088	41425.938	59899.062	0.075	0.9250	0.0019116	0.0235918	0.0255034	0.0852909	1.0526	1.1379	8.54
0.4826	48898.989	52426.011	0.0985	0.9015	0.0024856	0.0227458	0.0252315	0.1109033	1.0149	1.1258	8.54
0.5415	54868.378	46456.622	0.1216	0.8784	0.0030354	0.0219357	0.0249711	0.1354305	0.9787	1.1141	8.54
0.5897	59754.816	41570.184	0.1441	0.8559	0.0035632	0.0211578	0.0247211	0.1589833	0.944	1.103	8.54
0.63	63833.125	37491.875	0.1663	0.8337	0.0040712	0.0204093	0.0244805	0.1816463	0.9106	1.0923	8.54
0.6641	67291.023	34033.977	0.1881	0.8119	0.0045607	0.019688	0.0242486	0.2034861	0.8784	1.0819	8.54
0.6934	70261.426	31063.574	0.2095	0.7905	0.0050329	0.018992	0.024025	0.2245569	0.8474	1.0719	8.54
0.7189	72841.272	28483.728	0.2305	0.7695	0.005489	0.01832	0.023809	0.2449038	0.8174	1.0623	8.54
0.8622	87361.168	13963.832	0.423	0.5770	0.00[illegible]1057	0.0126955	0.0220012	0.4151958	0.5664	0.9816	8.54
0.9228	93501.197	7823.8028	0.5834	0.4166	0.01[illegible]0707	0.0086208	0.0206915	0.5385641	0.3846	0.9232	8.54
0.9549	96750.515	4574.4853	0.7125	0.2875	0.0140681	0.0056773	0.0197454	0.6276848	0.2533	0.881	8.54
0.9737	98655.979	2669.0211	0.8124	0.1876	0.015493	0.0035775	0.0190705	0.6912596	0.1596	0.8509	8.54
0.9852	99826.919	1498.081	0.8865	0.1135	0.0164876	0.0021118	0.0185994	0.7356354	0.0942	0.8299	8.54
0.9924	100552.13	772.87164	0.9384	0.0616	0.0171569	0.0011256	0.0182824	0.7654967	0.0502	0.8157	8.54
0.9967	100986.66	338.3414	0.9722	0.0278	0.0175795	0.0005027	0.0180822	0.7843548	0.0224	0.8068	8.54
0.999	101223.22	101.77792	0.9915	0.0085	0.0178169	0.0001529	0.0179698	0.7949457	0.0068	0.8018	8.54
1	101325	0	1	0.0000	0.0179207	0	0.0179207	0.7995751	0	0.7996	.....

Extended Langmuir Model for CH4-CO / Turkish clinoptilolite at 40.0°C and 101325 Pa total pressure

Averaging approach

y1 (CH4)	P1 (CH4) [Pa]	P2 (CO) [Pa]	x1 (CH4)	x2 (CO)	vm [m3 STP/kg]	v1 (CH4) [m3 STP/kg]	v2 (CO) [m3 STP/kg]	vt [m3 STP/kg]	n1 (CH4) [mol/kg]	n2 (CO) [mol/kg]	nt [mol/kg]	alpha21 CO/CH
0	0	101325	0	1	0.023531	0	0.0211077	0.0211077	0	0.9418	0.9418	-------
0.0701	7101.6757	94223.324	0.0379	0.9621	0.0232716	0.0007893	0.0200117	0.020801	0.0352	0.8929	0.9281	1.91
0.1338	13554.891	87770.109	0.0748	0.9252	0.0230252	0.0015336	0.0189765	0.0205101	0.0684	0.8467	0.9151	1.91
0.1918	19434.087	81890.913	0.1105	0.8895	0.0227914	0.0022352	0.0179993	0.0202345	0.0997	0.8031	0.9028	1.91
0.2448	24803.705	76521.295	0.145	0.8550	0.0225694	0.0028966	0.0170769	0.0199735	0.1292	0.7619	0.8912	1.91
0.2933	29719.672	71605.328	0.1784	0.8216	0.0223589	0.0035198	0.0162063	0.0197261	0.157	0.7231	0.8801	1.91
0.3378	34230.652	67094.348	0.2107	0.7893	0.0221592	0.0041073	0.0153846	0.0194919	0.1833	0.6864	0.8697	1.91
0.3788	38379.104	62945.896	0.2419	0.7581	0.0219698	0.0046611	0.014609	0.01927	0.208	0.6518	0.8598	1.91
0.4165	42202.173	59122.827	0.2719	0.7281	0.0217902	0.0051833	0.0138766	0.0190599	0.2313	0.6191	0.8504	1.91
0.4513	45732.438	55592.562	0.3009	0.6991	0.0216197	0.0056758	0.013185	0.0188608	0.2532	0.5883	0.8415	1.91
0.4836	48998.559	52326.441	0.3289	0.6711	0.0214579	0.0061405	0.0125315	0.018672	0.274	0.5591	0.8331	1.91
0.7057	71503.589	29821.411	0.5565	0.4435	0.0202247	0.0095947	0.007647	0.0172417	0.4281	0.3412	0.7693	1.91
0.8240	83495.612	17829.388	0.7102	0.2898	0.019469	0.0116281	0.0047451	0.0163732	0.5188	0.2117	0.7305	1.91
0.8930	90481.247	10843.753	0.8137	0.1863	0.0189915	0.0128781	0.0029494	0.0158275	0.5746	0.1316	0.7062	1.91
0.9353	94767.376	6557.6243	0.8832	0.1168	0.0186833	0.0136693	0.0018076	0.0154769	0.6099	0.0806	0.6905	1.91
0.9620	97469.859	3855.1406	0.9297	0.0703	0.0184828	0.0141777	0.0010716	0.0152493	0.6326	0.0478	0.6804	1.91
0.9789	99188.964	2136.0364	0.9605	0.0395	0.0183526	0.0145049	0.0005969	0.0151018	0.6472	0.0266	0.6738	1.91
0.9896	100273.95	1051.0473	0.9804	0.0196	0.0182693	0.0147129	0.0002947	0.0150076	0.6565	0.0131	0.6696	1.91
0.9962	100939.96	385.03601	0.9928	0.0072	0.0182178	0.0148412	0.0001082	0.0149494	0.6622	0.0048	0.667	1.91
1	101325	0	1	0.0000	0.0181879	0.0149155	0	0.0149155	0.6655	0	0.6655	------

Extended Langmuir Model for CH4-CO / Turkish clinoptilolite at 40.0°C and 101325 Pa total pressure

Direct approach

y1 (CH4)	P1 (CH4) [Pa]	P2 (CO) [Pa]	x1 (CH4)	x2 (CO)	v1 (CH4) [m3 STP/kg]	v2 (CO) [m3 STP/kg]	vt [m3 STP/kg]	n1 (CH4) [mol/kg]	n2 (CO) [mol/kg]	nt [mol/kg]	alpha21 CO/CH4
0	0	101325	0	1	0	0.0211077	0.0211077	0	0.9418	0.9418	.....
0.0701	7101.6757	94223.324	0.0296	0.9704	0.0006169	0.0202348	0.0208516	0.0275225	0.9028	0.9303	2.47
0.1338	13554.891	87770.109	0.0588	0.9412	0.0012114	0.0193934	0.0206048	0.0540494	0.8653	0.9193	2.47
0.1918	19434.087	81890.913	0.0876	0.9124	0.0017838	0.0185834	0.0203672	0.0795869	0.8291	0.9087	2.47
0.2448	24803.705	76521.295	0.1159	0.8841	0.0023342	0.0178044	0.0201387	0.1041476	0.7944	0.8985	2.47
0.2933	29719.672	71605.328	0.1437	0.8563	0.0028632	0.0170558	0.019919	0.1277494	0.761	0.8887	2.47
0.3378	34230.652	67094.348	0.1711	0.8289	0.0033712	0.016337	0.0197082	0.1504139	0.7289	0.8793	2.47
0.3788	38379.104	62945.896	0.1978	0.8022	0.0038587	0.0156471	0.0195058	0.1721659	0.6981	0.8703	2.47
0.4165	42202.173	59122.827	0.224	0.7760	0.0043264	0.0149852	0.0193116	0.1930324	0.6686	0.8616	2.47
0.4513	45732.438	55592.562	0.2497	0.7503	0.0047748	0.0143506	0.0191254	0.2130416	0.6403	0.8533	2.47
0.4836	48998.559	52326.441	0.2747	0.7253	0.0052048	0.0137422	0.018947	0.2322232	0.6131	0.8454	2.47
0.7057	71503.589	29821.411	0.4923	0.5077	0.0086284	0.0088972	0.0175256	0.3849799	0.397	0.7819	2.47
0.8240	83495.612	17829.388	0.6545	0.3455	0.0108629	0.0057351	0.016598	0.4846762	0.2559	0.7406	2.47
0.8930	90481.247	10843.753	0.7714	0.2286	0.0123332	0.0036544	0.0159876	0.5502763	0.163	0.7133	2.47
0.9353	94767.376	6557.6243	0.8539	0.1461	0.0133068	0.0022766	0.0155834	0.593717	0.1016	0.6953	2.47
0.9620	97469.859	3855.1406	0.9109	0.0891	0.0139515	0.0013643	0.0153158	0.6224795	0.0609	0.6834	2.47
0.9789	99188.964	2136.0364	0.9494	0.0506	0.0143747	0.0007654	0.01514	0.6413631	0.0341	0.6755	2.47
0.9896	100273.95	1051.0473	0.9747	0.0253	0.0146473	0.0003796	0.0150269	0.6535258	0.0169	0.6705	2.47
0.9962	100939.96	385.03601	0.9907	0.0093	0.0148168	0.0001397	0.0149565	0.6610879	0.0062	0.6673	2.47
1	101325	0	1	0.0000	0.0149155	0	0.0149155	0.6654936	0	0.6655	.....

Extended Langmuir Model for N2-CH4 / Turkish clinoptilolite at 22.6-22.8°C and 101325 Pa total pressure

Averaging approach

y1 (N2)	P1 (N2) [Pa]	P2 (CH4) [Pa]	x1 (N2)	x2 (CH4)	vm [m3 STP/kg]	v1 (N2) [m3 STP/kg]	v2 (CH4) [m3 STP/kg]	vt [m3 STP/kg]	n1 (N2) [mol/kg]	n2 (CH4) [mol/kg]	nt [mol/kg]	alpha21 CH4/N2
0	0	101325	0	1	0.0209926	0	0.0179207	0.0179207	0	0.7996	0.7996	.....
0.0458	4640.763	96684.237	0.0607	0.9393	0.0203793	0.0010586	0.0163784	0.017437	0.0472	0.7308	0.778	0.74
0.1247	12634.421	88690.579	0.161	0.839	0.0194415	0.0026875	0.0140102	0.0166977	0.1199	0.6251	0.745	0.74
0.2384	24159.363	77165.637	0.2966	0.7034	0.0183021	0.0046858	0.0111145	0.0158003	0.2091	0.4959	0.705	0.74
0.3786	38363.953	62961.047	0.4507	0.5493	0.017159	0.0067159	0.0081851	0.014901	0.2996	0.3652	0.6648	0.74
0.5288	53578.305	47746.695	0.6018	0.3982	0.0161694	0.0084988	0.0056245	0.0141233	0.3792	0.2509	0.6301	0.74
0.6712	68010.387	33314.613	0.7333	0.2667	0.0153963	0.0099112	0.0036054	0.0135166	0.4422	0.1609	0.6031	0.74
0.793	80354.630	20970.370	0.8377	0.1623	0.0148333	0.0109526	0.0021226	0.0130752	0.4887	0.0947	0.5834	0.74
0.8882	89992.249	11332.751	0.9145	0.0855	0.0144447	0.0116786	0.0010922	0.0127708	0.5211	0.0487	0.5698	0.74
0.9561	96878.248	4446.752	0.967	0.033	0.0141903	0.0121572	0.0004144	0.0125716	0.5424	0.0185	0.5609	0.74
1	101325	0	1	0	0.0140353	0.0124503	0	0.0124503	0.5555	0	0.5555	.....

Direct approach

y1 (N2)	P1 (N2) [Pa]	P2 (CH4) [Pa]	x1 (N2)	x2 (CH4)	v1 (N2) [m3 STP/kg]	v2 (CH4) [m3 STP/kg]	vt [m3 STP/kg]	n1 (N2) [mol/kg]	n2 (CH4) [mol/kg]	nt [mol/kg]	alpha21 CH4/N2
0	0	101325	0	1	0	0.0179207	0.0179207	0	0.7996	0.7996	.....
0.0458	4640.763	96684.237	0.0414	0.9586	0.0007291	0.0168713	0.0176003	0.0325292	0.7528	0.7853	1.11
0.1247	12634.421	88690.579	0.1137	0.8863	0.0019402	0.015128	0.0170682	0.0865667	0.675	0.7615	1.11
0.2384	24159.363	77165.637	0.2199	0.7801	0.0035934	0.0127484	0.0163418	0.1603283	0.5688	0.7291	1.11
0.3786	38363.953	62961.047	0.3542	0.6458	0.0054933	0.0100137	0.0155071	0.2450979	0.4468	0.6919	1.11
0.5288	53578.305	47746.695	0.5026	0.4974	0.0073771	0.0073022	0.0146794	0.3291492	0.3258	0.655	1.11
0.6712	68010.387	33314.613	0.6476	0.3524	0.009035	0.0049159	0.0139509	0.4031205	0.2193	0.6225	1.11
0.793	80354.63	20970.37	0.7753	0.2247	0.0103633	0.003004	0.0133673	0.4623839	0.134	0.5964	1.11
0.8882	89992.249	11332.751	0.8773	0.1227	0.0113476	0.0015873	0.0129348	0.5063013	0.0708	0.5771	1.11
0.9561	96878.248	4446.752	0.9515	0.0485	0.0120244	0.000613	0.0126375	0.5364997	0.0274	0.5639	1.11
1	101325	0	1	0	0.0124503	0	0.0124503	0.5555029	0	0.5555	.....

Extended Langmuir Model for N2-CH4 / Turkish clinoptilolite at 40.0°C and 101325 Pa total pressure

Averaging approach

y1 (N2)	P1 (N2) [Pa]	P2 (CH4) [Pa]	x1 (N2)	x2 (CH4)	vm [m3 STP/kg]	v1 (N2) [m3 STP/kg]	v2 (CH4) [m3 STP/kg]	vt [m3 STP/kg]	n1 (N2) [mol/kg]	n2 (CH4) [mol/kg]	nt [mol/kg]	alpha21 CH4/N2
0	0	101325	0	1	0.0181879	0	0.0149155	0.0149155	0	0.6655	0.6655	.....
0.0458	4640.763	96684.237	0.063	0.937	0.017586	0.0009118	0.0135571	0.0144689	0.0407	0.6049	0.6456	0.71
0.1247	12634.421	88690.579	0.1664	0.8336	0.0166805	0.0022959	0.0115017	0.0137976	0.1024	0.5132	0.6156	0.71
0.2384	24159.363	77165.637	0.3049	0.6951	0.0156038	0.0039643	0.0090363	0.0130006	0.1769	0.4032	0.5801	0.71
0.3786	38363.953	62961.047	0.4606	0.5394	0.0145488	0.0056287	0.0065924	0.0122211	0.2511	0.2941	0.5453	0.71
0.5288	53578.305	47746.695	0.6113	0.3887	0.0136549	0.0070675	0.0044947	0.0115622	0.3153	0.2005	0.5159	0.71
0.6712	68010.387	33314.613	0.741	0.259	0.012969	0.0081935	0.0028643	0.0110577	0.3656	0.1278	0.4934	0.71
0.793	80354.63	20970.37	0.843	0.157	0.0124761	0.0090166	0.0016793	0.0106959	0.4023	0.0749	0.4772	0.71
0.8882	89992.249	11332.751	0.9175	0.0825	0.012139	0.0095873	0.0008616	0.0104489	0.4278	0.0384	0.4662	0.71
0.9561	96878.248	4446.752	0.9683	0.0317	0.0119197	0.0099621	0.0003263	0.0102884	0.4445	0.0146	0.459	0.71
1	101325	0	1	0	0.0117867	0.0101911	0	0.0101911	0.4547	0	0.4547	.....

Direct approach

y1 (N2)	P1 (N2) [Pa]	P2 (CH4) [Pa]	x1 (N2)	x2 (CH4)	v1 (N2) [m3 STP/kg]	v2 (CH4) [m3 STP/kg]	vt [m3 STP/kg]	n1 (N2) [mol/kg]	n2 (CH4) [mol/kg]	nt [mol/kg]	alpha21 CH4/N2
0	0	101325	0	1	0	0.0149155	0.0149155	0	0.6655	0.6655	.....
0.0458	4640.763	96684.237	0.0418	0.9582	0.0006111	0.0140211	0.0146322	0.0272675	0.6256	0.6529	1.10
0.1247	12634.421	88690.579	0,1145	0.8855	0.0016223	0.0125411	0.0141634	0.0723842	0.5596	0.6319	1.10
0.2384	24159.363	77165.637	0.2214	0.7786	0.0029945	0.0105328	0.0135273	0.1336084	0.4699	0.6036	1.10
0.3786	38363.953	62961.047	0.3562	0.6438	0.0045601	0.0082414	0.0128015	0.2034612	0.3677	0.5712	1.10
0.5288	53578.305	47746.695	0.5047	0.4953	0.0061005	0.0059868	0.0120874	0.2721909	0.2671	0.5393	1.10
0.6712	68010.387	33314.613	0.6496	0.3504	0.0074465	0.0040169	0.0114634	0.3322453	0.1792	0.5115	1.10
0.793	80354.63	20970.37	0.7768	0.2232	0.0085184	0.0024481	0.0109665	0.3800697	0.1092	0.4893	1.10
0.8882	89992.249	11332.751	0.8782	0.1218	0.009309	0.001291	0.0106	0.4153453	0.0576	0.4729	1.10
0.9561	96878.248	4446.752	0.9519	0.0481	0.0098509	0.0004979	0.0103488	0.4395206	0.0222	0.4617	1.10
1	101325	0	1	0	0.0101911	0	0.0101911	0.4546999	0	0.4547	.....

Extended Langmuir Model for N2-CO / Cuban clinoptilolite at 40.0-40.1°C and 101325 Pa total pressure

Averaging approach

y1 (N2)	P1 (N2) [Pa]	P2 (CO) [Pa]	x1 (N2)	x2 (CO)	vm [m3 STP/kg]	v1 (N2) [m3 STP/kg]	v2 (CO) [m3 STP/kg]	vt [m3 STP/kg]	n1 (N2) [mol/kg]	n2 (CO) [mol/kg]	nt [mol/kg]	alpha21 CO/N2
0	0.000	101325.000	0	1	0.0150452	0	0.0124417	0.0124417	0	0.5551	0.5551	.....
0.0990	10030.936	91294.064	0.0334	0.9666	0.0150817	0.0004113	0.0119054	0.0123167	0.0184	0.5312	0.5495	3.18
0.2647	26824.553	74500.447	0.1017	0.8983	0.015157	0.0012277	0.0108432	0.0120709	0.0548	0.4838	0.5386	3.18
0.4545	46048.385	55276.615	0.2076	0.7924	0.015275	0.0024317	0.0092826	0.0117144	0.1085	0.4142	0.5227	3.18
0.6198	62805.311	38519.689	0.3389	0.6611	0.0154241	0.0038331	0.0074759	0.011309	0.171	0.3336	0.5046	3.18
0.7454	75529.863	25795.137	0.4794	0.5206	0.0155867	0.0052326	0.0056829	0.0109155	0.2335	0.2536	0.487	3.18
0.8352	84622.674	16702.326	0.6144	0.3856	0.0157463	0.0064948	0.0040765	0.0105713	0.2898	0.1819	0.4717	3.18
0.8984	91032.098	10292.902	0.7355	0.2645	0.0158923	0.0075669	0.0027208	0.0102876	0.3376	0.1214	0.459	3.18
0.9434	95589.462	5735.538	0.8398	0.1602	0.0160202	0.0084486	0.0016121	0.0100607	0.377	0.0719	0.4489	3.18
0.9759	98888.020	2436.980	0.9273	0.0727	0.0161291	0.0091632	0.0007181	0.0098813	0.4088	0.032	0.4409	3.18
1	101325.000	0.000	1	0	0.0162207	0.0097396	0	0.0097396	0.4346	0	0.4346	.....

Direct approach

y1(N2)	P1 (N2) [Pa]	P2 (CO) [Pa]	x1 (N2)	x2 (CO)	v1 (N2) [m3 STP/kg]	v2 (CO) [m3 STP/kg]	vt [m3 STP/kg]	n1(N2) [mol/kg]	n2 (CO) [mol/kg]	nt [mol/kg]	alpha21 (CO/N2)
0	0.000	101325.000	0	1	0	0.0124417	0.0124417	0	0.5551	0.5551	.....
0.0990	10030.936	91294.064	0.0359	0.9641	0.0004424	0.0118765	0.012319	0.0197395	0.5299	0.5496	2.95
0.2647	26824.553	74500.447	0.1088	0.8912	0.0013139	0.0107633	0.0120772	0.0586225	0.4802	0.5389	2.95
0.4545	46048.385	55276.615	0.2202	0.7798	0.0025823	0.009143	0.0117253	0.1152147	0.4079	0.5232	2.95
0.6198	62805.311	38519.689	0.356	0.6440	0.004031	0.0072923	0.0113233	0.1798553	0.3254	0.5052	2.95
0.7454	75529.863	25795.137	0.4982	0.5018	0.0054455	0.0054855	0.0109309	0.2429628	0.2447	0.4877	2.95
0.8352	84622.674	16702.326	0.632	0.3680	0.0066905	0.003895	0.0105855	0.2985131	0.1738	0.4723	2.95
0.8984	91032.098	10292.902	0.7499	0.2501	0.0077232	0.0025757	0.010299	0.3445913	0.1149	0.4595	2.95
0.9434	95589.462	5735.538	0.8496	0.1504	0.0085544	0.001514	0.0100684	0.3816764	0.0675	0.4492	2.95
0.9759	98888.020	2436.980	0.9322	0.0678	0.0092152	0.0006698	0.009885	0.411159	0.0299	0.441	2.95
1	101325.000	0.000	1	0.0000	0.0097396	0	0.0097396	0.4345548	0	0.4346	.....

Extended Langmuir Model for CH4-CO / Cuban clinoptilolite at 39.9-40.1°C and 101325 Pa total pressure

Averaging approach

y1 (CH4)	P1 (CH4) [Pa]	P2 (CO) [Pa]	x1 (CH4)	x2 (CO)	vm [m3 STP/kg]	v1 (CH4) [m3 STP/kg]	v2 (CO) [m3 STP/kg]	vt [m3 STP/kg]	n1 (CH4) [mol/kg]	n2 (CO) [mol/kg]	nt [mol/kg]	alpha21 CO/CH4
0	0.000	101325.000	0	1	0.0150452	0	0.0124417	0.0124417	0	0.5551	0.5551	-------
0.0189	1913.090	99411.910	0.0504	0.9496	0.0152627	0.0000872	0.0125077	0.0125949	0.0039	0.5581	0.562	0.36
0.1076	10905.627	90419.373	0.2498	0.7502	0.016187	0.0005533	0.0126641	0.0132173	0.0247	0.565	0.5897	0.36
0.2875	29133.731	72191.269	0.527	0.4730	0.0176755	0.0017944	0.0122756	0.0140701	0.0801	0.5477	0.6278	0.36
0.5017	50837.504	50487.496	0.7354	0.2646	0.0189886	0.0038806	0.0106396	0.0145203	0.1731	0.4747	0.6479	0.36
0.6800	68905.864	32419.136	0.8544	0.1456	0.0198292	0.0062982	0.0081806	0.0144788	0.281	0.365	0.646	0.36
0.8039	81453.365	19871.635	0.9188	0.0812	0.0203162	0.0084928	0.0057201	0.0142128	0.3789	0.2552	0.6341	0.36
0.8852	89688.405	11636.595	0.9551	0.0449	0.0206014	0.0102451	0.0036697	0.0139148	0.4571	0.1637	0.6208	0.36
0.9387	95111.398	6213.602	0.9769	0.0231	0.0207763	0.0115693	0.0020866	0.0136559	0.5162	0.0931	0.6093	0.36
0.9748	98773.957	2551.043	0.9907	0.0093	0.0208891	0.012554	0.0008951	0.0134491	0.5601	0.0399	0.6001	0.36
1	101325.000	0.000	1	0	0.0209652	0.0132884	0	0.0132884	0.5929	0	0.5929	-------

Direct approach

y1 (CH4)	P1 (CH4) [Pa]	P2 (CO) [Pa]	x1 (CH4)	x2 (CO)	v1 (CH4) [m3 STP/kg]	v2 (CO) [m3 STP/kg]	vt [m3 STP/kg]	n1 (CH4) [mol/kg]	n2 (CO) [mol/kg]	nt [mol/kg]	alpha21 CO/CH4
0.0000	0.000	101325.000	0	1	0	0.0124417	0.0124417	0	0.5551	0.5551	-------
0.0189	1913.090	99411.910	0.0096	0.9904	0.0001198	0.0123296	0.0124493	0.0053435	0.5501	0.5555	1.98
0.1076	10905.627	90419.373	0.0574	0.9426	0.0007166	0.0117708	0.0124874	0.0319722	0.5252	0.5572	1.98
0.2875	29133.731	72191.269	0.1692	0.8308	0.0021284	0.0104489	0.0125773	0.0949644	0.4662	0.5612	1.98
0.5017	50837.504	50487.496	0.337	0.6630	0.0042846	0.0084301	0.0127147	0.191167	0.3761	0.5673	1.98
0.6800	68905.864	32419.136	0.5176	0.4824	0.006659	0.006207	0.012866	0.297108	0.2769	0.574	1.98
0.8039	81453.365	19871.635	0.6742	0.3258	0.0087641	0.004236	0.0130001	0.391032	0.189	0.58	1.98
0.8852	89688.405	11636.595	0.7955	0.2045	0.010426	0.00268	0.013106	0.4651825	0.1196	0.5848	1.98
0.9387	95111.398	6213.602	0.8854	0.1146	0.0116745	0.001511	0.0131856	0.5208878	0.0674	0.5883	1.98
0.9748	98773.957	2551.043	0.9513	0.0487	0.0125998	0.0006447	0.0132445	0.5621717	0.0288	0.5909	1.98
1	101325.000	0.000	1	0.0000	0.0132884	0	0.0132884	0.5928947	0	0.5929	-------

Extended Langmuir Model for N2-CH4 / Cuban clinoptilolite at 39.9-40.0°C and 101325 Pa total pressure

Averaging approach

y1 (N2)	P1 (N2) [Pa]	P2 (CH4) [Pa]	x1 (N2)	x2 (CH4)	vm [m3 STP/kg]	v1 (N2) [m3 STP/kg]	v2 (CH4) [m3 STP/kg]	vt [m3 STP/kg]	n1 (N2) [mol/kg]	n2 (CH4) [mol/kg]	nt [mol/kg]	alpha21 CH4/N2
0	0	101325.000	0	1	0.0209652	0	0.0132884	0.0132884	0	0.5929	0.5929	-------
0.1410	14291.598	87033.402	0.1248	0.8752	0.020227	0.0015886	0.0111436	0.0127322	0.0709	0.4972	0.5681	1.15
0.2750	27865.150	73459.850	0.2477	0.7523	0.0195487	0.0030278	0.0091944	0.0122222	0.1351	0.4102	0.5453	1.15
0.4009	40624.997	60700.003	0.3675	0.6325	0.0189303	0.0043212	0.0074371	0.0117583	0.1928	0.3318	0.5246	1.15
0.5180	52483.767	48841.233	0.4826	0.5174	0.0183717	0.0054732	0.0058669	0.0113401	0.2442	0.2618	0.506	1.15
0.6254	63364.543	37960.457	0.5917	0.4083	0.0178721	0.0064891	0.0044779	0.010967	0.2895	0.1998	0.4893	1.15
0.7225	73202.656	28122.344	0.6932	0.3068	0.0174308	0.0073747	0.0032634	0.0106381	0.329	0.1456	0.4746	1.15
0.8088	81947.021	19377.979	0.7859	0.2141	0.0170465	0.008136	0.0022161	0.0103522	0.363	0.0989	0.4619	1.15
0.8839	89560.987	11764.013	0.8686	0.1314	0.0167179	0.0087797	0.0013284	0.0101081	0.3917	0.0593	0.451	1.15
0.9477	96022.688	5302.312	0.9402	0.0598	0.0164433	0.0093121	0.0005923	0.0099044	0.4155	0.0264	0.4419	1.15
1	101325.000	0	1	0	0.0162207	0.0097396	0	0.0097396	0.4346	0	0.4346	-------

Direct approach

y1 (N2)	P1 (N2) [Pa]	P2 (CH4) [Pa]	x1 (N2)	x2 (CH4)	v1 (N2) [m3 STP/kg]	v2 (CH4) [m3 STP/kg]	vt [m3 STP/kg]	n1 (N2) [mol/kg]	n2 (CH4) [mol/kg]	nt [mol/kg]	alpha21 CH4/N2
0	0	101325.000	0	1	0	0.0132884	0.0132884	0	0.5929	0.5929	-------
0.1410	14291.598	87033.402	0.0993	0.9007	0.001274	0.0115502	0.0128242	0.0568406	0.5153	0.5722	1.49
0.2750	27865.150	73459.850	0.2031	0.7969	0.0025124	0.0098606	0.0123729	0.1120952	0.44	0.5521	1.49
0.4009	40624.997	60700.003	0.3101	0.6899	0.0037027	0.0082365	0.0119392	0.1652047	0.3675	0.5327	1.49
0.5180	52483.767	48841.233	0.4192	0.5808	0.0048324	0.0066951	0.0115276	0.2156112	0.2987	0.5143	1.49
0.6254	63364.543	37960.457	0.5286	0.4714	0.0058895	0.0052529	0.0111424	0.2627758	0.2344	0.4971	1.49
0.7225	73202.656	28122.344	0.6362	0.3638	0.0068627	0.0039251	0.0107878	0.3061964	0.1751	0.4813	1.49
0.8088	81947.021	19377.979	0.7396	0.2604	0.0077419	0.0027256	0.0104674	0.3454241	0.1216	0.467	1.49
0.8839	89560.987	11764.013	0.8364	0.1636	0.0085186	0.0016659	0.0101844	0.3800783	0.0743	0.4544	1.49
0.9477	96022.688	5302.312	0.924	0.0760	0.0091861	0.0007552	0.0099412	0.4098589	0.0337	0.4436	1.49
1	101325.000	0	1	0	0.0097396	0	0.0097396	0.4345548	0	0.4346	-------

Extended Langmuir Model for N2-CO / AlPO4-11 at 22.6-22.8°C and 101325 Pa total pressure

Averaging approach

y1 (N2)	P1 (N2) [Pa]	P2 (CO) [Pa]	x1 (N2)	x2 (CO)	nm [mol/kg]	n1 (N2) [mol/kg]	n2 (CO) [mol/kg]	nt [mol/kg]	v1 (N2) [m3 STP/kg]	v2 (CO) [m3 STP/kg]	vt [m3 STP/kg]	alpha21 CO/N2
0	0	101325	0	1	1.31864	0	0.18912	0.1891156	0	0.0042386	0.0042386	-------
0.1148	11635.982	89689.018	0.1867	0.8133	0.79335	0.02282	0.09945	0.1222775	0.0005115	0.002229	0.0027406	0.57
0.2442	24739.407	76585.593	0.3636	0.6364	0.57585	0.03473	0.06079	0.0955189	0.0007785	0.0013624	0.0021408	0.57
0.3851	39022.302	62302.698	0.5256	0.4744	0.46035	0.04314	0.03894	0.0820845	0.0009669	0.0008728	0.0018397	0.57
0.5316	53861.757	47463.243	0.6675	0.3325	0.39155	0.04988	0.02485	0.0747248	0.0011179	0.0005569	0.0016748	0.57
0.6738	68274.607	33050.393	0.7851	0.2149	0.34837	0.05543	0.01517	0.0706008	0.0012424	0.00034	0.0015824	0.57
0.7998	81042.272	20282.728	0.876	0.1240	0.32102	0.05986	0.00847	0.0683258	0.0013416	0.0001898	0.0015314	0.57
0.8982	91011.932	10313.068	0.9398	0.0602	0.30427	0.06308	0.00404	0.067125	0.0014139	0.0000906	0.0015045	0.57
0.9622	97490.509	3834.4906	0.9782	0.0218	0.29499	0.06509	0.00145	0.0665421	0.0014589	0.0000324	0.0014914	0.57
0.9927	100580.55	744.44592	0.9958	0.0042	0.29093	0.06603	0.00028	0.0663092	0.00148	6.19E-06	0.0014862	0.57
0.9998	101309.59	15.411533	0.9999	0.0001	0.29	0.06625	6E-06	0.0662581	0.0014849	1.28E-07	0.001485	0.57
1	101325	0	1	0	0.28998	0.06626	0	0.066257	0.001485	0	0.001485	-------

Direct approach

y1 (N2)	P1 (N2) [Pa]	P2 (CO) [Pa]	x1 (N2)	x2 (CO)	n1 (N2) [mol/kg]	n2 (CO) [mol/kg]	nt [mol/kg]	v1 (N2) [m3 STP/kg]	v2 (CO) [m3 STP/kg]	vt [m3 STP/kg]	alpha21 CO/N2
0	0	101325	0	1	0	0.18912	0.18912	0	0.0042386	0.0042386	-------
0.1148	11635.982	89689.018	0.048	0.9520	0.00834	0.1653	0.17365	0.000187	0.0037049	0.0038919	2.57
0.2442	24739.407	76585.593	0.1116	0.8884	0.01749	0.13919	0.15668	0.000392	0.0031197	0.0035117	2.57
0.3851	39022.302	62302.698	0.1959	0.8041	0.02718	0.11155	0.13872	0.0006091	0.0025001	0.0031092	2.57
0.5316	53861.757	47463.243	0.3062	0.6938	0.03694	0.08368	0.12062	0.0008279	0.0018755	0.0027034	2.57
0.6738	68274.607	33050.393	0.4455	0.5545	0.04614	0.05742	0.10356	0.0010341	0.0012869	0.0023211	2.57
0.7998	81042.272	20282.728	0.6085	0.3915	0.05407	0.03479	0.08886	0.0012118	0.0007797	0.0019915	2.57
0.8982	91011.932	10313.068	0.7744	0.2256	0.06012	0.01751	0.07763	0.0013475	0.0003925	0.00174	2.57
0.9622	97490.509	3834.4906	0.9082	0.0918	0.06399	0.00647	0.07046	0.0014342	0.000145	0.0015792	2.57
0.9927	100580.55	744.44592	0.9813	0.0187	0.06582	0.00125	0.06707	0.0014752	0.0000281	0.0015032	2.57
0.9998	101309.59	15.411533	0.9996	0.0004	0.06625	0.00003	0.06627	0.0014848	5.81E-07	0.0014854	2.57
1	101325	0	1	0	0.06626	0	0.06626	0.001485	0	0.001485	-------

Extended Langmuir Model for N2-CO / AlPO4-11 at 40.0°C and 101325 Pa total pressure

Averaging approach

y1 (N2)	P1 (N2) [Pa]	P2 (CO) [Pa]	x1 (N2)	x2 (CO)	nm [mol/kg]	n1 (N2) [mol/kg]	n2 (CO) [mol/kg]	nt [mol/kg]	v1 (N2) [m3 STP/kg]	v2 (CO) [m3 STP/kg]	vt [m3 STP/kg]	alpha21 CO/N2
0	0.00	101325	0	1	1.92467	0	0.14033	0.1403348	0	0.0031453	0.0031453	-------
0.0852	8629.93	92695.068	0.163	0.8370	1.09219	0.01409	0.07236	0.0864554	0.0003159	0.0016218	0.0019377	0.48
0.1897	19222.32	82102.683	0.3288	0.6712	0.75858	0.02162	0.04415	0.0657747	0.0004847	0.0009895	0.0014742	0.48
0.3155	31970.06	69354.94	0.4909	0.5091	0.58404	0.02742	0.02843	0.0558532	0.0006145	0.0006373	0.0012518	0.48
0.4611	46717.13	54607.871	0.6415	0.3585	0.4812	0.03264	0.01824	0.0508829	0.0007316	0.0004088	0.0011404	0.48
0.6181	62627.66	38697.337	0.772	0.2280	0.41753	0.03752	0.01108	0.0485991	0.0008409	0.0002484	0.0010892	0.48
0.7694	77955.97	23369.03	0.8747	0.1253	0.37815	0.04181	0.00599	0.0478068	0.0009372	0.0001343	0.0010715	0.48
0.8918	90358.64	10966.359	0.9452	0.0548	0.35514	0.04511	0.00262	0.0477218	0.0010109	0.0000586	0.0010696	0.48
0.9673	98011.25	3313.75	0.9841	0.0159	0.3436	0.04707	0.00076	0.0478316	0.001055	0.0000171	0.001072	0.48
0.9963	100945.58	379.41754	0.9982	0.0018	0.3396	0.04781	0.00009	0.0478993	0.0010716	1.93E-06	0.0010736	0.48
0.99998	101323.29	1.7052998	1	0.00001	0.339102	0.047908	4E-07	0.04790887	0.00107376	8.64E-09	0.00107377	0.48
1	101325.00	0	1	0	0.339100	0.047909	0	0.04790891	0.00107377	0	0.00107377	-------

Direct approach

y1 (N2)	P1 (N2) [Pa]	P2 (CO) [Pa]	x1 (N2)	x2 (CO)	n1 (N2) [mol/kg]	n2 (CO) [mol/kg]	nt [mol/kg]	v1 (N2) [m3 STP/kg]	v2 (CO) [m3 STP/kg]	vt [m3 STP/kg]	alpha21 CO/N2
0	0	101325	0	1	0	0.14033	0.14033	0	0.0031453	0.0031453	-------
0.0852	8629.9323	92695.068	0.0332	0.9668	0.00438	0.12752	0.13189	0.0000981	0.002858	0.0029561	2.71
0.1897	19222.317	82102.683	0.0794	0.9206	0.00967	0.11202	0.12169	0.0002167	0.0025107	0.0027273	2.71
0.3155	31970.06	69354.94	0.1452	0.8548	0.01592	0.0937	0.10962	0.0003568	0.0021001	0.0024569	2.71
0.4611	46717.129	54607.871	0.2397	0.7603	0.023	0.07295	0.09596	0.0005156	0.0016351	0.0021507	2.71
0.6181	62627.663	38697.337	0.3736	0.6264	0.03047	0.05108	0.08155	0.0006829	0.0011449	0.0018278	2.71
0.7694	77955.97	23369.03	0.5515	0.4485	0.0375	0.0305	0.068	0.0008404	0.0006835	0.001524	2.71
0.8918	90358.641	10966.359	0.7523	0.2477	0.04307	0.01418	0.05725	0.0009653	0.0003178	0.0012831	2.71
0.9673	98011.25	3313.75	0.916	0.0840	0.04645	0.00426	0.05072	0.0010412	0.0000955	0.0011367	2.71
0.9963	100945.58	379.41754	0.9899	0.0101	0.04774	0.00049	0.04823	0.00107	0.0000109	0.001081	2.71
0.99998	101323.29	1.7052998	1	0.0000	0.04791	2E-06	0.04791	0.0010738	4.90E-08	0.0010738	2.71
1	101325	0	1	0.0000	0.04791	0	0.04791	0.0010738	0	0.0010738	-------

Extended Langmuir Model for CH4-CO / AlPO4-11 at 22.6-22.8°C and 101325 Pa total pressure

Averaging approach

y1 (CH4)	P1 (CH4) [Pa]	P2 (CO) [Pa]	x1 (CH4)	x2 (CO)	nm [mol/kg]	n1 (CH4) [mol/kg]	n2 (CO) [mol/kg]	nt [mol/kg]	v1 (CH4) [m3 STP/kg]	v2 (CO) [m3 STP/kg]	vt [m3 STP/kg]	alpha12 CH4/CO
0	0	101325	0	1	1.31864	0	0.18912	0.1891156	0	0.0042386	0.0042386	-------
0.0427	4329.1907	96995.809	0.0498	0.9502	1.34664	0.00968	0.18468	0.1943615	0.0002169	0.0041392	0.0043562	1.17
0.0961	9741.197	91583.803	0.111	0.8890	1.38274	0.02233	0.17881	0.2011473	0.0005005	0.0040077	0.0045083	1.17
0.1608	16292.201	85032.799	0.1837	0.8163	1.42816	0.03852	0.1712	0.2097177	0.0008633	0.0038371	0.0047003	1.17
0.2373	24047.613	77277.387	0.2676	0.7324	1.48453	0.05898	0.16142	0.220402	0.0013219	0.0036179	0.0049398	1.17
0.3265	33084.229	68240.771	0.3628	0.6372	1.55404	0.08476	0.14889	0.2336468	0.0018997	0.003337	0.0052367	1.17
0.4292	43492.667	57832.333	0.4689	0.5311	1.63972	0.11727	0.1328	0.2500667	0.0026283	0.0029764	0.0056047	1.17
0.5466	55380.276	45944.724	0.586	0.4140	1.74581	0.15852	0.112	0.270524	0.0035529	0.0025103	0.0060632	1.17
0.6797	68874.723	32450.277	0.7136	0.2864	1.87839	0.21143	0.08483	0.2962605	0.0047386	0.0019014	0.00664	1.17
0.8303	84128.538	17196.462	0.8517	0.1483	2.04647	0.28032	0.0488	0.3291217	0.0062828	0.0010937	0.0073765	1.17
0.9821	99511.958	1813.0417	0.9847	0.0153	2.23948	0.36151	0.00561	0.3671194	0.0081024	0.0001257	0.0082281	1.17
1	101325	0	1	0	2.26401	0.37197	0	0.3719665	0.0083368	0	0.0083368	-------

Direct approach

y1 (CH4)	P1 (CH4) [Pa]	P2 (CO) [Pa]	x1 (CH4)	x2 (CO)	n1 (CH4) [mol/kg]	n2 (CO) [mol/kg]	nt [mol/kg]	v1 (CH4) [m3 STP/kg]	v2 (CO) [m3 STP/kg]	vt [m3 STP/kg]	alpha12 CH4/CO
0	0	101325	0	1	0	0.18912	0.18912	0	0.0042386	0.0042386	-------
0.0427	4329.1907	96995.809	0.0826	0.9174	0.01627	0.18084	0.19711	0.0003647	0.0040532	0.0044179	2.02
0.0961	9741.197	91583.803	0.1766	0.8234	0.03657	0.17052	0.20709	0.0008195	0.0038219	0.0046415	2.02
0.1608	16292.201	85032.799	0.2786	0.7214	0.06106	0.15807	0.21913	0.0013685	0.0035428	0.0049113	2.02
0.2373	24047.613	77277.387	0.3855	0.6145	0.08995	0.14338	0.23333	0.0020161	0.0032136	0.0052296	2.02
0.3265	33084.229	68240.771	0.4943	0.5057	0.12348	0.12634	0.24982	0.0027675	0.0028315	0.0055991	2.02
0.4292	43492.667	57832.333	0.6026	0.3974	0.16192	0.10679	0.26871	0.003629	0.0023936	0.0060225	2.02
0.5466	55380.276	45944.724	0.7085	0.1894	0.20557	0.0846	0.29017	0.0046075	0.0018961	0.0065035	2.02
0.6797	68874.723	32450.277	0.8106	0.0921	0.25483	0.05955	0.31438	0.0057114	0.0013348	0.0070462	2.02
0.8303	84128.538	17196.462	0.9079	0.0921	0.31012	0.03144	0.34156	0.0069506	0.0007047	0.0076554	2.02
0.9821	99511.958	1813.0417	0.991	0.0090	0.36547	0.0033	0.36877	0.0081912	0.000074	0.0082652	2.02
1	101325	0	1	0	0.37197	0	0.37197	0.0083368	0	0.0083368	-------

Extended Langmuir Model for CH4-CO / AlPO4-11 at 40.0°C and 101325 Pa total pressure

Averaging approach

y1 (CH4)	P1 (CH4) [Pa]	P2 (CO) [Pa]	x1 (CH4)	x2 (CO)	nm [mol/kg]	n1 (CH4) [mol/kg]	n2 (CO) [mol/kg]	nt [mol/kg]	v1 (CH4) [m3 STP/kg]	v2 (CO) [m3 STP/kg]	vt [m3 STP/kg]	alpha12 CH4/CO
0	0	101325	0	1	1.92467	0	0.14033	0.1403348	0	0.0031453	0.0031453	-------
0.0499	5060.2313	96264.769	0.0717	0.9283	1.96552	0.0105	0.13592	0.1464215	0.0002353	0.0030464	0.0032817	1.47
0.1058	10717.603	90607.397	0.1481	0.8519	2.01099	0.0227	0.13065	0.1533507	0.0005089	0.0029281	0.003437	1.47
0.1686	17084.078	84240.922	0.2296	0.7704	2.06189	0.03703	0.12427	0.1613031	0.0008299	0.0027853	0.0036152	1.47
0.2398	24301.438	77023.562	0.3167	0.6833	2.11926	0.05401	0.11651	0.1705132	0.0012104	0.0026112	0.0038217	1.47
0.3213	32551.909	68773.091	0.4102	0.5898	2.18442	0.07436	0.10693	0.1812907	0.0016666	0.0023966	0.0040632	1.47
0.4152	42073.658	59251.342	0.5106	0.4894	2.25906	0.09908	0.09497	0.1940519	0.0022207	0.0021286	0.0043492	1.47
0.5249	53184.023	48140.977	0.6188	0.3812	2.34541	0.12955	0.07982	0.2093694	0.0029036	0.0017889	0.0046925	1.47
0.6545	66315.304	35009.696	0.7357	0.2643	2.44643	0.16777	0.06028	0.2280493	0.0037601	0.0013511	0.0051112	1.47
0.81	82071.876	19253.124	0.8623	0.1377	2.5662	0.21667	0.0346	0.2512601	0.0048561	0.0007754	0.0056314	1.47
0.9791	99209.655	2115.3448	0.9857	0.0143	2.69472	0.27348	0.00397	0.2774535	0.0061295	0.000089	0.0062185	1.47
1	101325	0	1	0	2.71045	0.28075	0	0.280753	0.0062924	0	0.0062924	-------

Direct approach

y1 (CH4)	P1 (CH4) [Pa]	P2 (CO) [Pa]	x1 (CH4)	x2 (CO)	n1 (CH4) [mol/kg]	n2 (CO) [mol/kg]	nt [mol/kg]	v1 (CH4) [m3 STP/kg]	v2 (CO) [m3 STP/kg]	vt [m3 STP/kg]	alpha12 CH4/CO
0	0	101325	0	1	0	0.14033	0.14033	0	6.2613885	6.2613885	-------
0.0499	5060.2313	96264.769	0.0981	0.9019	0.01448	0.1331	0.14757	0.6458795	5.9385448	6.5844243	2.07
0.1058	10717.603	90607.397	0.1966	0.8034	0.0306	0.12504	0.15564	1.3653734	5.5789048	6.9442781	2.07
0.1686	17084.078	84240.922	0.2956	0.7044	0.04868	0.116	0.16468	2.1717814	5.1758206	7.347602	2.07
0.2398	24301.438	77023.562	0.395	0.6050	0.06907	0.10581	0.17488	3.0818079	4.7209426	7.8027505	2.07
0.3213	32551.909	68773.091	0.4948	0.5052	0.09227	0.09421	0.18648	4.1167238	4.2036385	8.3203623	2.07
0.4152	42073.658	59251.342	0.595	0.4050	0.11888	0.08091	0.19979	5.3040387	3.6101575	8.9141962	2.07
0.5249	53184.023	48140.977	0.6957	0.2033	0.14972	0.0655	0.21522	6.6799653	2.9223987	9.602364	2.07
0.6545	66315.304	35009.696	0.7967	0.1018	0.18587	0.04743	0.2333	8.2931466	2.1160478	10.409194	2.07
0.81	82071.876	19253.124	0.8982	0.1018	0.22884	0.02595	0.25479	10.210475	1.1576688	11.368143	2.07
0.9791	99209.655	2115.3448	0.9898	0.0102	0.27508	0.00283	0.27792	12.273463	0.1264812	12.399944	2.07
1	101325	0	1	0	0.28075	0	0.28075	12.526501	0	12.526501	-------

Extended Langmuir Model for N2-CH4 / AlPO4-11 at 22.8°C and 101325 Pa total pressure

Averaging approach

y1 (N2)	P1 (N2) [Pa]	P2 (CH4) [Pa]	x1 (N2)	x2 (CH4)	nm [mol/kg]	n1 (N2) [mol/kg]	n2 (CH4) [mol/kg]	nt [mol/kg]	v1 (N2) [m3 STP/kg]	v2 (CH4) [m3 STP/kg]	vt [m3 STP/kg]	alpha21 CH4/N2
0	0	101325	0	1	2.26401	0	0.37197	0.3719665	0	0.0083368	0.0083368	-------
0.1382	14007.584	87317.416	0.1946	0.8054	0.9738	0.03294	0.1363	0.1692446	0.0007383	0.003055	0.0037932	0.66
0.2902	29405.001	71919.999	0.3812	0.6188	0.62982	0.04417	0.07172	0.1158857	0.00099	0.0016073	0.0025973	0.66
0.4499	45585.16	55739.84	0.552	0.4480	0.47588	0.05108	0.04146	0.0925347	0.0011448	0.0009292	0.002074	0.66
0.6074	61547.64	39777.36	0.6998	0.3002	0.3928	0.05621	0.02412	0.0803282	0.0012599	0.0005405	0.0018004	0.66
0.7501	76003.897	25321.103	0.8189	0.1811	0.34436	0.06017	0.01331	0.0734818	0.0013487	0.0002983	0.0016469	0.66
0.8652	87667.424	13657.576	0.9063	0.0937	0.31579	0.06308	0.00652	0.0696044	0.0014138	0.0001462	0.00156	0.66
0.9441	95657.57	5667.4305	0.9622	0.0378	0.29987	0.06496	0.00256	0.0675194	0.001456	0.0000573	0.0015133	0.66
0.9857	99873.009	1451.9913	0.9904	0.0096	0.29242	0.06593	0.00064	0.0665652	0.0014776	0.0000143	0.0014919	0.66
0.9988	101208.15	116.84799	0.9992	0.0008	0.29017	0.06623	0.00005	0.0662814	0.0014844	1.14E-06	0.0014855	0.66
1	101324.85	0.1509742	1	0.0000	0.28998	0.06626	7E-08	0.066257	0.001485	1.47E-09	0.001485	0.66
1	101325	0	1	0	0.28998	0.06626	0	0.066257	0.001485	0	0.001485	-------

Direct approach

y1 (N2)	P1 (N2) [Pa]	P2 (CH4) [Pa]	x1 (N2)	x2 (CH4)	n1 (N2) [mol/kg]	n2 (CH4) [mol/kg]	nt [mol/kg]	v1 (N2) [m3 STP/kg]	v2 (CH4) [m3 STP/kg]	vt [m3 STP/kg]	alpha21 CH4/N2
0	0	101325	0	1	0	0.37197	0.37197	0	0.0083368	0.0083368	-------
0.1382	14007.584	87317.416	0.03	0.9700	0.00981	0.3169	0.32671	0.0002198	0.0071026	0.0073224	5.18
0.2902	29405.001	71919.999	0.0731	0.9269	0.02034	0.2578	0.27813	0.0004558	0.0057779	0.0062337	5.18
0.4499	45585.16	55739.84	0.1363	0.8637	0.03112	0.19724	0.22836	0.0006976	0.0044207	0.0051182	5.18
0.6074	61547.64	39777.36	0.2299	0.7701	0.0415	0.139	0.1805	0.0009301	0.0031153	0.0040454	5.18
0.7501	76003.897	25321.103	0.3667	0.6333	0.05067	0.08749	0.13817	0.0011357	0.001961	0.0030967	5.18
0.8652	87667.424	13657.576	0.5533	0.4467	0.05793	0.04677	0.1047	0.0012983	0.0010483	0.0023465	5.18
0.9441	95657.57	5667.4305	0.7651	0.2349	0.06282	0.01929	0.08211	0.001408	0.0004323	0.0018403	5.18
0.9857	99873.009	1451.9913	0.9299	0.0701	0.06538	0.00493	0.07031	0.0014653	0.0001104	0.0015757	5.18
0.9988	101208.15	116.84799	0.9941	0.0059	0.06619	0.0004	0.06658	0.0014834	8.88E-06	0.0014923	5.18
1	101324.85	0.1509742	1	0.0000	0.06626	5E-07	0.06626	0.001485	1.15E-08	0.001485	5.18
1	101325	0	1	0.0000	0.06626	0	0.06626	0.001485	0	0.001485	-------

Extended Langmuir Model for N2-CH4 / AlPO4-11 at 40.0°C and 101325 Pa total pressure

Averaging approach

y1 (N2)	P1 (N2) [Pa]	P2 (CH4) [Pa]	x1 (N2)	x2 (CH4)	nm [mol/kg]	n1 (N2) [mol/kg]	n2 (CH4) [mol/kg]	nt [mol/kg]	v1 (N2) [m3 STP/kg]	v2 (CH4) [m3 STP/kg]	vt [m3 STP/kg]	alpha21 CH4/N2
0	0	101325	0	1	2.71045	0	0.28075	0.280753	0	0.0062924	0.0062924	-------
0.1715	17380.736	83944.264	0.2277	0.7723	1.04561	0.02625	0.08906	0.1153115	0.0005884	0.001996	0.0025844	0.70
0.3421	34665.136	66659.864	0.4254	0.5746	0.68186	0.0339	0.04578	0.0796727	0.0007597	0.001026	0.0017857	0.70
0.5052	51188.784	50136.216	0.5925	0.4075	0.527	0.03841	0.02642	0.0648388	0.000861	0.0005922	0.0014532	0.70
0.6535	66212.943	35112.057	0.7286	0.2714	0.44467	0.04166	0.01552	0.057177	0.0009337	0.0003478	0.0012815	0.70
0.7798	79016.315	22308.685	0.8345	0.1655	0.3965	0.04409	0.00874	0.0528366	0.0009883	0.000196	0.0011842	0.70
0.8785	89013.569	12311.431	0.9115	0.0885	0.36757	0.04586	0.00445	0.0503103	0.0010278	0.0000998	0.0011276	0.70
0.9436	95612.782	5712.2182	0.9597	0.0403	0.35148	0.04697	0.00197	0.0489411	0.0010527	0.0000442	0.0010969	0.70
0.9842	99719.017	1605.983	0.9888	0.0112	0.34245	0.04765	0.00054	0.0481862	0.0010679	0.0000121	0.00108	0.70
0.9981	101136.53	188.47058	0.9987	0.0013	0.33949	0.04788	0.00006	0.047941	0.0010731	1.40E-06	0.0010745	0.70
0.999991	101324.04	0.960561	0.999993	7E-06	0.3391	0.04791	3E-07	0.0479091	0.0010738	7.15E-09	0.0010738	0.70
1	101325	0	1	0	0.3391	0.04791	0	0.0479089	0.0010738	0	0.0010738	-------

Direct approach

y1 (N2)	P1 (N2) [Pa]	P2 (CH4) [Pa]	x1 (N2)	x2 (CH4)	n1 (N2) [mol/kg]	n2 (CH4) [mol/kg]	nt [mol/kg]	v1 (N2) [m3 STP/kg]	v2 (CH4) [m3 STP/kg]	vt [m3 STP/kg]	alpha21 CH4/N2
0	0	101325	0	1	0	0.28075	0.28075	0	0.0062924	0.0062924	-------
0.1715	17380.736	83944.264	0.0356	0.9644	0.00851	0.23086	0.23937	0.0001908	0.0051741	0.0053649	5.61
0.3421	34665.136	66659.864	0.0848	0.9152	0.01686	0.18197	0.19883	0.0003778	0.0040784	0.0044562	5.61
0.5052	51188.784	50136.216	0.1539	0.8461	0.02472	0.1359	0.16062	0.000554	0.003046	0.0036	5.61
0.6535	66212.943	35112.057	0.2515	0.7485	0.03177	0.09458	0.12635	0.0007121	0.0021197	0.0028318	5.61
0.7798	79016.315	22308.685	0.3869	0.6131	0.03771	0.05977	0.09748	0.0008452	0.0013395	0.0021847	5.61
0.8785	89013.569	12311.431	0.5629	0.4371	0.0423	0.03285	0.07515	0.0009481	0.0007362	0.0016843	5.61
0.9436	95612.782	5712.2182	0.7489	0.2511	0.04532	0.0152	0.06051	0.0010156	0.0003406	0.0013563	5.61
0.9842	99719.017	1605.983	0.9171	0.0829	0.04718	0.00427	0.05145	0.0010575	0.0000956	0.0011531	5.61
0.9981	101136.53	188.47058	0.9896	0.0104	0.04782	0.0005	0.04832	0.0010719	0.0000112	0.0010831	5.61
0.999991	101324.04	0.960561	0.9999	0.0001	0.04791	3E-06	0.04791	0.0010738	5.71E-08	0.0010738	5.61
1	101325	0	1	0	0.04791	0	0.04791	0.0010738	0	0.0010738	-------

Extended Langmuir Model for N2-CO / AlPO4-18 at 40.1°C and 101325 Pa total pressure

Averaging approach

y1 (N2)	P1 (N2) [Pa]	P2 (CO) [Pa]	x1 (N2)	x2 (CO)	nm [mol/kg]	n1 (N2) [mol/kg]	n2 (CO) [mol/kg]	nt [mol/kg]	v1 (N2) [m3 STP/kg]	v2 (CO) [m3 STP/kg]	vt [m3 STP/kg]	alpha21 CO/N2
0	0	101325	0	1	0.839	0	0.22044	0.2204369	0	0.0049406	0.0049406	.....
8.3E-05	8.3847451	101316.62	5E-06	1.0000	0.83901	1E-06	0.22042	0.2204251	2.50E-08	0.0049403	0.0049403	16.36
5.9E-03	597.8175	100727.18	0.0004	0.9996	0.83923	0.00008	0.21952	0.219595	1.78E-06	0.0049199	0.0049217	16.36
0.0643	6515.7092	94809.291	0.0042	0.9958	0.84164	0.00088	0.21025	0.2111284	0.0000198	0.0047122	0.004732	16.36
0.1278	12948.867	88376.133	0.0089	0.9911	0.84462	0.00179	0.19985	0.2016434	0.0000401	0.0044793	0.0045194	16.36
0.2276	23062.115	78262.885	0.0177	0.9823	0.85028	0.00329	0.18282	0.1861086	0.0000738	0.0040974	0.0041712	16.36
0.3651	36994.409	64330.591	0.034	0.9660	0.86091	0.00555	0.15782	0.1633689	0.0001243	0.0035372	0.0036615	16.36
0.5225	52940.136	48384.864	0.0627	0.9373	0.88036	0.00848	0.12679	0.1352719	0.00019	0.0028418	0.0030318	16.36
0.6632	67200.556	34124.444	0.1074	0.8926	0.91246	0.01162	0.09653	0.1081502	0.0002604	0.0021635	0.0024239	16.36
0.8552	86651.054	14673.946	0.2652	0.7348	1.0471	0.01822	0.05049	0.0687168	0.0004084	0.0011317	0.0015401	16.36
0.9242	93644.608	7680.3924	0.427	0.5730	1.2338	0.02372	0.03183	0.055545	0.0005316	0.0007133	0.0012449	16.36
0.9708	98361.974	2963.0257	0.6698	0.3302	1.68465	0.03453	0.01702	0.0515481	0.0007739	0.0003814	0.0011553	16.36
0.9861	99920.014	1404.9856	0.813	0.1870	2.14701	0.04493	0.01034	0.0552632	0.0010069	0.0002317	0.0012386	16.36
0.993	100612.6	712.39581	0.8962	0.1038	2.55466	0.05395	0.00625	0.0601981	0.0012091	0.0001401	0.0013492	16.36
0.9966	100976.56	348.43844	0.9466	0.0534	2.88649	0.06125	0.00346	0.0647059	0.0013727	0.0000775	0.0014502	16.36
0.9987	101189.89	135.10979	0.9786	0.0214	3.1466	0.06695	0.00146	0.068417	0.0015006	0.0000328	0.0015334	16.36
0.9999	101313.88	11.124472	0.9982	0.0018	3.3299	0.07097	0.00013	0.0710973	0.0015906	2.86E-06	0.0015935	16.36
1	99920.014	1404.9856	1	0	3.34775	0.07005	0.01612	0.0861701	0.0015701	0.0003612	0.0019313	.....

Extended Langmuir Model for N2-CO / AlPO4-18 at 40.1°C and 101325 Pa total pressure

Direct approach

y1 (N2)	P1 (N2) [Pa]	P2 (CO) [Pa]	x1 (N2)	x2 (CO)	n1 (N2) [mol/kg]	n2 (CO) [mol/kg]	nt [mol/kg]	v1 (N2) [m3 STP/kg]	v2 (CO) [m3 STP/kg]	vt [m3 STP/kg]	alpha21 CO/N2
0	0	101325	0	1	0	0.22044	0.22044	0	0.0049406	0.0049406	-------
8.3E-05	8.3847451	101316.62	2E-05	1.0000	4E-06	0.22042	0.22043	9.97E-08	0.0049403	0.0049404	4.10
5.9E-03	597.8175	100727.18	0.0014	0.9986	0.00032	0.21946	0.21977	7.12E-06	0.0049186	0.0049257	4.10
0.0643	6515.7092	94809.291	0.0165	0.9835	0.00351	0.20959	0.2131	0.0000787	0.0046974	0.0047761	4.10
0.1278	12948.867	88376.133	0.0345	0.9655	0.00709	0.19852	0.20562	0.000159	0.0044495	0.0046085	4.10
0.2276	23062.115	78262.885	0.067	0.9330	0.01296	0.18039	0.19336	0.0002905	0.0040431	0.0043336	4.10
0.3651	36994.409	64330.591	0.123	0.8770	0.02157	0.15381	0.17538	0.0004834	0.0034472	0.0039307	4.10
0.5225	52940.136	48384.864	0.2106	0.7894	0.03224	0.12084	0.15308	0.0007226	0.0027083	0.0034309	4.10
0.6632	67200.556	34124.444	0.3244	0.6756	0.04263	0.08876	0.13139	0.0009554	0.0019894	0.0029447	4.10
0.8552	86651.054	14673.946	0.5902	0.4098	0.05826	0.04046	0.09872	0.0013058	0.0009068	0.0022126	4.10
0.9242	93644.608	7680.3924	0.7483	0.2517	0.06435	0.02164	0.086	0.0014424	0.0004851	0.0019274	4.10
0.9708	98361.974	2963.0257	0.8901	0.1099	0.06862	0.00848	0.07709	0.0015379	0.00019	0.0017279	4.10
0.9861	99920.014	1404.9856	0.9455	0.0545	0.07005	0.00404	0.07409	0.0015701	0.0000905	0.0016606	4.10
0.993	100612.6	712.39581	0.9718	0.0282	0.0707	0.00205	0.07275	0.0015845	0.000046	0.0016305	4.10
0.9966	100976.56	348.43844	0.986	0.0140	0.07104	0.00101	0.07204	0.0015921	0.0000225	0.0016146	4.10
0.9987	101189.89	135.10979	0.9946	0.0054	0.07123	0.00039	0.07162	0.0015966	8.74E-06	0.0016053	4.10
0.9999	101313.88	11.124472	0.9995	0.0005	0.07135	0.00003	0.07138	0.0015992	7.20E-07	0.0015999	4.10
1	99920.014	1404.9856	1	0.0000	0.07005	0.00404	0.07409	0.0015701	0.0000905	0.0016606	-------

Extended Langmuir Model for CH4-CO / AlPO4-18 at 40.0-40.1°C and 101325 Pa total pressure

Averaging approach

y1 (CH4)	P1 (CH4) [Pa]	P2 (CO) [Pa]	x1 (CH4)	x2 (CO)	nm [mol/kg]	n1 (CH4) [mol/kg]	n2 (CO) [mol/kg]	nt [mol/kg]	v1 (CH4) [m3 STP/kg]	v2 (CO) [m3 STP/kg]	vt [m3 STP/kg]	alpha21 CO/CH4
0	0	101325	0	1	0.839	0	0.22044	0.2204369	0	0.0049406	0.0049406	.....
4.9E-05	4.929056	101320.07	1E-05	1.0000	0.83901	3E-06	0.22043	0.2204328	6.50E-08	0.0049404	0.0049405	3.69
0.0195	1973.5506	99351.449	0.0053	0.9947	0.84159	0.00117	0.21762	0.2187907	0.0000262	0.0048775	0.0049037	3.69
0.082	8309.0269	93015.973	0.0236	0.9764	0.85052	0.00504	0.20841	0.2134523	0.0001129	0.0046711	0.004784	3.69
0.2234	22639.871	78685.129	0.0722	0.9278	0.87529	0.01453	0.18657	0.2011026	0.0003256	0.0041816	0.0045073	3.69
0.3036	30757.42	70567.58	0.1055	0.8945	0.89307	0.02047	0.17351	0.193976	0.0004587	0.0038888	0.0043475	3.69
0.3924	39759.697	61565.303	0.1488	0.8512	0.91731	0.02768	0.15835	0.1860211	0.0006203	0.003549	0.0041692	3.69
0.4836	49000.636	52324.364	0.2022	0.7978	0.94912	0.03597	0.14193	0.1778968	0.0008062	0.003181	0.0039872	3.69
0.5701	57769.031	43555.969	0.2641	0.7359	0.98887	0.04501	0.12538	0.170389	0.0010087	0.0028102	0.0038189	3.69
0.6466	65520.768	35804.232	0.3312	0.6688	1.03586	0.05437	0.10977	0.1641385	0.0012185	0.0024603	0.0036788	3.69
0.7845	79491.973	21833.027	0.4963	0.5037	1.17305	0.07702	0.07816	0.1551778	0.0017262	0.0017518	0.003478	3.69
0.8632	87466.477	13858.523	0.6307	0.3693	1.31484	0.0967	0.05661	0.1533168	0.0021674	0.0012689	0.0034362	3.69
0.9373	94976.581	6348.4186	0.8019	0.1981	1.55408	0.12626	0.03118	0.1574439	0.0028298	0.0006989	0.0035287	3.69
0.9688	98164.515	3160.4848	0.8937	0.1063	1.72198	0.14567	0.01733	0.1629971	0.0032648	0.0003884	0.0036532	3.69
0.9849	99793.423	1531.577	0.9463	0.0537	1.8358	0.15847	0.00899	0.1674598	0.0035518	0.0002014	0.0037532	3.69
0.9942	100734	590.9963	0.9788	0.0212	1.91376	0.16713	0.00362	0.1707492	0.0037458	0.0000812	0.003827	3.69
0.9995	101276.46	48.538728	0.9982	0.0018	1.96375	0.17263	0.00031	0.1729397	0.0038692	6.85E-06	0.003876	3.69
1	101325	6348.4186	1	0	1.96843	0.15992	0.0395	0.1994217	0.0035843	0.0008853	0.0044696	.....

Extended Langmuir Model for CH4-CO / AlPO4-18 at 40.0-40.1°C and 101325 Pa total pressure

Direct approach

y1 (CH4)	P1 (CH4) [Pa]	P2 (CO) [Pa]	x1 (CH4)	x2 (CO)	n1 (CH4) [mol/kg]	n2 (CO) [mol/kg]	nt [mol/kg]	v1 (CH4) [m3 STP/kg]	v2 (CO) [m3 STP/kg]	vt [m3 STP/kg]	alpha21 CO/CH4
0	0	101325	0	1	0	0.22044	0.22044	0	0.0049406	0.0049406	.....
4.9E-05	4.929056	101320.07	3E-05	1.0000	7E-06	0.22043	0.22044	1.53E-07	0.0049404	0.0049405	1.57
0.0195	1973.5506	99351.449	0.0125	0.9875	0.00274	0.21695	0.21969	0.0000613	0.0048625	0.0049238	1.57
0.082	8309.0269	93015.973	0.0537	0.9463	0.01166	0.20559	0.21725	0.0002614	0.0046079	0.0048692	1.57
0.2234	22639.871	78685.129	0.1545	0.8455	0.03267	0.17884	0.21151	0.0007323	0.0040083	0.0047406	1.57
0.3036	30757.42	70567.58	0.2168	0.7832	0.04511	0.163	0.20812	0.0010111	0.0036534	0.0046645	1.57
0.3924	39759.697	61565.303	0.2908	0.7092	0.05939	0.14483	0.20422	0.0013311	0.003246	0.0045771	1.57
0.4836	49000.636	52324.364	0.3729	0.6271	0.0746	0.12546	0.20006	0.001672	0.0028119	0.0044839	1.57
0.5701	57769.031	43555.969	0.4572	0.5428	0.08959	0.10638	0.19597	0.0020079	0.0023843	0.0043922	1.57
0.6466	65520.768	35804.232	0.5375	0.4625	0.10331	0.08891	0.19222	0.0023155	0.0019927	0.0043082	1.57
0.7845	79491.973	21833.027	0.698	0.3020	0.12924	0.0559	0.18514	0.0028966	0.0012529	0.0041495	1.57
0.8632	87466.477	13858.523	0.8003	0.1997	0.14477	0.03613	0.1809	0.0032447	0.0008097	0.0040544	1.57
0.9373	94976.581	6348.4186	0.9048	0.0952	0.15992	0.01684	0.17676	0.0035843	0.0003773	0.0039617	1.57
0.9688	98164.515	3160.4848	0.9517	0.0483	0.16652	0.00844	0.17496	0.0037321	0.0001892	0.0039213	1.57
0.9849	99793.423	1531.577	0.9764	0.0236	0.16992	0.00411	0.17403	0.0038084	0.0000921	0.0039005	1.57
0.9942	100734	590.9963	0.9908	0.0092	0.1719	0.00159	0.17349	0.0038527	0.0000356	0.0038883	1.57
0.9995	101276.46	48.538728	0.9992	0.0008	0.17304	0.00013	0.17318	0.0038784	2.93E-06	0.0038813	1.57
1	101325	0	1	0.0000	0.17315	0	0.17315	0.0038807	0	0.0038807	.....

Extended Langmuir Model for N2-CH4 / AlPO4-18 at 40.0-40.1°C and 101325 Pa total pressure

Averaging approach

y1 (N2)	P1 (N2) [Pa]	P2 (CH4) [Pa]	x1 (N2)	x2 (CH4)	nm [mol/kg]	n1 (N2) [mol/kg]	n2 (CH4) [mol/kg]	nt [mol/kg]	v1 (N2) [m3 STP/kg]	v2 (CH4) [m3 STP/kg]	vt [m3 STP/kg]	alpha21 CH4/N2
0	0	101325	0	1	1.96843	0	0.17315	0.1731474	0	0.0038807	0.0038807	.....
0.1997	20237.157	81087.843	0.0534	0.9466	2.01267	0.0081	0.14363	0.1517287	0.0001814	0.0032192	0.0034007	4.43
0.3692	37404.785	63920.215	0.1167	0.8833	2.06787	0.01555	0.11771	0.1332613	0.0003486	0.0026381	0.0029867	4.43
0.5098	51657.045	49667.955	0.1902	0.8098	2.1358	0.02241	0.0954	0.1178107	0.0005022	0.0021382	0.0026405	4.43
0.6255	63379.204	37945.796	0.2739	0.7261	2.21881	0.0288	0.07634	0.1051387	0.0006454	0.001711	0.0023564	4.43
0.7205	73001.693	28323.307	0.3679	0.6321	2.32012	0.03492	0.05999	0.0949088	0.0007826	0.0013446	0.0021272	4.43
0.7986	80920.183	20404.817	0.4725	0.5275	2.44422	0.04101	0.04579	0.086792	0.000919	0.0010262	0.0019452	4.43
0.8632	87467.61	13857.39	0.5877	0.4123	2.59736	0.04732	0.0332	0.0805179	0.0010606	0.000744	0.0018046	4.43
0.917	92914.805	8410.1949	0.7139	0.2861	2.78864	0.05418	0.02172	0.0758962	0.0012143	0.0004867	0.001701	4.43
0.962	97477.217	3847.7834	0.8512	0.1488	3.03167	0.062	0.01084	0.0728339	0.0013895	0.0002429	0.0016324	4.43
0.9965	100968.31	356.6873	0.9846	0.0154	3.31201	0.07033	0.0011	0.0714324	0.0015763	0.0000247	0.001601	4.43
1	101325	0	1	0	3.34775	0.07136	0	0.0713608	0.0015994	0	0.0015994	.....

Direct approach

y1 (N2)	P1 (N2) [Pa]	P2 (CH4) [Pa]	x1 (N2)	x2 (CH4)	n1 (N2) [mol/kg]	n2 (CH4) [mol/kg]	nt [mol/kg]	v1 (N2) [m3 STP/kg]	v2 (CH4) [m3 STP/kg]	vt [m3 STP/kg]	alpha21 CH4/N2
0	0	101325	0	1	0	0.17315	0.17315	0	0.0038807	0.0038807	.....
0.1997	20237.157	81087.843	0.0875	0.9125	0.01347	0.14048	0.15394	0.0003018	0.0031485	0.0034502	2.60
0.3692	37404.785	63920.215	0.1835	0.8165	0.02518	0.11205	0.13723	0.0005644	0.0025112	0.0030757.	2.60
0.5098	51657.045	49667.955	0.2854	0.7146	0.03512	0.08793	0.12305	0.0007872	0.0019707	0.0027579	2.60
0.6255	63379.204	37945.796	0.3908	0.6092	0.04345	0.06773	0.11118	0.0009738	0.001518	0.0024917	2.60
0.7205	73001.693	28323.307	0.4975	0.5025	0.05038	0.0509	0.10128	0.0011292	0.0011407	0.00227	2.60
0.7986	80920.183	20404.817	0.6037	0.3963	0.05616	0.03687	0.09304	0.0012588	0.0008264	0.0020852	2.60
0.8632	87467.61	13857.39	0.708	0.2920	0.06099	0.02516	0.08615	0.001367	0.0005639	0.0019309	2.60
0.917	92914.805	8410.1949	0.8093	0.1907	0.06504	0.01533	0.08037	0.0014578	0.0003436	0.0018014	2.60
0.962	97477.217	3847.7834	0.9068	0.0932	0.06846	0.00704	0.0755	0.0015344	0.0001577	0.0016921	2.60
0.9965	100968.31	356.6873	0.9909	0.0091	0.07109	0.00065	0.07175	0.0015933	0.0000147	0.001608	2.60
1	101325	0	1	0.0000	0.07136	0	0.07136	0.0015994	0	0.0015994	.....

Ideal Adsorbed Solution Theory for N2-CO / 5A at 22.6-22.7°C and 101325 Pa total pressure

y1 (N2)	x1 (N2)	P10 (N2) [Pa]	P20 (CO) [Pa]	v10 (N2) [m3 STP/kg]	v20 (CO) [m3 STP/kg]	vt [m3 STP/kg]	v1 (N2) [m3 STP/kg]	v2 (CO) [m3 STP/kg]	alpha21 CO/N2	nt [mol/kg]	n1 (N2) [mol/kg]	n2 (CO) [mol/kg]
0	0	undefined	101325	0	0.0183944	0.0183944	0	0.0183944	.....	0.8207	0	0.8207
0.2822	0.0958	298439	80440.8	0.0176085	0.0166647	0.0167507	0.0016047	0.015146	3.710	0.7474	0.0716	0.6758
0.4720	0.1927	248185	66270	0.0159403	0.0151834	0.0153236	0.0029529	0.0123708	3.745	0.6837	0.1317	0.552
0.6071	0.2905	211753	56110.9	0.0145335	0.0139125	0.0140873	0.0040924	0.009995	3.774	0.6285	0.1826	0.446
0.7076	0.3893	184169	48515	0.0133329	0.0128167	0.0130129	0.0050659	0.007947	3.796	0.5806	0.226	0.3546
0.7850	0.4890	162653	42637.8	0.012301	0.0118652	0.0120744	0.0059044	0.00617	3.815	0.5387	0.2634	0.2753
0.8462	0.5897	145413	37973.3	0.0114053	0.0110345	0.0112502	0.0066337	0.0046165	3.829	0.502	0.296	0.206
0.8962	0.6922	131192	34157.1	0.0106148	0.0102983	0.0105153	0.0072787	0.0032366	3.841	0.4692	0.3248	0.1444
0.9367	0.7934	119630	31048.4	0.0099343	0.0096563	0.0098755	0.0078348	0.0020408	3.853	0.4406	0.3496	0.0911
0.9709	0.8964	109755	28421	0.009324	0.0090813	0.0092983	0.0083345	0.0009638	3.862	0.4149	0.3719	0.043
1	1	101325	undefined	0.0087804	0	0.0087804	0.0087804	0	.....	0.3918	0.3918	0

Ideal Adsorbed Solution Theory for N2-CO / 5A at 39.8-40.0°C and 101325 Pa total pressure

y1(N2)	x1(N2)	P10 [Pa]	P20 [Pa]	v10 [m3STP/kg]	v20 [m3STP/kg]	vt [m3STP/kg]	v1 [m3STP/kg]	v2 [m3STP/kg]	alpha21 CO/N2	nt [mol/kg]	n1 [mol/kg]	n2 [mol/kg]
0	0	undefined	101325	0	0.01336	0.0133604	0	0.0133604	.....	0.5961057	0	0.5961
0.3711	0.0898	418727	70010	0.01265	0.01085	0.0109885	0.0009868	0.0100017	5.9809433	0.4902793	0.04402708	0.4463
0.5890	0.1874	318527	51251	0.01	0.00887	0.0090639	0.0016981	0.0073658	6.2150811	0.4044085	0.07576594	0.3286
0.7232	0.2903	252431	39516	0.00814	0.00738	0.0075866	0.0022024	0.0053842	6.3881582	0.3384953	0.09826517	0.2402
0.8104	0.3965	207116	31835	0.0068	0.00627	0.0064719	0.0025658	0.0039061	6.5059445	0.2887599	0.11447884	0.1743
0.8697	0.5032	175134	26565	0.00583	0.00544	0.0056275	0.0028318	0.0027957	6.5925601	0.2510857	0.12634633	0.1247
0.9120	0.6090	151732	22813	0.0051	0.0048	0.0049792	0.0030324	0.0019469	6.6510774	0.2221616	0.13529644	0.0869
0.9431	0.7120	134213	20019	0.00454	0.00431	0.004473	0.0031848	0.0012882	6.7042625	0.199576	0.14209811	0.0575
0.9668	0.8120	120639	17907	0.00411	0.00392	0.0040708	0.0033055	0.0007653	6.7369668	0.1816309	0.14748426	0.0341
0.9853	0.9080	109946	16240	0.00376	0.0036	0.003746	0.0034013	0.0003446	6.7702492	0.167135	0.15175861	0.0154
1	1	101325	undefined	0.00348	0	0.0034795	0.0034795	0	.....	0.1552469	0.15524692	0

Ideal Adsorbed Solution Theory for CH4-CO / 5A at 22.6-22.8°C and 101325 Pa total pressure

y1 (CH4)	x1 (CO)	P10 (CH4) [Pa]	P20 (CO) [Pa]	v10 (CH4) [m3STP/kg]	v20 (CO) [m3STP/kg]	vt [m3STP/kg]	v1 (CH4) [m3STP/kg]	v2 (CO) [m3STP/kg]	alpha21 CO/CH4	nt [mol/kg]	n1 (CH4) [mol/kg]	n2 (CO) [mol/kg]
0	0	undefined	101325	0	0.0183944	0.0183944	0	0.0183944	.....	0.8207	0	0.8207
0.1332	0.0326	414520	90787.5	0.0166687	0.0175787	0.0175475	0.0005712	0.0169763	4.566	0.7829	0.0255	0.7574
0.3731	0.1165	324468	71900.9	0.0150923	0.0158081	0.0157212	0.0018315	0.0138897	4.513	0.7014	0.0817	0.6197
0.592	0.2455	244341	54790.4	0.013207	0.0137317	0.0135991	0.0033386	0.0102605	4.460	0.6068	0.1490	0.4578
0.7384	0.3897	192000	43425.5	0.0116064	0.0119986	0.0118427	0.0046151	0.0072276	4.421	0.5284	0.2059	0.3225
0.831	0.5279	159498	36276.4	0.0104067	0.0107138	0.0105495	0.0055691	0.0049804	4.397	0.4707	0.2485	0.2222
0.8913	0.652	138519	31640.6	0.0095257	0.0097817	0.0096133	0.0062679	0.0033454	4.378	0.4289	0.2797	0.1493
0.9325	0.7599	124345	28467.2	0.0088747	0.0090917	0.0089258	0.0067828	0.0021431	4.368	0.3982	0.3026	0.0956
0.9619	0.8528	114294	26220	0.0083823	0.0085748	0.0084101	0.0071717	0.0012384	4.359	0.3752	0.3200	0.0553
0.9836	0.9321	106918	24546.6	0.0080033	0.0081735	0.0080147	0.0074705	0.0005442	4.356	0.3576	0.3333	0.0243
1	1	101325	undefined	0.0077054	0	0.0077054	0.0077054	0	.....	0.3438	0.3438	0

Ideal Adsorbed Solution Theory for CH4-CO / 5A at 40.0-40.1°C and 101325 Pa total pressure

y1 (CH4)	x1 (CH4)	P10 (CH4) [Pa]	P20 (CO) [Pa]	v10 (CH4) [m3STP/kg]	v20 (CO) [m3STP/kg]	vt [m3STP/kg]	v1 (CH4) [m3STP/kg]	v2 (CO) [m3STP/kg]	alpha21 CO/CH4	nt [mol/kg]	n1 (CH4) [mol/kg]	n2 (CO) [mol/kg]
0	0	undefined	101325	0	0.0133604	0.0133604	0	0.0133604	.....	0.5961	0	0.5961
0.0242	0.0063	387179	99500.3	0.0139756	0.0132347	0.0132391	0.000084	0.0131552	3.891	0.5907	0.0037	0.587
0.0482	0.0128	380529	97695.4	0.0138331	0.0131082	0.013117	0.0001683	0.0129487	3.895	0.5852	0.0075	0.5777
0.0719	0.0195	373913	95911.2	0.0136894	0.012981	0.0129941	0.000253	0.012741	3.899	0.5798	0.0113	0.5685
0.0952	0.0263	367385	94148	0.0135455	0.012853	0.0128703	0.0003381	0.0125323	3.902	0.5742	0.0151	0.5592
0.1183	0.0332	360946	92406.4	0.0134016	0.0127245	0.0127459	0.0004233	0.0123226	3.906	0.5687	0.0189	0.5498
0.1411	0.0403	354563	90687.1	0.0132569	0.0125954	0.0126207	0.0005088	0.012112	3.910	0.5631	0.0227	0.5404
0.1635	0.0476	348244	88990.7	0.0131117	0.0124658	0.012495	0.0005945	0.0119006	3.913	0.5575	0.0265	0.531
0.1856	0.0550	342024	87317.4	0.0129668	0.0123357	0.0123688	0.0006802	0.0116886	3.917	0.5519	0.0303	0.5215
0.2074	0.0626	335871	85668.1	0.0128214	0.0122054	0.0122422	0.0007661	0.0114761	3.921	0.5462	0.0342	0.512
0.2289	0.0703	329789	84043.2	0.0126757	0.0120748	0.0121151	0.000852	0.0112632	3.924	0.5405	0.038	0.5025
0.424	0.1568	273951	69214.1	0.0112384	0.0107726	0.0108431	0.0017006	0.0091425	3.958	0.4838	0.0759	0.4079
0.5823	0.2591	227762	57116.3	0.0098945	0.0095379	0.0096278	0.0024942	0.0071336	3.988	0.4296	0.1113	0.3183
0.7051	0.3734	191329	47690.5	0.0087172	0.0084436	0.0085437	0.0031902	0.0053535	4.012	0.3812	0.1423	0.2389
0.7972	0.4937	163623	40589.7	0.0077421	0.007528	0.0076322	0.0037676	0.0038646	4.031	0.3405	0.1681	0.1724
0.865	0.6130	142979	35339.7	0.0069653	0.006793	0.0068976	0.0042284	0.0026692	4.046	0.3078	0.1887	0.1191
0.9149	0.7259	127694	31476.1	0.0063598	0.006217	0.00632	0.004588	0.001732	4.057	0.282	0.2047	0.0773
0.9517	0.8289	116333	28618	0.005892	0.0057701	0.0058708	0.0048663	0.0010045	4.065	0.2619	0.2171	0.0448
0.9792	0.9203	107807	26475.5	0.0055303	0.0054226	0.0055216	0.0050815	0.0004401	4.072	0.2464	0.2267	0.0196
1	1	101325	undefined	0.0052491	0	0.0052491	0.0052491	0	.....	0.2342	0.2342	0

Ideal Adsorbed Solution Theory for N2-CH4 / 5A at 22.7-22.8°C and 101325 Pa total pressure

y1 (N2)	x1 (N2)	P10 (N2) [Pa]	P20 (CH4) [Pa]	v10 (N2) [m3STP/kg]	v20 (CH4) [m3STP/kg]	vt [m3STP/kg]	v1 (N2) [m3STP/kg]	v2 (CH4) [m3STP/kg]	alpha12 N2/CH4	nt [mol/kg]	n1 (N2) [mol/kg]	n2 (CH4) [mol/kg]
0	0	undefined	101325	0	0.0077054	0.0077054	0	0.0077054	---------	0.3438	0	0.3438
0.0868	0.0963	91313.8	102392	0.0081058	0.0077629	0.0077947	0.0007506	0.0070441	1.1213	0.3478	0.0335	0.3143
0.1778	0.1952	92317.2	103510	0.0081749	0.0078229	0.0078892	0.00154	0.0063492	1.1212	0.352	0.0687	0.2833
0.2727	0.2961	93310.9	104696	0.008243	0.0078861	0.0079885	0.0023653	0.0056232	1.1220	0.3564	0.1055	0.2509
0.3707	0.398	94386.5	105912	0.0083164	0.0079505	0.0080922	0.0032207	0.0048715	1.1221	0.3611	0.1437	0.2174
0.4716	0.5006	95457.1	107206	0.008389	0.0080184	0.0081997	0.0041044	0.0040954	1.1231	0.3659	0.1831	0.1827
0.5757	0.6039	96595.3	108534	0.0084658	0.0080877	0.0083119	0.0050191	0.0032927	1.1236	0.3709	0.2239	0.1469
0.6805	0.7054	97748.7	109888	0.0085432	0.0081578	0.0084259	0.0059436	0.0024823	1.1242	0.3759	0.2652	0.1108
0.7866	0.8058	98915.5	111323	0.008621	0.0082315	0.0085425	0.0068836	0.001659	1.1254	0.3811	0.3071	0.074
0.8927	0.9035	100110	112699	0.0087003	0.0083017	0.0086601	0.0078244	0.0008357	1.1258	0.3864	0.3491	0.0373
1	1	101325	undefined	0.0087804	0	0.0087804	0.0087804	0	---------	0.3918	0.3918	0

Ideal Adsorbed Solution Theory for N2-CH4 / 5A at 39.8-40.1°C and 101325 Pa total pressure

y1 (N2)	x1 (N2)	P10 (N2) [Pa]	P20 (CH4) [Pa]	v10 (N2) [m3STP/kg]	v20 (CH4) [m3STP/kg]	vt [m3STP/kg]	v1 (N2) [m3STP/kg]	v2 (CH4) [m3STP/kg]	alpha12 CH4/N2	nt [mol/kg]	n1 (N2) [mol/kg]	n2 (CH4) [mol/kg]
0	0	undefined	101325	0	0.0052491	0.0052491	0	0.0052491	---------	0.2342	0	0.2342
0.1488	0.0969	155628	95501.8	0.005222	0.0049917	0.0050131	0.0004855	0.0045276	1.630	0.2237	0.0217	0.202
0.2839	0.1954	147262	90172.5	0.0049588	0.004752	0.0047911	0.0009359	0.0038551	1.633	0.2138	0.0418	0.172
0.4065	0.295	139611	85304.8	0.0047164	0.0045297	0.0045832	0.001352	0.0032312	1.637	0.2045	0.0603	0.1442
0.5175	0.3955	132581	80875.7	0.0044923	0.0043244	0.0043893	0.001736	0.0026533	1.639	0.1958	0.0775	0.1184
0.6181	0.4963	126198	76817.5	0.0042877	0.0041337	0.0042087	0.0020888	0.0021199	1.643	0.1878	0.0932	0.0946
0.7094	0.5974	120326	73129.7	0.0040984	0.0039584	0.0040409	0.002414	0.0016269	1.645	0.1803	0.1077	0.0726
0.7924	0.6984	114963	69744.7	0.0039248	0.0037956	0.0038849	0.0027132	0.0011717	1.648	0.1733	0.1211	0.0523
0.868	0.7994	110014	66697.3	0.0037638	0.0036475	0.0037399	0.0029897	0.0007502	1.649	0.1669	0.1334	0.0335
0.9369	0.8998	105504	63796.8	0.0036165	0.0035052	0.003605	0.0032438	0.0003612	1.654	0.1608	0.1447	0.0161
1	1	101325	undefined	0.0034795	0	0.0034795	0.0034795	0	---------	0.1552	0.1552	0

Ideal Adsorbed Solution Theory for N2-CO / Turkish clinoptilolite at 22.6-22.8°C and 101325 Pa total pressure

y1 (N2)	x1 (N2)	P10 (N2) [Pa]	P20 (CO) [Pa]	v10 (N2) [m3 STP/kg]	v20 (CO) [m3 STP/kg]	vt [m3 STP/kg]	v1 (N2) [m3 STP/kg]	v2 (CO) [m3 STP/kg]	alpha21 CO/N2	nt [mol/kg]	n1 (N2) [mol/kg]	n2 (CO) [mol/kg]
0	0	undefined	101325	0	0.0264088	0.0264088	0	0.0264088	-	1.1783	0	1.1783
0.0688	0.0005	1E+07	94405.7	0.0140221	0.02636	0.0263482	0.0000134	0.0263348	144.91	1.1756	0.0006	1.175
0.1272	0.0011	1E+07	88530.9	0.0140204	0.0263127	0.0262882	0.0000279	0.0262603	136.96	1.1729	0.0012	1.1717
0.1776	0.0017	1E+07	83463	0.0140186	0.0262668	0.0262288	0.0000435	0.0261853	130.08	1.1703	0.0019	1.1683
0.2218	0.0023	9803005	79034.3	0.0140168	0.026222	0.0261697	0.00006	0.0261097	124.03	1.1676	0.0027	1.165
0.2608	0.0030	8915463	75122.2	0.014015	0.0261781	0.0261109	0.0000774	0.0260335	118.68	1.165	0.0035	1.1616
0.2956	0.0037	8158410	71635.2	0.0140131	0.0261351	0.0260524	0.0000956	0.0259567	113.89	1.1624	0.0043	1.1581
0.3269	0.0044	7506453	68502.8	0.0140112	0.0260929	0.025994	0.0001147	0.0258793	109.58	1.1598	0.0051	1.1547
0.3552	0.0052	6939120	65670	0.0140092	0.0260514	0.0259358	0.0001345	0.0258013	105.67	1.1572	0.006	1.1512
0.3811	0.0060	6441465	63093	0.0140072	0.0260106	0.0258777	0.0001551	0.0257226	102.09	1.1546	0.0069	1.1477
0.4047	0.0068	6002100	60736.6	0.0140052	0.0259703	0.0258196	0.0001764	0.0256432	98.82	1.152	0.0079	1.1441
0.5654	0.0167	3423377	44784.3	0.0139826	0.0255925	0.0252417	0.0004224	0.0248193	76.44	1.1262	0.0188	1.1074
0.6559	0.0290	2290341	35909.3	0.0139567	0.0252468	0.0246678	0.0007158	0.023952	63.78	1.1006	0.0319	1.0687
0.715	0.0432	1675308	30181.5	0.013928	0.0249244	0.0241015	0.0010423	0.0230593	55.51	1.0754	0.0465	1.0288
0.7571	0.0591	1298587	26158.2	0.0138972	0.0246213	0.0235478	0.0013911	0.0221568	49.64	1.0506	0.0621	0.9886
0.7887	0.0762	1048612	23171.5	0.0138647	0.0243351	0.0230107	0.0017537	0.0212569	45.25	1.0267	0.0782	0.9484
0.8135	0.0944	873097	20865.9	0.0138309	0.0240643	0.0224931	0.0021236	0.0203696	41.84	1.0036	0.0947	0.9088
0.8335	0.1134	744489	19032.9	0.0137962	0.023808	0.0219972	0.0024953	0.019502	39.12	0.9815	0.1113	0.8701
0.8499	0.1331	647016	17542	0.0137609	0.0235652	0.021524	0.0028649	0.0186592	36.88	0.9603	0.1278	0.8325
0.8637	0.1532	571258	16306.4	0.0137254	0.0233349	0.0210744	0.0032286	0.0178458	35.03	0.9403	0.1441	0.7962
0.9345	0.3552	266572	10295.8	0.0133875	0.0215867	0.0177297	0.0062976	0.0114321	25.89	0.7911	0.281	0.5101
0.9617	0.5260	185257	8185.04	0.0131217	0.0205116	0.015824	0.0083234	0.0075006	22.63	0.706	0.3714	0.3347
0.9759	0.6585	150175	7150.27	0.0129251	0.019815	0.014667	0.0096575	0.0050095	21.00	0.6544	0.4309	0.2235
0.9844	0.7591	131402	6548.5	0.0127807	0.0193376	0.0139175	0.0105648	0.0033527	20.07	0.621	0.4714	0.1496
0.99	0.8359	120013	6167.19	0.0126732	0.0190013	0.0134061	0.0112055	0.0022006	19.46	0.5981	0.5	0.0982
0.9939	0.8945	112575	5908.16	0.0125924	0.0187557	0.0130445	0.0116687	0.0013758	19.05	0.582	0.5206	0.0614
0.9966	0.9395	107476	5727.41	0.0125313	0.0185753	0.0127828	0.01201	0.0007728	18.77	0.5703	0.5359	0.0345
0.9986	0.9740	103885	5595.32	0.0124851	0.0184385	0.012591	0.012263	0.000328	18.57	0.5618	0.5471	0.0146
1	1	101325	undefined	0.0124503	0	0.0124503	0.0124503	0	-	0.5555	0.5555	0

Ideal Adsorbed Solution Theory for N2-CO / Turkish clinoptilolite at 40.0°C and 101325 Pa total pressure

y1 (N2)	x1 (N2)	P10 (N2) [Pa]	P20 (CO) [Pa]	v10 (N2) [m3 STP/kg]	v20 (CO) [m3 STP/kg]	vt [m3 STP/kg]	v1 (N2) [m3 STP/kg]	v2 (CO) [m3 STP/kg]	alpha12 CO/N2	nt [mol/kg]	n1 (N2) [mol/kg]	n2 (CO) [mol/kg]
0	0	undefined	101325	0	0.0211077	0.0211077	0	0.0211077	-------	0.9418	0	0.9418
0.0222	0.0016	1415881	99229.7	0.011656	0.0210619	0.0210349	0.0000335	0.0210014	14.27	0.9385	0.0015	0.937
0.0434	0.0032	1362660	97241.2	0.011651	0.0210168	0.0209624	0.0000676	0.0208948	14.01	0.9353	0.003	0.9323
0.0636	0.0049	1315313	95350.3	0.011646	0.0209724	0.0208904	0.0001023	0.0207881	13.79	0.9321	0.0046	0.9275
0.0828	0.0066	1270900	93549.8	0.011641	0.0209286	0.0208189	0.0001375	0.0206814	13.59	0.9289	0.0061	0.9228
0.1012	0.0083	1229342	91832.9	0.011636	0.0208854	0.0207478	0.0001731	0.0205747	13.39	0.9257	0.0077	0.918
0.1189	0.0101	1190216	90193.9	0.011632	0.0208428	0.0206771	0.0002092	0.0204679	13.20	0.9226	0.0093	0.9132
0.1357	0.0119	1153540	88627	0.011627	0.0208008	0.0206069	0.0002457	0.0203612	13.02	0.9194	0.011	0.9085
0.1520	0.0138	1118842	87127.6	0.011622	0.0207593	0.0205372	0.0002826	0.0202545	12.84	0.9163	0.0126	0.9037
0.1675	0.0156	1086135	85691.1	0.011617	0.0207184	0.0204678	0.0003199	0.020148	12.68	0.9132	0.0143	0.899
0.1825	0.0175	1055301	84313.3	0.011612	0.0206781	0.020399	0.0003574	0.0200416	12.52	0.9102	0.0159	0.8942
0.3059	0.0378	819759	73094	0.011563	0.0203003	0.0197364	0.0007462	0.0189902	11.22	0.8806	0.0333	0.8473
0.3962	0.0600	669411	65083.5	0.011514	0.0199629	0.0191214	0.0011467	0.0179747	10.29	0.8532	0.0512	0.802
0.4657	0.0833	566223	59057.8	0.011465	0.0196588	0.0185538	0.0015463	0.0170075	9.59	0.8278	0.069	0.7588
0.5212	0.1075	491453	54354.6	0.011418	0.0193828	0.0180312	0.0019376	0.0160936	9.04	0.8045	0.0865	0.7181
0.5667	0.1320	435152	50578.6	0.011372	0.019131	0.0175509	0.0023159	0.015235	8.60	0.7831	0.1033	0.6797
0.6048	0.1566	391408	47479.6	0.011328	0.0189003	0.0171096	0.0026787	0.0144309	8.24	0.7634	0.1195	0.6439
0.6372	0.1811	356569	44890.2	0.011285	0.0186882	0.0167039	0.0030245	0.0136794	7.94	0.7453	0.1349	0.6103
0.6652	0.2053	328244	42694.5	0.011243	0.0184925	0.0163306	0.0033531	0.0129775	7.69	0.7286	0.1496	0.579
0.6896	0.2292	304810	40809.4	0.011204	0.0183114	0.0159865	0.0036645	0.012322	7.47	0.7133	0.1635	0.5498
0.8306	0.4385	191922	30564.3	0.010887	0.0170441	0.0136569	0.005989	0.0076679	6.28	0.6093	0.2672	0.3421
0.8943	0.5936	152645	26360.4	0.010677	0.0163263	0.0124241	0.0073751	0.005049	5.79	0.5543	0.3291	0.2253
0.9305	0.7079	133197	24096.6	0.010532	0.0158698	0.0116798	0.0082677	0.0034121	5.53	0.5211	0.3689	0.1522
0.9537	0.7934	121796	22701.4	0.010428	0.0155585	0.0111906	0.0088788	0.0023118	5.37	0.4993	0.3962	0.1031
0.9696	0.8585	114440	21768.5	0.010352	0.0153359	0.0108507	0.0093151	0.0015356	5.26	0.4841	0.4156	0.0685
0.9809	0.9085	109401	21116	0.010294	0.0151726	0.0106059	0.0096357	0.0009702	5.18	0.4732	0.4299	0.0433
0.9892	0.9472	105822	20643.9	0.010250	0.0150503	0.0104256	0.0098752	0.0005504	5.13	0.4652	0.4406	0.0246
0.9954	0.9771	103224	20296.4	0.010217	0.014958	0.0102912	0.0100555	0.0002357	5.09	0.4592	0.4487	0.0105
1.0000	1	101325	undefined	0.010191	0	0.0101911	0.0101911	0	-------	0.4547	0.4547	0

Ideal Adsorbed Solution Theory for CH4-CO / Turkish clinoptilolite at 22.6-22.8°C and 101325 Pa total pressure

y1 (CH4)	x1 (CH4)	P10 (CH4) [Pa]	P20 (CO) [Pa]	v10 (CH4) [m3STP/kg]	v20 (CO) [m3STP/kg]	vt [m3STP/kg]	v1 (CH4) [m3STP/kg]	v2 (CO) [m3STP/kg]	alpha21 CO/CH4	nt [mol/kg]	n1 (CH4) [mol/kg]	n2 (CO) [mol/kg]
0	0	undefined	101325	0	0.0264088	0.0264088	0	0.0264088	.....	1.1783	0	1.1783
0.0221	0.0012	1932289	99199.6	0.0208056	0.0263945	0.0263863	0.0000306	0.0263557	19.48	1.1773	0.0014	1.1759
0.0433	0.0023	1881735	97167	0.0208006	0.0263803	0.0263638	0.0000614	0.0263024	19.37	1.1763	0.0027	1.1735
0.0635	0.0035	1834346	95220.7	0.0207957	0.0263661	0.0263413	0.0000925	0.0262489	19.26	1.1753	0.0041	1.1712
0.0830	0.0047	1789055	93355.2	0.0207908	0.026352	0.0263189	0.0001237	0.0261952	19.16	1.1743	0.0055	1.1688
0.1017	0.0059	1745726	91565.5	0.0207858	0.0263379	0.0262964	0.0001551	0.0261413	19.07	1.1733	0.0069	1.1664
0.1196	0.0071	1704232	89846.7	0.0207808	0.0263238	0.026274	0.0001868	0.0260872	18.97	1.1723	0.0083	1.1639
0.1368	0.0083	1664459	88194.7	0.0207758	0.0263098	0.0262516	0.0002187	0.0260329	18.87	1.1713	0.0098	1.1615
0.1534	0.0096	1626302	86605.5	0.0207708	0.0262959	0.0262292	0.0002508	0.0259784	18.78	1.1703	0.0112	1.1591
0.1694	0.0108	1590252	85075.1	0.0207658	0.026282	0.0262068	0.0002829	0.0259239	18.69	1.1693	0.0126	1.1567
0.1849	0.012	1555357	83600.6	0.0207608	0.0262681	0.0261844	0.0003153	0.0258691	18.60	1.1683	0.0141	1.1542
0.3135	0.025	1273241	71337.5	0.0207101	0.0261313	0.0259617	0.0006477	0.025314	17.85	1.1583	0.0289	1.1294
0.4088	0.0386	1073489	62303.3	0.0206584	0.0259974	0.0257407	0.0009933	0.0247474	17.23	1.1485	0.0443	1.1042
0.4826	0.0529	925066	55351.9	0.0206057	0.025866	0.0255216	0.0013491	0.0241726	16.71	1.1387	0.0602	1.0785
0.5415	0.0677	810943	49828	0.0205524	0.0257368	0.0253049	0.0017121	0.0235928	16.27	1.129	0.0764	1.0527
0.5897	0.0829	720415	45330.1	0.0204984	0.0256095	0.0250906	0.0020811	0.0230095	15.89	1.1195	0.0929	1.0266
0.6300	0.0987	647001	41595.7	0.0204438	0.0254842	0.0248791	0.0024546	0.0224245	15.55	1.11	0.1095	1.0005
0.6641	0.1147	586670	38443.4	0.020389	0.0253607	0.0246707	0.0028297	0.021841	15.26	1.1007	0.1263	0.9745
0.6934	0.1311	535938	35750.5	0.0203336	0.0252392	0.0244654	0.0032074	0.021258	14.99	1.0916	0.1431	0.9485
0.7189	0.1478	492953	33422.4	0.0202781	0.0251194	0.0242634	0.0035853	0.0206782	14.75	1.0826	0.16	0.9226
0.8622	0.3215	271730	20580.4	0.0197314	0.0240271	0.0224554	0.0072194	0.015236	13.20	1.0019	0.3221	0.6798
0.9228	0.4905	190644	15354.3	0.0192397	0.0231359	0.0210457	0.0103218	0.0107238	12.42	0.939	0.4605	0.4785
0.9549	0.6389	151433	12668.2	0.0188326	0.0224409	0.0199934	0.0127738	0.0072196	11.95	0.8921	0.5699	0.3221
0.9737	0.7602	129776	11130.2	0.0185146	0.0219207	0.0192312	0.0146196	0.0046116	11.66	0.858	0.6523	0.2058
0.9852	0.8530	117030	10191	0.0182796	0.0215417	0.0186958	0.0159475	0.0027483	11.48	0.8342	0.7115	0.1226
0.9924	0.9197	109331	9624.8	0.0181148	0.0212851	0.0183341	0.0168618	0.0014722	11.36	0.818	0.7523	0.0657
0.9967	0.9635	104808	9279.8	0.0180082	0.0211168	0.0181054	0.0174453	0.0006601	11.29	0.8078	0.7784	0.0295
0.9990	0.9888	102369	9095.44	0.0179474	0.0210228	0.0179769	0.0177757	0.0002012	11.25	0.8021	0.7931	0.009
1	1	101325	undefined	0.0179207	0	0.0179207	0.0179207	0	.....	0.7996	0.7996	0

Ideal Adsorbed Solution Theory for CH4-CO / Turkish clinoptilolite at 40.0°C and 101325 Pa total pressure

y1 (CH4)	x1 (CH4)	P10 (CH4) [Pa]	P20 (CO) [Pa]	v10 (CH4) [m3STP/kg]	v20 (CO) [m3STP/kg]	vt [m3STP/kg]	v1 (CH4) [m3STP/kg]	v2 (CO) [m3STP/kg]	alpha21 CO/CH4	nt [mol/kg]	n1 (CH4) [mol/kg]	n2 (CO) [mol/kg]
0	0	undefined	101325	0	0.0211077	0.0211077	0	0.0211077	.....	0.9418	0	0.9418
0.0701	0.0131	542527	95473.1	0.017472	0.0209753	0.0209204	0.0002738	0.0206466	5.6825	0.9334	0.0122	0.9212
0.1338	0.0267	507047	90180.9	0.017424	0.0208425	0.0207337	0.0005543	0.0201794	5.6226	0.9251	0.0247	0.9004
0.1918	0.0409	475161	85383.1	0.017375	0.0207095	0.0205482	0.0008404	0.0197078	5.565	0.9168	0.0375	0.8793
0.2448	0.0555	446592	81021.2	0.0173255	0.0205767	0.0203644	0.001131	0.0192334	5.512	0.9086	0.0505	0.8581
0.2933	0.0706	420750	77047.6	0.0172752	0.0204443	0.0201828	0.0014256	0.0187572	5.4609	0.9005	0.0636	0.8369
0.3378	0.0861	397453	73417.4	0.0172245	0.0203126	0.0200037	0.0017228	0.0182809	5.4136	0.8925	0.0769	0.8156
0.3788	0.102	376340	70094.1	0.0171735	0.0201817	0.0198275	0.002022	0.0178055	5.3691	0.8847	0.0902	0.7944
0.4165	0.1182	357040	67047.9	0.0171218	0.020052	0.0196544	0.0023232	0.0173313	5.3252	0.8769	0.1037	0.7733
0.4513	0.13	339614	64243.6	0.0170705	0.0199234	0.0194849	0.0026238	0.0168611	5.2863	0.8694	0.1171	0.7523
0.4836	0.1514	323636	61662.1	0.0170189	0.0197964	0.019319	0.0029249	0.0163941	5.2485	0.862	0.1305	0.7315
0.7057	0.3257	219515	44228	0.0165154	0.0186308	0.0178846	0.0058256	0.012059	4.9632	0.798	0.2599	0.538
0.8240	0.4943	168917	35256.8	0.0160727	0.0176933	0.0168533	0.0083306	0.0085227	4.791	0.752	0.3717	0.3803
0.8930	0.6406	141256	30167.6	0.0157148	0.0169825	0.0161481	0.0103437	0.0058044	4.6824	0.7205	0.4615	0.259
0.9353	0.7581	125006	27108.8	0.0154418	0.0164655	0.0156776	0.0118852	0.0037924	4.6113	0.6995	0.5303	0.1692
0.9620	0.847	115077	25197	0.0152433	0.0160987	0.0153682	0.0130169	0.0023513	4.5671	0.6857	0.5808	0.1049
0.9789	0.911	108879	24000.4	0.0151041	0.0158492	0.0151675	0.0138176	0.0013499	4.5366	0.6767	0.6165	0.0602
0.9896	0.9548	105024	23237.8	0.0150106	0.0156812	0.0150397	0.0143595	0.0006802	4.5195	0.671	0.6407	0.0304
0.9962	0.9831	102675	22783.2	0.0149509	0.0155775	0.0149611	0.0147082	0.0002528	4.5066	0.6675	0.6562	0.0113
1	1	101325	undefined	0.0149155	0	0.0149155	0.0149155	0	.....	0.6655	0.6655	0

Ideal Adsorbed Solution Theory for N2-CH4 / Turkish clinoptilolite at 22.6-22.8°C and 101325 Pa total pressure

y1 (N2)	x1 (N2)	P10 (N2) [Pa]	P20 (CH4) [Pa]	v10 (N2) [m3STP/kg]	v20 (CH4) [m3STP/kg]	vt [m3STP/kg]	v1 (N2) [m3STP/kg]	v2 (CH4) [m3STP/kg]	alpha21 CH4/N2	nt [mol/kg]	n1 (N2) [mol/kg]	n2 (CH4) [mol/kg]
0	0	undefined	101325	0	0.0179207	0.0179207	0	0.0179207	.....	0.7996	0	0.7996
0.0556	0.0273	206880	98368	0.0132115	0.0178422	0.0176734	0.0004816	0.0171918	2.103	0.7885	0.0215	0.7671
0.1529	0.0803	192994	93321.3	0.013156	0.0176985	0.0172211	0.0013829	0.0158382	2.068	0.7684	0.0617	0.7067
0.2822	0.1631	175342	86900.1	0.0130735	0.0174957	0.0165809	0.0027043	0.0138766	2.018	0.7398	0.1207	0.6191
0.4252	0.2736	157491	80173.2	0.0129728	0.0172545	0.0158256	0.0043294	0.0114962	1.964	0.7061	0.1932	0.5129
0.5646	0.4039	141638	74010	0.0128638	0.0170024	0.0150471	0.0060775	0.0089696	1.914	0.6714	0.2712	0.4002
0.6894	0.5428	128707	68823.2	0.0127568	0.0167623	0.0143216	0.0077731	0.0065486	1.870	0.639	0.3468	0.2922
0.795	0.6788	118661	64680.7	0.0126592	0.0165487	0.0136927	0.0092953	0.0043975	1.835	0.6109	0.4147	0.1962
0.8808	0.8035	111067	61490.2	0.0125749	0.0163689	0.0131749	0.0105861	0.0025889	1.806	0.5878	0.4723	0.1155
0.9483	0.9113	105437	59078.4	0.0125054	0.016223	0.0127649	0.0116326	0.0011322	1.785	0.5695	0.519	0.0505
1	1	101325	undefined	0.0124503	0	0.0124503	0.0124503	0	.....	0.5555	0.5555	0

Ideal Adsorbed Solution Theory for N2-CH4 / Turkish clinoptilolite at 40.0°C and 101325 Pa total pressure

y1 (N2)	x1 (CH4)	P10 (N2) [Pa]	P20 (CH4) [Pa]	v10 (N2) [m3STP/kg]	v20 (CH4) [m3STP/kg]	vt [m3STP/kg]	v1 (N2) [m3STP/kg]	v2 (CH4) [m3STP/kg]	alpha21 CH4/N2	nt [mol/kg]	n1 (N2) [mol/kg]	n2 (CH4) [mol/kg]
0	0	undefined	101325	0	0.0149155	0.0149155	0	0.0149155	.....	0.6655	0	0.6655
0.0458	0.0232	199968	98981.3	0.0109203	0.0148523	0.0147292	0.0003418	0.0143873	2.020	0.6572	0.0153	0.6419
0.1247	0.0669	188997	95044.3	0.0108739	0.0147403	0.014398	0.0009625	0.0134355	1.989	0.6424	0.0429	0.5995
0.2384	0.1383	174713	89548.4	0.0108055	0.0145708	0.0139009	0.0019222	0.0119787	1.951	0.6202	0.0858	0.5345
0.3786	0.2426	158169	83122.4	0.0107122	0.0143501	0.0132581	0.0032157	0.0100423	1.903	0.5915	0.1435	0.4481
0.5288	0.3772	142042	76664.6	0.0106025	0.0140995	0.0125395	0.0047299	0.0078096	1.853	0.5595	0.211	0.3484
0.6712	0.5304	128225	70942.5	0.0104889	0.0138484	0.0118375	0.0062786	0.0055589	1.807	0.5282	0.2801	0.248
0.793	0.684	117478	66361.9	0.0103843	0.0136241	0.0112281	0.00768	0.0035481	1.770	0.501	0.3427	0.1583
0.8882	0.8201	109733	62994.7	0.0102979	0.0134438	0.0107504	0.0088164	0.001934	1.742	0.4797	0.3934	0.0863
0.9561	0.9267	104541	60665.1	0.0102337	0.0133104	0.0104101	0.009647	0.0007631	1.723	0.4645	0.4304	0.034
1	1	101325	undefined	0.0101911	0	0.0101911	0.0101911	0	.....	0.4547	0.4547	0

Ideal Adsorbed Solution Theory for N2-CO / Cuban clinoptilolite at 40.0-40.1°C and 101325 Pa total pressure

y1 (N2)	x1 (N2)	P10 (N2) [Pa]	P20 (CO) [Pa]	v10 (N2) [m3STP/kg]	v20 (CO) [m3STP/kg]	vt [m3STP/kg]	v1 (N2) [m3STP/kg]	v2 (CO) [m3STP/kg]	alpha21 CO/N2	nt [mol/kg]	n1 (N2) [mol/kg]	n2 (CO) [mol/kg]
0	0	undefined	101325	0	0.0124417	0.0124417	0	0.0124417	.....	0.5551	0	0.5551
0.0990	0.0387	259197	94969.4	0.0128722	0.0122993	0.0123205	0.0004768	0.0118437	2.7293	0.5497	0.0213	0.5284
0.2647	0.116	231246	84276.5	0.0125588	0.0120209	0.0120809	0.0014014	0.0106795	2.7439	0.539	0.0625	0.4765
0.4545	0.2315	198913	71927.9	0.0121143	0.0116199	0.0117307	0.0027157	0.0090151	2.7655	0.5234	0.1212	0.4022
0.6198	0.3697	169882	61113.3	0.0116119	0.0111699	0.0113293	0.0041885	0.0071409	2.7798	0.5055	0.1869	0.3186
0.7454	0.5117	147606	52826.4	0.0111345	0.0107361	0.0109363	0.0055961	0.0053402	2.7942	0.488	0.2497	0.2383
0.8352	0.6436	131483	46864	0.0107222	0.0103586	0.0105897	0.0068156	0.0037742	2.8056	0.4725	0.3041	0.1684
0.8984	0.7586	120008	42629.5	0.0103856	0.0100477	0.0103019	0.0078145	0.0024874	2.8151	0.4596	0.3487	0.111
0.9434	0.8552	111770	39618.3	0.0101173	0.0098003	0.0100702	0.0086123	0.0014579	2.8212	0.4493	0.3843	0.065
0.9759	0.9349	105774	37434.4	0.009906	0.0096049	0.0098859	0.0092423	0.0006436	2.8256	0.4411	0.4124	0.0287
1	1	101325	undefined	0.0097396	0	0.0097396	0.0097396	0	.....	0.4346	0.4346	0

Ideal Adsorbed Solution Theory for CH4-CO / Cuban clinoptilolite at 39.9-40.1°C and 101325 Pa total pressure

y1 (CH4)	x1 (CH4)	P10 (CH4) [Pa]	P20 (CO) [Pa]	v10 (CH4) [m3STP/kg]	v20 (CO) [m3STP/kg]	vt [m3STP/kg]	v1 (CH4) [m3STP/kg]	v2 (CO) [m3STP/kg]	alpha21 CO/CH4	nt [mol/kg]	n1 (CH4) [mol/kg]	n2 (CO) [mol/kg]
0	0	undefined	101325	0	0.0124417	0.0124417	0	0.0124417	.....	0.5551	0	0.5551
0.0189	0.013	146884	100724	0.014991	0.0124289	0.0124566	0.0001622	0.0122944	1.4583	0.5558	0.0072	0.5485
0.1076	0.0761	143382	97862.8	0.0148874	0.012366	0.0125274	0.0009528	0.0115745	1.4651	0.5589	0.0425	0.5164
0.2875	0.2142	136012	91869.8	0.0146571	0.012224	0.0126747	0.0027149	0.0099598	1.4805	0.5655	0.1211	0.4444
0.5017	0.4014	126666	84335.6	0.0143388	0.0120226	0.0128561	0.0051598	0.0076963	1.5019	0.5736	0.2302	0.3434
0.6800	0.5828	118232	77706.5	0.0140227	0.01182	0.0130111	0.0075829	0.0054282	1.5215	0.5805	0.3383	0.2422
0.8039	0.7274	111986	72883.3	0.0137684	0.0116547	0.0131196	0.0095426	0.0035771	1.5365	0.5854	0.4258	0.1596
0.8852	0.8328	107701	69576.1	0.0135828	0.0115312	0.0131903	0.0109842	0.0022061	1.548	0.5885	0.4901	0.0984
0.9387	0.9078	104777	67356.1	0.0134507	0.0114431	0.0132364	0.0120154	0.0012211	1.5556	0.5906	0.5361	0.0545
0.9748	0.9613	102755	65850.4	0.0133564	0.0113808	0.0132672	0.0127532	0.000514	1.5604	0.5919	0.569	0.0229
1	1	101325	undefined	0.0132884	0	0.0132884	0.0132884	0	.....	0.5929	0.5929	0

Ideal Adsorbed Solution Theory for N2-CH4 / Cuban clinoptilolite at 39.9-40.0°C and 101325 Pa total pressure

y1 (N2)	x1 (N2)	P10 (N2) [Pa]	P20 (CH4) [Pa]	v10 (N2) [m3STP/kg]	v20 (CH4) [m3STP/kg]	vt [m3STP/kg]	v1 (N2) [m3STP/kg]	v2 (CH4) [m3STP/kg]	alpha21 CH4/N2	nt [mol/kg]	n1 (N2) [mol/kg]	n2 (CH4) [mol/kg]
0	0	undefined	101325	0	0.0132884	0.0132884	0	0.0132884	.....	0.5929	0	0.5929
0.1410	0.086	166181	95222.5	0.0115389	0.0129837	0.0128454	0.0011047	0.0117407	1.745	0.5731	0.0493	0.5238
0.2750	0.179	155671	89476.1	0.0113184	0.0126738	0.0124078	0.002221	0.0101868	1.740	0.5536	0.0991	0.4545
0.4009	0.278	146133	84072	0.0110994	0.0123596	0.0119814	0.0033308	0.0086506	1.738	0.5346	0.1486	0.386
0.5180	0.384	136676	79287.7	0.0108621	0.0120609	0.0115705	0.0044431	0.0071275	1.724	0.5162	0.1982	0.318
0.6254	0.494	128268	75020.7	0.0106319	0.0117764	0.0111818	0.0055238	0.005658	1.710	0.4989	0.2465	0.2524
0.7225	0.605	120996	71195.8	0.0104162	0.0115055	0.0108209	0.0065466	0.0042742	1.699	0.4828	0.2921	0.1907
0.8088	0.7135	114852	67636.9	0.0102205	0.0112387	0.0104929	0.0074867	0.0030062	1.698	0.4682	0.334	0.1341
0.8839	0.818	109488	64637.4	0.0100386	0.0110018	0.0102011	0.0083445	0.0018566	1.694	0.4551	0.3723	0.0828
0.9477	0.915	104943	62380.1	0.0098756	0.0108158	0.0099491	0.0091034	0.0008457	1.682	0.4439	0.4062	0.0377
1	1	101325	undefined	0.0097396	0	0.0097396	0.0097396	0	.....	0.4346	0.4346	0

Ideal Adsorbed Solution Theory for N2-CO / AlPO4-11 at 22.6-22.8°C and 101325 Pa total pressure

y1 (N2)	x1 (N2)	P10 (N2) [Pa]	P20 (CO) [Pa]	n10 (N2) [mol/kg]	n20 (CO) [mol/kg]	nt [mol/kg]	n1 (N2) [mol/kg]	n2 (CH4) [mol/kg]	alpha21 CO/N2	vt [m3STP/kg]	v1 (N2) [m3STP/kg]	v2 (CO) [m3STP/kg]
0	0	undefined	101325	0	0.1891	0.1891	0	0.1891156	.....	0.0042386	0	0.0042386
0.1148	0.0371	313875	93142	0.1387	0.1759	0.1742	0.0065	0.1676955	3.370	0.0039032	0.0001447	0.0037585
0.2442	0.0896	276202	84120.2	0.1295	0.1609	0.1575	0.0141	0.1433962	3.283	0.0035301	0.0003162	0.0032139
0.3851	0.164	238006	74520.7	0.119	0.1446	0.1396	0.0229	0.1167490	3.194	0.0031298	0.0005131	0.0026167
0.5316	0.2676	201251	64808.2	0.1074	0.1276	0.1215	0.0325	0.0889477	3.105	0.0027221	0.0007285	0.0019936
0.6738	0.4059	168205	55631	0.0956	0.111	0.1042	0.0423	0.0618944	3.024	0.002335	0.0009478	0.0013872
0.7998	0.5749	140980	47707.2	0.0846	0.0964	0.0892	0.0513	0.0379408	2.955	0.0020001	0.0011498	0.0008504
0.8982	0.7524	120957	41657.2	0.0757	0.0849	0.0778	0.0586	0.0192670	2.904	0.0017443	0.0013124	0.0004318
0.9622	0.8985	108499	37793.1	0.0698	0.0775	0.0705	0.0634	0.0071558	2.871	0.0015807	0.0014204	0.0001604
0.9927	0.9793	102707	35963.6	0.067	0.074	0.0671	0.0657	0.0013886	2.856	0.0015035	0.0014724	0.0000311
0.9998	0.9996	101354	35535	0.0663	0.0731	0.0663	0.0662	0.0000287	2.852	0.0014854	0.0014847	6.44E-07
1	1	101325	undefined	0.0663	0	0.0663	0.0663	0	.....	0.001485	0.001485	0

Ideal Adsorbed Solution Theory for N2-CO / AlPO4-11 at 40.0°C and 101325 Pa total pressure

y1 (N2)	x1 (N2)	P10 (N2) [Pa]	P20 (CO) [Pa]	n10 (N2) [mol/kg]	n20 (CO) [mol/kg]	nt [mol/kg]	n1 (N2) [mol/kg]	n2 (CO) [mol/kg]	alpha21 CO/N2	vt [m3STP/kg]	v1 (N2) [m3STP/kg]	v2 (CO) [m3STP/kg]
0	0	undefined	101325	0	0.140335	0.140335	0	0.140335	.....	0.00314528	0	0.0031453
0.08517	0.02804	307811	95368.9	0.113005	0.132654	0.132011	0.003701	0.128309	3.228	0.00295872	0.00008295	0.00287576
0.18971	0.06847	280741	88137.5	0.106178	0.123240	0.121898	0.008346	0.113552	3.185	0.00273208	0.00018707	0.00254501
0.31552	0.12816	249454	79550.1	0.097757	0.111930	0.109889	0.014083	0.095805	3.136	0.00246290	0.00031565	0.00214726
0.46106	0.21737	214925	69774.4	0.087726	0.098882	0.096222	0.020915	0.075307	3.080	0.00215661	0.00046877	0.00168784
0.61809	0.3487	179603	59415.5	0.076564	0.084819	0.081764	0.028511	0.053253	3.023	0.00183255	0.00063901	0.00119354
0.76937	0.52906	147348	49622.1	0.065468	0.071382	0.068126	0.036043	0.032083	2.969	0.00152690	0.00080782	0.00071908
0.89177	0.73785	122463	41831.6	0.056246	0.060528	0.057309	0.042285	0.015024	2.928	0.00128444	0.00094772	0.00033672
0.9673	0.91065	107628	37085.2	0.050446	0.053852	0.050733	0.046199	0.004533	2.902	0.00113706	0.00103546	0.00010160
0.99626	0.98924	102043	35276.6	0.048200	0.051296	0.048231	0.047713	0.000519	2.893	0.00108100	0.00106937	0.00001163
0.99998	0.99995	101328	35041.6	0.047910	0.050963	0.047910	0.047908	0.000002	2.892	0.00107380	0.00107375	0.00000005
1	1	101325	undefined	0.047909	0	0.047909	0.047909	0	.....	0.00107377	0.0010738	0

Ideal Adsorbed Solution Theory for CH4-CO / AlPO4-11 at 22.6-22.8°C and 101325 Pa total pressure

y1 (CH4)	x1 (CH4)	P10 (CH4) [Pa]	P20 (CO) [Pa]	n10 (CH4) [mol/kg]	n20 (CO) [mol/kg]	nt [mol/kg]	n1 (CH4) [mol/kg]	n2 (CO) [mol/kg]	alpha12 CH4/CO	vt [m3STP/kg]	v1 (CH4) [m3STP/kg]	v2 (CO) [m3STP/kg]
0	0	undefined	101325	0	0.18912	0.18912	0	0.18912	.....	0.0042386	0	0.0042386
0.0427	0.0852	50813.6	106029	0.20318	0.19659	0.19713	0.0168	0.18034	2.087	0.0044183	0.0003764	0.0040418
0.0961	0.1819	53552.5	111947	0.2131	0.20585	0.20713	0.03768	0.16945	2.090	0.0046423	0.0008444	0.0037979
0.1608	0.2864	56881.2	119164	0.22503	0.21693	0.21919	0.06278	0.15641	2.095	0.0049127	0.0014071	0.0035056
0.2373	0.3953	60840	127786	0.23904	0.22989	0.23342	0.09226	0.14116	2.100	0.0052316	0.0020679	0.0031638
0.3265	0.5053	65474.4	137944	0.25519	0.24477	0.24993	0.12629	0.12364	2.107	0.0056016	0.0028305	0.0027711
0.4292	0.6139	70848.2	149780	0.27361	0.26161	0.26885	0.16504	0.10381	2.114	0.0060256	0.003699	0.0023266
0.5466	0.719	77026.2	163493	0.29436	0.28047	0.29032	0.20873	0.08159	2.123	0.0065069	0.0046783	0.0018286
0.6797	0.819	84094.1	179303	0.31758	0.30139	0.31453	0.2576	0.05692	2.132	0.0070494	0.0057736	0.0012758
0.8303	0.9129	92152.4	197498	0.3434	0.32445	0.34166	0.31191	0.02975	2.143	0.0076576	0.0069908	0.0006668
0.9821	0.9916	100354	216192	0.36898	0.34708	0.36879	0.36569	0.00309	2.154	0.0082655	0.0081962	0.0000693
1	1	101325	undefined	0.37197	0	0.37197	0.37197	0	.....	0.0083368	0.0083368	0

Ideal Adsorbed Solution Theory for CH4-CO / AlPO4-11 at 40.0°C and 101325 Pa total pressure

y1 (CH4)	x1 (CH4)	P10 (CH4) [Pa]	P20 (CO) [Pa]	n10 (CH4) [mol/kg]	n20 (CO) [mol/kg]	nt [mol/kg]	n1 (CH4) [mol/kg]	n2 (CO) [mol/kg]	alpha12 CH4/CO	vt [m3STP/kg]	v1 (CH4) [m3STP/kg]	v2 (CO) [m3STP/kg]
0	0	undefined	101325	0	0.14033	0.14033	0	0.14033	---------	0.0031453	0	0.0031453
0.0499	0.0991	51046.4	106858	0.1491	0.14741	0.14758	0.01463	0.13295	2.093	0.0033076	0.0003279	0.0029797
0.1058	0.1986	53972.6	113058	0.15716	0.15527	0.15564	0.03091	0.12474	2.095	0.0034884	0.0006927	0.0027957
0.1686	0.2983	57271.5	120053	0.16617	0.16406	0.16469	0.04913	0.11556	2.096	0.003691	0.001101	0.00259
0.2398	0.3983	61012.9	128010	0.17632	0.17395	0.17489	0.06966	0.10523	2.098	0.0039197	0.0015612	0.0023585
0.3213	0.4985	65299.7	137135	0.18785	0.18516	0.18649	0.09297	0.09353	2.100	0.0041798	0.0020836	0.0020962
0.4152	0.5989	70256.8	147706	0.20105	0.19796	0.19980	0.11965	0.08015	2.102	0.0044781	0.0026818	0.0017964
0.5249	0.6993	76053.2	160096	0.21632	0.21274	0.21523	0.15051	0.06472	2.105	0.0048239	0.0033733	0.0014505
0.6545	0.7976	83139.4	173007	0.23473	0.22786	0.23330	0.18609	0.04721	2.081	0.005229	0.0041709	0.0010581
0.8100	0.9000	91187.4	192600	0.25531	0.25031	0.25480	0.22933	0.02547	2.112	0.0057108	0.0051399	0.0005709
0.9791	0.9900	100209	212070	0.27798	0.27204	0.27792	0.27515	0.00277	2.116	0.0062289	0.0061668	0.0000621
1	1	101325	undefined	0.28075	0	0.28075	0.28075	0	---------	0.0062924	0.0062924	0

Ideal Adsorbed Solution Theory for N2-CH4 / AlPO4-11 at 22.8°C and 101325 Pa total pressure

y1 (N2)	x1 (N2)	P10 (N2) [Pa]	P20 (CH4) [Pa]	n10 (N2) [mol/kg]	n20 (CH4) [mol/kg]	nt [mol/kg]	n1 (N2) [mol/kg]	n2 (CH4) [mol/kg]	alpha21 CH4/N2	vt [m3STP/kg]	v1 (N2) [m3STP/kg]	v2 (CH4) [m3STP/kg]
0	0	undefined	101325	0	0.37197	0.37197	0	0.37197	---------	0.0083368	0	0.0083368
0.138244	0.016648	841397	88795.7	0.20615	0.33273	0.32936	0.00548	0.32388	9.476	0.0073819	0.0001229	0.0072591
0.290205	0.045215	650344	75325.8	0.19002	0.28869	0.28207	0.01275	0.26932	8.634	0.006322	0.0002858	0.0060361
0.449891	0.094320	483303	61544.7	0.16979	0.24151	0.23226	0.02191	0.21035	7.853	0.0052055	0.000491	0.0047145
0.607428	0.177400	346943	48355.7	0.146	0.19419	0.18345	0.03254	0.15091	7.175	0.0041116	0.0007294	0.0033822
0.750100	0.311600	243915	36782.5	0.12069	0.15081	0.13993	0.0436	0.09633	6.631	0.0031362	0.0009772	0.002159
0.865210	0.507200	172846	27714.2	0.09733	0.11553	0.10552	0.05352	0.052	6.237	0.002365	0.0011995	0.0011655
0.944067	0.738170	129587	21645.5	0.07966	0.09125	0.0824	0.06083	0.02158	5.987	0.0018468	0.0013633	0.0004836
0.985670	0.921470	108384	18489.6	0.06976	0.07841	0.07037	0.06485	0.00553	5.862	0.0015772	0.0014534	0.0001239
0.998847	0.993322	101889	17497.5	0.06654	0.07434	0.06659	0.06614	0.00044	5.823	0.0014924	0.0014824	9.97E-06
0.999999	0.999991	101326	17411.4	0.06626	0.07398	0.06626	0.06626	6E-07	5.820	0.001485	0.001485	1.29E-08
1	1	101325	undefined	0.06626	0	0.06626	0.06626	0	---------	0.001485	0.001485	0

Ideal Adsorbed Solution Theory for N2-CH4 / AlPO4-11 at 40.0°C and 101325 Pa total pressure

y1 (N2)	x1 (N2)	P10 (N2) [Pa]	P20 (CH4) [Pa]	n10 (N2) [mol/kg]	n20 (CH4) [mol/kg]	nt [mol/kg]	n1 (N2) [mol/kg]	n2 (CH4) [mol/kg]	alpha21 CH4/N2	vt [m3STP/kg]	v1 (N2) [m3STP/kg]	v2 (CH4) [m3STP/kg]
0	0	undefined	101325	0	0.280753	0.280753	0	0.28075	.....	0.00629244	0	0.0062924
0.17153	0.02532	686443	86124.9	0.178740	0.242403	0.240236	0.006083	0.23415	7.970	0.00538435	0.00013633	0.005248
0.34212	0.06487	534379	71284.1	0.157540	0.203773	0.199966	0.012972	0.18699	7.496	0.00448178	0.00029073	0.0041911
0.50519	0.12603	406163	57366.1	0.134763	0.166430	0.161643	0.020372	0.14127	7.080	0.00362285	0.00045659	0.0031663
0.65347	0.21889	302501	44951.2	0.111698	0.132168	0.127071	0.027814	0.09926	6.730	0.002848	0.00062339	0.0022246
0.77983	0.35444	222933	34557.1	0.090126	0.102766	0.097899	0.034699	0.0632	6.451	0.00219419	0.00077771	0.0014165
0.8785	0.53653	165906	26563.6	0.071964	0.079694	0.075351	0.040428	0.03492	6.246	0.00168883	0.00090611	0.0007827
0.94362	0.7324	130547	21346.1	0.059309	0.064413	0.060594	0.044379	0.01621	6.116	0.00135808	0.00099465	0.0003634
0.98415	0.91139	109414	18124.2	0.051157	0.054887	0.051467	0.046906	0.00456	6.037	0.00115351	0.0010513	0.0001022
0.99814	0.98893	102269	17018.4	0.048292	0.051602	0.048326	0.047791	0.00054	6.009	0.00108312	0.00107112	0.000012
0.99999	0.99994	101330	16869.7	0.047911	0.051160	0.047911	0.047908	3E-06	6.007	0.00107382	0.00107376	6.11E-08
1	1	101325	undefined	0.047909	0	0.047909	0.047909	0	.....	0.00107377	0.00107377	0

Ideal Adsorbed Solution Theory for N2-CO / AlPO4-18 at 40.1°C and 101325 Pa total pressure

y1	x1	P10 [Pa]	P20 [Pa]	n10 [mol/kg]	n20 [mol/kg]	nt [mol/kg]	n1 [mol/kg]	n2 [mol/kg]	alpha21 CO/N2	vt [m3STP/kg]	v1 [m3STP/kg]	v2 [m3STP/kg]
0	0	undefined	101325	0	0.22044	0.22044	0	0.22044	.....	0.0049406	0	0.0049406
8.3E-05	0.00002	369274	101319	0.24619	0.22043	0.22043	5E-06	0.22042	3.645	0.0049404	1.12E-07	0.0049403
5.9E-03	0.00173	367888	100891	0.24534	0.21974	0.21978	0.00036	0.21942	3.646	0.0049258	8.00E-06	0.0049178
0.06431	0.01842	353788	96588.2	0.2366	0.21274	0.21314	0.00393	0.20922	3.663	0.0047771	0.000088	0.0046891
0.1278	0.03828	338236	91894.2	0.2269	0.20493	0.20569	0.00787	0.19782	3.681	0.0046102	0.0001765	0.0044337
0.22761	0.07359	313406	84479.3	0.2113	0.19218	0.19347	0.01424	0.17923	3.710	0.0043362	0.0003191	0.0040171
0.36511	0.13292	278331	74191.8	0.18898	0.17362	0.17552	0.02333	0.15219	3.752	0.0039339	0.0005229	0.003411
0.52248	0.2235	236866	62311.7	0.16219	0.15082	0.15322	0.03425	0.11898	3.801	0.0034341	0.0007675	0.0026666
0.66322	0.33852	198516	51587.6	0.13701	0.12885	0.1315	0.04451	0.08699	3.848	0.0029473	0.0009977	0.0019496
0.85518	0.6013	144106	36804.5	0.10059	0.09616	0.09877	0.05939	0.03938	3.915	0.0022137	0.0013311	0.0008826
0.9242	0.75573	123913	31442.2	0.08686	0.08354	0.08602	0.06501	0.02101	3.941	0.001928	0.001457	0.000471
0.97076	0.89347	110090	27812.7	0.07739	0.07476	0.0771	0.06889	0.00821	3.958	0.0017281	0.001544	0.0001841
0.98613	0.9472	105490	26609.6	0.07423	0.0718	0.0741	0.07018	0.00391	3.964	0.0016607	0.001573	0.0000877
0.99297	0.97268	103439	26076	0.07282	0.07048	0.07275	0.07076	0.00199	3.967	0.0016305	0.001586	0.0000445
0.99656	0.98649	102359	25795.9	0.07207	0.06979	0.07204	0.07107	0.00097	3.968	0.0016146	0.0015928	0.0000218
0.99867	0.99473	101726	25627.8	0.07164	0.06937	0.07162	0.07125	0.00038	3.969	0.0016053	0.0015968	8.46E-06
0.99989	0.99956	101358	25538.3	0.07138	0.06915	0.07138	0.07135	0.00003	3.969	0.0015999	0.0015992	6.97E-07
1	1	99920	undefined	0.07039	0	0.07039	0.07039	0	.....	0.0015777	0.0015777	0

Ideal Adsorbed Solution Theory for CH4-CO / AlPO4-18 at 40.0-40.1°C and 101325 Pa total pressure

y1 (CH4)	x1 (CH4)	P10 (CH4) [Pa]	P20 (CO) [Pa]	n10 (CH4) [mol/kg]	n20 (CO) [mol/kg]	nt [mol/kg]	n1 (CH4) [mol/kg]	n2 (CO) [mol/kg]	alpha21 CO/CH4	vt [m3STP/kg]	v1 (CH4) [m3STP/kg]	v2 (CH4) [m3STP/kg]
0	0	undefined	101325	0	0.22044	0.22044	0	0.22044	---------	0.0049406	0	0.0049406
4.9E-05	0.00003	145750	101323	0.23981	0.22043	0.22044	7E-06	0.22043	1.4385	0.0049406	1.67E-07	0.0049404
0.01948	0.01361	144959	100723	0.23867	0.21947	0.21971	0.00299	0.21672	1.4392	0.0049243	0.00067	0.0048573
0.082	0.05836	142383	98780.5	0.23493	0.21633	0.21733	0.01268	0.20465	1.4414	0.004871	0.0002843	0.0045868
0.22344	0.1659	136467	94335.4	0.2263	0.20902	0.21170	0.03512	0.17658	1.4466	0.0047448	0.0007872	0.0039576
0.30355	0.23117	133051	91785.7	0.22127	0.20475	0.20834	0.04816	0.16018	1.4496	0.0046696	0.0010795	0.0035901
0.3924	0.30771	129212	88929.9	0.21558	0.1999	0.20447	0.06292	0.14156	1.4530	0.0045828	0.0014102	0.0031726
0.4836	0.39135	125211	85967.2	0.20962	0.19478	0.20033	0.0784	0.12193	1.4565	0.00449	0.0017571	0.0027328
0.57014	0.47604	121355	83127.6	0.20383	0.1898	0.19623	0.09341	0.10282	1.4599	0.0043981	0.0020936	0.0023044
0.64664	0.55572	117902	80589.3	0.19862	0.18529	0.19247	0.10696	0.08551	1.4630	0.0043137	0.0023972	0.0019165
0.78452	0.71257	111558	75958.1	0.18895	0.17689	0.18532	0.13205	0.05327	1.4687	0.0041535	0.0029597	0.0011939
0.86323	0.81088	107866	73279	0.18328	0.17192	0.18102	0.14679	0.03423	1.4720	0.0040572	0.0032899	0.0007673
0.93735	0.91025	104342	70730.5	0.17784	0.16714	0.17682	0.16095	0.01587	1.4752	0.003963	0.0036073	0.0003557
0.96881	0.95462	102831	69641	0.17549	0.16507	0.17499	0.16705	0.00794	1.4766	0.003922	0.003744	0.000178
0.98488	0.97783	102056	69083.3	0.17429	0.16401	0.17404	0.17019	0.00386	1.4773	0.0039008	0.0038143	0.0000865
0.99417	0.99141	101607	68760.5	0.17359	0.16339	0.17349	0.172	0.00149	1.4777	0.0038885	0.0038551	0.0000334
0.99952	0.99929	101348	68576.9	0.17318	0.16304	0.17318	0.17305	0.00012	1.4779	0.0038813	0.0038786	2.75E-06
1	1	101325	undefined	0.17315	0	0.17315	0.17315	0	---------	0.0038807	0.0038807	0

Ideal Adsorbed Solution Theory for N2-CH4 / AlPO4-18 at 40.0-40.1°C and 101325 Pa total pressure

y1 (N2)	x1 (N2)	P10 (N2) [Pa]	P20 (CH4) [Pa]	n10 (N2) [mol/kg]	n20 (CH4) [mol/kg]	nt [mol/kg]	n1 (N2) [mol/kg]	n2 (CH4) [mol/kg]	alpha21 CH4/N2	vt [m3STP/kg]	v1 (N2) [m3STP/kg]	v2 (CH4) [m3STP/kg]
0	0	undefined	101325	0	0.17315	0.17315	0	0.17315	---------	0.0038807	0	0.0038807
0.19973	0.08883	227819	88993.1	0.15629	0.15372	0.15394	0.01367	0.14027	2.560	0.0034503	0.0003065	0.0031438
0.36916	0.18577	201355	78503.4	0.13889	0.13686	0.13723	0.02549	0.11174	2.565	0.0030758	0.0005714	0.0025044
0.50982	0.28817	179260	69774.9	0.12421	0.12259	0.12305	0.03546	0.08759	2.569	0.002758	0.0007948	0.0019632
0.6255	0.39367	160998	62582.2	0.11198	0.11066	0.11118	0.04377	0.06741	2.573	0.0024918	0.0009809	0.0015109
0.72047	0.5002	145945	56669.3	0.10183	0.10074	0.10128	0.05066	0.05062	2.575	0.0022701	0.0011355	0.0011346
0.79862	0.60605	133521	51795.4	0.0934	0.09249	0.09304	0.05639	0.03665	2.578	0.0020853	0.0012638	0.0008215
0.86324	0.70987	123217	47762.2	0.08638	0.0856	0.08615	0.06116	0.025	2.580	0.0019309	0.0013707	0.0005602
0.917	0.8106	114625	44404.4	0.0805	0.07982	0.08037	0.06515	0.01522	2.581	0.0018014	0.0014602	0.0003412
0.96203	0.90748	107415	41588.7	0.07555	0.07496	0.0755	0.06851	0.00699	2.583	0.0016921	0.0015356	0.0001566
0.99648	0.99095	101890	39432.6	0.07175	0.07121	0.07175	0.0711	0.00065	2.584	0.001608	0.0015935	0.0000145
1	1	101325	undefined	0.07136	0	0.07136	0.07136	0	---------	0.0015994	0.0015994	0